UNIVERSITA' DEGLI STUDI DEL PIEMONTE ORIENTALE "AMEDEO AVOGADRO"

Dottorato in Scienze delle Sostanze Bioattive

Dipartimento di Scienze del Farmaco

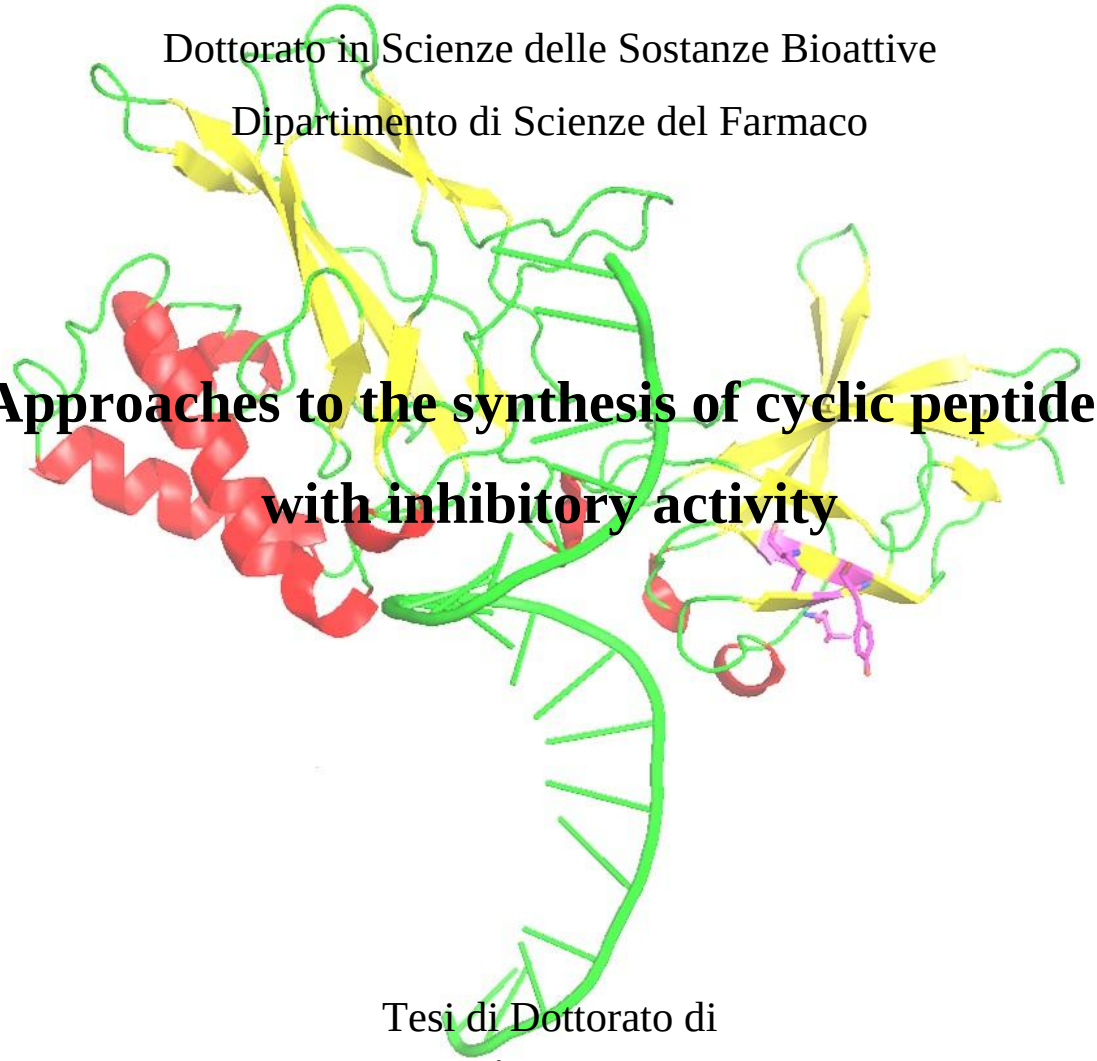

Approaches to the synthesis of cyclic peptides with inhibitory activity

Tesi di Dottorato di

Monica Varese

XXVI Ciclo

UNIVERSITA' DEGLI STUDI DEL PIEMONTE ORIENTALE "AMEDEO AVOGADRO"

Dipartimento di Scienze del Farmaco

Dottorato di Ricerca in Scienza delle Sostanze Bioattive

Ciclo XXVI a.a. 2010-2013

Approaches to the synthesis of cyclic peptides with inhibitory activity

Monica Varese

Supervised by Prof. Luigi PANZA

PhD program coordinator: Prof. Luigi PANZA

Contents

PART II

Development of a cyclic peptides library to modulate EGF-EGFR and VEGF-VEGFR interactions

Chapter 1. Introduction

Chapter 2. Results and discussion

Abbreviations and annex

Abbreviations

1.1. Analytics

^{13}C-NMR	Carbon 13 Nuclear Magnetic Resonance
^{1}H-NMR	Proton Nuclear Magnetic Resonance
Calcd	Calculated
COSY	Correlation Spectroscopy
DEPT	Distortionless Enhancement by Polarization Transfer
ESI	Electrospray Ionization
FP	Fluorescence Polarization
G	HPLC gradient
HPLC	High Pressure Liquid Chromatography
HR	High Resolution
HSQC	Heteronuclear Single Quantum Coherence
MALDI-TOF	Matrix Assisted Lased Desorption Ionization Time Of Flight
MS	Mass Spectroscopy
P*e*	Effective permeability
R_f	Retention factor
RP	Reverse Phase
TLC	Thin Layer Chromatography
t_R	Retention time
z	Charge

1.2. Solvents

ACN	Acetonitrile
AcOEt	Ethyl acetate
DCM	Dichloromethane
DMF	*N*,*N*-Dimethylformamide
DMSO	Dimethyl sulfoxide
*i*PrOH	Isopropanol
MeOH	Methanol
PE	Petroleum ether
TEA	Triethylamine
TFA	Trifluoroacetic acid
THF	Tetrahydrofuran
TBME	*tert*-Butyl methyl ether

1.3. Chemicals and reagents

Ac_2O	Acetic anhydride
Ac	Acetyl
Ala	L-Alanine
Alloc	Allyloxycarbonyl
Arg	L-Arginine
Asp	L-Aspartic acid

Bn	Benzyl
Boc	*tert*-Butyloxycarbonyl
Bzl	Benzyl
Cbz	Carboxybenzyl
CPP	Cell-Penetrating Peptide
Cf	5(6)-Carboxyfluorescein
CF_3	4,4,4-Trifluoro-3-(trifluoromethyl)butanoic acid
2Cl-Z	2-Chlorobenzyloxy-carbonyl
CNS	Central Nervous System
Cl-Trt	2-Chlorotrityl resin
Cys	L-Cysteine
Dap	2,3-Diaminopropionic acid
DBU	1,8-Diazabicyclo[5.4.0]undec-7-ene
DIBAL	Diisobutylaluminum hydride
DIC	N,N'-Diisopropylcarbodiimide
DIPEA	N,N-Diisopropylethylamine
DKP	Diketopiperazine
DMAP	4-Dimethylaminopyridine
DPPA	Diphenylphosphoryl azide
DTT	Dithiothreitol
EDC•HCl	1-Ethyl-3-(3-dimethylaminopropyl)carbodiimide hydrochloride
EDT	1,2-Ethanedithiol
Fm	Fluorenylmethyl
Fmoc	Fluorenylmethyloxycarbonyl
Fmoc-O_2O	Fmoc-8-amino-3,6-dioxaoctanoic acid
Gln	L-Glutamine
Glu	L-Glutamic acid
HATU	O-(7-Azabenzotriazol-1-yl)-N,N,N',N'-tetramethyluronium hexafluorophosphate
HBTU	O-Benzotriazole-N,N,N',N'-tetramethyl-uronium-hexafluorophosphate
His	L-Histidine
HOAc	Acetic acid
HOAt	1-Hydroxy-7-azabenzotriazole
HOBt	1-Hydroxybenzotriazole
Leu	L-Leucine
Lys	L-Lysine
NHS	N-Hydroxysuccinimide
NTCP	N-Tetrachlorophthaloyl
Pbf	2,2,4,6,7-Pentamethyl-dihydrobenzofurane-5-sulfonyl
Phe	L-Phenylalanine
Phe(4-NH_2)	4-Amino-L-phenylalanine
PPAA	Propane phosphonic acid anhydride
Pro	L-Proline

PS-DCC	Polymer supported cyclohexylcarbodiimide
Py	Pyridine
PyBOP	1H-Benzotriazol-1-yloxytris(pyrrolidino)phosphonium hexafluorophosphate
SAA	Sugar Amino Acid
Ser	L-Serine
TBTU	O-(Benzotriazol-1-yl)-N,N,N′,N′-tetramethyl-uronium tetrafluoroborate
*t*Bu	*tert*-Butyl
TFA	Trifluoroacetic acid
TIS	Triisopropylsilane
Trp	L-Tryptophan
Trt	Trityl
Tyr	L-Tyrosine
Val	L-Valine
Z	Carboxybenzyl

1.4. Symbols and other abbreviations

1D	One-dimensional
2D	Two-dimensional
abs	Absorbance
BBB	Blood-Brain Barrier
c	Concentration
eq	Equivalent
h	Hours
J	Coupling constant
K_D	Dissociation constant
M	Molar concentration
mM	Millimolar concentration
MW	Microwave
nm	Nanometer
PAMPA	Parallel Artificial Membrane Permeability Assay
PPI	Protein-Protein Interaction
SPPS	Solid-Phase Peptide Synthesis
min	Minutes
s	Seconds
r.t.	Room temperature
Δ	Difference
δ	Chemical shift
λ	Wavelength
μm	Micrometer

Annex I: Amino acids*

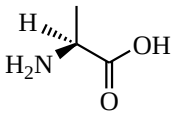	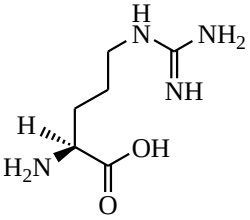	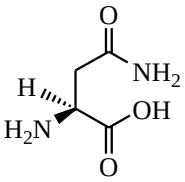	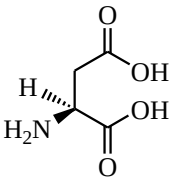
L-Alanine Ala A	L-Arginine Arg R	L-Aspargine Asn N	L-Aspartic acid Asp D
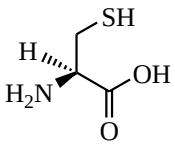	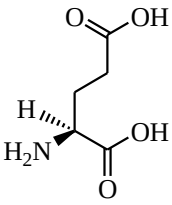	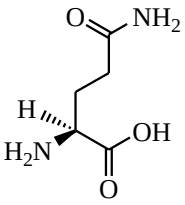	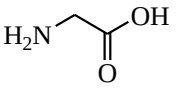
L-Cysteine Cys C	L-Glutamic acid Glu E	L-Glutamine Gln Q	L-Glycine Gly G
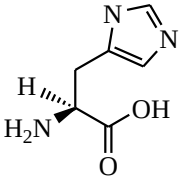	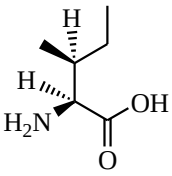	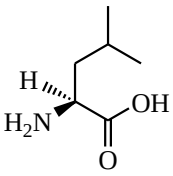	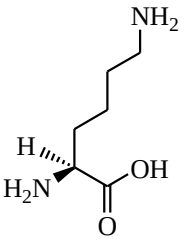
L-Hystidine Hys H	L-Isoleucine Ile I	L-Leucine Leu L	L-Lysine Lys K
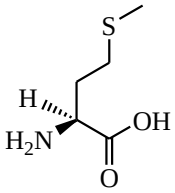	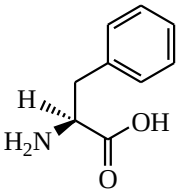	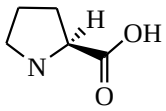	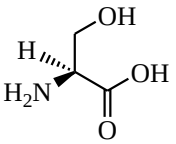
L-Methionine Met M	L-Phenilalanine Phe F	L-Proline Pro P	L-Serine Ser S
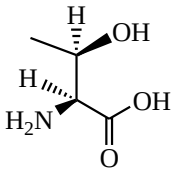	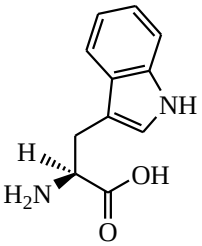	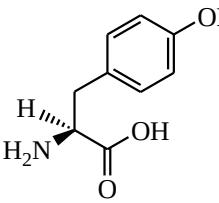	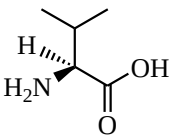
L-Threonine Thr T	L-Tryptophan Trp W	L-Tyrosine Tyr Y	L-Valine Val V

* Amino acids abbreviations follow the rules of the Comission on Biochemical Nomenclature of the IUPAC-IUB as specified in *Eur. J. Biochem.* **1984**; *138*, 9-37 and *Eur. J. Biochem.* **1993**; *213*, 2.

Annex II: protecting groups

Name	Abbreviation	Structure
2,2,4,6,7-Pentamethyl-dihydrobenzofurane-5-sulfonyl	Pbf	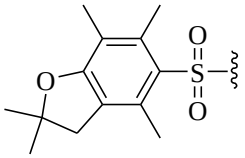
9-Fluorenylmethoxycarbonyl	Fmoc	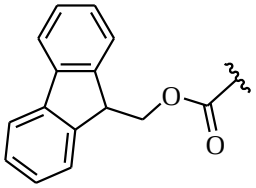
9-Fluorenylmethyl	Fm	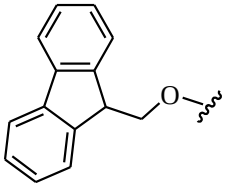
Acetyl	Ac	
Allyloxycarbonyl	Alloc	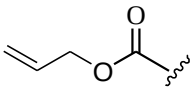
Benzyl	Bzl (Bn)	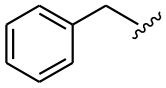
Benzyloxycarbonyl	Cbz (Z)	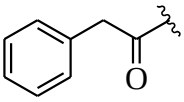
Tetrachlorophthaloyl	TCP	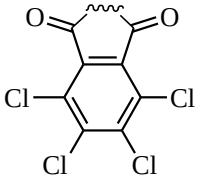
Tert-butoxycarbonyl	Boc	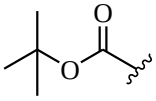
Tert-butyl	*t*Bu	
Trityl	Trt	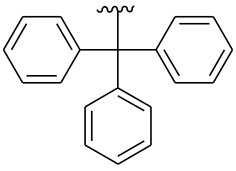

Annex III: coupling reagents and additives

Name	Abbreviation	Structure
N,*N*′-Diisopropylcarbodiimide	DIC	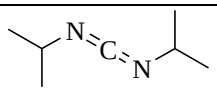
Diphenylphosphoryl azide	DPPA	
N-(3-Dimethylaminopropyl)-*N'*-ethylcarbodiimide hydrochloride	EDC	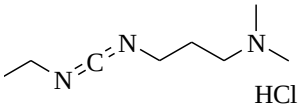
O-(7-Azabenzotriazol-1-yl)-N,N,N',N'-tetramethyluronium hexafluorophosphate	HATU	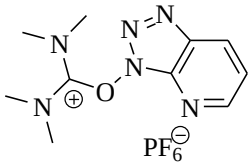
O-Benzotriazole-N,N,N',N'-tetramethyl-uronium-hexafluorophosphate	HBTU	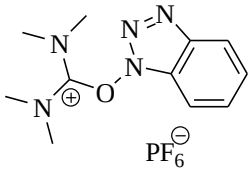
1-Hydroxy-7-azabenzotriazole	HOAt	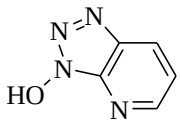
Hydroxybenzotriazole	HOBt	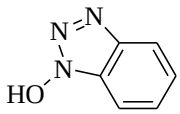
Propane phosphonic acid anhydride	PPAA	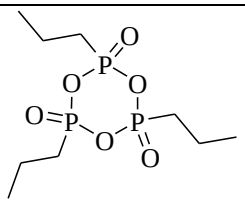
1H-benzotriazol-1-yloxytris (pyrrolidino)phosphonium hexafluorophosphate	PyBOP	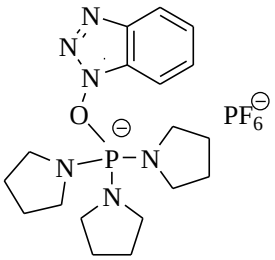
O-(Benzotriazol-1-yl)-*N,N,N′,N*′-tetramethyl-uronium tetrafluoroborate	TBTU	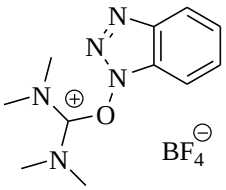

Annex IV: resins and linkers

Name	Structure
Aminomethyl-ChemMatrix-AB	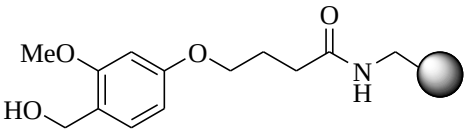
2-Chlorotrityl resin	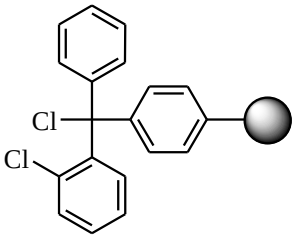
N-Cyclohexylcarbodiimide-*N*'-methyl polistirene	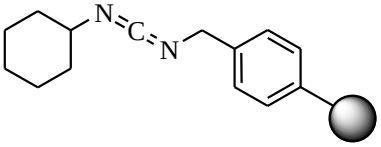
AB Fmoc-Rink linker	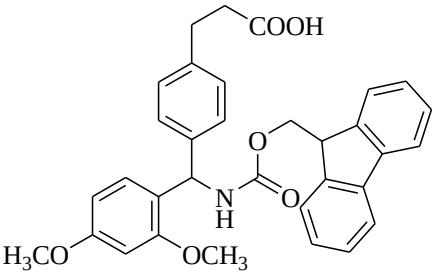

Nomenclature

The nomenclature used in this work to define the cyclic peptides was based on an innovative system propose by Spengler et al.[1] in which the *head-to-tail* cyclopeptides are represented in one-line text formulae using a three-letter symbols. According to this nomenclature system the '&' represents the start or the end of a chemical bond, thus the two '&' symbols placed at the beginning and end of the peptide sequence represent the amide bond between the *N*- and *C*-terminal amino acids. Indeed, otherwise than is required by this nomenclature, the amino acids were placed in the same order of the correspondent linear peptide.

The peptides with the same amino acids sequences were identify with the same product number. An alphabetic letter or a symbol (') were added to indicate a differentiation among the structures with the same amino acid residues but with a different stereochemistry, bearing or not protecting groups or synthesized using different methodology. Roman numerals were used to define the intermediates of the linear peptide synthesis in solution.

The cyclopeptides (except those conjugated with the glycosidic carrier) are identified with the same number of the corresponding linear peptide preceded by the prefix *cyclo*.

(1) Spengler, J.; Jimenez, J. C.; Burger, K.; Giralt, E.; Albericio, F. Abbreviated nomenclature for cyclic and branched homo- and hetero-detic peptides. *The journal of peptide research: official journal of the American Peptide Society* **2005**, *65*, 550-555.

Perspectives and objectives

Perspectives

Protein–protein interactions (PPIs) control the functions of living cells, such as signal transduction, cell cycle, proliferation and metabolism, representing a promising new class of attractive therapeutic targets for the development of future drugs.
The advancement in drug discovery efforts towards PPIs has been recently referred as 'the unmined biology gold reserve'.[1] Worldwide research efforts have driven recent pharmaceutical successes, and consequently, the emerging role of PPIs as drug targets has been widely recognized by the scientific community. Quantitative, functional and structural studies of PPI enable the understanding of these processes at the cellular and molecular levels and provide a basis for designing drugs that inhibit or stimulate PPIs.

The use of peptides to study PPIs introduces several substantial advantages over the small molecule drugs featured by their high affinity and specificity to interact with their targets together with their low toxicity profiles.[2] Nevertheless, the main shortcoming of using linear peptides for therapeutic purposes is their wide conformational range and short lifetime. The peptide cyclization is considered one of the best methods to improve the stability of peptides and to capture their bioactive conformations. Cyclization imposes conformational constraints on the peptides and, by stabilizing peptides, conveys higher binding affinity, selectivity and bioavailability and enables peptides to be used as lead compounds for drug design.

Peptides that modulate PPIs may be rationally developed based on a structural information of the binding site within a known protein that participates to the PPI,[3] or from the screening of peptide sequences that do not originate from natural proteins.[4]
In this contest, the *in silico* drug design has became a widely used computational method that helps to take rational decisions at the different steps of the drug discovery process. Indeed, the *in silico* approach is useful for the identification of a biomolecular target of therapeutic interest, but also for the selection or the design of new lead compounds and their modification to obtain better affinities, as well as pharmacokinetic and pharmacodynamic properties.
Once a tight binding potential peptide sequence is identified, the peptide can be modified to enhance stability, uptake and delivery. Typically, this could be achieved through the introduction of non-natural amino acids, additional constrains and moiety as vector or shuttle to promote the transport.
This modified peptide is a peptidomimetic, which has the properties of the peptide with respect to binding mechanism but also has higher stability and uptake potential than a natural peptide ligand.

Objectives

This thesis was developed on two distinct projects that share a common topic regarding the development of cyclic peptides as modulators of the protein-protein interactions with a potential therapeutic effect.

The first project, (Part **I**) mainly develop at the University of "Piemonte Orientale" under the supervision of Prof. Panza, was focused on the protein p50 NF-κB, member of the Rel/NF-κB family of transcription factors, which homodimerization was described as a pivotal determinant of polarized M2 inflammatory responses in TAM (Tumour Associated Macrophage) which promote the tumour progression.

In this context, it is becoming clear the involvement of p50 NF-κB in the defective NF-κB function in TAM. This defective function has been attributed to the overexpression of nuclear p50 and the consequent formation of p50 homo-dimers, responsible for the inhibition of the transcription of pro-inflammatory NF-κB-dependent genes.[5] This concept is also supported by the observation that TAM from p50 deficient mice, regained a pro-inflammatory (M1) phenotype associated with reduced tumour growth; which may be attributed to the restoration of a canonical NF-κB activity.
Therefore, the role of NF-κB in tumorigenesis and cancer therapy becomes increasingly evident and the inhibition of p50 homodimerization could represent an innovative method to modulate the TAM phenotype with a consequent therapeutic effect.

Over the years several strategies to therapeutically modulate NF-κB activation with different degree of specificity have been developed.[6,7] In the field of peptides, were reported cell-permeable peptides that contain the nuclear localizing sequence of p50 which inhibits nuclear translocation of p50-containing dimers by saturating the nuclear import machinery. The most commonly used peptide of this family is the SN50[8] which was demonstrated that not only acts on NF-κB signalling but also blocks nuclear translocation of a number of non-NF-κB transcription.[9]
Recently has been also develop a short peptide against the NF-κB p50 which seems to bind the NF-κB p50 subunit inhibiting the NF-κB activation and suppress the inflammation.[10]

In this context, the goal was to develop a class of cyclic peptides able to selectively interact with the homodimerization binding site of the p50 NF-κB protein preventing its homodimerization. The objectives of this thesis are listed below:

1. Development and synthesis of cyclic peptides and peptidomimetics with high structural analogy towards p50, able to modulate the interaction between two p50 subunits inhibiting the homodimerization process.

2. Tune, if possible, the chemical and conformational properties of the cyclopeptides in order to investigate their role in the PPIs and to increase the possibility to identify a lead compound with a good binding affinity with the target protein.

3. Explore the role of a sugar amino acid (SAAs) in the PPI and on the peptidomimetic properties.

4. Establish a suitable method for the effective cyclopeptides cellular transport by conjugation of peptides onto carrier to promote the drug delivery.

The second project (Part **II**) named "*Cancertec*", in which I was involved during my stage in Prof. Giralt's group at the Institute for Research in Biomedicine (IRB Barcelona), has, as main topic, the development of novel pharmacological compounds that would cross the blood-brain barrier (BBB) and target glioma. The two selected target PPIs are represented by EGF-EGFR and VEGF-VEGFR that are two of the most important cancer-enabling PPIs.

The overactivation of the EGF signaling pathway is associated with several human carcinomas and may cause uncontrolled cell growth. For this reason, in a clinical context, hEGF is a popular target for anti-cancer therapies because of its potent growth-stimulating effect on a variety of cancer cells that overexpress EGFR on the cell surface, including non-small cell lung cancer (NSCLC) cells.
On the other hand, VEGF is a major regulator of developmental and reproductive angiogenesis. VEGF is also an important mediator of blood vessel growth associated with cancer, rheumatoid arthritis and proliferative retinopathy. Inhibitors of VEGF-VEGFR interactions could be beneficial as therapeutics for diseases caused by dysfunctional angiogenesis (e.g., cancer).

The aim of the project was the development of cyclic peptides able to interact directly with EGF and VEGF blocking the interaction with their receptors. For the VEGF have already been reported short disulfide-constrained peptides that bind VEGF inhibiting its interaction with VEGFR;[11] for EGF, in the field of peptides, only inhibitors that interact with EGFR are known. Therefore, targeting the EGF molecule itself could represent a new way to prevent the binding of the growth factor to the receptor and, thus, inhibit EGFR activation and downstream events.
In this context, the task assigned was to develop a class of cyclic peptides able to interact with the EGF and/or VEGF preventing the interaction with their receptors.
Most part of these tasks became the objectives of this thesis work, which are listed below:

1. Development and synthesis of an explorative library of cyclic hexapeptides looking for anti-EGF and anti-VEGF binders.

2. Explore the protein-ligand interactions by spectroscopic or thermodynamic methods.

3. Investigation, by *in vitro* assays, of the ability of compounds to cross the blood-brain barrier.

4. Explore the effect of a BBB-shuttle on the transport of the cyclopeptides and on its activity.

References

(1) Mullard, A. Protein-protein interaction inhibitors get into the groove. *Nat. Rev. Drug Discov.* **2012**, *11*, 173-175.

(2) Jenssen, H.; Aspmo, S. I. Serum stability of peptides. *Methods Mol. Biol.* **2008**, *494*, 177-186.

(3) Eichler, J. Peptides as protein binding site mimetics. *Curr. Opin. Chem. Biol.* **2008**, *12*, 707-713.

(4) Hecht, I.; Rong, J.; Sampaio, A. L.; Hermesh, C.; Rutledge, C.; Shemesh, R.; Toporik, A.; Beiman, M.; Dassa, L.; Niv, H.; Cojocaru, G.; Zauberman, A.; Rotman, G.; Perretti, M.; Vinten-Johansen, J.; Cohen, Y. A novel peptide agonist of formyl-peptide receptor-like 1 (ALX) displays anti-inflammatory and cardioprotective effects. *J. Pharmacol. Exp. Ther.* **2009**, *328*, 426-434.

(5) Saccani, A.; Schioppa, T.; Porta, C.; Biswas, S. K.; Nebuloni, M.; Vago, L.; Bottazzi, B.; Colombo, M. P.; Mantovani, A.; Sica, A. p50 nuclear factor-kappaB overexpression in tumor-associated macrophages inhibits M1 inflammatory responses and antitumor resistance. *Cancer Res.* **2006**, *66*, 11432-11440.

(6) Karin, M.; Yamamoto, Y.; Wang, Q. M. The IKK NF-kappa B system: a treasure trove for drug development. *Nat. Rev. Drug Discov.* **2004**, *3*, 17-26.

(7) Gilmore, T. D.; Herscovitch, M. Inhibitors of NF-kappaB signaling: 785 and counting. *Oncogene* **2006**, *25*, 6887-6899.

(8) Boothby, M. Specificity of SN50 for NF-[kappa]B? *Nat Immunol* **2001**, *2*, 471-471.

(9) Lin, Y. Z.; Yao, S. Y.; Veach, R. A.; Torgerson, T. R.; Hawiger, J. Inhibition of nuclear translocation of transcription factor NF-kappa B by a synthetic peptide containing a cell membrane-permeable motif and nuclear localization sequence. *J. Biol. Chem.* **1995**, *270*, 14255-14258.

(10) Wang, Y. F.; Xu, X.; Fan, X.; Zhang, C.; Wei, Q.; Wang, X.; Guo, W.; Xing, W.; Yu, J.; Yan, J. L.; Liang, H. P. A cell-penetrating peptide suppresses inflammation by inhibiting NF-kappaB signaling. *Mol. Ther.* **2011**, *19*, 1849-1857.

(11) Fairbrother, W. J.; Christinger, H. W.; Cochran, A. G.; Fuh, G.; Keenan, C. J.; Quan, C.; Shriver, S. K.; Tom, J. Y. K.; Wells, J. A.; Cunningham, B. C. Novel Peptides Selected to Bind Vascular Endothelial Growth Factor Target the Receptor-Binding Site. *Biochemistry* **1998**, *37*, 17754-17764.

Part I

Development of p50 NF-κB homodimerization inhibitors

Chapter 1

Introduction

1.1. NF-κB: biological background

1.1.1. Recruitment of myeloid cells at the tumour site: monocyte-macrophages

A prominent component of solid tumours is represented by non-tumoural cells, including stromal cells (fibroblasts and endothelial cells) and leukocytes. In the late 1970s it was found that the tumor-associated macrophages (TAM) are the major leukocyte population present in tumors able to promote tumour growth and invasion.[1,2] The origin of TAM has been studied in terms of recruitment, survival and proliferation starting from the observation of leukocyte infiltrations into malignant tissues, which suggested that cancers arise at regions of chronic inflammation. TAMs derive from circulating monocytes and are recruited at the tumour site by a tumour-derived chemotactic factor for monocytes[3] identified as the chemokine CCL2/MCP-1.[4,5]

Among these, CCL2 is probably the most frequently found CC chemokine in tumours and its levels of expression correlate with the increased infiltration of macrophages.[2,6,7]

Along with the supposed pro-tumoural role of TAM, the local production of chemokines and the extent of TAM infiltration have been studied as prognostic factors.[8-10]

A variety of chemokines have been detected in neoplastic tissues as products of either tumour cells or stromal elements. These molecules play an important role in tumour progression by direct stimulation of neoplastic growth, promotion of inflammation and induction of angiogenesis.[11]

Macrophages are also recruited by molecules other than chemokines. In particular, tumour-derived cytokines interacting with tyrosine kinase receptors, such as vascular endothelial growth factor (VEGF) and macrophage colony stimulating factor (M-CSF), promoting macrophage recruitment, as well as macrophage survival and proliferation.[12,13]

1.1.1.1. Distinct properties of M1 and M2 macrophages

Macrophages are able to express distinct functional programs in response to different micro-environmental signals, in particular during pathological conditions such as infections and cancer.[14,15] This plays a central role in the activation of specific transcriptional program expressed by tumor-associated leukocytes, either mediating pro- or anti-tumor functions.[2,16]

Chronic infections can tightly regulate the immune responses, being able to trigger highly polarized type I or type II inflammation and immunity. Central to the development of type I or type II polarization is the specificity of the host–pathogen interaction.

Several studies on tumour–host interaction have highlighted the importance of inflammatory responses in the early steps of carcinogenesis,[17] as well as in established progressive tumours and are beginning now to identify the contribution of polarized inflammatory responses in cancer progression.

For a long period, classical or M1 macrophage activation was recognized as the unique activation program in response to microbial products and interferon-c. Recently it became clear that anti-inflammatory molecules, such as glucocorticoid hormones, IL-4, IL-13 and IL-10, are also able to induce distinct M2 activation programs.[2,18-20]

Classical or M1 macrophage activation is characterized by: high capacity to present antigen; high interleukin-12 (IL-12) and IL-23 production[21] and consequent activation of a

polarized type I response. Furthermore, M1 is associated with high production of toxic intermediates (nitric oxide (NO) and reactive oxygen intermediates (ROI)). Based on this, M1 macrophages are generally considered to be potent effector cells that kill micro-organisms and tumour cells and produce copious amounts of pro-inflammatory cytokines.
Type II macrophages (M2) tune inflammatory responses and adaptive Th1 immunity, scavenge debris, and promote angiogenesis, tissue remodeling and repair. Various signals cause different M2 activation forms that commonly share selected functional properties.[2,14,19,22,23]
Polarized macrophages differ also in terms of receptor expression, cytokine production and effector function chemokine repertoires.

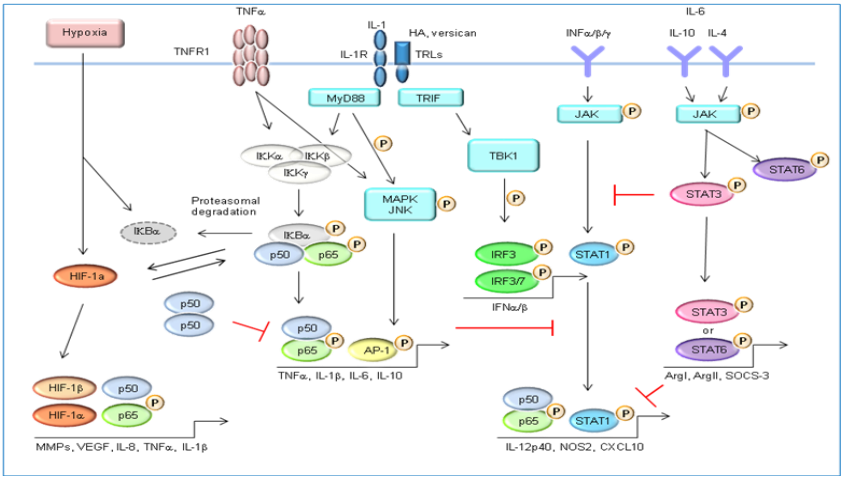

Figure 1. Signaling pathways regulating TAM phenotype and function. (Adapted from *Clinical Cancer Research*; **2010** *16*, 784-789.

Overall, evidence suggests that signals inducing M2 polarization down-regulate NF-κB and STAT1 activities, and thus act as a common mechanism to limit the induction of inflammatory chemokines associated with the development of type I immunity and inflammation. Defective NF-κB activation in TAM correlates with impaired expression of NF-κB-dependent inflammatory functions and cytokines (TNFα, IL-1, IL-12).[24] Restoration of NF-κB activity in TAM is therefore a potential strategy to restore M1 inflammation and intra-tumoural cytotoxicity. It became clear that differential involvement of NF-κB driven inflammation in early step of carcinogenesis as compared with advanced neoplasia, where the established tumour micro-environment would guide TAM functions toward an M2 suppressive and tumour-promoting phenotype.

Recent evidence suggests that homodimers of the p50 subunit of NF-κB (a negative regulator of the NF-κB pathway) are responsible for the slow activation of NF-κB in TAMs and for the pro-tumor phenotype of these cells.[25] It seems that NF-κB functions can be tuned to different levels, a property that enables the extent of inflammation to be regulated. Such regulation allows to the vigorous inflammation that predisposes individuals towards developing cancer to be sustained, and enables TAMs to support the smouldering inflammatory microenvironment present in established metastatic neoplasia.

By investigation the molecular basis which drives M2 polarization of TAM, it has been demonstrated that these cells are characterized by massive nuclear localization of the

inhibitory p50 NF-κB homodimer. Strikingly, in p50 deficient tumor-bearing mice TAMs express cytokines characteristic of M1 inflammation and splenocytes produce Th1 cytokines, an immune profile associated with tumor growth inhibition *in vivo*.[25] Thus p50 NF-κB nuclear accumulation appears to promote persistent M2-inflammation associated with tumour progression.[26] The massive accumulation of p50 NF-κB in LPS-tolerant macrophages is parallel by their expression of an M2-associated profile suggesting that p50 NF-κB is a pivotal determinant of polarized M2 inflammatory responses. Preliminary results have also confirmed a similar activity of p50 NF-κB in myeloid-derived suppressor cells (MDSC), in terms of both functional M2-polarization and suppressive activity, further indicating that targeting this molecule in the myelomonocytic compartment may restore M1 inflammation and anticancer activity in vivo.

1.1.2. Dimeric transcription factors: Rel/NF-κB family

Nuclear factor-κB (NF-κB) has been shown as an important regulator of TAM transcriptional programs. NF-κB is a generic term for a family of transcription factors that play pivotal roles in inflammation and immunity. In particular, the Rel/NF-κB family of dimeric transcription factors is involved in a wide array of cellular activities, such as cellular immune responses, growth, development and apoptosis.[27,28] In mammals, these dimers arise from the combinatorial association of five polypeptides; RelA (p65), RelB, c-Rel, NF-κB1 (p105/p50), NF-κB2 (p100/p52).[29]

Rel/NF-kB polypeptides share a homologous amino-terminal region composed of approximately 300 amino acid residues; this homologous portion, known as the rel homology region (RHR), contains the amino acid sequences responsible for DNA binding, subunit dimerization, nuclear localization and for the interaction with the cytosolic inhibitor κB molecule (IκB).[30-32]

Primary sequence comparison of the Rel/NF-κB polypeptides shows 38% amino acid identity and more than 75% homology across the family.

The crystal structures of the DNA-bound p50, p52, and p65 RHR homodimers and the p50-p65 heterodimer [33-37] show that the RHR can be divided into three sub-regions: i) the large *N*-terminal region, contains approximately 200 amino acid residues folded into an immunoglobulin (Ig)-like domain, which is the major contributor of DNA-contacting amino acids. ii) The central region, also an Ig-like domain, consists of approximately 100 amino acids, responsible for subunit association and iii) the short carboxyl-terminal region harbors a nuclear translocation signal. This last segment containing the 14 amino acids of the nuclear localization sequence (NLS), does not display a folded structure[38,39] and its last four amino acids are known to interact with the NF-κB inhibitor protein IκB.[30]

1.1.2.1. Canonical and non-canonical pathway

The NF-κB subunits fall into two categories, named class 1 and class 2. Class 1 includes the p50 and p52 subunits, they are encoded by the genes nfκb1 and nfκb2 and synthesized as precursor proteins p105 and p100 respectively. Class 2 subunits include RelA, RelB and c-Rel, encoded by the genes rela, relb and c-rel and are synthesized in an active form. All subunits contain the *N*-terminal Rel homology domain (RHD) but only the class 2 subunits

have a transactivation domain (TAD) allowing for direct control of transcription.[40]
In resting cells, NF-κB/Rel dimers are bound to IκBs and retained in an inactive form in the cytoplasm.[41,42] Like NF-κB, IκBs are also members of a multigene family containing seven known mammalian members including IκBα, IκBβ, IκBγ , IκBε, bcl-3, the precursor Rel-proteins p100 and p105.[43,44] The IκB family is characterized by the presence of multiple copies of ankyrin repeats, which are protein-protein interaction motifs that interact with NF-κB *via* the RHD.[45-47] Upon appropriate stimulation, IκB is phosphorylated mainly by the IκB kinases (IKKs), polyubiquitinated and degraded by the 26S proteasome.[48,49]
Close to the *C*-terminal end of the RHD lies the Nuclear Localization Signal (NLS) which is essential for the transport of active NF-κB complex into the nucleus. The RHD contains a phosphorylation site for Protein Kinase A, the phosphorylation of this site has been described to be essential for nuclear localization of NF-κB.[50] Consequently, NF-κB is released and is translocated into the nucleus to bind to the target DNA and initiate gene expression.[51,52]

Activation of NF-κB occurs through canonical and non-canonical pathways.
The canonical pathway is triggered by microbial products and proinflammatory cytokines, such as tumor necrosis factor α (TNFα), IL-1β, and most commonly leads to the activation of RelA-p50 complexes. The alternative pathway[53] is activated by lymphotoxin β (LTβ),[54] CD40 ligand (CD40L),[53] B-cell activating factor (BAFF)[55] and RANK ligand (RANKL)[56] and results in activation of RelB-p52. NF-κB proteins are usually held inactive in the cytoplasm of resting cells by association with inhibitor of NF-κB (IκB) proteins which upon stimulation are phosphorylated by IκB kinase complex (IKK). IKK consists of two active kinase subunits: IKKα (IKK1) and IKKβ (IKK2), and a regulatory subunit IKKγ (NEMO). The canonical pathway for NF-κB activation requires IKKβ-mediated IκBα phosphorylation, whereas the alternative pathway is regulated by IKKα-mediated phosphorylation and processing of p100.[40,41]

Each subunit has distinct biological functions and with 12 known dimeric combinations binding DNA the range of NF-κB functions is diverse.[57]

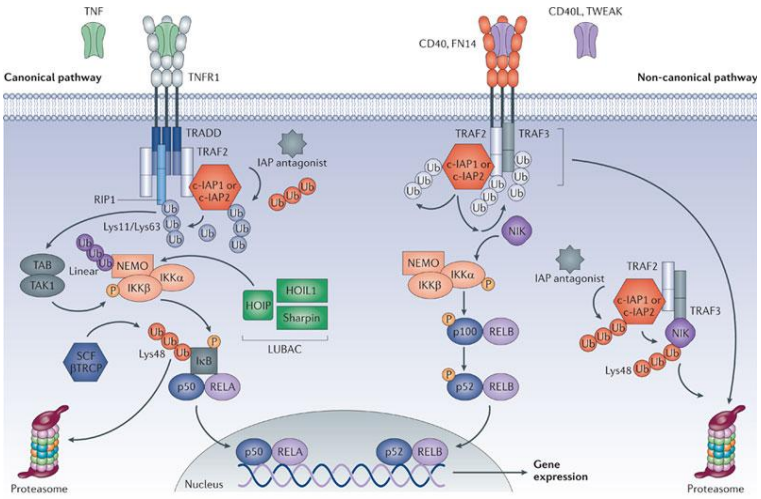

Figure 2. Canonical and non-canonical NF-κB signalling pathways.(Adapted from *Nature* Reviews *Drug Discovery*. **2012**, *11*, 109-124).[58]

1.1.2.2. Rel/NF-κB polypeptides dimerization

The five mammalian Rel/NF-κB polypeptides dimerize to form, in principle, 15 unique homo- and heterodimers but experimental evidences suggest that Rel/NF-κB family transcription factors exhibit variable preferences for dimer formation, because p50-p65 heterodimer and p50 homodimer have been identified as the most prevalent NF-κB dimers in various tissues.[32]
The crystal structures of the dimerization domains of p50, p52, and p65[33,34,38,39,59] illustrate how the dimer interfaces are created by two symmetrical beta sandwich domains which pack against one another. The structures reveal that a set of 14 amino acid residues from each monomer is primarily responsible for mediating dimer formation.[38] Two of these residues participate only through their backbone, whereas the side-chains of the other 12 residues form the dimer interface. Of these 12 seemingly critical dimer-forming residues, seven are identical throughout the Rel/NF-κB family and the other five are homologous. These residues appear to mediate similar protein-protein interactions for the various subunit associations within the NF-κB family. Selective dimerization of these family members plays a central role in the regulation of transcription for specific Rel/NF-κB-dependent genes.[60]

The diversity provided by dimerization between the different members of the Rel/NF-κB family regulates NF-κB signaling at two levels. First, it enhances the repertoire of DNA sequences that are regulated by these dimers. Each of the Rel/NF-κB dimers has distinct DNA binding affinity, which determines the fate of transactivation potentials, as the dimers have differential transcriptional activities. Second, specific Rel/NF-κB dimers display preferential affinity for members of the inhibitor protein family (IκB)[60] thus, preferential sequestration of Rel/NF-κB dimers in the cytoplasm by IκB proteins blocks early activation of the NF-κB regulated genes.

1.1.2.3. The p50 dimer interface[61]

The dimer interface of p50 is comprised of roughly 40 contacts between the two monomers. Approximately 62% of the total buried surface area of the p50dd dimer is hydrophobic; the other 38% is composes of seven hydrogen bonds and four salt bridges.
A total of 14 amino acids are involved in formation of the p50dd dimer interface and 1471 $Å^2$ solvent-accessible surface area are buried in the dimerization process. Based on their role in forming the interface, these residues can be divided into three classes: i) residues involved in Van der Waals interactions (Val251, Met253, Leu269, Phe307, Ala308, and Val310), ii) residues involved in both Van der Waals interactions and polar contacts (Arg252, Asp254, Tyr267, Cys270, Asp302, His304, and Arg305) and residue that makes only polar contacts (Glu265). Moreover, the side chains of Met253 and Cys270 are oriented in the opposite direction to the interface and thus contribute to dimer formation only through their backbone carbonyl oxygen atoms.
The effects of alanine substitutions reveal that four residues (Y267, V310, L269, and D302) are the most critical for stabilizing the p50 dimer interface and define the hot-spot of binding energy. Among these, Y267 is by far the most critical determinant for the stability of the p50 homodimer, because Y267 contacts six different residues emanating from the

opposing subunit, making a total of three hydrogen bonds and a number of Van der Waals contacts in each subunit (six total H-bonds). Therefore, mutation of this residue to alanine reduces sensibly the stability of the interface.

The K_d for p50 homodimer is in the order of 10^{-6} M^{-1}, which reveals that the dimerization affinity for p50 is relatively low considering the extensive buried surface area upon p50 dimer formation.[62]

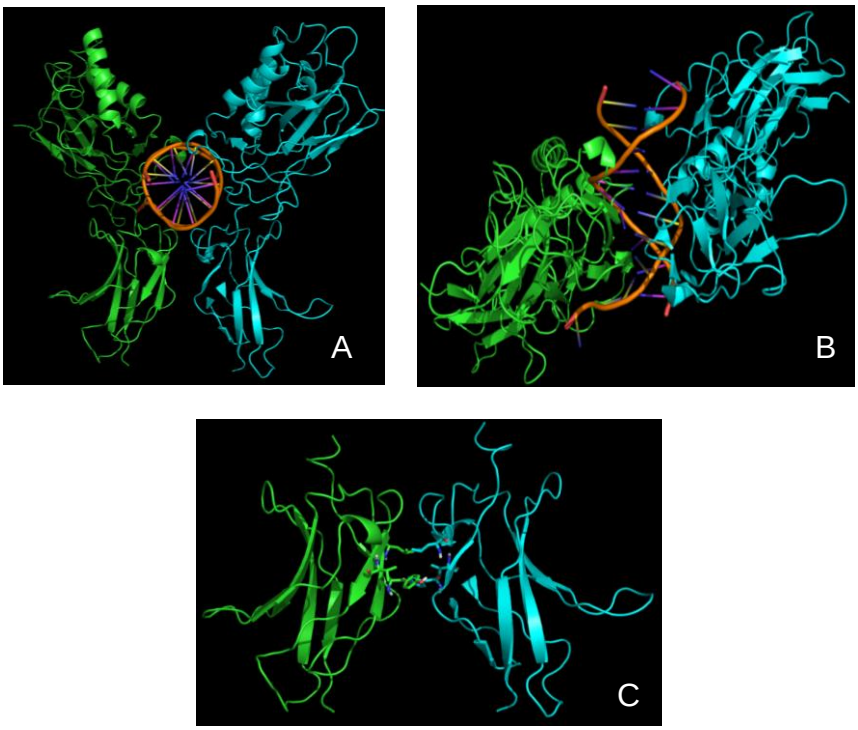

Figure 3. (A) Overall view of p50 NF-κB dimer bound to DNA. Depicted are residues 39 to 350 of both subunits and the central 11pb of DNA. The color coding is green and light blue for the two p50 subunits and orange-violet for the DNA. (B) View perpendicular to the direction of the DNA. (C) The ribbon diagram for the p50 homodimerization region and the main residues involved in the interaction Y267, L269 and V310. These figures were produced using PyMOL.

1.1.3. TAM as targets in cancer therapy

Given the strong association between macrophages and cancer progression TAM have emerged as a promising target in the battle against cancer, based on the concept to restore the antitumor activity of TAM and fight the cancer from within. NF-κB activation in macrophages has been shown to contribute to carcinogenesis in several models of inflammation-associated cancer.[63-65] Nowadays, several existing anticancer agents, such as paclitaxel, have been proposed to act at least in part to inhibit TAM recruitment or function.[66-68] Interestingly, most of these agents activate TAM to produce pro-inflammatory mediators by activating NF-κB. However, as with all current anticancer treatments, due to a lack of specificity, there are serious side effects associated with these agents.[69] Conversely, strategies to target NF-κB activation in TAM are also likely to show success on the basis of evidence from experimental models,[64,70] indeed targeting NF-κB activation in both malignant cells and TAM may be of added benefit due to the role of NF-κB in malignant cell survival.[64,71]

Systemically targeting NF-κB may also have adverse effects given its fundamental role in innate immunity,[55] but specific targeting of NF-κB in macrophages has been shown to

increase immunity to infection associated with activation of M1 macrophages,[72] again suggesting the specific targeting of NF-κB in TAM would avoid these adverse effects.

1.1.3.1. NF-kB inhibition approach

Most NF-κB inhibitors developed to date inhibit either NF-κB protein activation or IκB phosphorylation and degradation, thus preventing the release of free NF-κB and its entry into the nucleus. Another approach that directly inhibits NF-κB DNA binding, by interfering with the DNA binding of NF-κB to the promoter of targeted genes, also appears amenable to designing specific inhibitors. However, only a limited number of agents have been developed based on this approach.[73]

Despite a variety of agents exhibit various degrees of effectiveness in suppressing NF-κB signaling, few of these compounds are specific, and some side effects have been reported. For example, glucocorticoids, which are considered as the most powerful nonspecific inhibitors of NF-κB, resulted in reduced bone formation and suppression of hypothalamic–pituitary–adrenal axis function.[74,75]

NF-κB activation or function can be inhibited by more specific means. For example, the NF-κB essential modifier (NEMO)-binding domain peptide inhibits p65 phosphorylation, and the SN50 peptide inhibits NF-κB nuclear transport.[76-78] Among various strategies aimed at inhibiting NF-κB activation, blocking the binding of the p65 or p50 subunit with the κB site may be more specific[17,79] because a higher degree of specificity may be achieved by the inhibition of NF-κB–mediated transcription.

In this regard, recently it has been reported a study in which a linear pentapeptide AIP6 (RLRWR) was developed mimicking the DNA-binding motif in p50. AIP6 is able to selectively bind with κB elements and prevents the binding of active NF-κB complexes. This peptide (AIP6) seems to interact directly with p65 to inhibit the DNA-binding, the transcriptional activities of NF-κB and the production of inflammatory mediators *in vitro*.[80] This inhibitory effect of AIP6 on NF-κB appeared specific and did not involve IκB degradation, IkBα phosphorylation, or p65 nuclear import. The observation that the local administration of AIP6 inhibit inflammatory responses induced by zymosan in the joints and soft tissues in mice[81] suggest that AIP inhibits inflammation by binding the NF-κB p50 subunit resulting in the inhibition of NF-κB activation.

1.2. Protein–protein interactions as emerging therapeutic targets

Protein–protein interactions (PPIs) control the function of living cells, such as signal transduction, cell cycle, proliferation and metabolism and, for this reason, represent a promising new class of attractive therapeutic targets. Quantitative, functional and structural studies of PPI enable the understanding of these processes at the cellular and molecular levels and provide a basis for designing drugs that inhibit or stimulate PPIs. Disruption of PPIs is a viable strategy for example in the treatment of many types of cancer, age-related macular degeneration (AMD), and also in diseases that are the result of protein misfolding and aggregation, for example Alzheimer's disease, Duchenne muscular dystrophy and Huntington's disease.

However, PPIs are still considered as extremely difficult for targeting by small-molecules due to the structural characteristics of the interface.[82] The inter-protein surfaces are generally large (approximately 1500–3000 Å), flat and lack distinguishing features,[83] making the design of small molecule antagonists a difficult task.[84,85] Thereby, successes in drug discovery developments against PPI targets face two major issues, i.e. predictability of the chemical space dedicated to these interaction interfaces and druggability of each potential new PPI target identified in a biological program. Even so, recent successes in the inhibition of PPI with small molecules and peptidomimetics have emerged as a new way to modulate the activity of proteins and generate new drugs against this huge reservoir of potential targets. Small peptide or peptidomimetic ligands have been developed, often to facilitate interaction with hydrophobic α-helix, β-turn, or β-sheet binding channels or clefts.[86]

1.2.1. Peptides to modulate PPI and their use as therapeutic agents

Peptides are often used as ligands for recognition of protein surfaces[50,51] representing one of the main sources for small molecule inhibitors of PPIs, leading to a successful development of small-molecule modulators for some of the most clinically important PPI.[87-91]

Peptides that modulate PPIs may be rationally developed based on a binding site within a known protein that participates in a certain PPI,[92] or from the screening of peptide sequences that do not originate from natural proteins.[93]

The main shortcoming of using linear peptides for therapeutic purposes is their wide conformational range and short lifetime, a reason why many peptide drugs with exciting pharmacological activities *in vitro* have proven to be ineffective *in vivo*.

The short half life is primarily due to its fast renal clearance, connected to its hydrophilic property and small size, and its poor metabolic stability and biodegradability as a result of enzymatic degradation by proteolytic enzymes (proteases and peptidases) of the blood, liver, and kidney. Hence different strategies for targeted modifications of peptide drugs in order to prolong their plasma half lives are highly demanded to improve drugs' pharmacokinetic profiles.[94,95]

The peptide cyclization is considered one of the best methods to improve the stability of peptides[96] and to capture their bioactive conformations. By stabilizing peptides and imposing conformational constraints, cyclization conveys higher binding affinity, selectivity and bioavailability and enables peptides to be used as lead compounds for drug design.

In addition, there are many different conformational restrictions to increase the affinity and the selectivity towards the target, for instance, compounds that mimic *β-turn* motif can promote additionally intra-molecular hydrogen bond formation which will increase the rigidity of the molecule. The introduction of *N*-methyl amino acids along the backbone of the peptide may have an impact in different preferred conformations. *N*-methylation or introduction of proline increases the formation of *cis*-peptide bonds which has a relevant effect on the backbone conformation of cyclic peptides. Then the cyclic peptide conformation depends on the steric interaction between the introduced *N*-methyl group and the carbonyl oxygen and/or the alpha-substitution of the constituent amino acids, and not by the functionality of the side chains. Then by varying the specific points of *N*-methylation in

the backbone we can fine-tune the selectivity of the peptide for a specific protein target. The advantage of *N*-methylation in front of the incorporation of proline is the addition of more functional groups into the bioactive compound.
Moreover, protease resistance can be conferred by substituting the natural amino acids by unnatural amino acids (D-), *N*-methyl-alpha-amino acids, or beta-amino acids. The amide bond between two amino acids may be replaced, the *N*- or *C*-termini may be blocked and carbohydrate chains can be added.

Peptide cyclization approach evolved both in nature[97-99] and in synthetic work. In nature, there are several cyclic and bicyclic peptides which have presumably evolved to confer stability and binding advantages to these complex structures over the linear peptides. Moreover, many natural peptides display two or more disulfide bridges, which enhance the stability of these compounds owing to the reduction of their sensitivity to proteolytic cleavage.[100] The common feature of all of them is the imposed rigidity.

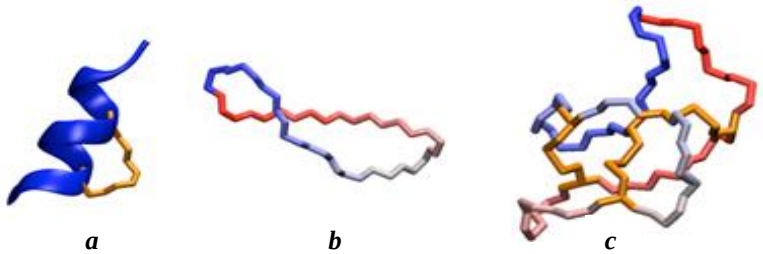

Figure 4. Some examples of constrained peptides. **a**) Cyclotide with three disulfide bridges shown in gold. **b**) Cyclic beta-hairpin. **c**) Stapled peptide with the so-called staple, or hydrocarbon link shown in gold.

Today, there are more than 50 peptide drugs that have been approved for clinical use and the increasing number of peptides entering clinical trials now supports the notion that peptide drugs have a long and secure future.[101] The targeted therapeutic areas of these peptides include, but are not limited to oncology, metabolic, cardiovascular and infectious diseases, all of which represent important markets.[102]
Currently, most of the peptide drugs are peptide hormones (such as insulin) or peptides that mimic hormones.[103] However, the number of peptide drugs that act as enzyme inhibitors[104] or as antimicrobial peptides[105] is increasing.

1.3. Peptide delivery

An important limitation in the use of peptides as drug candidates is their poor uptake and low ability to cross biological barriers,[95] thus different peptide carriers or delivery systems have been proposed to address this problem.
For peptides which target membrane receptors, delivery to the target sites may be made possible with the application of liposomes or nano- and micro-particles which also enhance the local availability of peptides, protecting them from proteolytic action. These particles effected bioadhesion (residence time and absorption), biodegradability (release kinetics), and biocompatibility.
Thanks to the nanotechnological advances applicable to peptide delivery,[106-108] are receiving increasing attention sustained delivery systems based on biodegradable polymers from renewable resources (e.g. chitosan and its derivatives) or derived from petroleum resources (e.g. PLGA (poly-lactic-coglycolic acid) or PGA (polyglycolide)).

Peptide-based strategies offer considerable advantages over other delivery systems. Peptides are not immunogenic molecules and they allow rapid delivery of cargoes, such as proteins, other peptides or nucleic acids, into cells. Furthermore, they are stable in physiological buffers and are usually not highly toxic.
In this field, cell penetrating peptides (CPPs)[109] is a novel approach to deliver drug molecules which involves the use of peptides to facilitate uptake of the cargo. Indeed, it was discovered that short peptides derived from protein-transduction domains can be internalized in most cell types and, more importantly, allow the cellular delivery of conjugated (or fused) biomolecules.[110,111]
The interest for CPPs is mainly due to their low cytotoxicity and to the fact that there is no limitation for the type of cargo. Although CPPs have been used to improve delivery of cargo that varies greatly in size and nature (small molecules, oligonucleotide, plasmid DNA, peptide, protein, nanoparticle, lipid-based formulation, virus, quantum dots) most of the applications describe the delivery of oligopeptide/protein and nucleic acids or analogs.

Always in the field of peptides, BBB shuttles represent another class of transporter with a peptidic nature that have demonstrated to be able to overcome the blood-brain barrier and carry therapeutic compounds that cannot cross unaided.[112]

1.4. Peptide synthesis

In 1901, Emil Fischer initiated peptide chemistry by the synthesis of the dipeptide glycylglycine, obtained by hydrolysis of the diketopiperazine of glycine. This is the first reported synthesis of a dipeptide and is also the first instance of the term “peptide” used to refer to a polymer of amino acids.[113]
However, already twenty years ago, Theodor Curtius synthesized the first *N*-protected dipeptide, benzoylglycylglycine, by treating the silver salt of glycine with benzoyl chloride.[114] Furthermore in 1904, he developed the first practical method for peptide synthesis, the azide coupling procedure, which enabled the synthesis of benzoylglycine peptides of various length.[115] In addition, only one year later, Emil Fischer presented a new method for the synthesis of peptides via acylchlorides, prepared from the corresponding free amino acid using PCl_5 in acetyl chloride as solvent.[116]
After these first simple examples, the research in the field of peptide synthesis has undergone prodigious advances leading to the development of innovative and efficient methodologies that allow the preparation of complex molecules as well as proteins.

1.4.1. From solution to solid-phase peptide synthesis

The solution-phase peptide synthesis (SPS) method was based on the coupling of peptide fragments or a single amino acid in solution. It offers many inherent benefits: in principle, the whole repertoire of organic reactions can be employed; reactions can be monitored in real time using conventional techniques (TLC, NMR, LC-MS); the product is characterized after each coupling and no additional steps are required to attach and cleave substrates from the solid support. On the other hand, this approach imply a purification step after each coupling which is time consuming and can associate with product losses.

Solid-phase peptide synthesis (SPPS) was introduce for the first time in 1963 when Bruce

Merrifield published a historic paper describing the principles and the applications of his invention.[117] In contrast to the solution-phase methodology, the growing peptide in the solid-phase approach is linked to an insoluble support and therefore, after each reaction step, the byproducts are simply removed by filtration and washing. Moreover the solid-phase synthesis offers the ability to use excess quantities of reagents to drive reactions to completion. Furthermore, because of the repetitive nature of peptide synthesis (deprotection, washing, coupling, washing, deprotection), the use of an insoluble support in a single reaction vessel allows the automatization of the processes. The mechanization of the SPPS process permits, in a fully automatic manner, the incorporation of more than 10 amino acid residues per day and for this reason this techniques have been considered the method of choice for the production of chemical libraries.

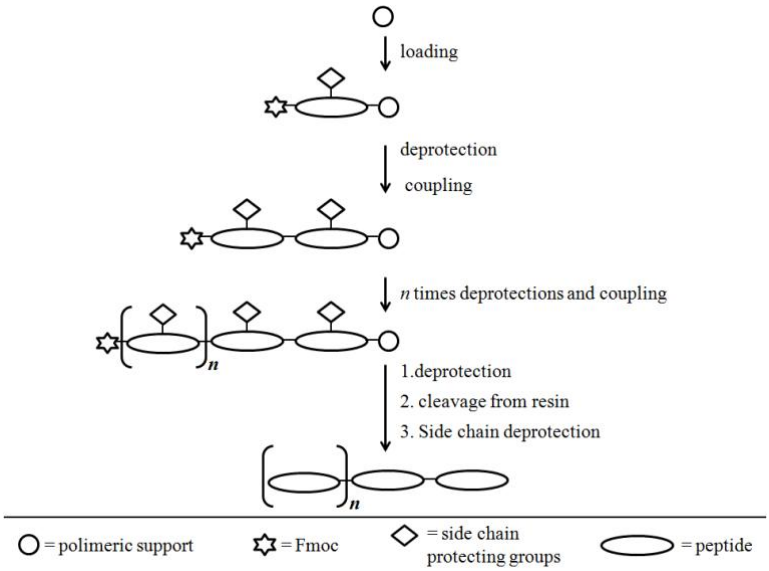

Scheme 1. Schematic principle of solid-phase peptide synthesis.

Generally, peptide synthesis is based on the appropriate combination of protecting groups and an efficient method for the activation of the carboxyl group prior to reaction with the amino terminal. Protecting groups have to prevent on one hand bond formation between two incoming amino acids (*N*-terminal protecting group), and on the other hand formations between the incoming amino acids and side chain functionalities (side chain protecting groups). In the Merrifield synthesis, the *C*-terminal is protected by the polymeric carrier.

Mainly, two protection schemes have been developed for the Merrifield synthesis. The first one is the *tert*-butoxycarbonyl (Boc)/benzyl (Bzl) strategy, which depends on the different acid lability of the *N*-terminal protecting group (Boc) and the side-chain protecting group (Bzl) as described in the original publication of Merrifield.[117] The main drawback of this strategy is the use of hydrogen fluoride (HF) for the final cleavage and deprotection of the peptide. This procedure leads to various side reactions, such as Friedel-Crafts reactions between aromatic groups of the resin and the side chains of the peptide, and/or promotion of a N→O acyl shift involving the side-chain groups of serine and threonine.

The second protection strategy was developed by Carpino and Han[118] and is based on the use of the base labile 9-fluorenylmethyloxycarbonyl (Fmoc) group for the protection of α–amino groups. This approach allows the orthogonal protection of side-chain functions with acid labile protecting groups.

1.4.1.1. Solid support

The first solid support used in solid-phase peptide synthesis was a styrene-divinylbenzene co-polymer, functionalized by chlorination of benzyl groups. The benzyl chloride was then be used to anchor the *C*-terminal amino acid via an ester linkage to the solid support. Thus, when the product of the SPPS was cleaved from the solid support a carboxylic acid was obtained at the *C*-terminal. Later on, a broad variety of resins were developed leading to different functionalities at the *C*-terminal such as acids (Wang resin, 2-Chlorotrityl resin), amide (Rink amide (RAM), 4-methylbenzhydrylamine (MBHA) resin), thioesters (4-sulfamylbutyryl resin), or alcohols (4-hydroxymethylbenzoic acid (HMBA) resin).
Among this solid support 2-Chlorotrityl chloride (Cl-Trt) resin is one of the most useful resins for the solid-phase synthesis of *C*-terminal acid peptides[119-122] which can be used for the preparation of both protected and unprotected peptides. Cl-Trt resin offers many advantages because, allows the release of the peptide under mild acidic conditions (1% Trifluoroacetic Acid (TFA), 10% Hexafluoro-2-Propanol (HFIP)),[84] it reduces the formation of diketopiperazine (DKP),[85] minimizes the racemization during the incorporation of the first amino acid; and it allows the incorporation of partially protected amino acids through the side chain or the amino function.

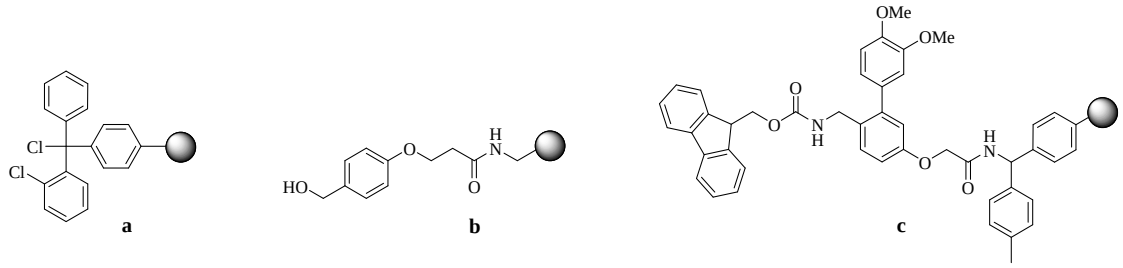

Figure 5. Some examples of solid support resins: **a**) 2-Chlorotrityl resin, **b**) Aminomethyl ChemMatrix-AB, **c**) Fmoc-Rink amide *p*-MBHA resin.

1.4.1.2. Amide bond formation and condensing agent development

The formation of the amide bond is a key step in the synthesis of any peptide; this step occurs through the activation of a carboxylic acid group which is carried out with different condensing agents, additives and active species.[123]
Carboxylic acids are generally activated either by carbodiimides, formation of symmetrical anhydrides (anhydride formed from equivalent of the same amino acid), or formation of active esters. Since low yields, racemization, or degradation often accompany amide formation, coupling procedures are optimized not only to provide high yields, but also to prevent the racemization. To this purpose numerous coupling reagents have been developed and become commercially available.[124]

In solution-phase peptide synthesis, racemization is encountered upon activation of the acid (**i** – **iii**), which might lead to the formation of an oxazolone (**iv**). Under mild basic conditions, the oxazolone is deprotonated into a conjugated anionic intermediate (**v**). Since reprotonation occurs not enantioselectively, racemates of oxazolones are obtained (**vi** and **viii**). Because both react with the amino terminal of the growing peptide chains, chirality gets lost leading to a DL- (**vii**) and a LL-peptide (**ix**) (Scheme **2**).

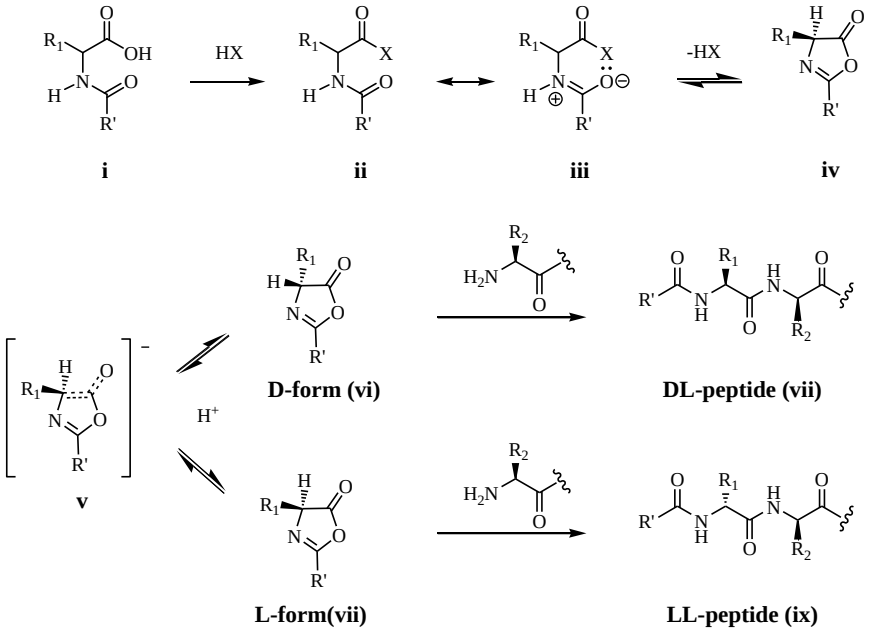

Scheme 2. Racemization via oxazolone mechanism. R_1, R_2: side chain residues.

In SPPS, this mechanism is prevented due to the fact that peptides are grown at the *N*-terminus and Nα-protected amino acids are used. Nevertheless, racemization might also occur due to a reversible proton exchange on the Cα-atom forming the carbanion as observed with activated cysteine or histidine residues.[125,126] Similar to the oxazolone mechanism, reattachment of the proton is able to occur from both sides leading again to a racemic mixture. Activation of the carboxylic acid allows to overcome the thermodynamic restrictions of the peptide bond formation as already mentioned above.

1.4.1.2.1. Carbodiimides

Carbodiimides rank as one of the most important classes of reagents in organic synthesis due to their accessibility, versatile chemical properties, and utility as *in situ* activating reagents in coupling reactions.[127,128]

The most widely used carbodiimide is dicyclohexylcarbodiimide (DCC), which serves as a versatile coupling agent in the preparation of amides, esters and anhydrides.[129] The mechanism of the reaction[130] is depicted in Scheme **3**.

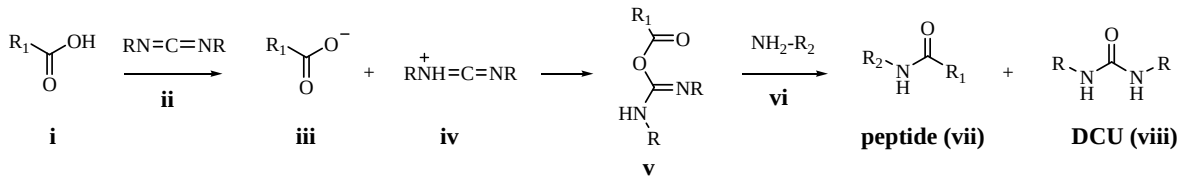

Scheme 3. Peptide coupling via carbodiimide. R: cyclohexyl residue. R_1: carboxy moiety; R_2: amino moiety.

The anion of the carboxylate (**iii**) is added to the protonated carbodiimide (**iv**) forming the highly reactive *O*-acyl-isourea (**v**), which further reacts with amine **vi** to form amide **vii** and dicyclohexylurea (DCU, **viii**) as a byproduct.

The carbodiimide activation method has, however, a high propensity for racemization because of the high reactivity of the *O*-acyl-isourea, which can lead, through intramolecular

cyclization, to the formation of an oxazolone; this cyclic intermediate can easily racemize via an aromatic intermediate.

Moreover, complete removal of the dicyclohexylurea (DCU) byproduct is difficult because of its low solubility and usually necessitates additional cumbersome purifications. This limitation has prompted the development of an array of surrogate DCC coupling reagents including water-soluble carbodiimide derivatives such as diisopropylcarbodiimide (DIC)[131] and EDC (1-ethyl-3-(3-dimethylaminopropyl)-carbodiimide hydrochloride) which form more soluble products.[132]

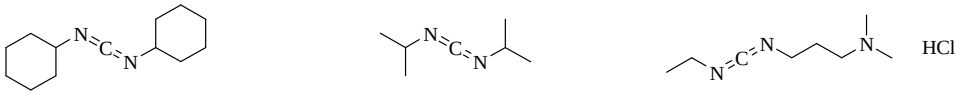

DCC **DIC** **EDC**

Figure 6. Commonly used carbodiimides.

In addition, in the contest of the solution phase synthesis assisted by solid-phase reagents[133-137] polymer-bound carbodiimides have been developed, such as polystyrene isopropylcarbodiimie as viable replacement for DCC.[138-142]

The use of polymer-supported reagents is emerging as a leading strategy that combines the advantages of product isolation and purification of solid-phase chemistry with the benefits of traditional solution-phase reactions.[143] Despite this, only a few polymer-supported coupling reagents are available; in particular, DCC,[127] DIC[138] and EDC[142] have been successfully immobilised and applied to the synthesis of amides.[144] However, these carbodiimides maintain the same drawbacks as their solution-phase equivalents, particularly in terms of epimerization in the absence of an additive.

1.4.1.2.2. Use of additives

In order to reduce the epimerisation level when using carbodiimides as coupling reagents, has been proposed to add a nucleophile which reacting faster than the competing acyl transfer generates an intermediate still active enough to couple with the amine and also prevents the side reactions. In this field HOBt (1-Hydroxybenzotriazole) has been introduced as the first additive,[145,146] showing that, when it is used, yields were higher and epimerisation levels lower.

HOBt is believed to work by initially reacting with the *O*-acylurea to give the OBt active ester (**ii**), which enhances the reactivity of the activated ester.[147]

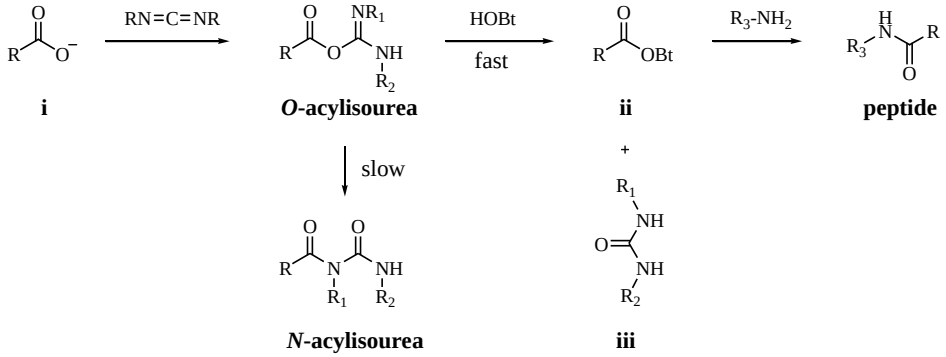

i ***O*-acylisourea** **ii** **peptide**

***N*-acylisourea** **iii**

Scheme 4. Schematic representation of the amide bond formation using HOBt as additive to minimize the formation of unreactive *N*-acylurea.

The successful active ester method has been extensively studied[148] and is nowadays the most widely used approach in solid-phase peptide synthesis. The amino group of R_3NH_2 (**i**) nucleophilicly attacks the carboxyl carbon of **ii** leading to the tetrahedral intermediate **iii** (Scheme **5**).

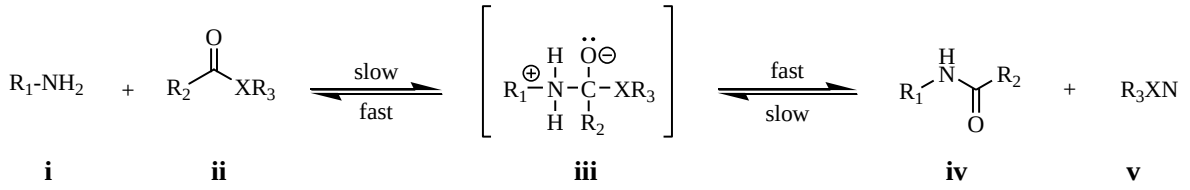

Scheme 5. Formation of peptide bond by activation ester mechanism. R_1: amino moiety; R_2: carboxyl moiety; R_3: leaving group.

The formation of **iii** is the rate determining step in this reaction. It can be positively influenced by activating the carboxyl component with electron withdrawing groups. The second step, the peptide bond formation, is fast, if the C-X bond in **iii** is highly polarized.
Since the acceptance of HOBt as epimerization suppressant, other benzotriazole derivatives were proposed such as 1-hydroxy-6-chlorobenzotriazole (Cl-HOBt) and 1-hydroxy-7-azabenzotriazole (HOAt), that are reported to be more efficient additives than HOBt, because speed up the coupling process and reduce racemization.

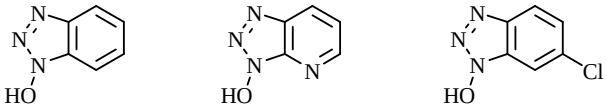

HOBt **HOAt** **Cl-HOBt**

Figure 7. Several common additives.

1.4.1.2.3. Coupling reagents based on 1H-benzotriazole

Several coupling reagents based on the HOBt/HOAt system and uronium/aminium salts, have been developed; by reaction with the carboxylic acids they form OAt/OBt active esters, which then react with amines.[149] A side-reaction can often take place with the amine reacting with the coupling reagent to form a guanidinium by-product,[150] nevertheless, coupling with aminium/uronium salts in the presence of a base have proven to be more effective than those carried out with carbodiimide in the presence of hydroxylamine derivatives.[123]

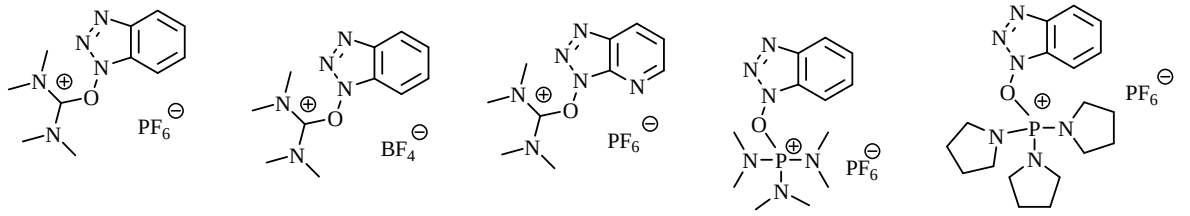

HBTU **TBTU** **HATU** **BOP** **PyBOP**

Figure 8. Structures of the most common phosphonium or uronium salts coupling reagents to form active esters for peptide coupling.

Castro *et al*. developed another family of coupling reagents based on HOBt/HOAt but that uses a phosphonium group.[151] Phosphonium salts have the advantage of not yielding guanidinium by-products via reaction of the coupling reagent with amines. The first phosphonium salt introduced was BOP but its use has been limited due to the carcinogenicity and respiratory toxicity associated with HMPA (hexamethylphosphoramide) generated when BOP is used in coupling reactions, leading to the development of the pyrrolidino derivative PyBOP.[152] Moreover, the cytotoxic aminium salt HBTU is often replaced by the tetrafluoro borate TBTU.[153]

It has been proven that coupling reagents based on HOAt (compared to HOBt) give faster, more efficient couplings with less epimerisation.[154] This is due to the 1*H*-hydroxy-7-azabenzotriazole (OAt) esters which show an increased reactivity owing to the formation of a transition state stabilized by an additional H-bond.[147] This increases the aminolytic reactivity and additionally inhibits racemization with a high efficiency. In the transition state the amino component is fixed in a certain orientation facilitating the nucleophilic attack, whereas the oxazolone formation is significantly reduced due to the low activation of the ester group (Scheme **6**).

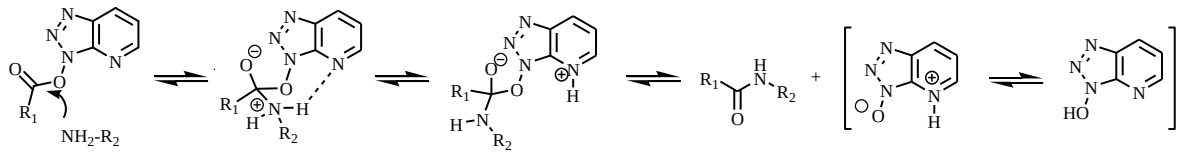

Scheme 6. Intramolecular base catalysis of HATU during aminolysis of OAt esters. R_1: carboxy moiety; R_2: amino moiety.

Comparative studies using HBTU[155] and TBTU[156] showed that the counter-anion had no practical influence on the outcome of coupling reactions using these reagents. Moreover, reagents based on phosphonium salts are preferred to their aminium/uronium counterparts for cyclization, because the latter compounds can give guanilidation reactions on the amino group.

1.4.1.2.4. Phosphonic acid derivatives

A wide variety of phosphonic acid derivatives is available. Diphenylphosphoryl azide (DPPA) and diethylphosphoryl cyanide were the first phosphonic acid derivatives to be used in peptide synthesis. DPPA reacts with free carboxyl groups to form acid azides.[157]

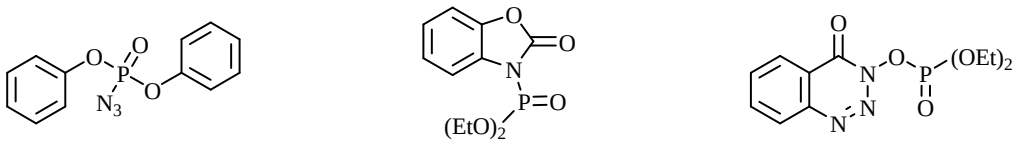

DPPA **DEPBO** **DEPBT**

Figure 9. Coupling reagents derived from phosphonic acids.

DPPA (diphenylphosphoryl azide) was introduced as a reagent for organic synthesis in 1972[157,158] and in the field of peptide synthesis, has been demonstrated that DPPA is a coupling reagent with little epimerization and racemization and it is inactive to the functional groups of many amino acids avoid unwanted side chain reactions. The reaction

mechanism of the amide bond formation using DPPA would be as shown in Scheme **7**. The carboxylate anion **i** would attack to the phosphorus atom in DPPA **ii** to give the acyl phosphates **iii**. The acyl azide **iv** would be formed by SN_2 type reaction of **iii** with the azide anion, which by reaction with the amine forms the corresponding amide **v**.

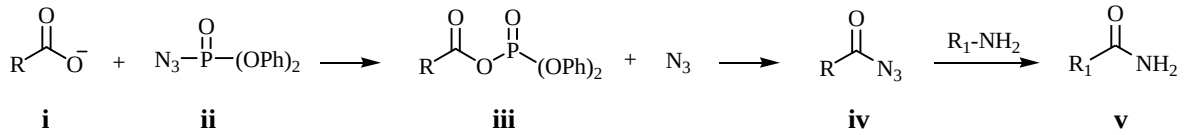

Scheme 7. Reaction mechanism of amide bond formation using DPPA as coupling regent.

In the macrocyclization DPPA is often utilized under high dilution conditions, combined with a inorganic base (sodium hydrogen carbonate, $NaHCO_3$) instead of organic bases such as triethylamine.

Propane phosphonic acid anhydride (PPAA) has been reported as an excellent reagent for amide/peptide bond formation characterized by excellent reaction selectivity, low epimerization with high product purities and yields. PPAA is a commercially available trimeric reagent that has been used in solution phase peptide synthesis and in cyclization reactions. It gave better results than BOP-Cl, and was found superior to HATU for cyclization reactions, especially for sterically hindered peptides.[159,160]

Among the many advantages of this coupling reagent the main is represented by the fact that the salt by-product is completely water soluble. Thus, it is readily removed via an aqueous wash at the conclusion of the reaction.

The reaction mechanism involved PPAA provide the conversions of the oxygen of the carboxylic acid into a leaving group and the by-product formed by the leaving group can be easily extracted by use of an aqueous work-up.

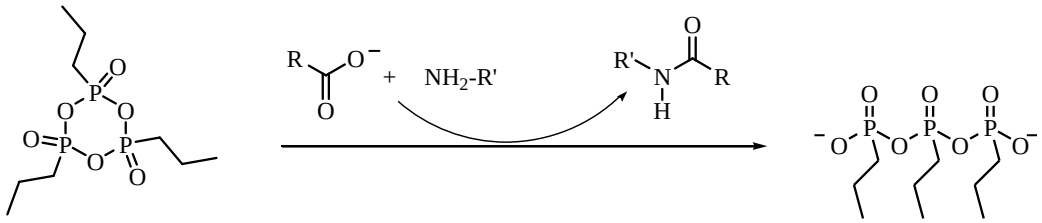

Scheme 8. The reaction mechanism involved PPAA.

1.4.2. Diketopiperazines (DKP)

One of the most serious side reactions during peptide synthesis on solid phase, is the formation of diketopiperazines (2,5-piperazinediones), which are the smallest cyclic peptides.[161-164]

DKPs are formed by intramolecular aminolysis at the dipeptide level and its formation has been established to be either acid-[162] or base-catalysed[165,166] and is strongly dependent on the nature and the sequence of the amino acids. Thus, the reaction is favoured by the presence, in either the first or second position, of amino acids (Gly, Pro, or N-alkyl) that can easily adopt a *cis*-conformation in the resulting amide bond. Another favourable combination is to have one L- and one D-amino acid in the dipeptide, due to the minimal steric interference between the two side-chains.[167] Furthermore, rates of DKP formation differ considerably depending on the *C*-carboxyl ester protecting groups, or the structures of

the peptide-resin linkages in the solid-phase approach.
The formation of DKP is most commonly seen in convergent solid-phase synthesis. The main consequence of the formation of DKPs was thought to be a decrease in the overall yield of the final peptide, since the hydroxyl sites formed on the polymer were considered to be poor nucleophiles, and therefore not predisposed to suffer acylation by the following protected amino acids, which would have started new peptide chains.
Either the use of halogenomethyl resins, where the first amino acid is incorporated via a nucleophilic substitution, or the use of preformed handles isolated, purified, and characterized in a step preceding the incorporation into the polymer, are advisable.[168] Furthermore, the loading of the starting polymer has importance with regard to the quality of the final product. Thus, the Cl-Trt-resin with a limited incorporation of the first amino acid is suggested to be the method of choice for the preparation of protected Fmoc/tBu peptides.

1.4.3. Peptide cyclization

The peptide macrocyclization is generally considered a significant synthetic challenge.[169-171] As peptide macrocycles have found applications ranging from drug discovery to nanomaterials, many efforts were directed to develop and optimize synthetic methodologies for their production.[156,157]
Depending on its functional groups, a peptide can be cyclized in four different ways: head-to-tail (*C*-terminus to *N*-terminus), head-to-side chain, side chain-to-tail or side-chain-to-side-chain. Of the various methods of synthesizing cyclic peptides, most often the final ring-closing reaction is a lactamization,[124] a lactonization[171] or the formation of a disulfide bridge.
Ring size is the most important factor that governs the success of a *head-to-tail* peptide macrocyclization, because for small-to-medium-sized rings, the ground-state *E* geometry of the peptide bond prevents the peptides from attaining the ring-like conformation conducive to cyclization. On the other hand, larger ring sizes do not pose this problem because they can accommodate *E* peptide bonds. Thus, despite the synthesis of large peptides containing more than seven amino acids is not problematic and generally straightforward, smaller peptides can often be troublesome, if not impossible, to cyclize.
Considering that, the ring-closure process is favored when the various structural elements of a linear precursor can accommodate the angular requirements for both termini in the transition state with the least amount of strain.[172]
Over the years, various strategies for directing macrocyclizations using conformational pre-organization have been developed.[173] These strategies can be classified under two categories: (i) ‘internal’ conformational elements, which encompass covalent modifications of the peptide chain to facilitate the union of its ends, and (ii) ‘external’ conformational elements, which involve the use of molecular scaffolds that are neither covalently attached to the peptide, nor consumed during the course of the ring closure.

Internal conformational elements

One of the most important aspect during the planning of the cyclopeptide synthesis is the carefully chosen of ring disconnection which[174] should be not sterically encumbered by *N*-

alkyl, α,α-substituted or β-branched amino acids (that is, Val or Ile).
The incorporation of β-turns elements embedded midway along the linear precursor represents another important feature able to promote macrocyclization, because β-turns elements, such as proline, β-amino and *N*-Methyl amino acids have the potential to introduce *cis*-amide bonds into peptide sequences giving a fast cyclization.
Recently, it has been also introduced the concept of Pseudo-prolines as a powerful temporary turn-inducing elements in the synthesis of short constrained cyclic peptides.[175,176]
Pseudo-prolines were first introduced as structure-disrupting building blocks that prevent the aggregation and self-association of peptides during solid-phase synthesis.[177] They are modified heterocyclic amino acids derived from serine, threonine ((4*S*)-oxazolidine-4-carboxylic acid) and cysteine ((4*R*)-thiazolidine-4-carboxylic acid). When incorporated into a peptide chain, these residues predominantly induce *cisoid* conformations of the amide bond preceding them, establishing type-VI β-turn structures.[178] These residues, following cyclization can be cleaved under acidic conditions to free the respective residue and thus yield cyclic peptides devoid of turn-inducing elements.

The chirality is another important feature which influences the peptide cycliziation. Indeed, peptides contains only all L- or all D-amino acids prefer to adopt extended conformations as a result of the tendency to minimize allylic strain[179] placing their reactive termini far away from each other resulting in unfavored macrocyclizations.
The incorporation of D-amino acids into peptides plays a turn-inducing effects and promote the cyclization and in general, it has been demonstrated that macrocyclization is favourites when occurs between two residues of opposite stereochemical configuration and if the linear peptide contain alternating D and L residues favor cyclization.[180]

External conformational elements

Many different methods based on the use of external conformational elements have been proposed to promote the peptide cyclization.
One of these approaches is represented by the use of external templates for assisting peptide macrocyclization which operate on the basis of a site-isolation mechanism.
Polymeric scaffolds that can create reaction cavities large enough for only one linear peptide molecule to enter and cyclize at a time have been developed.[181] Such distinct nanoenvironments isolate the peptide from the bulk solution and as a result of the isolation effect, these internal cavities create significantly decreases the likelihood of cyclooligomerization. An alternative method is represents by the molecularly imprinted cavities[182] which is based on the maintaining a turn structure with *cis*-amide conformations of a linear peptide enforced by a nano-sized cavity.

Metal ions have been introduced to conformationally pre-organize a peptide and facilitate the macrocyclization.[183] To date, various alkali metals have been shown to enhance the cyclization of peptides.
For instance, lithium salts was demonstrated to mediate cyclodimerization of two un-activated dipeptide methyl esters under basic conditions avoiding the use of high dilution conditions, protecting or activating groups, or coupling reagents.[184] Whereas sodium and

caesium ions have demonstrated to promote peptide macrocyclization by coordination of the *N*- and *C*-terminus of a peptide and the amidic oxygen atoms along the chain, inducing the linear peptide to form a strong turn structure, thus bringing the *N*- and *C*-termini in close proximity for cyclization (Scheme **9**).[185]

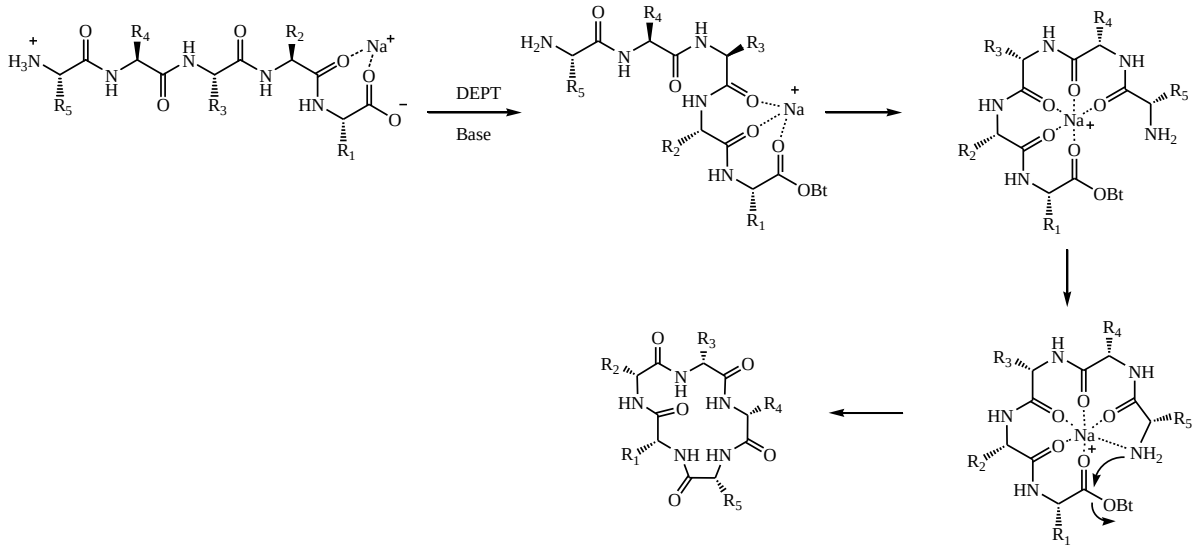

Scheme 9. Sodium ions used to enhance the *head-to-tail* cyclization of peptide through tandem coordination of amidic oxygen atoms along the peptide chain.

It has been also shown how the silver ions could promote cyclization of thioester linear peptides playing a dual role as an entropic and enthalpic activator for the macrocyclization for an acyl-transfer ring closure.[186] Through its thiophilic nature, Ag^+ generates the enthalpic activation on complexation with the thioester, making it a better leaving group and thus facilitating the acyl-transfer reaction. Unprotected peptides can be cyclized individually or as a mixture of peptides in solution. In addition, when tyrosine and lysine, which are competitive nucleophilic residues, are incorporated into the backbone of the peptide, the chemoselectivity of the cyclization becomes dependent on the pH of the solution. However, like any method of macrocyclization that proceeds through a highly activated *C*-terminal ester, also with Ag^+-ion-promoted activation the epimerization can be occur and this effect will be greater only if the ring closes slowly.

Regarding the sulphur mediated cyclization many different methods for the *head-to-tail* synthesis have been reported, such as the direct aminolysis of peptide thioesters in the presence of imidazole,[187] or the macrocyclization of thioesters with Sanger's reagent.[188] Moreover, it was defined the bridge between two internal cysteine thiol groups as one of the most convenient and straightforward method for constraining a peptide into a macrocycle, because the resulting intramolecular disulfide bridges can stabilize secondary structure motifs. In addition, the cysteine thiol functionality can be exploited in an intramolecular thiol-ene reaction to generate peptide macrocycles.

In ligation strategies based on the capture/rearrangement mechanism to link two peptide fragments together, the native chemical ligation displays the power to link peptide fragments under mild conditions.[189] The process involves a reaction between two peptide fragments, one of which is a weakly activated *C*-terminal thioester, and the other one an unprotected *N*-terminal cysteine residue. The thermodynamic strength of an amide bond

over a thioester is the driving force behind this reaction, made possible through a proximity-driven *S*-to-*N* acyl migration. The selectivity of the reaction allows the use of unprotected peptide fragments. The characteristics of the chemical ligation methodology overcomes all the limitations of the traditional convergent approach for the synthesis of large peptides or proteins (i.e. poor solubility and difficulty in purifying the fully protected peptide fragments), and provides access to new synthetic systems.
The native chemical ligation strategy has been applied to the *end-to-end* cyclization of large peptides that are rich in cysteine residues,[190] moreover has been recently developed a method through the native chemical ligation approach to cyclize peptides that do not contain cysteine residues[191] in which after an initial native chemical macrocyclization between an *N*-terminal cysteine residue and a *C*-terminal thioester, the cyclic peptide can be devoid of its cysteine sulfur through a desulfurization reaction with Raney nickel.

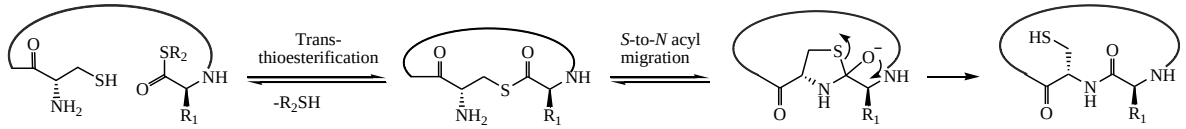

Scheme 10. Native chemical ligation applied to the *head-to-tail* cyclization of peptides. An *N*-terminal cysteine residue undergoes a macrocyclic *trans*-thioesterification with a *C*-terminal thioester. A subsequent *S*-to-*N* acyl transfer furnishes the desired lactamization product.

The traceless Staudinger ligation was also developed as thioester-based macrocyclization strategy.[192] With this approach a phosphine tethered to a thioester at the *C*-terminus of a peptide reacts intramolecularly with an azide present at the *N*-terminus to form a cyclic iminophosphorane. This ring then contracts to form an amide bond as the aza ylide attacks the thioester electrophile. This macrolactamization process was shown to be amenable to the cyclization of several globally deprotected peptides providing direct access to a cyclic peptide without further deprotection steps.

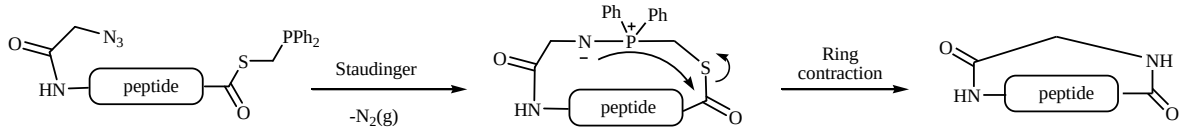

Scheme 11. Schematic representation of peptides *head-to-tail* macrocyclization through a traceless Staudinger ligation strategy.

In addition, many other classical reactions were used in the fields of peptide and peptoid macrocyclization such as the clik chemistry, the Ugi four-component reaction (U-4CR)[193,194] and the ring closing metathesis exploiting Grubb's catalyst.[195,196]

1.4.3.1. Peptide cyclization: synthetic approaches

Cyclic peptides have commonly being prepared entirely in solution or, on the other hand, taking advantage of the straightforward methodology of solid phase peptide synthesis (SPPS) followed by release of the linear chain from the solid support and a last step of cyclization in solution.
The peptide cyclization in solution is typically performed under high dilution (submillimolar concentrations) to minimize unwanted intermolecular processes such as oligo- and polymerizations.
Alternatively, different strategies have been designed to perform the *head to tail* cyclization

on the solid support, which simplified the removal of the coupling reagents, and the organic solvent. Each of these strategies requires a different type of linker. The solid-support may be attached to the *C*-terminus of the peptide through a 'safety catch linker' or an activated linker, or alternatively, the solid support may be linked to the peptide through a side chain, or through an amide bond nitrogen. Probably, the last one is the most robust and it is sequence independent but all first amino acid must be previously prepared in solution as H-AA-CO-PG and no proline or *N*-methyl amino acid can be used at this position.

In cyclization on solid phase anchoring the reactive molecule to an insoluble polymer[197] not only creates a pseudodilution phenomenon, but it is less prone to encounter one another relative to independent molecules in solution that can freely diffuse. Moreover, in the macrocyclizations on solid-supported the purification is accomplished by simple washing and filtration.

References

(1) Balkwill, F.; Mantovani, A. Inflammation and cancer: back to Virchow? *Lancet* **2001**, *357*, 539-545.

(2) Mantovani, A.; Sozzani, S.; Locati, M.; Allavena, P.; Sica, A. Macrophage polarization: tumor-associated macrophages as a paradigm for polarized M2 mononuclear phagocytes. *Trends in immunology* **2002**, *23*, 549-555.

(3) Bottazzi, B.; Polentarutti, N.; Acero, R.; Balsari, A.; Boraschi, D.; Ghezzi, P.; Salmona, M.; Mantovani, A. Regulation of the macrophage content of neoplasms by chemoattractants. *Science* **1983**, *220*, 210-212.

(4) Matsushima, K.; Larsen, C. G.; DuBois, G. C.; Oppenheim, J. J. Purification and characterization of a novel monocyte chemotactic and activating factor produced by a human myelomonocytic cell line. *J. Exp. Med.* **1989**, *169*, 1485-1490.

(5) Yoshimura, T.; Robinson, E. A.; Tanaka, S.; Appella, E.; Kuratsu, J.; Leonard, E. J. Purification and amino acid analysis of two human glioma-derived monocyte chemoattractants. *J. Exp. Med.* **1989**, *169*, 1449-1459.

(6) Balkwill, F. Cancer and the chemokine network. *Nat. Rev. Cancer* **2004**, *4*, 540-550.

(7) Conti, I.; Rollins, B. J. CCL2 (monocyte chemoattractant protein-1) and cancer. *Semin. Cancer Biol.* **2004**, *14*, 149-154.

(8) Azenshtein, E.; Luboshits, G.; Shina, S.; Neumark, E.; Shahbazian, D.; Weil, M.; Wigler, N.; Keydar, I.; Ben-Baruch, A. The CC chemokine RANTES in breast carcinoma progression: regulation of expression and potential mechanisms of promalignant activity. *Cancer Res.* **2002**, *62*, 1093-1102.

(9) Saji, H.; Koike, M.; Yamori, T.; Saji, S.; Seiki, M.; Matsushima, K.; Toi, M. Significant correlation of monocyte chemoattractant protein-1 expression with neovascularization and progression of breast carcinoma. *Cancer* **2001**, *92*, 1085-1091.

(10) Nesbit, M.; Schaider, H.; Miller, T. H.; Herlyn, M. Low-level monocyte chemoattractant protein-1 stimulation of monocytes leads to tumor formation in nontumorigenic melanoma cells. *J. Immunol.* **2001**, *166*, 6483-6490.

(11) Sica, A.; Schioppa, T.; Mantovani, A.; Allavena, P. Tumour-associated macrophages are a distinct M2 polarised population promoting tumour progression: potential targets of anti-cancer therapy. *Eur. J. Cancer* **2006**, *42*, 717-727.

(12) Lin, E. Y.; Nguyen, A. V.; Russell, R. G.; Pollard, J. W. Colony-stimulating factor 1 promotes progression of mammary tumors to malignancy. *J. Exp. Med.* **2001**, *193*, 727-740.

(13) Duyndam, M. C.; Hilhorst, M. C.; Schluper, H. M.; Verheul, H. M.; van Diest, P. J.; Kraal, G.; Pinedo, H. M.; Boven, E. Vascular endothelial growth factor-165 overexpression stimulates angiogenesis and induces cyst formation and macrophage infiltration in human ovarian cancer xenografts. *Am. J. Pathol.* **2002**, *160*, 537-548.

(14) Mantovani, A.; Sica, A.; Sozzani, S.; Allavena, P.; Vecchi, A.; Locati, M. The chemokine system in diverse forms of macrophage activation and polarization. *Trends in immunology* **2004**, *25*, 677-686.

(15) Sher, A.; Pearce, E.; Kaye, P. Shaping the immune response to parasites: role of dendritic cells. *Curr. Opin. Immunol.* **2003**, *15*, 421-429.

(16) Mantovani, A.; Bottazzi, B.; Colotta, F.; Sozzani, S.; Ruco, L. The origin and function of tumor-associated macrophages. *Immunol. Today* **1992**, *13*, 265-270.

(17) Uwe, S. Anti-inflammatory interventions of NF-kappaB signaling: potential applications and risks. *Biochem. Pharmacol.* **2008**, *75*, 1567-1579.

(18) Anderson, C. F.; Mosser, D. M. A novel phenotype for an activated macrophage: the type 2 activated macrophage. *J. Leukoc. Biol.* **2002**, *72*, 101-106.

(19) Goerdt, S.; Orfanos, C. E. Other functions, other genes: alternative activation of

antigen-presenting cells. *Immunity* **1999**, *10*, 137-142.
(20) Mantovani, A.; Allavena, P.; Sica, A. Tumour-associated macrophages as a prototypic type II polarised phagocyte population: role in tumour progression. *Eur. J. Cancer* **2004**, *40*, 1660-1667.
(21) Verreck, F. A.; de Boer, T.; Langenberg, D. M.; Hoeve, M. A.; Kramer, M.; Vaisberg, E.; Kastelein, R.; Kolk, A.; de Waal-Malefyt, R.; Ottenhoff, T. H. Human IL-23-producing type 1 macrophages promote but IL-10-producing type 2 macrophages subvert immunity to (myco)bacteria. *PNAS* **2004**, *101*, 4560-4565.
(22) Gordon, S. Alternative activation of macrophages. *Nat. Rev. Immunol.* **2003**, *3*, 23-35.
(23) Mosser, D. M. The many faces of macrophage activation. *J. Leukoc. Biol.* **2003**, *73*, 209-212.
(24) Galliera, E.; Jala, V. R.; Trent, J. O.; Bonecchi, R.; Signorelli, P.; Lefkowitz, R. J.; Mantovani, A.; Locati, M.; Haribabu, B. beta-Arrestin-dependent constitutive internalization of the human chemokine decoy receptor D6. *J. Biol Chem.* **2004**, *279*, 25590-25597.
(25) Saccani, A.; Schioppa, T.; Porta, C.; Biswas, S. K.; Nebuloni, M.; Vago, L.; Bottazzi, B.; Colombo, M. P.; Mantovani, A.; Sica, A. p50 nuclear factor-kappaB overexpression in tumor-associated macrophages inhibits M1 inflammatory responses and antitumor resistance. *Cancer Res.* **2006**, *66*, 11432-11440.
(26) Cavaillon, J. M.; Adib-Conquy, M. Bench-to-bedside review: endotoxin tolerance as a model of leukocyte reprogramming in sepsis. *Crit. Care* **2006**, *10*, 233.
(27) Bodinka, A.; Schmidt, H.; Henkel, B.; Flemmig, T. F.; Klaiber, B.; Karch, H. Polymerase chain reaction for the identification of Porphyromonas gingivaliscollagenase genes. *Oral Microbiol. Immunol.* **1994**, *9*, 161-165.
(28) Ghosh, S.; May, M. J.; Kopp, E. B. NF-kappa B and Rel proteins: evolutionarily conserved mediators of immune responses. *Annu. Rev. Immunol.* **1998**, *16*, 225-260.
(29) Ghosh, S.; Karin, M. Missing pieces in the NF-kappaB puzzle. *Cell* **2002**, *109 Suppl*, S81-96.
(30) Baeuerle, P. A.; Henkel, T. Function and activation of NF-kappa B in the immune system. *Annu. Rev. Immunol.* **1994**, *12*, 141-179.
(31) Baldwin, A. S., Jr. The NF-kappa B and I kappa B proteins: new discoveries and insights. *Annu. Rev. Immunol.* **1996**, *14*, 649-683.
(32) Siebenlist, U.; Franzoso, G.; Brown, K. Structure, regulation and function of NF-kappa B. *Annu. Rev. Cell. Biol.* **1994**, *10*, 405-455.
(33) Chen, F. E.; Huang, D. B.; Chen, Y. Q.; Ghosh, G. Crystal structure of p50/p65 heterodimer of transcription factor NF-kappaB bound to DNA. *Nature* **1998**, *391*, 410-413.
(34) Cramer, P.; Larson, C. J.; Verdine, G. L.; Muller, C. W. Structure of the human NF-kappaB p52 homodimer-DNA complex at 2.1 A resolution. *EMBO J.* **1997**, *16*, 7078-7090.
(35) Cramer, P.; Muller, C. W. Engineering of diffraction-quality crystals of the NF-kappaB P52 homodimer:DNA complex. *FEBS Lett.* **1997**, *405*, 373-377.
(36) Ghosh, S.; Ojala, W. H.; Gleason, W. B.; Grant, D. J. Relationships between crystal structures, thermal properties, and solvate stability of dialkylhydroxypyridones and their formic acid solvates. *J. Pharm. Sci.* **1995**, *84*, 1392-1399.
(37) Wagner, U. G.; Muller, N.; Schmitzberger, W.; Falk, H.; Kratky, C. Structure determination of the biliverdin apomyoglobin complex: crystal structure analysis of two crystal forms at 1.4 and 1.5 A resolution. *J. Mol. Biol.* **1995**, *247*, 326-337.
(38) Ghosh, G.; van Duyne, G.; Ghosh, S.; Sigler, P. B. Structure of NF-kappa B p50 homodimer bound to a kappa B site. *Nature* **1995**, *373*, 303-310.

(39) Muller, C. W.; Rey, F. A.; Sodeoka, M.; Verdine, G. L.; Harrison, S. C. Structure of the NF-kappa B p50 homodimer bound to DNA. *Nature* **1995**, *373*, 311-317.
(40) Fullard, N.; Wilson, C. L.; Oakley, F. Roles of c-Rel signalling in inflammation and disease. *Int. J. Biochem. Cell. Biol.* **2012**, *44*, 851-860.
(41) Baeuerle, P. A.; Baltimore, D. NF-kappa B: ten years after. *Cell* **1996**, *87*, 13-20.
(42) Wulczyn, F. G.; Krappmann, D.; Scheidereit, C. The NF-kappa B/Rel and I kappa B gene families: mediators of immune response and inflammation. *J. Mol. Med.* **1996**, *74*, 749-769.
(43) Ray, A.; Siegel, M. D.; Prefontaine, K. E.; Ray, P. Anti-inflammation: direct physical association and functional antagonism between transcription factor NF-KB and the glucocorticoid receptor. *Chest* **1995**, *107*, 139.
(44) Henkel, T.; Machleidt, T.; Alkalay, I.; Kronke, M.; Ben-Neriah, Y.; Baeuerle, P. A. Rapid proteolysis of I kappa B-alpha is necessary for activation of transcription factor NF-kappa B. *Nature* **1993**, *365*, 182-185.
(45) Phelps, C. B.; Sengchanthalangsy, L. L.; Huxford, T.; Ghosh, G. Mechanism of I kappa B alpha binding to NF-kappa B dimers. *J. Biol. Chem.* **2000**, *275*, 29840-29846.
(46) Jacobs, M. D.; Harrison, S. C. Structure of an IkappaBalpha/NF-kappaB complex. *Cell* **1998**, *95*, 749-758.
(47) Malek, S.; Huxford, T.; Ghosh, G. Ikappa Balpha functions through direct contacts with the nuclear localization signals and the DNA binding sequences of NF-kappaB. *J. Biol. Chem.* **1998**, *273*, 25427-25435.
(48) Palombella, V. J.; Rando, O. J.; Goldberg, A. L.; Maniatis, T. The ubiquitin-proteasome pathway is required for processing the NF-kappa B1 precursor protein and the activation of NF-kappa B. *Cell* **1994**, *78*, 773-785.
(49) Groll, M.; Clausen, T. Molecular shredders: how proteasomes fulfill their role. *Curr. Opin. Struct. Biol.* **2003**, *13*, 665-673.
(50) May, M. J.; Ghosh, S. Signal transduction through NF-kappa B. *Immunol. Today* **1998**, *19*, 80-88.
(51) Phelps, C. B.; Sengchanthalangsy, L. L.; Malek, S.; Ghosh, G. Mechanism of kappa B DNA binding by Rel/NF-kappa B dimers. *J. Biol. Chem.* **2000**, *275*, 24392-24399.
(52) Berkowitz, B.; Huang, D. B.; Chen-Park, F. E.; Sigler, P. B.; Ghosh, G. The x-ray crystal structure of the NF-kappa B p50.p65 heterodimer bound to the interferon beta -kappa B site. *J. Biol. Chem.* **2002**, *277*, 24694-24700.
(53) Senftleben, U.; Cao, Y.; Xiao, G.; Greten, F. R.; Krahn, G.; Bonizzi, G.; Chen, Y.; Hu, Y.; Fong, A.; Sun, S. C.; Karin, M. Activation by IKKalpha of a second, evolutionary conserved, NF-kappa B signaling pathway. *Science* **2001**, *293*, 1495-1499.
(54) Dejardin, E.; Droin, N. M.; Delhase, M.; Haas, E.; Cao, Y.; Makris, C.; Li, Z. W.; Karin, M.; Ware, C. F.; Green, D. R. The lymphotoxin-beta receptor induces different patterns of gene expression via two NF-kappaB pathways. *Immunity* **2002**, *17*, 525-535.
(55) Bonizzi, G.; Bebien, M.; Otero, D. C.; Johnson-Vroom, K. E.; Cao, Y.; Vu, D.; Jegga, A. G.; Aronow, B. J.; Ghosh, G.; Rickert, R. C.; Karin, M. Activation of IKKalpha target genes depends on recognition of specific kappaB binding sites by RelB:p52 dimers. *The EMBO journal* **2004**, *23*, 4202-4210.
(56) Novack, D. V.; Yin, L.; Hagen-Stapleton, A.; Schreiber, R. D.; Goeddel, D. V.; Ross, F. P.; Teitelbaum, S. L. The IkappaB function of NF-kappaB2 p100 controls stimulated osteoclastogenesis. *J. Exp. Med.* **2003**, *198*, 771-781.
(57) Lo, J. C.; Basak, S.; James, E. S.; Quiambo, R. S.; Kinsella, M. C.; Alegre, M. L.;

Weih, F.; Franzoso, G.; Hoffmann, A.; Fu, Y. X. Coordination between NF-kappaB family members p50 and p52 is essential for mediating LTbetaR signals in the development and organization of secondary lymphoid tissues. *Blood* **2006**, *107*, 1048-1055.

(58) Fulda, S.; Vucic, D. Targeting IAP proteins for therapeutic intervention in cancer. *Nature rev. Drug discov.* **2012**, *11*, 109-124.

(59) Muller, C. W.; Harrison, S. C. The structure of the NF-kappa B p50:DNA-complex: a starting point for analyzing the Rel family. *FEBS Lett.* **1995**, *369*, 113-117.

(60) Verma, I. M.; Stevenson, J. K.; Schwarz, E. M.; Van Antwerp, D.; Miyamoto, S. Rel/NF-kappa B/I kappa B family: intimate tales of association and dissociation. *Genes & development* **1995**, *9*, 2723-2735.

(61) Sengchanthalangsy, L. L.; Datta, S.; Huang, D. B.; Anderson, E.; Braswell, E. H.; Ghosh, G. Characterization of the dimer interface of transcription factor NFkappaB p50 homodimer. *J. Mol. Biol.* **1999**, *289*, 1029-1040.

(62) Huang, D. B.; Huxford, T.; Chen, Y. Q.; Ghosh, G. The role of DNA in the mechanism of NFkappaB dimer formation: crystal structures of the dimerization domains of the p50 and p65 subunits. *Structure* **1997**, *5*, 1427-1436.

(63) Karin, M.; Greten, F. R. NF-kappaB: linking inflammation and immunity to cancer development and progression. *Nat. Rev. Immunol.* **2005**, *5*, 749-759.

(64) Greten, F. R.; Eckmann, L.; Greten, T. F.; Park, J. M.; Li, Z. W.; Egan, L. J.; Kagnoff, M. F.; Karin, M. IKKbeta links inflammation and tumorigenesis in a mouse model of colitis-associated cancer. *Cell* **2004**, *118*, 285-296.

(65) Pikarsky, E.; Porat, R. M.; Stein, I.; Abramovitch, R.; Amit, S.; Kasem, S.; Gutkovich-Pyest, E.; Urieli-Shoval, S.; Galun, E.; Ben-Neriah, Y. NF-kappaB functions as a tumour promoter in inflammation-associated cancer. *Nature* **2004**, *431*, 461-466.

(66) Allavena, P.; Signorelli, M.; Chieppa, M.; Erba, E.; Bianchi, G.; Marchesi, F.; Olimpio, C. O.; Bonardi, C.; Garbi, A.; Lissoni, A.; de Braud, F.; Jimeno, J.; D'Incalci, M. Anti-inflammatory properties of the novel antitumor agent yondelis (trabectedin): inhibition of macrophage differentiation and cytokine production. *Cancer Res.* **2005**, *65*, 2964-2971.

(67) Ghosh, D.; Maiti, T. K. Effects of native and heat-denatured Abrus agglutinin on tumor-associated macrophages in Dalton's lymphoma mice. *Immunobiology* **2007**, *212*, 667-673.

(68) Hwang, S.; Ding, A. Activation of NF-kappa B in murine macrophages by taxol. *Cancer Biochem. Biophys.* **1995**, *14*, 265-272.

(69) Swain, S. M.; Arezzo, J. C. Neuropathy associated with microtubule inhibitors: diagnosis, incidence, and management. *Clin. Adv. Hematol. Oncol.* **2008**, *6*, 455-467.

(70) Hagemann, T.; Lawrence, T.; McNeish, I.; Charles, K. A.; Kulbe, H.; Thompson, R. G.; Robinson, S. C.; Balkwill, F. R. "Re-educating" tumor-associated macrophages by targeting NF-kappaB. *J. Exp. Med.* **2008**, *205*, 1261-1268.

(71) Maeda, S.; Kamata, H.; Luo, J. L.; Leffert, H.; Karin, M. IKKbeta couples hepatocyte death to cytokine-driven compensatory proliferation that promotes chemical hepatocarcinogenesis. *Cell* **2005**, *121*, 977-990.

(72) Fong, C. H.; Bebien, M.; Didierlaurent, A.; Nebauer, R.; Hussell, T.; Broide, D.; Karin, M.; Lawrence, T. An antiinflammatory role for IKKbeta through the inhibition of "classical" macrophage activation. *J. Exp. Med.* **2008**, *205*, 1269-1276.

(73) Pande, V.; Ramos, M. J. Nuclear factor kappa B: a potential target for anti-HIV chemotherapy. *Curr. Med. Chem.* **2003**, *10*, 1603-1615.

(74) Mader, R.; Lavi, I.; Luboshitzky, R. Evaluation of the pituitary-adrenal axis function

following single intraarticular injection of methylprednisolone. *Arthritis Rheum.* **2005**, *52*, 924-928.

(75) Weitoft, T.; Larsson, A.; Saxne, T.; Ronnblom, L. Changes of cartilage and bone markers after intra-articular glucocorticoid treatment with and without postinjection rest in patients with rheumatoid arthritis. *Ann. Rheum. Dis.* **2005**, *64*, 1750-1753.

(76) Jimi, E.; Aoki, K.; Saito, H.; D'Acquisto, F.; May, M. J.; Nakamura, I.; Sudo, T.; Kojima, T.; Okamoto, F.; Fukushima, H.; Okabe, K.; Ohya, K.; Ghosh, S. Selective inhibition of NF-kappa B blocks osteoclastogenesis and prevents inflammatory bone destruction in vivo. *Nature medicine* **2004**, *10*, 617-624.

(77) Takada, Y.; Singh, S.; Aggarwal, B. B. Identification of a p65 peptide that selectively inhibits NF-kappa B activation induced by various inflammatory stimuli and its role in down-regulation of NF-kappaB-mediated gene expression and up-regulation of apoptosis. *J. Biol. Chem.* **2004**, *279*, 15096-15104.

(78) Kang, M. I.; Henrich, C. J.; Bokesch, H. R.; Gustafson, K. R.; McMahon, J. B.; Baker, A. R.; Young, M. R.; Colburn, N. H. A selective small-molecule nuclear factor-kappaB inhibitor from a high-throughput cell-based assay for "activator protein-1 hits". *Mol. Cancer Ther.* **2009**, *8*, 571-581.

(79) Piccagli, L.; Fabbri, E.; Borgatti, M.; Bianchi, N.; Bezzerri, V.; Mancini, I.; Nicolis, E.; Dechecchi, C. M.; Lampronti, I.; Cabrini, G.; Gambari, R. Virtual screening against p50 NF-kappaB transcription factor for the identification of inhibitors of the NF-kappaB-DNA interaction and expression of NF-kappaB upregulated genes. *ChemMedChem* **2009**, *4*, 2024-2033.

(80) Wang, Y. F.; Xu, X.; Fan, X.; Zhang, C.; Wei, Q.; Wang, X.; Guo, W.; Xing, W.; Yu, J.; Yan, J. L.; Liang, H. P. A cell-penetrating peptide suppresses inflammation by inhibiting NF-kappaB signaling. *Mol. Ther.* **2011**, *19*, 1849-1857.

(81) Wang, Z.-p.; Cai, S.-x.; Liu, D.-b.; Xu, X.; Liang, H.-p. Anti-inflammatory effects of a novel peptide designed to bind with NF-κB p50 subunit1. *Acta Pharmacol. Sin.* **2006**, *27*, 1474-1478.

(82) Wells, J. A.; McClendon, C. L. Reaching for high-hanging fruit in drug discovery at protein-protein interfaces. *Nature* **2007**, *450*, 1001-1009.

(83) Blundell, T. L.; Mizuguchi, K. Structural genomics: an overview. *Prog. Biophys. Mol. Biol.* **2000**, *73*, 289-295.

(84) Blundell, T. L.; Sibanda, B. L.; Montalvao, R. W.; Brewerton, S.; Chelliah, V.; Worth, C. L.; Harmer, N. J.; Davies, O.; Burke, D. Structural biology and bioinformatics in drug design: opportunities and challenges for target identification and lead discovery. *Philos. Trans. R. Soc Lond. B Biol. Sci.* **2006**, *361*, 413-423.

(85) Hopkins, A. L.; Groom, C. R. The druggable genome. *Nature Rev.. Drug Discov.* **2002**, *1*, 727-730.

(86) Morelli, X.; Bourgeas, R.; Roche, P. Chemical and structural lessons from recent successes in protein-protein interaction inhibition (2P2I). *Curr. Opin. Chem. Biol.* **2011**, *15*, 475-481.

(87) Murray, J. K.; Gellman, S. H. Targeting protein-protein interactions: lessons from p53/MDM2. *Biopolymers* **2007**, *88*, 657-686.

(88) Yin, H.; Frederick, K. K.; Liu, D.; Wand, A. J.; Degrado, W. F. Arylamide derivatives as peptidomimetic inhibitors of calmodulin. *Org. Lett.* **2006**, *8*, 223-225.

(89) Sun, H.; Nikolovska-Coleska, Z.; Lu, J.; Meagher, J. L.; Yang, C. Y.; Qiu, S.; Tomita, Y.; Ueda, Y.; Jiang, S.; Krajewski, K.; Roller, P. P.; Stuckey, J. A.; Wang, S. Design, synthesis, and characterization of a potent, nonpeptide, cell-permeable, bivalent Smac mimetic that concurrently targets both the BIR2 and BIR3 domains in XIAP. *J. Am. Chem. Soc.* **2007**, *129*, 15279-15294.

(90) Yin, H.; Lee, G. I.; Sedey, K. A.; Kutzki, O.; Park, H. S.; Orner, B. P.; Ernst, J. T.;

Wang, H. G.; Sebti, S. M.; Hamilton, A. D. Terphenyl-Based Bak BH3 alpha-helical proteomimetics as low-molecular-weight antagonists of Bcl-xL. *J. Am. Chem. Soc.* **2005**, *127*, 10191-10196.

(91) Zinzalla, G.; Thurston, D. E. Targeting protein-protein interactions for therapeutic intervention: a challenge for the future. *Future Med. Chem.* **2009**, *1*, 65-93.

(92) Eichler, J. Peptides as protein binding site mimetics. *Curr. Opin. Chem. Biol.* **2008**, *12*, 707-713.

(93) Hecht, I.; Rong, J.; Sampaio, A. L.; Hermesh, C.; Rutledge, C.; Shemesh, R.; Toporik, A.; Beiman, M.; Dassa, L.; Niv, H.; Cojocaru, G.; Zauberman, A.; Rotman, G.; Perretti, M.; Vinten-Johansen, J.; Cohen, Y. A novel peptide agonist of formyl-peptide receptor-like 1 (ALX) displays anti-inflammatory and cardioprotective effects. *J. Pharmacol. Exp. Ther.* **2009**, *328*, 426-434.

(94) Jenssen, H.; Aspmo, S. I. Serum stability of peptides. *Methods Mol. Biol.* **2008**, *494*, 177-186.

(95) Werle, M.; Bernkop-Schnurch, A. Strategies to improve plasma half life time of peptide and protein drugs. *Amino acids* **2006**, *30*, 351-367.

(96) Henchey, L. K.; Jochim, A. L.; Arora, P. S. Contemporary strategies for the stabilization of peptides in the alpha-helical conformation. *Curr. Opin. Chem. Biol.* **2008**, *12*, 692-697.

(97) Craik, D. J. Chemistry. Seamless proteins tie up their loose ends. *Science* **2006**, *311*, 1563-1564.

(98) Craik, D. J. Circling the enemy: cyclic proteins in plant defence. *Trends Plant Sci.* **2009**, *14*, 328-335.

(99) Daly, N. L.; Rosengren, K. J.; Craik, D. J. Discovery, structure and biological activities of cyclotides. *Adv. Drug Deliv. Rev.* **2009**, *61*, 918-930.

(100) Daly, N. L.; Craik, D. J. Bioactive cystine knot proteins. *Curr. Opin. Chem. Biol.* **2011**, *15*, 362-368.

(101) Baeriswyl, V.; Heinis, C. Polycyclic peptide therapeutics. *ChemMedChem* **2013**, *8*, 377-384.

(102) Pechon. development trends for peptide therapeutics. *Peptide therapeutics foundation, report 2010* **2010**.

(103) Vlieghe, P.; Lisowski, V.; Martinez, J.; Khrestchatisky, M. Synthetic therapeutic peptides: science and market. *Drug Discov. Today* **2010**, *15*, 40-56.

(104) Lovshin, J. A.; Drucker, D. J. Incretin-based therapies for type 2 diabetes mellitus. *Nat. Rev. Endocrinol.* **2009**, *5*, 262-269.

(105) Nguyen, L. T.; Haney, E. F.; Vogel, H. J. The expanding scope of antimicrobial peptide structures and their modes of action. *Trends Biotechnol.* **2011**, *29*, 464-472.

(106) Keijzer, C.; Slutter, B.; van der Zee, R.; Jiskoot, W.; van Eden, W.; Broere, F. PLGA, PLGA-TMC and TMC-TPP nanoparticles differentially modulate the outcome of nasal vaccination by inducing tolerance or enhancing humoral immunity. *PloS one* **2011**, *6*, 26684.

(107) Fonte, P.; Andrade, F.; Araujo, F.; Andrade, C.; Neves, J.; Sarmento, B. Chitosan-coated solid lipid nanoparticles for insulin delivery. *Methods Enzymol.* **2012**, *508*, 295-314.

(108) Morishita, M.; Peppas, N. A. Is the oral route possible for peptide and protein drug delivery? *Drug Discov. Today* **2006**, *11*, 905-910.

(109) Richard, J. P.; Melikov, K.; Vives, E.; Ramos, C.; Verbeure, B.; Gait, M. J.; Chernomordik, L. V.; Lebleu, B. Cell-penetrating peptides. A reevaluation of the mechanism of cellular uptake. *J. Biol. Chem.* **2003**, *278*, 585-590.

(110) Lindgren, M.; Hallbrink, M.; Prochiantz, A.; Langel, U. Cell-penetrating peptides. *Trends Pharmacol. Sci.* **2000**, *21*, 99-103.

(111) Schwarze, S. R.; Hruska, K. A.; Dowdy, S. F. Protein transduction: unrestricted delivery into all cells? *Trends Cell. Biol.* **2000**, *10*, 290-295.
(112) Malakoutikhah, M.; Teixido, M.; Giralt, E. Shuttle-mediated drug delivery to the brain. *Angew. Chem. Int. Ed. Engl.* **2011**, *50*, 7998-8014.
(113) Fischer E, F. E. Ueber einige Derivate des Glykocolls. *Ber. Deutsch. Chem. Ges.* **1901**, *34*, 2868–2877.
(114) Curtius, T. Ueber einige neue Hippursäureanalog constituierte synthetisch dargestellte Aminosäuren. *J. Prakt. Chem.* **1882**, *26*, 145-208.
(115) Curtius, T. Verkettung von Aminosäuren. *J. Prakt. Chem.* **1904**, *70*, 51-108.
(116) Fischer, E. Synthese von Polypeptiden, IX. Chloride der Aminosäuren und ihrer Acylderivate. *Ber. Dtsch. Chem. Ges.* **1905**, *38*, 605-620.
(117) Merrifield, R. B. Solid Phase Peptide Synthesis. I. The Synthesis of a Tetrapeptide. *J. Am. Chem. Soc.* **1963**, *85*, 2149-2154.
(118) Carpino, L. A., and Han, G. Y. . 9-Fluorenylmethoxycarbonyl Function, a New Base-Sensitive Amino-Protecting Group. *J. Am. Chem. Soc.* **1970**, *92*, 5748.
(119) García-Martín, F.; Bayó-Puxan, N.; Cruz, L. J.; Bohling, J. C.; Albericio, F. Chlorotrityl Chloride (CTC) Resin as a Reusable Carboxyl Protecting Group. *QSAR & Comb. Sci.* **2007**, *26*, 1027-1035.
(120) Chatzi, K. B. O.; Gatos, D.; Stavropoulos, G. 2-Chlorotrityl chloride resin. *Int. J. Pept. Protein Res.* **1991**, *37*, 513-520.
(121) Barlos, K.; Gatos, D.; Kapolos, S.; Poulos, C.; SchÄFer, W.; Wenqing, Y. A. O. Application of 2-chlorotrityl resin in solid phase synthesis of (Leu15)-gastrin I and unsulfated cholecystokinin octapeptide. *Int. J. Pept. Protein Res.* **1991**, *38*, 555-561.
(122) Barlos, K.; Chatzi, O.; Gatos, D.; Stavropoulos, G. 2-Chlorotrityl chloride resin. Studies on anchoring of Fmoc-amino acids and peptide cleavage. *Int. J. Pept. Protein Res.* **1991**, *37*, 513-520.
(123) Albericio F, C. R., Dodsworth DJ, Najera, C. New trends in peptide coupling reagents. *Org. Prep. Proced. Int.* **2001**, *33*, 203-303.
(124) Montalbetti, C. A. G. N.; Falque, V. Amide bond formation and peptide coupling. *Tetrahedron* **2005**, *61*, 10827-10852.
(125) Robertson, N.; Jiang, L.; Ramage, R. Racemisation studies of a novel coupling reagent for solid phase peptide synthesis. *Tetrahedron* **1999**, *55*, 2713-2720.
(126) Han, Y.; Albericio, F.; Barany, G. Occurrence and Minimization of Cysteine Racemization during Stepwise Solid-Phase Peptide Synthesis(1)(,)(2). *J. Org. Chem.* **1997**, *62*, 4307-4312.
(127) Zhang, M.; Vedantham, P.; Flynn, D. L.; Hanson, P. R. High-Load, Soluble Oligomeric Carbodiimide: Synthesis and Application in Coupling Reactions. *J. Org. Chem.* **2004**, *69*, 8340-8344.
(128) Mikoz.xl; lajczyk, M.; Kiez.xl; lbasiński, P. Recent developments in the carbodiimide chemistry. *Tetrahedron* **1981**, *37*, 233-284.
(129) Bodanszky, M. Peptide Chemistry: A Practical Textbook. **1988**.
(130) Rich, D. H., and Singh, J. The Carbodiimide Method. *The Peptides: Analysis, Synthesis, Biology* **1975-1987**.
(131) Sheehan, J. C.; Hess, G. P. A New Method of Forming Peptide Bonds. *J. Am. Chem. Soc.* **1955**, *77*, 1067-1068.
(132) Newman, M.; Boden, H. Notes- N-Methylpyrrolidone as Solvent for Reaction of Aryl Halides with Cuprous Cyanide. *J. Org. Chem.* **1961**, *26*, 2525-2525.
(133) Kirschning, A.; Monenschein, H.; Wittenberg, R. Functionalized Polymers-Emerging Versatile Tools for Solution-Phase Chemistry and Automated Parallel Synthesis. *Angew. Chem. Int. Ed. Engl.* **2001**, *40*, 650-679.
(134) Parlow, J. J.; Devraj, R. V.; South, M. S. Solution-phase chemical library synthesis

using polymer-assisted purification techniques. *Curr. Opin. Chem. Biol.* **1999**, *3*, 320-336.
(135) Parlow, J. J. Polymer-assisted solution-phase chemical library synthesis. *Curr. Opin. Drug Discov. Devel.* **2005**, *8*, 757-775.
(136) Clapham, B.; Reger, T. S.; Janda, K. D. Polymer-supported catalysis in synthetic organic chemistry. *Tetrahedron* **2001**, *57*, 4637-4662.
(137) Dendrinos, K. G.; Kalivretenos, A. G. Synthesis of N-hydroxysuccinimide esters using polymer bound HOBT. *Tetrahedron Lett.* **1998**, *39*, 1321-1324.
(138) Weinshenker, N. M.; Shen, C. M. Polymeric reagents I. Synthesis of an insoluble polymeric carbodiimide. *Tetrahedron Lett.* **1972**, *13*, 3281-3284.
(139) Parlow, J. J.; Mischke, D. A.; Woodard, S. S. Utility of Complementary Molecular Reactivity and Molecular Recognition (CMR/R) Technology and Polymer-Supported Reagents in the Solution-Phase Synthesis of Heterocyclic Carboxamides. *J. Org. Chem.* **1997**, *62*, 5908-5919.
(140) Salimi, H.; Rahimi, A.; Pourjavadi, A. Applications of Polymeric Reagents in Organic Synthesis. *Monatsh. Chem. Chem. Mon.* **2007**, *138*, 363-379.
(141) Adamczyk, M.; Fishpaugh, J. R.; Mattingly, P. G. An easy preparation of hapten active esters via solid supported EDAC. *Tetrahedron Lett.* **1995**, *36*, 8345-8346.
(142) Desai, M. C.; Stephens Stramiello, L. M. Polymer bound EDC (P-EDC): A convenient reagent for formation of an amide bond. *Tetrahedron Lett.* **1993**, *34*, 7685-7688.
(143) Gonthier, E.; Breinbauer, R. Solid-supported reagents and catalysts for the preparation of large ring compounds. *Mol. Divers* **2005**, *9*, 51-62.
(144) Lannuzel, M.; Lamothe, M.; Perez, M. An efficient one-pot, purification-free, preparation of amides using polymer-supported reagents. *Tetrahedron Lett.* **2001**, *42*, 6703-6705.
(145) König, W.; Geiger, R. Eine neue Methode zur Synthese von Peptiden: Aktivierung der Carboxylgruppe mit Dicyclohexylcarbodiimid unter Zusatz von 1-Hydroxy-benzotriazolen. *Chem. Ber.* **1970**, *103*, 788-798.
(146) König, W.; Geiger, R. Racemisierung bei Peptidsynthesen. *Chem. Ber.* **1970**, *103*, 2024-2033.
(147) Carpino, L. A. 1-Hydroxy-7-azabenzotriazole. An efficient peptide coupling additive. *J. Am. Chem. Soc.* **1993**, *115*, 4397-4398.
(148) Fields, G. B.; Noble, R. L. Solid phase peptide synthesis utilizing 9-fluorenylmethoxycarbonyl amino acids. *Int. J. Pept. Protein Res.* **1990**, *35*, 161-214.
(149) Albericio, F.; Bofill, J. M.; El-Faham, A.; Kates, S. A. Use of Onium Salt-Based Coupling Reagents in Peptide Synthesis. *J. Org. Chem.* **1998**, *63*, 9678-9683.
(150) Nájera, C. From α-Amino Acids to Peptides: All You Need for the Journey. *Synlett.* **2002**, *2002*, 1388-1404.
(151) Castro, B.; Dormoy, J. R.; Evin, G.; Selve, C. Reactifs de couplage peptidique I (1) - l'hexafluorophosphate de benzotriazolyl N-oxytrisdimethylamino phosphonium (B.O.P.). *Tetrahedron Lett.* **1975**, *16*, 1219-1222.
(152) Coste, J.; Le-Nguyen, D.; Castro, B. PyBOP®: a new peptide coupling reagent devoid of toxic by-product. *Tetrahedron Lett.* **1990**, *31*, 205-208.
(153) Chen, S.; Xu, J. A new coupling reagent for peptide synthesis. Benzotriazolvyloxy-bis (pyrroltdino) -carbonium hexaflouorophosphate (BBC). *Tetrahedron Lett.* **1992**, *33*, 647-650.
(154) Carpino, L. A.; El-Faham, A.; Albericio, F. Racemization studies during solid-phase peptide synthesis using azabenzotriazole-based coupling reagents. *Tetrahedron Lett.* **1994**, *35*, 2279-2282.
(155) Dourtoglou, V.; Ziegler, J.-C.; Gross, B. L'hexafluorophosphate de O-

benzotriazolyl-N,N-tetramethyluronium: Un reactif de couplage peptidique nouveau et efficace. *Tetrahedron Lett.* **1978**, *19*, 1269-1272.
(156) Knorr, R.; Trzeciak, A.; Bannwarth, W.; Gillessen, D. New coupling reagents in peptide chemistry. *Tetrahedron Lett.* **1989**, *30*, 1927-1930.
(157) Shioiri, T.; Ninomiya, K.; Yamada, S. Diphenylphosphoryl azide. New convenient reagent for a modified Curtius reaction and for peptide synthesis. *J. Am. Chem. Soc.* **1972**, *94*, 6203-6205.
(158) L'Abbé, G.; Ykman, P.; Smets, G. Reactions of azides with α-ester phosphorus ylids. *Tetrahedron* **1969**, *25*, 5421-5426.
(159) Bailen, M. A.; Chinchilla, R.; Dodsworth, D. J.; Najera, C. 2-Mercaptopyridone 1-Oxide-Based Uronium Salts: New Peptide Coupling Reagents. *J. Org. Chem.* **1999**, *64*, 8936-8939.
(160) Chesworth, R.; Zawistoski, M. P.; Lefker, B. A.; Cameron, K. O.; Day, R. F.; Mangano, F. M.; Rosati, R. L.; Colella, S.; Petersen, D. N.; Brault, A.; Lu, B.; Pan, L. C.; Perry, P.; Ng, O.; Castleberry, T. A.; Owen, T. A.; Brown, T. A.; Thompson, D. D.; DaSilva-Jardine, P. Tetrahydroisoquinolines as subtype selective estrogen agonists/antagonists. *Bioorg. Med. Chem. Lett.* **2004**, *14*, 2729-2733.
(161) Chiva, C.; Vilaseca, M.; Giralt, E.; Albericio, F. An HPLC-ESMS study on the solid-phase assembly of C-terminal proline peptides. *J. Pept. Sci.* **1999**, *5*, 131-140.
(162) Giralt, E.; Eritja, R.; Pedroso, E. Diketopiperazine formation in acetamido-and nitrobenzamido-bridgedpolymeric supports. *Tetrahedron Lett.* **1981**, *22*, 3779-3782.
(163) Pedroso, E.; Grandas, A.; de las Heras, X.; Eritja, R.; Giralt, E. Diketopiperazine formation in solid phase peptide synthesis using p-alkoxybenzyl ester resins and Fmoc-amino acids. *Tetrahedron Lett.* **1986**, *27*, 743-746.
(164) Lloyd-Williams, P.; Merzouk, A.; Guibé, F.; Albericio, F.; Giralt, E. Solid-phase synthesis of peptides using allylic anchoring groups 2. Palladium-catalysed cleavage of Fmoc-protected peptides. *Tetrahedron Lett.* **1994**, *35*, 4437-4440.
(165) Goodman, M.; Stueben, K. C. Peptide Synthesis via Amino Acid Active Esters. II.1 Some Abnormal Reactions during Peptide Synthesis. *J. Am. Chem. Soc.* **1962**, *84*, 1279-1283.
(166) Khosla, M. C.; Smeby, R. R.; Bumpus, F. M. Failure sequence in solid-phase peptide synthesis due to the presence of an N-alkylamino acid. *J. Am. Chem. Soc.* **1972**, *94*, 4721-4724.
(167) Lloyd-Williams, P. A., F.; Giralt, E. . Chemical Approaches to the Synthesis of Peptides and Proteinss *CRC Press: Boca Raton, FL* **1997**.
(168) Albericio, F.; Barany, G. Improved approach for anchoring Nα-9-fluorenylmethyloxycarbonylamino acids as p-alkoxybenzyl esters in solid-phase peptide synthesis. *Int. J. Pept. Protein Res.* **1985**, *26*, 92-97.
(169) Marsault, E.; Peterson, M. L. Macrocycles are great cycles: applications, opportunities, and challenges of synthetic macrocycles in drug discovery. *J. Med. Chem.* **2011**, *54*, 1961-2004.
(170) White, C. J.; Yudin, A. K. Contemporary strategies for peptide macrocyclization. *Nat. Chem.* **2011**, *3*, 509-524.
(171) Parenty, A.; Moreau, X.; Campagne, J. M. Macrolactonizations in the total synthesis of natural products. *Chem. Rev.* **2006**, *106*, 911-939.
(172) Cavelier-Frontin, F.; Pepe, G.; Verducci, J.; Siri, D.; Jacquier, R. Prediction of the best linear precursor in the synthesis of cyclotetrapeptides by molecular mechanic calculations. *J. Am. Chem. Soc.* **1992**, *114*, 8885-8890.
(173) Blankenstein, J.; Zhu, J. Conformation-Directed Macrocyclization Reactions. *Eur. J. Org. Chem.* **2005**, *2005*, 1949-1964.
(174) Humphrey, J. M.; Chamberlin, A. R. Chemical Synthesis of Natural Product

Peptides: Coupling Methods for the Incorporation of Noncoded Amino Acids into Peptides. *Chem. Rev.* **1997**, *97*, 2243-2266.

(175) Rückle, T.; de Lavallaz, P.; Keller, M.; Dumy, P.; Mutter, M. Pseudo-prolines in cyclic peptides: Conformational stabilisation of cyclo[Pro-Thr(ψMe,Mepro)-Pro]. *Tetrahedron* **1999**, *55*, 11281-11288.

(176) Skropeta, D.; Jolliffe, K. A.; Turner, P. Pseudoprolines as Removable Turn Inducers: Tools for the Cyclization of Small Peptides. *J. Org. Chem.* **2004**, *69*, 8804-8809.

(177) Wöhr, T.; Wahl, F.; Nefzi, A.; Rohwedder, B.; Sato, T.; Sun, X.; Mutter, M. Pseudo-Prolines as a Solubilizing, Structure-Disrupting Protection Technique in Peptide Synthesis. *J. Am. Chem. Soc.* **1996**, *118*, 9218-9227.

(178) Dumy, P.; Keller, M.; Ryan, D. E.; Rohwedder, B.; Wöhr, T.; Mutter, M. Pseudo-Prolines as a Molecular Hinge: Reversible Induction of cis Amide Bonds into Peptide Backbones. *J. Am. Chem. Soc.* **1997**, *119*, 918-925.

(179) Hoffmann, R. W. Flexible Molecules with Defined Shape—Conformational Design. *Angew. Chem. Int. Ed. Engl.* **1992**, *31*, 1124-1134.

(180) Tang, Y.-c.; Xie, H.-b.; Tian, G.-l.; Ye, Y.-h. Synthesis of cyclopentapeptides and cycloheptapeptides by DEPBT and the influence of some factors on cyclization. *J. Pept. Res.* **2002**, *60*, 95-103.

(181) Amore, A.; van Heerbeek, R.; Zeep, N.; van Esch, J.; Reek, J. N. H.; Hiemstra, H.; van Maarseveen, J. H. Carbosilane Dendrimeric Carbodiimides: Site Isolation as a Lactamization Tool. *J. Org. Chem.* **2006**, *71*, 1851-1860.

(182) Tai, D.-F.; Lin, Y.-F. Molecularly imprinted cavities template the macrocyclization of tetrapeptides. *ChemComm.* **2008**, 5598-5600.

(183) Haas, K.; Ponikwar, W.; Nöth, H.; Beck, W. Facile Synthesis of Cyclic Tetrapeptides from Nonactivated Peptide Esters on Metal Centers. *Angew. Chem. Int. Ed. Engl.* **1998**, *37*, 1086-1089.

(184) Yep, Y.-h.; Gao, X.-m.; Liu, M.; Tang, Y.-c.; Tian, G.-l. Studies on the Synthetic Methodology of Head to Tail Cyclization of Linear Peptides. *Int. J. Pept. Res. Ther.* **2003**, *10*, 571-579.

(185) Liu, M.; Tang, Y. C.; Fan, K. Q.; Jiang, X.; Lai, L. H.; Ye, Y. H. Cyclization of several linear penta- and heptapeptides with different metal ions studied by CD spectroscopy*. *J. Pept. Res.* **2005**, *65*, 55-64.

(186) Zhang, L.; Tam, J. P. Metal ion-assisted peptide cyclization. *Tetrahedron Lett.* **1997**, *38*, 4375-4378.

(187) Li, Y.; Yongye, A.; Giulianotti, M.; Martinez-Mayorga, K.; Yu, Y.; Houghten, R. A. Synthesis of Cyclic Peptides through Direct Aminolysis of Peptide Thioesters Catalyzed by Imidazole in Aqueous Organic Solutions. *J. Comb. Chem.* **2009**, *11*, 1066-1072.

(188) Sasaki, K.; Crich, D. Cyclic peptide synthesis with thioacids. *Org. Lett.* **2010**, *12*, 3254-3257.

(189) Dawson, P.; Muir, T.; Clark-Lewis, I.; Kent, S. Synthesis of proteins by native chemical ligation. *Science* **1994**, *266*, 776-779.

(190) Tam, J. P.; Lu, Y.-A.; Yu, Q. Thia Zip Reaction for Synthesis of Large Cyclic Peptides: Mechanisms and Applications. *J. Am. Chem. Soc.* **1999**, *121*, 4316-4324.

(191) Yan, L. Z.; Dawson, P. E. Synthesis of Peptides and Proteins without Cysteine Residues by Native Chemical Ligation Combined with Desulfurization. *J. Am. Chem. Soc.* **2001**, *123*, 526-533.

(192) Kleineweischede, R.; Hackenberger, C. P. R. Chemoselective Peptide Cyclization by Traceless Staudinger Ligation. *Angew. Chem. Int. Ed. Engl.* **2008**, *47*, 5984-5988.

(193) Vercillo, O. E.; Andrade, C. K.; Wessjohann, L. A. Design and synthesis of cyclic RGD pentapeptoids by consecutive Ugi reactions. *Organic letters* **2008**, *10*, 205-208.
(194) Hebach, C.; Kazmaier, U. Via Ugi reactions to conformationally fixed cyclic peptides. *ChemComm.* **2003**, 596-597.
(195) Miller, S. J.; Blackwell, H. E.; Grubbs, R. H. Application of Ring-Closing Metathesis to the Synthesis of Rigidified Amino Acids and Peptides. *J. Am. Chem. Soc.* **1996**, *118*, 9606-9614.
(196) Illesinghe, J.; Guo, C. X.; Garland, R.; Ahmed, A.; van Lierop, B.; Elaridi, J.; Jackson, W. R.; Robinson, A. J. Metathesis assisted synthesis of cyclic peptides. *ChemComm.* **2009**, 295-297.
(197) Mazur, S.; Jayalekshmy, P. Chemistry of polymer-bound o-benzyne. Frequency of encounter between substituents on crosslinked polystyrenes. *J. Am. Chem. Soc.* **1979**, *101*, 677-683.

Chapter 2

Development and synthesis of cyclic peptides as p50 NF-κB homodimerization inhibitors

Introduction

p50 NF-κB nuclear accumulation seems to promote a persistent M2 inflammation associated with tumour progression.[1] Preliminary results have also confirmed a similar activity of p50 NF-κB in MDSC (myeloid-derived suppressor cells) in terms of both functional M2 polarization and suppressive activity, which further indicated that, targeting this molecule in the myelomonocytic compartment may restore the M1 inflammation and the anticancer activity *in vivo*.

The crystallographic data of the p50 homodimerization[2] domain reveal that just a few numbers of amino acids located in the binding region are directly involved in the homodimerization process. Among them, Leu269, Val310 and Tyr267 seem to be the most important in the stabilization of p50 dimer interface, defining the hot-spot of the binding energy.

In order to prevent the proteins dimerization either the natural binding sequence or some analogues could be exploited prompting the design and the investigation of peptides analogues with high affinity towards the p50 NF-κB binding site. These molecules will efficiently inhibit the protein dimerization by competitive effect.

Nowadays, the use of peptides as therapeutic agents has been significantly increased due to their potential benefits, which consists on high potency and target specificity, as well as, low toxicity. The peptide cyclization is one of the most diffused approach to constrain small peptides into specific global secondary structures (α-helices, β-sheets, extended structures and β-turns), and to establish their biological active conformation.[3-7] In addition, this allows to overcome their limited pharmacokinetics properties and to extend the peptide half-live.

Based on these considerations, the goal of the present thesis work was to develop new cyclic peptides able to prevent the p50 NF-κB homodimerization and subsequently restore the M1 inflammation and anticancer activity. The idea is to develop structures that mimicking the p50 dimerization binding site could interact with the p50 subunits blocking their interaction.

2.1. Peptidomimetic design and candidate selection

The peptidomimetic rational design was based on previous reported data,[8] where investigations by X-ray crystallography together with site-directed mutagenesis have identified the minimal sequence and the amino-acid residues needed involved in the binding process between two p50 subunits.

Several cyclopeptides bearing the key residues (leucine, valine and tyrosine) but different in ring size were underwent to a virtual screening *in silico*. The ring size was varied, from tetra to octapeptides, considering the relative proximity among the key-residues and the similar previously reported scaffolds typically employed in drug discovery. This structural design allows the construction of a cyclopeptides library in which the backbone flexibility, the orientation and spatial position of the amino acidic side chains can be modulated.

The structures after being built using the graphical interface of Maestro, were solvated in explicit water and minimized with Amber11.
One of the main problems encountered during this part of the work, was the loading of the pdb files generate with Maestro in the Amber software. Since this program was developed to perform studies of molecular dynamics of proteins and peptides, it does not recognize cyclic peptides that do not contain carboxyl and amine as terminal groups, showing a stiffness of the program. Nevertheless, the problem was solved by introducing new parameters that define the connectivity between the *N*- and *C*- terminal.
The analysis of the results was performed by plotting the energy from the output file. The graphic profiles show that the kinetic energy is stable and also the total and potential energy plots show a similar trend suggesting a significantly structural rigidity of the cyclopeptides backbone mostly for the cyclopeptides with smaller size such as tetra-, penta- and hexa-peptides.

The minimized structures have been superimposed with the p50 "hot spot" region to evaluate which one present an analogue spatial presentation to that in the natural protein.
The results obtaining during this qualitative structural analysis, show that the cyclopeptides contain five amino acids have a properly size to generate a good overlap with the three keys residues of the natural protein. In addition the high rigidity of these structures can results in a high specificity toward the binding site of the target protein.

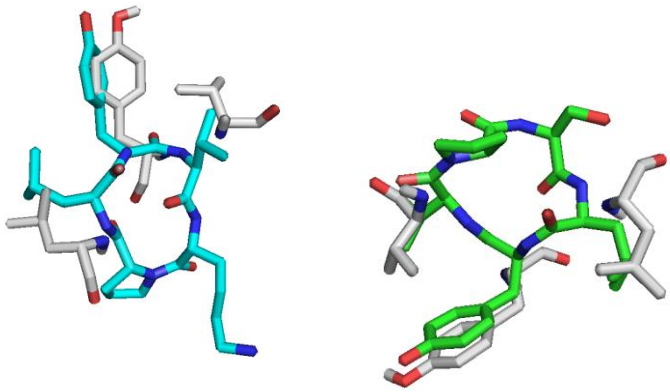

Figure 1. Example of the penta cyclopeptide analyzed *in silico* and subjected to conformational analysis studies.

The following step, after the identification of the most promising ring size mimicking the protein binding region, consisted in the evaluation of the structures contain five amino acid residues. A molecular modelling investigation based on several penta cyclopeptides developed *in silico*, have suggested that the key residues must be inserted sequentially in the ring in order to increase the affinity to the protein. Other than the key-sequence (Leu-Val-Tyr) two more amino acid had to be chosen in order to maximize the peptide cyclization and to allow structural differentiation. To achieve this goal, β-turn elements (e.g. Pro, D-amino acids) and residues functionalizable on the side chain were inserted in the cyclopeptidic sequence.
The small size of these structures provides high structural analogy with the relevant amino acids of p50 homodimerization site, nevertheless, the cyclopeptides can differ one from another just by a single amino acid in the sequence in order to keep remarkable degree of similarity to the natural target. Complementary, once fixed the peptidic backbone, which is

the most challenging step, the evaluation of different side chain to better understand the binding requirements and improve the interaction with the target protein is relatively easy.
Based on these considerations, we have proposed two different cyclic pentapeptides which differ by a lysine or a serine as functionalizable amino acid (Figure **2**).

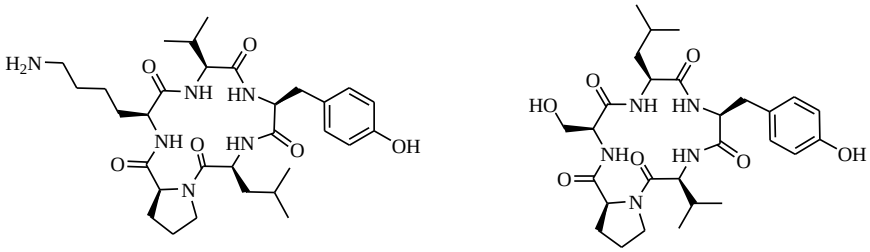

&Val-Tyr-Leu-Pro-Lys&
***cyclo*-1**

&Leu-Tyr-Val-Pro-Ser&
***cyclo*-2**

Figure 2. Structures of the two different cyclic pentapeptides proposed.

The proline role is to pre-organize the linear peptides in a more suitable conformation for the cyclization introducing a *cis*-amide bond in the peptide chain. In the same time, the presence of a lysine (Lys) and a serine (Ser) allowed furthermore modifications in the cyclic peptides in order to modulate or fine tune the binding affinity towards the target molecule. Additionally, the Lys and Ser side functional groups could be exploited to conjugate the cyclopeptide to a *carrier* able to promote the delivery inside the cells.
As previously mentioned, both cyclic pentapeptides contained the key residues but placed in a opposite order in the sequence (Val-Tyr-Leu in the ***cyclo*-1** and Leu-Tyr-Val in the ***cyclo*-2**). This generates a total different conformation of the cyclopeptides which may be reflected by different interactions with the natural target and, probably, different biological activity.

2.2. Peptide synthesis

2.2.1. Synthesis planning and preliminary considerations

The synthesis of linear peptides is, in general, a straightforward pathway whereas the *head to tail* cyclization is often troublesome especially in the case of peptides shorter than seven residues, the case of cyclic pentapeptides is among the most challenging.
Although several cyclization methodology have been reported,[9] many variable are still present affecting the ring closure such as the nature of the linear precursor, the coupling reagents, the concentration of the reaction solution and the reaction temperature. Among all these factors, the nature of the linear precursor may play a predominant role in the cyclization reactions as previously reported.[10,11] Nevertheless it is hard, in general, to predict with accuracy the optimal linear sequence for a cyclization but some general guidelines can facilitate the synthetic plan of a linear peptide with good cyclization potential.
The cyclization position plays an important role in ring closure, and this imply that the ring disconnection must be carefully chosen identifying a macrocyclization site not sterically hindered by any *N*-alkyl, α,α-substituted or β-branched amino acids.

Moreover, the cyclization could be promoted in other two ways: realizing the ring closure between two residues with opposite stereochemical configuration or, by the introduction of β-turn promoting structural element in the linear precursor main chain
Based on the above considerations, different epimers of a linear peptide were synthesized in order to identify the more efficient position in which the D-amino acid can pre-organize the linear peptides towards the cyclization.

2.2.2. Synthesis of the linear peptides in solution

The synthesis of the linear peptides was initially performed in solution using the Fmoc/Boc chemistry with orthogonally protected groups along the amino acid side chains.
The carboxylic acid on the first residues was protected at the beginning of the synthetic pathway as fluorenylmethyl ester. The esterification of the carboxylic group was performed with EDC in the presence of catalytic amount of DMAP. The peptide sequence was grown up by coupling with Boc-protected amino acids using the standard procedure with carbodiimide (EDC) in presence of HOBt and DIPEA as base.
Despite the formation of secondary amides (standard amide bond) could be carried out equally with different condensing agents, however for the formation of tertiary amide, phosphonium and uronium reagents consistently gave higher yield than carbodiimides[12,13] and for this reason the coupling with the proline amino group was performed using the uronium reagent HBTU.
Fluorenylmethyloxycarbonil *N*-protected amino acid has been used as *N*-terminal, allowing a final treatment with 20% of piperidine able to simultaneously remove the protecting group on the *C*- and *N*- terminal leading the desiderate linear pentapeptides.

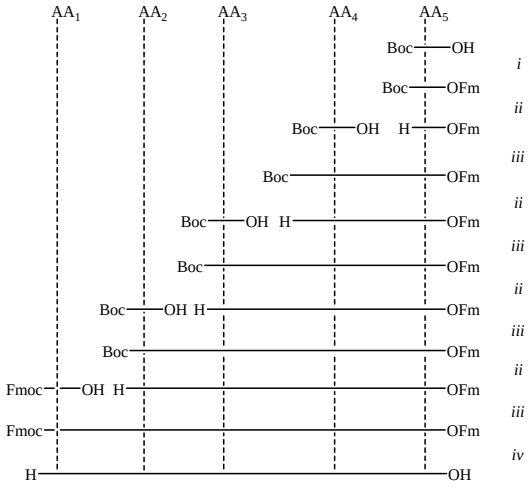

Scheme 1. Schematic representation of the linear peptide synthesis in solution. *i)* FmOH, EDC, DMAP, *ii)* TFA 40% in DCM; *iii)* EDC/HOBt or HBTU, DIPEA, *iv)* piperidine 20% in DMF. AA_1= Val, AA_2= Tyr, AA_3= Leu, AA_4= Pro, AA_5= Lys.

In parallel, commercially available PPAA (propane phosphonic acid anhydride), which is reported as an excellent coupling reagent for sterically hindered peptides[14,15] was tested. The main advantage of PPAA is due to the formation, during the reactions, of water soluble by-products easily removable but, in our case, it did not produce any significant increase in the reaction yield.

The average coupling yield for each condensation step was more than 90%. After each coupling the product was isolated, purified by silica gel column flash chromatography and completely characterized. The linear peptide purity, determined by ^{1}H-NMR, reached more than 95% for all the synthesized molecules.

n	*Linear peptide*	*Overall yield%*	*Purity%*
1a	H-Val-Tyr(OBzl)-Leu-Pro-Lys(Z)-OH	20	>95
1b	H-Val-Tyr(OBzl)-Leu-Pro-**D**-Lys(2Cl-Z)-OH	25	>95
1c	H-Val-Tyr(OBzl)-Leu-**D**-Pro-Lys(Z)-OH	25	>95

Table 1. Linear peptides synthesized. The overall yields are referred to the amount of isolate final products after five couplings and relative purification steps. The purities were determined by ^{1}H-NMR.

2.2.3. Head-to-tail cyclization reaction

2.2.3.1. Preliminary investigations and reaction set up

Chemical synthesis of cyclic peptides is more challenging than that of linear peptides. The cyclization is an intramolecular process which is usually carried out in a highly dilute solution (1–0.5 mM). Nevertheless, cyclic dimers and oligomers are produces also in this condition.

The synthesis of the cyclic peptide was performed in solution in high dilution condition by *head-to-tail* approach which consists in the formation of an amide bond between the *C*- and *N*- terminal of the linear sequence.

A preliminary investigation was performed to evaluate all the possible variables, including the possible *C*-terminal epimerization,[16-18] that can affect the *head-to-tail* cyclization.

2.2.3.1.1. Effect of different coupling reagents on cyclization

In order to study the effect of the coupling reagents on the cyclization reaction three commercially available condensing agents (PyBOP, HATU and PPAA) were chosen to cyclize the linear peptide **1a** (shown in Table **1**) which was selected as model peptides during these preliminarily investigations.

The aim of this investigation was to identify the best coupling reagent in terms of yield in the desired compound and formation of by-products, mainly derived by *C*-terminal epimerization or dimerization.

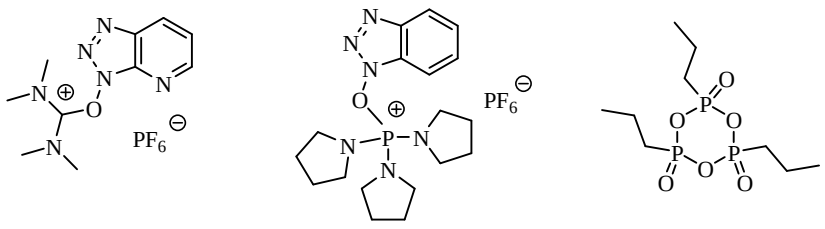

HATU **PyBOP** **PPAA**

Figure 3. Condensing reagents tested during the preliminary investigation of the cyclization reactions in solution.

The uronium reagent HATU and the phosphonium one PyBOP were chosen due to their well-known capability to maximize the cyclization yield while inducing a low

racemisation.[13] PPAA was selected due to the generation of water soluble by-products easily removable at the end of the reaction[14,15] and because it is commercially available as DCM solution which allow to perform the coupling reaction in a low boiling point media speeding up the reaction work-up and the product isolation.

All the cyclization reactions were carried out in highly dilute solution and monitored by TLC, although, due to the diluted condition it was not easy to follow the reaction progress. In the three reactions tested, after 72-56 hours, no traces of linear precursor were detected which suggested that, for this cyclization, the choice of the coupling reagent had no a great effect on the reaction time.

The cyclization products were purified by silica gel column chromatography obtaining the final cyclic pentapeptides with purity higher than 90%, as analyzed by ^{1}H-NMR.

The experimental data (listed in the Table **2**) show that the yield of cyclization using PPAA is much higher (56%) to the one obtained with HATU (20%) or PyBOP (12%).

Nevertheless, the NMR characterization of the cyclopeptide **1c** has shown a double set of signals. As consequence, a variable temperature NMR characterization was performed to clarify the data. The observed proton patters did not change at different temperatures (25-60 °C) and this might suggest that the signals are related to a mixture of epimers rather than rotamers.

In order to confirm this hypothesis a new cyclization reaction was carried out using again PPAA as coupling reagent but with a different linear peptide (**1b)** which differs from the previous sequence for a D-Lys instead of the natural one. The reaction was performed under the same experimental condition describe before, but in this case, during the product purification were isolated two distinct products that were characterized by mass spectrometry and nuclear magnetic resonance.

MS-HPLC analysis indicate that the two compounds have the same molecular mass, whereas, their ^{1}H-NMR spectrums evidences negligible differences except for the signals at 4.00 ppm which correspond to one of the $^{\delta}$H proton of proline.

Temperature dependence ^{1}H-NMR investigation was performed to further characterize the conformation of the cyclopeptides. The spectra showed the presence of a single defined conformation for each peptide excluding that the two compounds were conformers. These results suggested that the two products should be different diastereoisomers due to a *C*-epimerization induced by PPAA during the reaction.

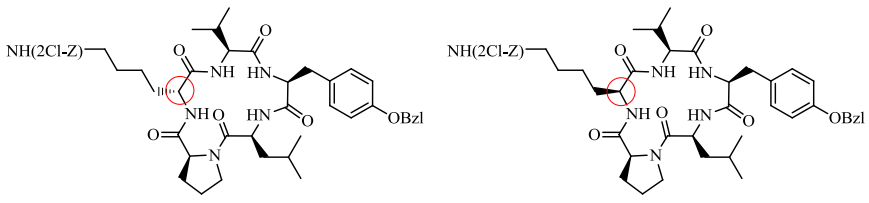

Figure 4. The two different diastereoisomers due to a *C*-epimerization induced by PPAA.

Differently, the cyclopeptides obtained using PyBOP and HATU have been isolated as single product by flash chromatography and the subsequent characterization confirmed the optical purity of both.

The obtained results suggest that, despite PPAA provides higher cyclization yield, it could induce the epimerization on the *C*-terminal leading to a mixture of the two epimers. On the other hand, the uroniun (HATU) and phosophonium (PyBOP) activating coupling reagents

provided cyclopeptides in moderate yields but strereochemically pure. Moreover, PyBOP and HATU provide similar yield in the desired compound but HATU was preferred due to the lower amount of by-products generated during the reaction.

n	*Cyclic peptide*	*Condensing agent*	*Yield %*
***cyclo*-1a**	&Val-Tyr(OBzl)-Leu-Pro-Lys(Z)&	PyBOP	12
***cyclo*-1a**	&Val-Tyr(OBzl)-Leu-Pro-Lys(Z)&	HATU	20
***cyclo*-1a**	&Val-Tyr(OBzl)-Leu-Pro-Lys(Z)&	PPAA	56[a]
***cyclo*-1b**	&Val-Tyr(OBzl)-Leu-Pro-**D**-Lys(2Cl-Z)&	PPAA	50[a]

Table 2. Effects of different coupling reagents on the cyclization yields. The yields are referred to the isolated products after purification by column chromatography. The purities were determined by ^{1}H-NMR. a: mixture of two epimers.

2.2.3.1.2. The role of the solvent

Standard peptide coupling are normally performed in DMF to ensure a complete solubility of all the reagents. Nevertheless, mixing the DMF with lower boiling point solvents could simplify the reaction work-up and speed up the product isolation reducing the risk of the product decomposition. For this reason, the effect on the conversion in the cyclized product of reaction mixture between DMF and DCM, in one case, and ACN in the second was investigated. DMF was kept as major solvent to ensure a complete solubility of the coupling reagent, and 1:2 mixtures with DCM or ACN were tested. The experimental results have shown that the presence of DCM or ACN was not affecting the yield in the desired product compared to the reaction in pure DMF.

2.2.3.1.3. Influence of D amino acid along the sequence

In addition to the steric hindrance, another important factor for an efficient peptide cyclization is the conformation of the linear peptide in solution. In fact, when the secondary structure of the linear peptide is ready to form turn-induced structures, it may provide proximity between the *N*- and the *C*-terminus and increase the chance for ring closure. A well-known way to induce a turn-structures is to introduce in the linear precursor residues with D-L alternating configuration.[19,20]

Moreover, the yield of cyclization could be increased if the ring closure occurs between two residues of opposite stereochemical configuration and when the β-turn-induced structural elements are embedded midway along the linear precursor.

Based on these considerations, we synthesized a subset of linear analogues of the peptidomimetics ***cyclo-1*** (Figure **2**) characterized by the same residues in the peptide sequence but with different chirality (Table **3**).

The cyclization reactions of these analogues were performed with the aim to identify the best position in which the D-amino acid may pre-organize the linear peptide into a suitable structural conformational that promote the cyclization.

A L-lysine or a L-proline were replaced with a D-lysine or a D-proline to form an alternated configuration structure, and the cyclization was carried out in high dilution conditions in DMF using HATU in presence of HOAt as coupling reagent.

The experimental data (listed in the Table **3)** show that the linear peptides contain a D-proline could provide a much higher cyclization yields compared to the structures containing all L-natural amino acid residues or a D-lysine.
These results agree with the consideration that a D-amino acid is able to introduce a *cis*-conformation in the relative amide bond, but its position along the sequence has different degrees of influence.[21]
A D-amino acid in the position (*i*+1) generates a *cis* conformation in the middle of the peptide sequence, resulting in an enhanced cyclization yield. The D-amino acid in position (*i*), although introduces again a *cis*- conformation, produces a weaker positive effect due to the different position along the chain, on the intramolecular cyclization.

n	***Cyclic peptide***	***Condensing agent***	***Time (h)***	***Yield %***
***cyclo*-1a**	&Val-Tyr(OBzl)-Leu-Pro-Lys(Z)&	HATU	72	20
***cyclo*-1b**	&Val-Tyr(OBl)-Leu-Pro-**D**-Lys(2Cl-Z)&	HATU	56	25
***cyclo*-1c**	&Val-Tyr(OBzl)-Leu-**D**-Pro-Lys(Z)&	HATU	56	45

Table 3. Results relative to the investigation of D-amino acids position along the sequence on peptide cyclization. The yields are referred to the isolated products after purification by column chromatography. The purities were determined by ^{1}H-NMR.

The present study suggested that an improvement of the *head-to-tail* intramolecular cyclization yield can be obtained by the introduction of a D-amino acid in the position (*i*+1) along the chain.
Moreover, the characterization of the cyclopeptide **1b** has provided the NMR spectra of the enantiomeric pure product which was used as references to quantify the racemisation rate obtained during the cyclization of the same product with PPAA as condensing agent. Expected stereoisomer and its Lys epimer are in ratio 2:1.

These preliminary investigations, besides providing useful guidelines about the reaction conditions and the linear peptides structural features, have lead to the synthesis of three different cyclic pentapeptides (Figure **5**) characterized by exactly the same residues but with a different stereochemistry. Thus, these products will show different conformational properties and allow exploring a wider conformational space, giving more chance to identify a possible candidate as p50 NF-*k*B homodimerization inhibitors.

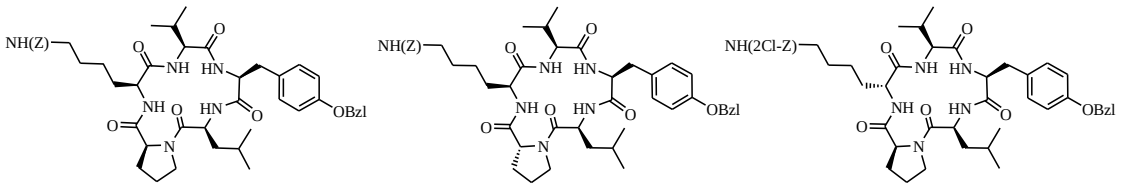

&Val-Tyr-Leu-Pro-Lys&
***cyclo*-1a**

&Val-Tyr-Leu-**D**-Pro-Lys&
***cyclo*-1b**

&Val-Tyr-Leu-Pro-**D**-Lys&
***cyclo*-1c**

Figure 5. Cyclic pentapeptides synthesized during the first part of this project devoted to the identification of the best reaction conditions and linear peptide features that promote the peptide cyclization.

2.2.3.2. Cyclic peptides deprotection

The fully deprotected cyclopeptides were achieved after the removal of the benzyl (Tyr) and carboxybenzyl (Lys) protecting groups by hydrogenolysis palladium catalyzed. The reaction was performed on the pure cyclopeptides under the standard conditions with $Pd(OH)_2$ on activated charcoal in hydrogen atmosphere. The progress of the reaction was monitored by TLC and the product formation was confirmed by MS-HPLC of the reaction mixture.

Despite both TLC and MS analysis confirm the product formation and the successful outcome of the reaction, after the catalyst removal and the solvent evaporation, the final product is poorly soluble in many solvents (including MeOH in which was carried out the hydrogenolysis reaction) also at high temperature (50 °C), thus complicating the product characterization. Because of the small quantity of final product, deuterated DMSO was not used to attempt a NMR characterization, as would result in the loss of the product.
At this point it was decided not to devote too much effort to search an alternative deprotection procedure but to settle for a limited characterization of these products.

We suppose that the low solubility of the cyclopeptide in pure solvents could be related to the amphipathic character of the molecule. The hydrophilic moieties amino (Lys) and hydroxyl (Tyr) groups together with hydrophobic hydrocarbon (Val and Leu) and aromatic (Tyr) side chains provide an overall amphiphilic nature to the peptide lowering its solubility both in polar and apolar solvents. It has been also supposed that the pi-pi stacking between the Tyr aromatic rings could promoted the peptides aggregation decreasing the solubility.

2.2.3.3. Development of serine containing cyclopeptide

Based on the results obtained during the preliminary trials, the synthesis of a second cyclic pentapeptide ***cyclo*-2a,** similar to the previous one but with a serine instead of the lysine, has been designed. In addition, considering the important role of the cyclization position, an appropriate disconnection has been evaluated, avoiding the use of a β-branched amino acid as *C*- or *N*-terminal. To this end, we have designed a new linear peptide in which the *head-to-tail* amide bond will be performed between a serine and a leucine.

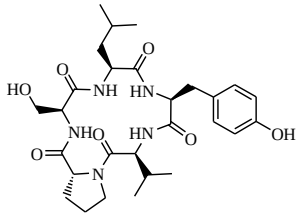

&Leu-Tyr-Val-**D**-Pro-Ser&

***cyclo*-2a**

Figure 6. Pentacyclic peptide synthesized based on the sequence *cyclo*-(LYVPS).

Based on the previous investigation, for this sequence only the analogue with a D-proline has been synthesized. The synthesis of this linear peptide was performed in solution using orthogonally protected amino acids and the standard reaction conditions protocol. The final product was purified by silica gel column chromatography obtaining good overall yield and a high degree of purity. (Table **4**)

n	*Linear peptide*	*Yield %*	*Purity %*
2	H-Leu-Tyr(OBzl)-Val-**D**-Pro-Ser-OH	25	> 95

Table 4. Linear peptide synthesized. The overall yield is referred to the amount of isolate final products after five couplings and relative purification steps. The purity was determined by ^{1}H-NMR.

The cyclization of the linear peptide **2** (Figure **6**) was performed in solution using the *head-to-tail* approach in accordance with the best conditions previously identified (HATU as coupling reagent, in presence of HOAt at room temperature under high DMF/DCM dilution). The progress of the synthesis was checked at different stages by TLC and after 48 hours the linear precursor was completely consumed.
The crude purification by silica gel column chromatography provides the desired cyclic peptide ***cyclo*-2** in very good yield. (Table **5**)

The results related to this synthesis show that for this sequence the product yield is significantly higher, suggesting how the peptide disconnection in the precursor sequence could determines the success of a cyclization reaction. The removal of the tyrosine benzyl group by hydrogenolysis palladium catalyzed afforded the final deprotected ***cyclo*-2a** with high yield and purity (95%).

Contrary to what was observed with the Lys containing cyclopeptides, the cyclopeptide ***cyclo*-2a** showed good solubility in polar solvents (e.g. MeOH and solvent mixture ACN/water). This difference could be related to a less hydrophobic character due to the shorter hydrocarbon side chain of the Ser compared to the Lys one. Moreover the hydroxyl groups (Ser and Tyr) could improve the solvation of the molecules forming a hydrogen bonds pattern with polar solvents.

n	*Cyclic peptide*	*Condensing agent*	*Time (h)*	*Yield %*
***cyclo*-2**	&Leu-Tyr(OBzl)-Val-**D**-Pro-Ser&	HATU	48	65

Table 5. Pentacyclic peptide synthesized. The yield is referred to the amount of isolate final product after the cyclization reaction and the relative purification step. The purity was determined by ^{1}H-NMR.

2.2.3.4. An alternative method for macrocyclization: cyclic peptide synthesis with thioacids.

The results obtained with the classic *head-to-tail* cyclization approach provided acceptable results in terms of yield. Nevertheless another innovative cyclization method, recently proposed by Crich and Sasaky,[22] was tested. In this procedure an amide-bond-forming sequence employing peptide thioacids in association with the Sanger's reagent (1-fluoro-2,4-dinitrobenzene) is viable for the cyclization of penta and hexapeptides. The power of this method, in which a carboxyl group is activated as a thioester and the cyclization occurs *in situ* in the presence of Sanger's reagent, is due to the much shorter time (5 minutes) compared to the classic cyclization condition (hours or days) and to the wide range of compatibility with functional groups such free carboxylic acid and hydroxyl moieties. Moreover the *C*-terminal epimerization, which typically plague this kind of reactions, is completely suppressed.

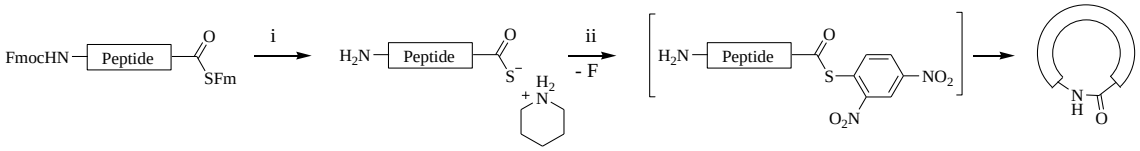

Scheme 2. Schematic representation of cyclopeptide synthesis with the thioacid approach. i) Piperidine 20% in DMF, (15 min), ii) Sanger's reagent (1-fluoro-2,4-dinitrobenzene) in DMF 5mM, (5 min).

In order to try this new synthetic approach, new linear peptides with *C*-terminal protected as fluorenylmethyl thioester (Fm) were prepared.

9-Fluorenylmethanethiol **6** was previously prepared and linked as *C*-terminal protecting group in order to avoid the potential racemization on the *C*-terminal.

The synthesis was performed following the reported methodology[23] starting from the commercially available 9-fluorenyl methanol **3**, that was subjected to nucleophylic substitution to give a 9-fluorenylmethyl *p*-toluenesulfonate **4**, further treatment with potassium thioacetate followed by DIBAL reduction gave 9-fluorenylmethanethiol **6**.

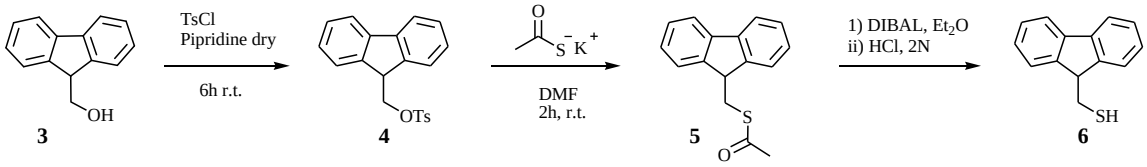

Scheme 3. Preparation of 9-Fluorenylmethyl (Fm).

Boc chemistry was used during the assembly of the linear peptide due to the incompatibility between the Fm thioester and the Fmoc chemistry conditions.[24] The tetrapeptide fluorenylmethyl thioester was constructed by standard solution phase Boc chemistry and the *N*-terminal Boc group was removed by TFA treatment. Finally the last amino acid was incorporate as Fmoc carbamate.

The cyclization was carried out by an initial treatment with piperidine of the *N*-terminal Fmoc-protected and *C*-terminal 9-fluorenylmethylthioester peptide which releases a *seco*-thioacid peptide. Without isolation, Sanger's reagent was added and the cyclization reaction occurs rapidly in only in 5 minutes at room temperature. The reaction proceeds through an initial SN_{Ar} reaction with Sanger's reagent to generate a reactive thioester *in situ* which can be attack by the *N*-terminal amino group forming the cyclopeptide.

The experimental results (Table **6**) show that, with this synthetic methodology, the linear precursor sequence determines the success of the cyclization reaction. The linear peptide **1a'** reacts providing the corresponding cyclo derivative in good yield, while the analog (**1c'**), with all L amino acids, under the same reaction conditions, was not able to cyclize. These data suggests that, for this sequence, a D-proline is crucial to obtain the desired final product. On the other hand, the linear peptide **2a'** characterized by a D-proline and a serine instead to a lysine gives the corresponding cyclopeptide, but in a considerable lower yield compared to the cyclization using HATU as coupling reagent (Table **5**, ***cyclo*-2**).

Despite the short reaction time, that positively characterizes this synthetic method, in our experiments no improvement in the final yields was observed. In addition, the multiple purification steps required to isolate the cyclic compounds, due to the large number of by-products formed, resulted in a considerable reduction of the overall yield of the peptides.

n	*Cyclic peptide*	*Time (min)*	*Yield %*	*Purity %*
***cyclo*-2'**	&Leu-Tyr(OBzl)-Val-**D**-Pro-Ser&	5	50	90
***cyclo*-1a'**	&Val-Tyr(OBzl)-Leu-Pro-Lys(Z)&	5	-	-
***cyclo*-1c'**	&Val-Tyr(OBzl)-Leu-**D**-Pro-Lys(Z)&	5	30	90

Table 6. Results of cyclic peptides synthesis using thioacids in association with Sanger's reagent. The yields are referred to the isolated products after purification by column chromatography. The purities were determined by ^{1}H-NMR.

2.2.4. Design and synthesis of a cyclic pentapeptide library

2.2.4.1. Synthesis on solid phase (Introduction)

During the last year of my PhD studies I have spent some months at the IRB institute in Barcelona as a visiting student in the Prof. Giralt's group. In this period I got the opportunity to learn and gain experience in the peptide solid phase synthesis (SPPS). This methodology, in which the peptide is synthesized keeping the *C*-terminus covalently bound to an insoluble polymeric support, presents many advantages over the classical solution phase method.[25,26] First for all the synthesis is faster. The reactions are driven to completion using an excess of reactants and reagents and the separation of the growing peptide from the by-products and the unreacted amino acids is performed by a simple filtration without any further purification.

No mechanical loss occurs due to the fact that the growing peptide is retained on the polymer in a single reaction vessel throughout the synthesis. The final peptide is released from the polymer support by a single cleavage step at the end of the synthesis. Moreover the side chain protecting groups can also be cleaved in the same step in order to simplify the work-up and the isolation of the final peptide.

2.2.4.2. Library design

The SPPS technique was exploited to synthesize a library of pentacyclic peptides, which will be screened as p50 NF-κB homodimerization inhibitors.

The library molecules are analogues of those developed using the peptide solution synthetic approach and differ one from another by a single amino acid in the sequence.

This differentiation among the components of the library allows the evaluation of the different side chains and functional groups effects on the interaction with the protein and the identification of peptide bioactive conformation.

Furthermore, this could provide key-information regarding the nature of interactions involved, which can direct further modification in order to increase and modulate the binding affinity.

Several amino acids have been selected for the construction of the library, in order to explore a wider range of different properties. The majority of them were natural occurring ones such: arginine (R), glutamic acid (E), tryptophan (W), alanine (A), cysteine (C) and glutamine (Q). To the mentioned below, two non-natural residues were also considered: 4-amino-phenylalanine (Phe(4NH_2)) and the α,β-diaminopropionic acid (Dap).

Amino acids with different charges, such as glutamic acid and arginine, have been selected to evaluate the electrostatic contribution and capability to form salt bridges with the p50 binding site.

Arginine residues are broadly employed for the specific biomolecular recognition, which exploits the potential of the bidentate electrostatic and hydrogen-bond interaction.[27] The R guanidinium group confers basic properties, due to the conjugation between the double bond and the nitrogen lone pairs, meaning that the positive charge is delocalized an enables the formation of multiple H-bonds (Figure **7**).
Hydrophobic residues such as tryptophan and alanine were selected considering the large number of hydrophobic interactions at the protein-protein interface. Over than providing hydrophobic character to the peptidomimetic, the tryptophan indole ring could be involved in stacking interactions with other aromatic residues of the protein. On the other hand, alanine, one of the simplest aliphatic α-amino acids, provides weaker hydrophobic character but due to a less steric hindrance and a reduced side chain flexibility could play a role in the affinity modulation towards the protein.

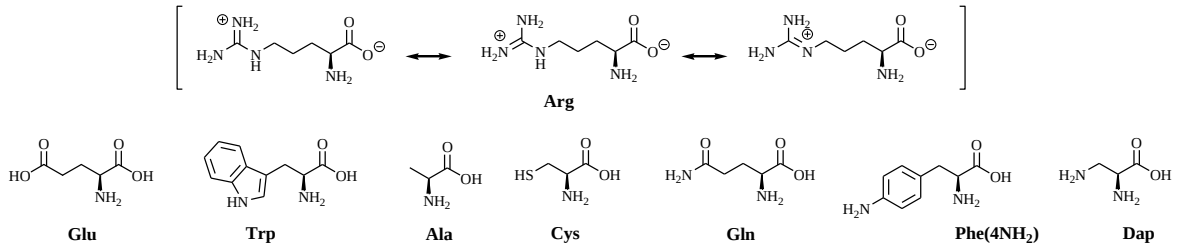

Figure 7. Subset of amino acids considered for the development of the cyclic pentapeptide library.

Cysteine and glutamine were selected to test the effect, respectively, of the thiol or the amide groups on the protein interaction and because these groups can allow a further chemical modification of the cyclopeptide.
We have also taken in account two non-natural amino acids: the 4-amino-phenylalanine (Phe($4NH_2$)) and the α,β-diaminopropionic acid (Dap). Both contain a primary amine group which can be exploited to conjugate or modify the cyclic peptide. Moreover, the 4-amino-phenylalanine should provide hydrophobic and stacking interactions due to the aromatic ring. The α,β-diaminopropionic acid (Dap), similar to a lysine in chemical properties terms, bears an amino functional group at the terminus of a shorter and less flexible hydrocarbon side chain, which could results in a different specific recognition with the target.

Based on these considerations we have designed a series of cyclic pentapeptides with a general formula *cyclo*-(R-Val-Tyr-Leu-D-Pro) where R is one of the amino acids with different functional groups described above. The target compounds common feature is based, as previously described, on the recognition sequence of the biological target, meaning that it will contain the three key amino acids involved in the p50 homodimerization. D-proline has been selected as a β-turn element based on the good results obtained during the preliminary investigation of this project.

2.2.4.3. Peptide synthesis

The linear peptides synthesis on solid phase was performed on the Barlos (2-Chlorotrityl chloride) resin[28] as solid support. This is one of the most useful resins for the SPPS of *C*-terminal peptide acids,[29-31] and minimizes the formation of diketopiperazine (DKP) due to the presence of the hindering trityl group and of the chlorine substituent in position 2.[32] This is of relevance in this case because the presence of consecutive L and D amino acids,

that are highly prone to form this stable cycle before the incorporation of the third residue, results in the loss of the two first amino acids and in deletions along the sequence.[33]
Moreover, Cl-Trt-resin reduces the risk of racemization during the incorporation of the first amino acid. This is related to a different coupling through a nucleophilic substitution instead of a carboxylic group activation required for the anchorage to hydroxyl-based resins. Finally, this resin allows the cleavage of the peptide under very mild acid conditions and in the presence of *t*Bu-based protecting groups.[34,35]

The synthesis was performed based on Fmoc/*t*Bu approach, which implies the use of orthogonal protecting groups, that can be, respectively, removed by treatment with piperidine and TFA.[36]
This approach is particularly efficient in the synthesis of complex peptides, in which orthogonality should be introduced.[37] An additional advantage of the Fmoc/*t*Bu strategy is that the use of strong acids, such as HF or trifluoromethanesulfonic acid is not required.
The peptides of the proposed library presented high structural analogy one to another which allowed us to perform a SPPS of a common building block containing the shared sequence Leu-Tyr-Val-D-Pro. Subsequently the resin was split in equal portions to perform the last coupling with the different selected amino acids for the library construction.

2.2.4.3.1. Preliminary investigations

Different amino acids have been considered as starting point for the synthesis of the linear peptide. In particular, the use of a proline as *C*-terminal has been evaluated because it would prevent the epimerization during the cyclization reaction. On the other hand anchoring a D-proline on the resin could lead to diketopiperazine (DPK) formation, lowering the yield of the synthesis.

n	*Linear sequence*	*DKP %*	*Epimerization %*	*Cyclic peptide %*	*Cyclic Dimer %*
7	H-Val-Tyr-Leu-**D**-Pro-Lys-OH	-	6	35	20
8	H-Lys-Val-Tyr-Leu-**D**-Pro-OH	30%	-	45	10

Table 7. Results of preliminary investigations.

In order to evaluate the percentage of DKP formation using a D-proline as the first amino acid, two different linear peptides containing the same residues have been synthesized. The first one with a D-proline directly attached on solid support, and the second with the D-proline in position (*i*+1).
The experimental results show that 30% of DKP was formed when the D-Pro was the *C*-terminal, despite the presence of the Cl-Trt moiety of the resin. On the other hand, DKP formation was not detected with the proline in the position (*i*+1).
In parallel, it has been evaluated how the D-proline position along the sequence can promote the peptide cyclization.
The reactions were carried out in solution under high dilution with DPPA/$NaHCO_3$ as a coupling reagent. The reaction progress was monitored by HPLC and in both cases, after 48 h the linear precursors were not detected. The fully deprotected cyclic peptides were obtained after removal of the *t*-Bu protecting groups by acidolysis with TFA. The purification was performed by column chromatography giving the final products.

The cyclization yield seems to be related to the position of the D-Pro along the sequence. When the D-Pro is present as *C*-terminal, the formation of side products (e.g. epimers, cyclo dimers) is reduced, on the contrary, the amount of undesired by-products derived from racemization and cyclo dimerization is increased when the D-Pro is shifted in the (*i*+1) position.

These observations are in contrast to what was concluded after the preliminary investigations at the beginning of this project, in which the D-Pro in (*i*+1) position was defined as the best driving force for the peptide cyclization. Probably the divergent results are associated with the different condensing agents employed. The cyclization of the linear peptide bearing a D-Pro in (*i*+1) and using DPPA yielded a low amount of the desired product while produced large formation of the cyclo dimer derivative. This may be due to the high reactivity of DPPA which promotes the peptide cyclization but also its cyclodimerization.
Based on these results and in order to obtain the final products in good quality and high yield, it was decided to perform the peptide cyclization lowering the DPPA equivalents (from 2 to 1.5) and placing the D-proline as C-terminal. As a consequence, the following efforts were directed to overcome the DKP formation.
The DKP formation, in this context, was promoted by the basic conditions for the Fmoc deprotection of the second amino acid in the sequence.[38-41]
Different approaches to avoid this problem have been evaluated. The simplest way consists in a shorter reaction time (2 cycles of 3 minutes) for the Fmoc removal from the second amino acid, which reduced but did not prevent the formation of DKP.
A more efficient approach consists in the replacement of the *N*-Fmoc of the second amino acid with a protecting group that can be removed in neutral conditions. *N*-allyloxycarbonyl (Alloc) was chosen as protecting group because of the orthogonality to the *t*-Bu and Fm groups and the neutral condition needed for the smooth cleavage.[42-46]

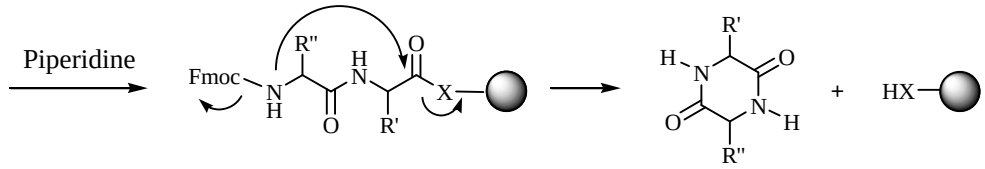

Scheme 4. Schematic representation of diketopiperazine (DKP) formation under basic conditions.

The removal of allyl carbamates involves a palladium-catalyzed transfer of the allylic unit to various nucleophiles/scavengers in presence of a proton source. $Pd(PPh_3)_4$ is probably the most used and well-known catalyst for this reaction while, special attention must be done on the choice of the nucleophile.[47] Nucleophilic secondary amine such as morpholine as allyl acceptor leads to deprotection of Fmoc group.[45] Similarly, the choice of Me_2NSiMe_3-CF_3CO_2SiMe is not compatible with *t*-Bu-based protecting groups.[48] Based on these considerations, we decided to use phenyltrihydrosilane ($PhSiH_3$) which has been reported as a neutral allyl group scavenger.[49]

Therefore, an Alloc-Leucine has been synthesized, considering that it is placed as second residues in the sequence of the design cyclopeptides. The synthesis was performed according to the reported procedure[50] in one pot, with free amino acids and sodium azide as

reagents.
Alloc-Cl reacts with NaN_3, forming the corresponding Alloc-azide, that lead to the final product by direct reaction with the free amino acid, without any intermediate purification.
This procedure does not require the temporary protection of the carboxyl function of the amino acid and, the formation of Alloc-dipeptide and by-products is significantly reduced compared to the one employing Alloc-Cl as acylating agent.[51-53]

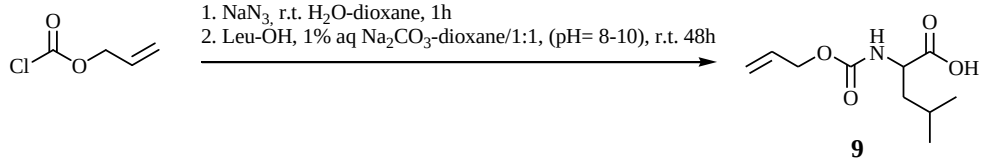

Scheme 5. Synthesis of Alloc-leucine.

2.2.4.3.2. Synthesis of linear peptides on solid phase

Ten linear pentapeptides were synthesized in a stepwise way with SPPS approach starting from a D-proline as *C*-terminal amino acid. The linear peptides were load on an acid labile Cl-Trt resin followed by the standard Fmoc/*t*Bu protocol.
In agreement with the developed synthetic strategy, after the removal of the Fmoc group on the fourth residue, the resin was split in ten equal portions; each one was coupled with one of the ten selected amino acids as *N*-terminal of the peptidic sequences.

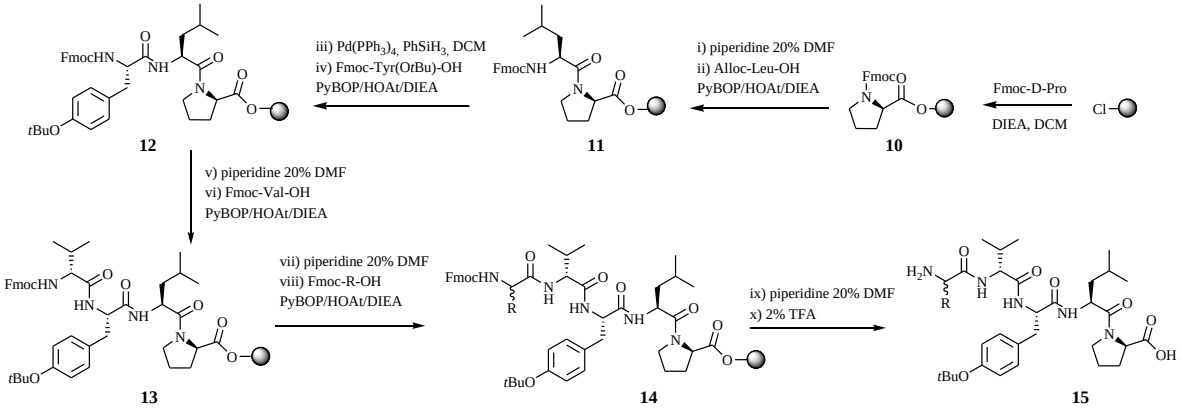

Scheme 6. Synthesis of the linear peptides members of the library. R= Lys, Dap, Cys, Glu, Gln, Arg, Ser, Ala, Phe($4NH_2$), Trp.

The peptide backbone elongation was carried out with PyBOP/HOAt/DIEA as coupling reagents and DIPEA as base. The reaction progress was monitored using the Kaiser test[54] for primary amines and De Clercq[55] or Chloranil[56] test for the secondary amines.
The Fmoc cleavage was performed according to the standard conditions (20% piperidine in DMF) whereas the removal of the Alloc group from the leucine was carried out under neutral conditions with a catalytic amount of $Pd(PPh_3)_4$ in presence of $PhSiH_3$ as scavenger.
After completion of the peptide chain assembly, the resin was cleaved in mild acidic condition (2% TFA in DCM) retaining the side chain protecting groups.
The products were completely characterized and the HPLC analysis show high degree of quality (purity > 90%). for each crudes (Results listed in Table **8**). As a consequence, the linear peptides were not further purified but directly subjected to cyclization.

2.2.4.3.3. Peptide cyclization

The peptides cyclization was performed in DMF solution [5 mM] with DPPA (Diphenylphosphoryl azide) as condensing agent together with $NaHCO_3$ as base.
These conditions were chosen based on the hexapeptides cyclization one developed with remarkable results in the *Cancertech* project (data reported in the chapter 2 *"Results and discussion"* of the Part **II** of this thesis).
The reaction progress was followed by HPLC and the cyclizations of the peptides were completed in a range of 16-48 hours (in relation to the amino acid sequence). $NaHCO_3$ was simply filtered out and the solvent was removed under vacuum. The fully deprotected cyclic peptides were obtained after the *t*Bu protecting groups removal by acidolytic treatment with TFA solution in presence of 5% of water and TIS (Triisopropylsilane) as carbocation scavenger.
The crude products were purified by RP-HPLC in a semi-preparative scale and the pure products were characterized by RP-HPLC, RP-HPLC-MS and ^{1}H-NMR. The desired cyclopeptides were obtained with purity higher than 95% (Table **8**). The overall yields of the desired molecules reach 15-54% and can be considered excellent taking in account the multistep pathway (synthesis linear peptide, cyclization reaction, side chain deprotection and HPLC-purification).

n	Peptide sequence	Linear peptide		Cyclic peptide			
		Yield %	Purity %	Reaction time (h)	Yield %	Purity %	Cyclic dimer %
16	H-Lys-Val-Tyr-Leu-D-Pro-OH	95	95	48	40	> 98	8
17	H-Phe(4-NH_2)-Val-Tyr-Leu-D-Pro-OH	94	85	24	35	> 98	-
18	H-Cys-Val-Tyr-Leu-D-Pro-OH	97	95	24	15	> 98	-
19	H-Glu-Val-Tyr-Leu-D-Pro-OH	80	95	24	45	> 97	-
20	H-Gln-Val-Tyr-Leu-D-Pro-OH	85	98	16	54	> 98	-
21	H-Arg-Val-Tyr-Leu-D-Pro-OH	93	90	16	16	> 98	-
22	H-Trp-Val-Tyr-Leu-D-Pro-OH	92	90	48	30	> 98	10
23	H-Ser-Val-Tyr-Leu-D-Pro-OH	83	90	48	20	> 98	5
24	H-Dap-Val-Tyr-Leu-D-Pro-OH	66	93	24	15	> 98	-
25	H-Ala-Val-Tyr-Leu-D-Pro-OH	74	98	48	46	> 98	6

Table 8. Results related to the synthesis of linear and cyclic peptides. For the linear peptides the purities were determined based on analytical HPLC analysis, whereas the yields were defined through the Fmoc UV quantification during the last Fmoc deprotection step. For the cyclic peptides, the overall yields are referred to the isolated final product (over 4 steps: synthesis linear peptide, cyclization, side chain deprotection and purification) and the purities were determined by HPLC analysis.

The cyclic peptide ***cyclo*-16** has the same sequence of the cyclic peptide **1c** previous synthesized in solution and it was synthesized again by SPPS with the aim to compare the different methodology adopted for their synthesis. As expected, the SPPS provided the linear peptide with significantly higher overall yield compare to the solution approach (95% instead of 20%).

Regard to the peptide cyclization, has been observed that the amide bond formation between a D-Pro (as *C*-terminal) and a Lys (as *N*-terminal) together with DPPA as condensing reagent prevents the epimerization and increase the cyclization reaction yield.

(Table **8**, *cyclo*-16). On the other hand, for the cyclopeptide **1c** for which were chosen a different disconnession and HATU as coupling reagents, has provided lower cyclization yield (Table **3**, *cyclo*-1c).

Finally, the fully deprotected cyclopeptide **9** was obtained after the cleavage of the *tert*-butyl ether (Tyr) and the Boc (Lys) protecting group by acidolytic TFA treatment. The final product was completely soluble in pure MeOH or in a mixture of ACN/H_2O, differently from what was observed for its analogue ***cyclo*-1c**. This different behavior may be due to the lysine side chain amino group which probably being in the protonated form as TFA salt enhanced the cyclopeptide amphiphilic character promoting its solubility in polar solvents.

&Lys-Val-Tyr-Leu-D-Pro& **(*cyclo*-16)**

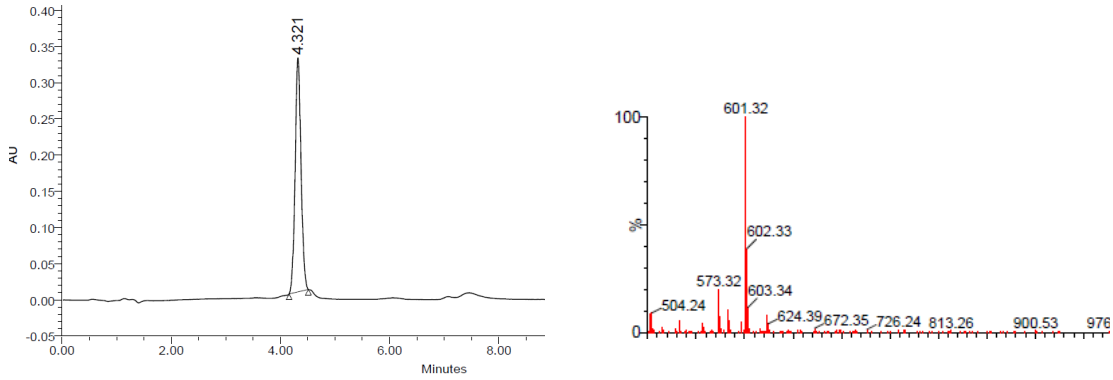

&Phe(4-NH_2)-Val-Tyr-Leu-D-Pro& **(*cyclo*-17)**

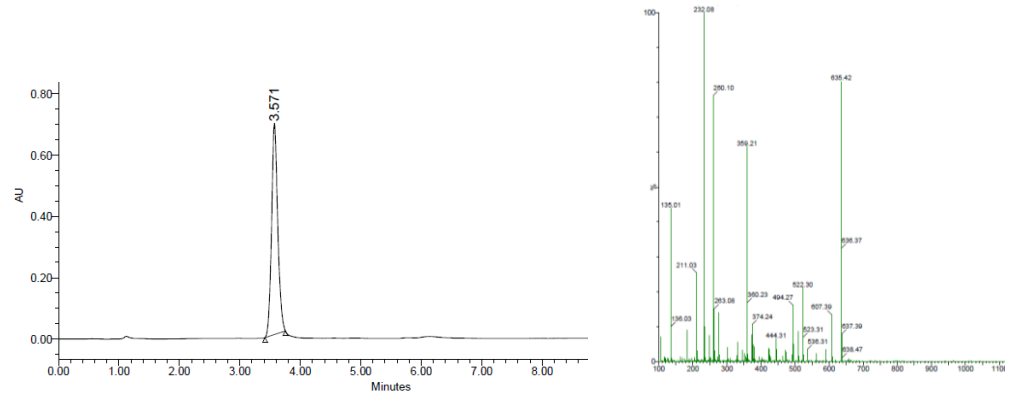

&Cys-Val-Tyr-Leu-D-Pro& **(*cyclo*-18)**

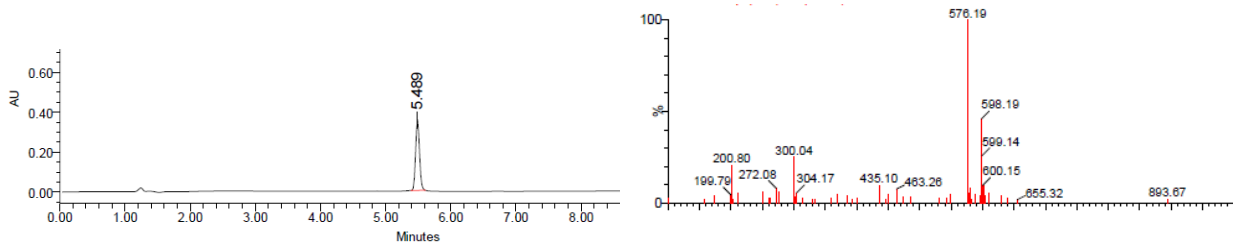

&Glu-Val-Tyr-Leu-D-Pro& **(*cyclo*-19)**

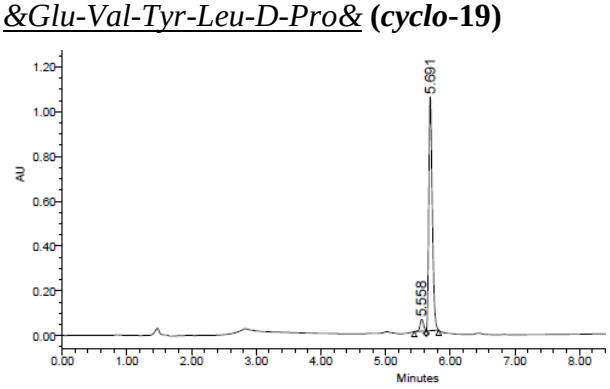

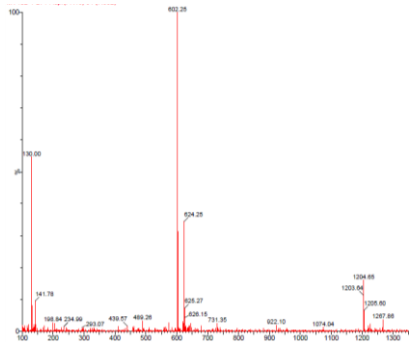

&Gln-Val-Tyr-Leu-D-Pro& **(*cyclo*-20)**

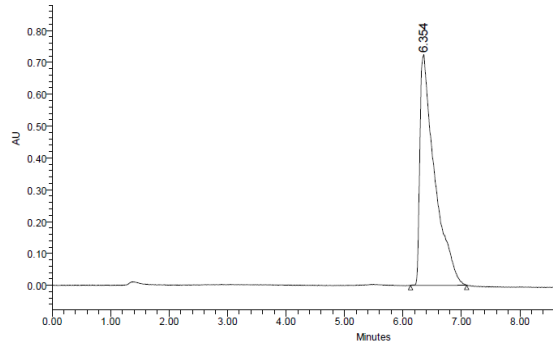

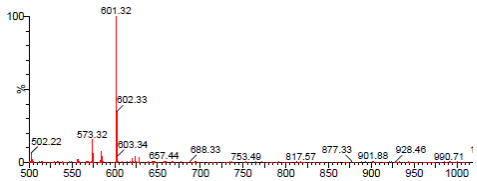

&Arg-Val-Tyr-Leu-D-Pro& **(*cyclo*-21)**

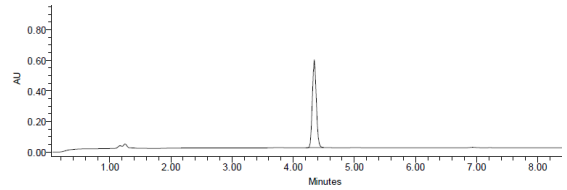

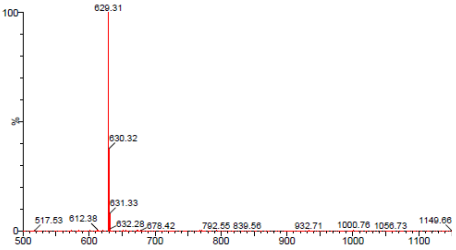

&Trp-Val-Tyr-Leu-D-Pro& **(*cyclo*-22)**

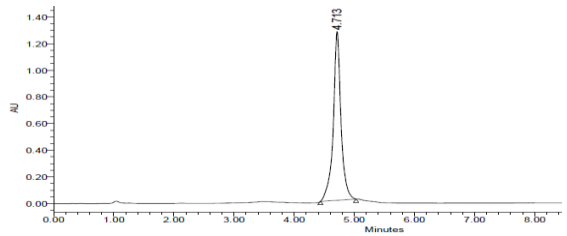

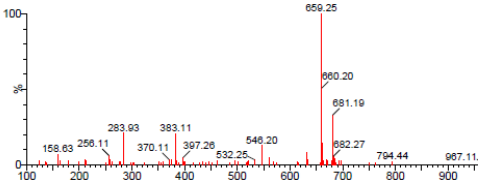

&Ser-Val-Tyr-Leu-D-Pro& **(*cyclo*-23)**

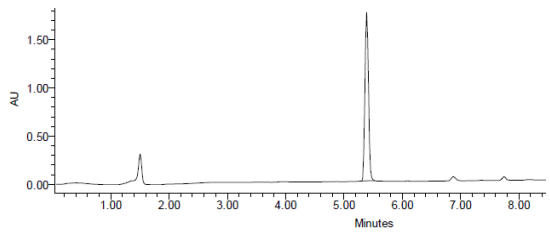

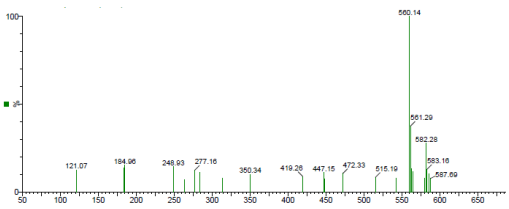

&Dap-Val-Tyr-Leu-D-Pro& **(*cyclo*-24)**

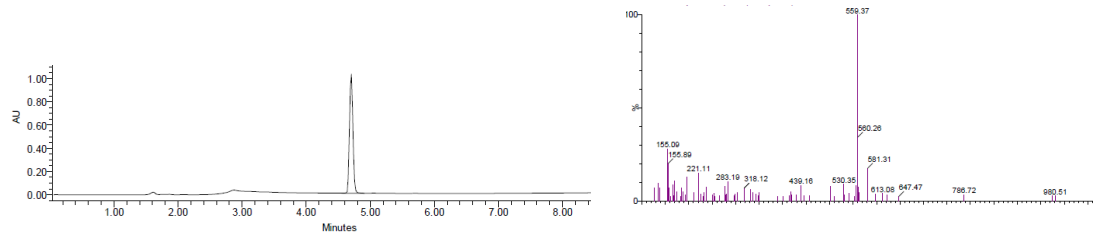

&Ala-Val-Tyr-Leu-D-Pro& **(*cyclo*-25)**

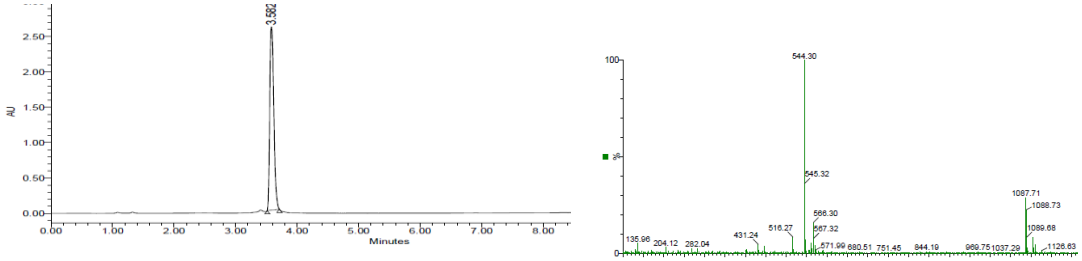

Figure 8. HPLC and RP-HPLC-MS traces of the cyclic pentapeptides of the library after synthesis and purification. HPLC were recorded using a 0-100% B gradient in 8 min (A = 0.045% TFA in H_2O, and B = 0.036% TFA in ACN).

2.2.5. Peptide functionalization on-solid phase

The SPPS methodology was also exploited to modify in solid state a cyclopeptide (***cyclo*-16**) by the acetylation of the lysine side chain amino group with the aim to evaluate the effect of the nitrogen electron pair (Lys-NH_2) on the binding site and on the specific protein recognition.

The synthesis of the linear peptide was performed using the same synthetic approach described before until the tetrapeptide **13**, then was introduced a Boc-Lys(Fmoc)-OH as last amino acid (Scheme **7**) which was deprotected by treatment with piperidine releasing the free amino group. The acetylation was carried out on solid phase using acetic anhydride and DIEA (DMF, 1 h). Subsequently, the peptide was cleaved from the resin and underwent to cyclization in high DMF dilution with DPPA. The product was purified by semipreparative RP-HPLC giving the final product in 30% overall yield.

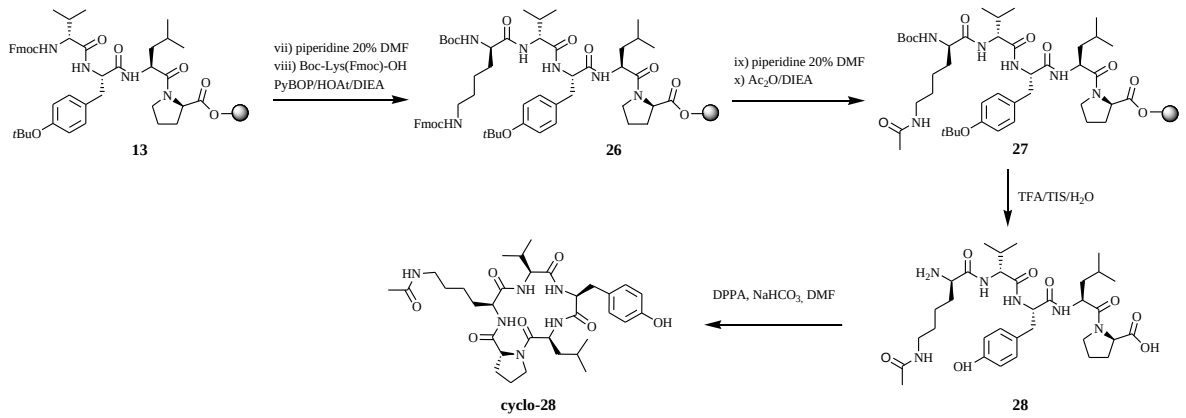

Scheme 7. Synthesis of the acylated version of linear peptides **16**.

&Lys(Ac)-Val-Tyr-Leu-D-Pro& **(*cyclo*-28)**

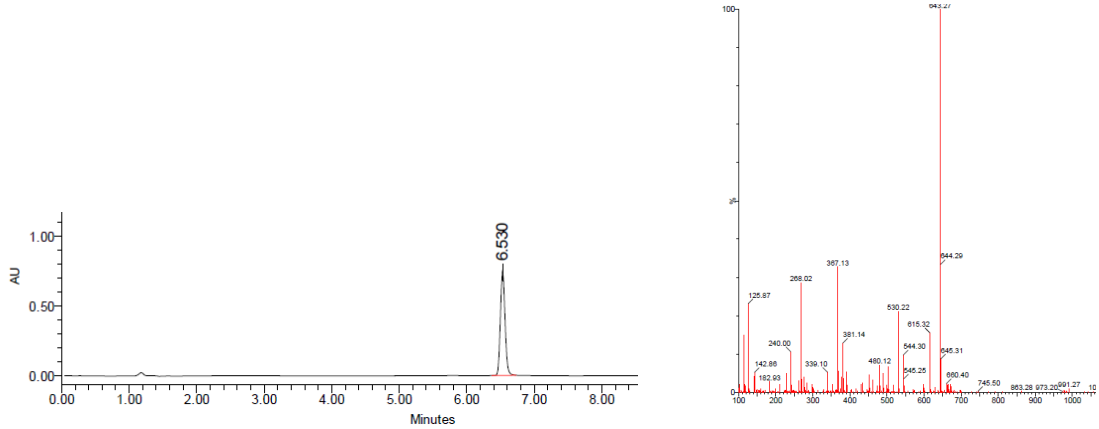

Figure 10. HPLC and MS-HPLC traces of the acylated cyclo peptide **28** after the synthesis and the purification. HPLC was recorded using a 0-100% B gradient in 8 min (A = 0.045% TFA in H_2O, and B = 0.036% TFA in ACN).

2.3. Conclusion

Several cyclic pentapeptides have been synthesized with the aim to explore and modulate the protein-protein interaction (PPI) between two p50 NF-κB subunits, preventing their homodimerization.

Despite the selection of pentacyclopeptides allow a limited structural variability, due to the possibility to introduce only one different amino acid in each sequence, has been generate a library of compounds with a moderate variability that, presenting different conformation and chemical properties, allow to explore a wide conformational range during their evaluation against the p50 homodimerization and maybe lead to identify a possible bioactive compound.

The linear peptides were synthesize using both the solution and solid synthetic approach, observing that SPPS is a more powerful method not only in terms of higher overall yield and reduction of work time to obtain the final product, but also for the possibility to achieve a fast peptide differentiation particularly important for a chemically library production.
The best results for the *head-to-tail* peptide cyclization were obtained using the standard approach in high diluted conditions, with HATU or DPPA as condensing reagents.

The diversity introduced in the cyclopeptides by using residues with different properties enables to largely investigate the defined binding sites and precisely identify the binding residues and the peptide bioactive conformation.
Once a cyclopentapeptide library is generated, the next step will be a quantitative characterization of the protein–peptide interactions, including its structural, biochemical and biophysical parameters. These may include, detecting the residues that mediate the interaction and their differential contribution, measuring the affinity of the interaction and studying its biological role in cells. Thus, a number of biological experiments will be performed on the cyclopeptides synthesized to determine whether some of these show promising results and may be further used as lead compounds to control the PPI as antagonists.

Additionally, these studies could provide important information to properly modifications by introduction of post-translational modifications (e.g., phosphorylation or acetylation), labels (e.g., biotin or fluorescein) or non-natural amino acids to increase the specificity toward the molecular target or to enhance their detection during the biological tests. The peptides can also served as the basis for further design of small molecules to target PPI.

References

(1) Saccani, A.; Schioppa, T.; Porta, C.; Biswas, S. K.; Nebuloni, M.; Vago, L.; Bottazzi, B.; Colombo, M. P.; Mantovani, A.; Sica, A. p50 nuclear factor-kappaB overexpression in tumor-associated macrophages inhibits M1 inflammatory responses and antitumor resistance. *Cancer Res.* **2006**, *66*, 11432-11440.

(2) Sengchanthalangsy, L. L.; Datta, S.; Huang, D.-B.; Anderson, E.; Braswell, E. H.; Ghosh, G. Characterization of the Dimer Interface of Transcription Factor NFκB p50 Homodimer. *J. Mol. Biol.* **1999**, *289*, 1029-1040.

(3) Kessler, H. Conformation and Biological Activity of Cyclic Peptides. *Angew. Chem. Int. Ed.* **1982**, *21*, 512-523.

(4) Hruby, V. J. Conformational restrictions of biologically active peptides via amino acid side chain groups. *Life Sci.* **1982**, *31*, 189-199.

(5) Hruby, V. J.; al-Obeidi, F.; Kazmierski, W. Emerging approaches in the molecular design of receptor-selective peptide ligands: conformational, topographical and dynamic considerations. *Biochem. J.* **1990**, *268*, 249-262.

(6) Toniolo, C. Conformationally restricted peptides through short-range cyclizations. *Int. J. Pept. Protein Res.* **1990**, *35*, 287-300.

(7) Hruby, V. J. Conformational and topographical considerations in the design of biologically active peptides. *Biopolymers* **1993**, *33*, 1073-1082.

(8) Ghosh, G.; van Duyne, G.; Ghosh, S.; Sigler, P. B. Structure of NF-kappa B p50 homodimer bound to a kappa B site. *Nature* **1995**, *373*, 303-310.

(9) White, C. J.; Yudin, A. K. Contemporary strategies for peptide macrocyclization. *Nat. Chem.* **2011**, *3*, 509-524.

(10) Tang, Y.-c.; Xie, H.-b.; Tian, G.-l.; Ye, Y.-h. Synthesis of cyclopentapeptides and cycloheptapeptides by DEPBT and the influence of some factors on cyclization. *J. Pept. Res.* **2002**, *60*, 95-103.

(11) Humphrey, J. M.; Chamberlin, A. R. Chemical Synthesis of Natural Product Peptides: Coupling Methods for the Incorporation of Noncoded Amino Acids into Peptides. *Chem. Rev.* **1997**, *97*, 2243-2266.

(12) Valeur, E.; Bradley, M. Amide bond formation: beyond the myth of coupling reagents. *Chem. Soc. Rev.* **2009**, *38*, 606-631.

(13) Albericio, F. Developments in peptide and amide synthesis. *Curr. Opin. Chem. Biol.* **2004**, *8*, 211-221.

(14) Bailen, M. A.; Chinchilla, R.; Dodsworth, D. J.; Najera, C. 2-Mercaptopyridone 1-Oxide-Based Uronium Salts: New Peptide Coupling Reagents. *J. Org. Chem.* **1999**, *64*, 8936-8939.

(15) Chesworth, R.; Zawistoski, M. P.; Lefker, B. A.; Cameron, K. O.; Day, R. F.; Mangano, F. M.; Rosati, R. L.; Colella, S.; Petersen, D. N.; Brault, A.; Lu, B.; Pan, L. C.; Perry, P.; Ng, O.; Castleberry, T. A.; Owen, T. A.; Brown, T. A.; Thompson, D. D.; DaSilva-Jardine, P. Tetrahydroisoquinolines as subtype selective estrogen agonists/antagonists. *Bioorg. Med. Chem. Lett.* **2004**, *14*, 2729-2733.

(16) McMurray, J. S.; Lewis, C. A.; Obeyesekere, N. U. Influence of solid support, solvent and coupling reagent on the head-to-tail cyclization of resin-bound peptides. *Pept. Res.* **1994**, *7*, 195-206.

(17) Plaue, S. Synthesis of cyclic peptides on solid support. Application to analogs of hemagglutinin of influenza virus. *Int. J. Pept. Protein Res.* **1990**, *35*, 510-517.

(18) Wadhwani, P.; Afonin, S.; Ieronimo, M.; Buerck, J.; Ulrich, A. S. Optimized protocol for synthesis of cyclic gramicidin S: starting amino acid is key to high yield. *J. Org. Chem.* **2006**, *71*, 55-61.

(19) Ji, A. X.; Bodanszky, M. Cyclization studies with a model pentapeptide. *Int. J. Pept. Protein Res.* **1983**, *22*, 590-596.

(20) Bomar, M. G.; Song, B.; Kibler, P.; Kodukula, K.; Galande, A. K. An enhanced beta turn in water. *Org. Lett.* **2011**, *13*, 5878-5881.
(21) Gierasch, L. M.; Deber, C. M.; Madison, V.; Niu, C. H.; Blout, E. R. Conformations of (X-L-Pro-Y)2 cyclic hexapeptides. Preferred beta-turn conformers and implications for beta turns in proteins. *Biochem.* **1981**, *20*, 4730-4738.
(22) Sasaki, K.; Crich, D. Cyclic peptide synthesis with thioacids. *Org. Lett.* **2010**, *12*, 3254-3257.
(23) Crich, D.; Sana, K.; Guo, S. Amino acid and peptide synthesis and functionalization by the reaction of thioacids with 2,4-dinitrobenzenesulfonamides. *Org. Lett.* **2007**, *9*, 4423-4426.
(24) Macmillan, D. Evolving strategies for protein synthesis converge on native chemical ligation. *Angew. Chem. Int. Ed.* **2006**, *45*, 7668-7672.
(25) Merrifield, R. B. Solid Phase Peptide Synthesis. I. The Synthesis of a Tetrapeptide. *J. Am. Chem. Soc.* **1963**, *85*, 2149-2154.
(26) Kimmerlin, T.; Seebach, D. '100 years of peptide synthesis': ligation methods for peptide and protein synthesis with applications to beta-peptide assemblies. *J. Pept. Res.* **2005**, *65*, 229-260.
(27) Balakrishnan, S.; Scheuermann, M. J.; Zondlo, N. J. Arginine mimetics using alpha-guanidino acids: introduction of functional groups and stereochemistry adjacent to recognition guanidiniums in peptides. *Eur. J. Chem. Biol.* **2012**, *13*, 259-270.
(28) Barlos, K.; Gatos, D.; Schäfer, W. Synthesis of Prothymosin α (ProTα)—a Protein Consisting of 109 Amino Acid Residues. *Angew. Chem. Int. Ed.* **1991**, *30*, 590-593.
(29) Barlos, K.; Gatos, D.; Kapolos, S.; Poulos, C.; SchÄFer, W.; Wenqing, Y. A. O. Application of 2-chlorotrityl resin in solid phase synthesis of (Leu15)-gastrin I and unsulfated cholecystokinin octapeptide. *Int. J. Pept. Prot. Res.* **1991**, *38*, 555-561.
(30) Chatzi, K. B. O.; Gatos, D.; Stavropoulos, G. 2-Chlorotrityl chloride resin. *Int. J. Pept. Prot. Res.* **1991**, *37*, 513-520.
(31) García-Martín, F.; Bayó-Puxan, N.; Cruz, L. J.; Bohling, J. C.; Albericio, F. Chlorotrityl Chloride (CTC) Resin as a Reusable Carboxyl Protecting Group. *QSAR & Combinatorial Science* **2007**, *26*, 1027-1035.
(32) Chiva, C.; Vilaseca, M.; Giralt, E.; Albericio, F. An HPLC-ESMS study on the solid-phase assembly of C-terminal proline peptides. *J. Pept. Sci.* **1999**, *5*, 131-140.
(33) Fischer, P. M. Diketopiperazines in peptide and combinatorial chemistry. *J. Pept. Sci.* **2003**, *9*, 9-35.
(34) Barlos, K.; Chatzi, O.; Gatos, D.; Stavropoulos, G. 2-Chlorotrityl chloride resin. Studies on anchoring of Fmoc-amino acids and peptide cleavage. *Int. J. Pept. Protein Res.* **1991**, *37*, 513-520.
(35) Bollhagen, R.; Schmiedberger, M.; Barlos, K.; Grell, E. A new reagent for the cleavage of fully protected peptides synthesised on 2-chlorotrityl chloride resin. *J. Chem. Soc., ChemComm.* **1994**, 2559-2560.
(36) Lloyd-Williams, P. A., F.; Giralt, E. . Chemical Approaches to the Synthesis of Peptides and Proteinss *CRC Press: Boca Raton, FL* **1997**.
(37) Chan, W. C., White, P. D., Eds. Fmoc Solid-Phase Peptide Synthesis. A Practical Approach. *J. Am. Chem. Soc.* **2000**
(38) Gisin, B. F.; Merrifield, R. B. Carboxyl-catalyzed intramolecular aminolysis. A side reaction in solid-phase peptide synthesis. *J. Am. Chem. Soc.* **1972**, *94*, 3102-3106.
(39) Rothe, M.; Mazanek, J. Side-reactions arising on formation of cyclodipeptides in solid-phase peptide synthesis. *Angew. Chem. Int. Ed.* **1972**, *11*, 293.
(40) Khosla, M. C.; Smeby, R. R.; Bumpus, F. M. Failure sequence in solid-phase peptide synthesis due to the presence of an N-alkylamino acid. *J. Am. Chem. Soc.* **1972**, *94*, 4721-4724.

(41) Giralt, E.; Eritja, R.; Pedroso, E. Diketopiperazine formation in acetamido-and nitrobenzamido-bridgedpolymeric supports. *Tetrahedron Lett.* **1981**, *22*, 3779-3782.
(42) Trzeciak, A.; Bannwarth, W. Synthesis of 'head-to-tail' cyclized peptides on solid support by Fmoc chemistry. *Tetrahedron Lett.* **1992**, *33*, 4557-4560.
(43) Handa, B. K.; Keech, E. FMOC solid phase synthesis of an endothelin converting enzyme substrate. Use of allyl ester as the third orthogonal protecting group. *Int. J. Pept. Protein Res.* **1992**, *40*, 66-71.
(44) Kates, S. A.; Solé, N. A.; Johnson, C. R.; Hudson, D.; Barany, G.; Albericio, F. A novel, convenient, three-dimensional orthogonal strategy for solid-phase synthesis of cyclic peptides. *Tetrahedron Lett.* **1993**, *34*, 1549-1552.
(45) Kates, S. A.; Daniels, S. B.; Albericio, F. Automated allyl cleavage for continuous-flow synthesis of cyclic and branched peptides. *Anal. Biochem.* **1993**, *212*, 303-310.
(46) Bloomberg, G. B.; Askin, D.; Gargaro, A. R.; Tanner, M. J. A. Synthesis of a branched cyclic peptide using a strategy employing Fmoc chemistry and two additional orthogonal protecting groups. *Tetrahedron Lett.* **1993**, *34*, 4709-4712.
(47) Thieriet, N.; Alsina, J.; Giralt, E.; Guibé, F.; Albericio, F. Use of Alloc-amino acids in solid-phase peptide synthesis. Tandem deprotection-coupling reactions using neutral conditions. *Tetrahedron Lett.* **1997**, *38*, 7275-7278.
(48) Merzouk, A.; Guibé, F.; Loffet, A. On the use of silylated nucleophiles in the palladium catalysed deprotection of allylic carboxylates and carbamates. *Tetrahedron Lett.* **1992**, *33*, 477-480.
(49) Dessolin, M.; Guillerez, M.-G.; Thieriet, N.; Guibé, F.; Loffet, A. New allyl group acceptors for palladium catalyzed removal of allylic protections and transacylation of allyl carbamates. *Tetrahedron Lett.* **1995**, *36*, 5741-5744.
(50) Cruz, L. J.; Beteta, N. G.; Ewenson, A.; Albericio, F. "One-Pot" Preparation of N-Carbamate Protected Amino Acids via the Azide. *Org. Process Res. Dev.* **2004**, *8*, 920-924.
(51) Tessier, M.; Albericio, F.; Pedroso, E.; Grandas, A.; Eritja, R.; Giralt, E.; Granier, C.; Van Rietschoten, J. Amino-acids condensations in the preparation of N alpha-9-fluorenylmethyloxycarbonylamino-acids with 9-fluorenylmethylchloroformate. *Int. J. Pept. Protein Res.* **1983**, *22*, 125-128.
(52) Sigler, G. F.; Fuller, W. D.; Chaturvedi, N. C.; Goodman, M.; Verlander, M. Formation of oligopeptides during the synthesis of 9-fluorenylmethyloxycarbonyl amino acid derivatives. *Biopolymers* **1983**, *22*, 2157-2162.
(53) Bolin, D. R.; Sytwu, I.-I.; Humiec, F.; Meienhofer, J. Preparation of oligomer-free Nα-Fmoc and Nα-urethane amino acids. *Int. J. Pept. Protein Res.* **1989**, *33*, 353-359.
(54) Kaiser, E.; Colescott, R. L.; Bossinger, C. D.; Cook, P. I. Color test for detection of free terminal amino groups in the solid-phase synthesis of peptides. *Anal. Biochem.* **1970**, *34*, 595-598.
(55) Madder, A.; Farcy, N.; Hosten, N. G. C.; De Muynck, H.; De Clercq, P. J.; Barry, J.; Davis, A. P. A Novel Sensitive Colorimetric Assay for Visual Detection of Solid-Phase Bound Amines. *Eur. J. Org. Chem.* **1999**, *1999*, 2787-2791.
(56) Christensen, T. Qualitative test for monitoring coupling completeness in solid-phase peptide-synthesis using chloranil. *Act. Chem. Scand. Series B-Organic Chemistry and Biochemistry* **1979**, *33*, 763-766.

Chapter 3

Peptidomimetics and Sugar Amino Acids (SAAs)

3.1. Introduction[1,2]

Peptidomimetics are compounds whose constituents (pharmacophore) mimic the natural peptides or proteins both in terms of 3D rearrangement and ability to interact with the biological targets producing the same biological effect.[3] Peptidomimetics are designed to overcome some problems associated with a natural peptides as, for instance, stability towards proteolysis[4] (duration of activity), poor bioavailability[5] and to improve other properties, such as receptor selectivity or potency.[6]
In the design of peptidomimetics sugars, the monosaccharides, particularly, represent an attractive molecular scaffold in which the amide backbone is replaced by a carbohydrate skeleton which keeps the proper orientation of the amino acidic substituents.[7] This concept was anticipated by Farmer in 1980, who reported the linkage of amino acidic side chains to a cyclohexane ring, creating the first non-peptide peptidomimetics.[8]

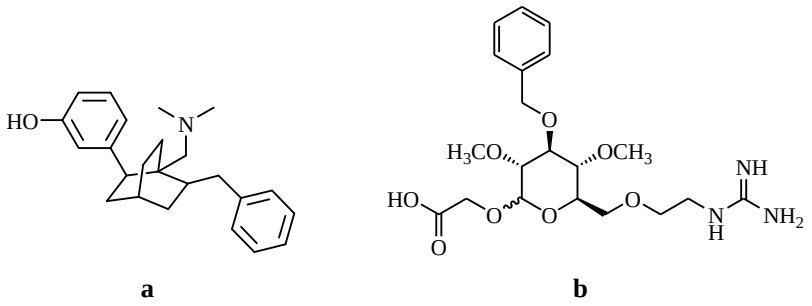

a **b**

Figure 1. **a**: non peptide peptidomimetic; **b**: carbohydrate-based mimic.

Sugar amino acids (SAAs) represent an important class of multifunctional building blocks that have found a wide range of applications, mainly in the area of peptidomimetic studies as rigid templates promoting secondary structures in peptides.[9,10] SAAs can adopt a robust secondary turn or helical structures which may allow them to mimic helices or sheets. SAAs can also be used to replace single amino acids or as dipeptide isosters.[11] When SAAs replace hydrophobic residues, the sugar can also be functionalized with hydrophobic side chains (e.g., benzyl groups); complementary, when hydrophilic residues are replaced or the solubility needs to be improved, the hydroxyl groups on the sugar moieties are, in general kept, unprotected or functionalized with hydrophilic residues.

In Kessler[12] definition, a sugar (carbohydrate) amino acid is a compound with direct linkages of both amino and carboxyl functionalities with a carbohydrate frame. Indeed, the SAAs are, essentially, hybrids of carbohydrate and amino acids where the amino and the carboxyl functional groups have been incorporated at the two termini of regular 2,5 or 2,6 anhydro sugar frameworks. SAAs can be found in nature largely as constitutive elements.[13]
The most prominent and well-known example is the sialic acid often located peripherally on glycoproteins. This family of natural SAAs consists of *N*- and *O*-acyl derivatives of neuraminic acid (Figure **2**).

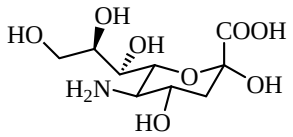

Figure 2. The naturally occurring sugar (carbohydrate) amino acid (SAA) sialic acid.

There are several advantages supporting the use of SAAs as building blocks. The rigid furan and pyran rings of these molecules provides an adequate conformational rigidity[14] and make them ideal candidates as non-peptide scaffolds in peptidomimetics. Moreover, they can be easily incorporated by using their carboxyl and amino termini. SAAs allow also an efficient exploitation of the structural diversities among carbohydrate molecules. The presence of several stereocenters allows different orientations of the hydroxyl groups and, by extension, of the substituents linked to them. Moreover, the protected/unprotected hydroxyl groups of sugar rings can be also exploit to modulate the hydrophobic/hydrophilic nature of these molecules, improving their solubility.

A different approach towards the preparation of SAAs consist in the direct coupling of the carbohydrate backbones with amino acidic residues by different synthetic methodologies.[12-14] Typically, the synthesis of SAAs is easily accomplished in few steps starting from commercially available or easily accessible monosaccharides, (glucose, glucosamine, diacetone glucose, galactose). The amino functionality of the SAA can be introduced as an azide, cyanide or nitromethane group, followed by subsequent reduction. The carboxylic function is directly installed as CO_2, by Wittig reaction as hydrolysable cyanide with a subsequent oxidation or by selective oxidation of a primary alcohol.
SAAs include both β-, γ-, and δ-SAA, as well as both furanoside and pyranoside ring forms (Figure **3**).

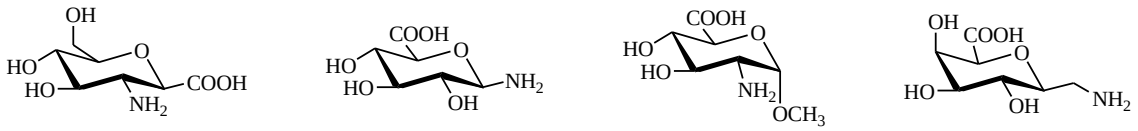

β-SAA **γ-SAA** **δ-SAA** **Dipeptide isoester**

Figure 3. Example of SAAs. The β-SAA can mimic a γ-turn when incorporated into a peptide, whereas the γ-SAA can mimic a β-turn. The δ-SAA illustrated has a linear alignment of amino and carboxylic acid functionalities. The dipeptide isoester can introduce a flexible a β-turn.

Sugar analogs in which the ring oxygen is replaced by a nitrogen atom can also be considered SAAs. This class of compounds has gained a large interest as inhibitors of glucosidases[12] and many of them, natural as well as synthetic, containing amino and carboxylic acid groups, are particularly well suited as peptidomimetic scaffolds.[15]

3.2. Development and synthesis of a peptidomimetics as p50 NF-κB homodimerization inhibitor

The many advantages related to the use of SAAs as peptidomimetics prompted us to develop and investigate a cyclic peptidomimetic as homodimerization inhibitor of p50 NF-κB. A glucose homolog (Figure **4**) bearing an amino and a carboxylic group was prepared and used as a peptide to mimic a proline β-turn residue.

This SAA, as analog of a β-amino acid and a γ-turn, could promote the peptide cyclization by pre-organizing the linear amino acidic sequence in a suitable conformation. Moreover it may lead to a cyclic structure with a proper conformational rigidity and metabolic stability. In addition, the three hydroxyl groups could play an important role enhancing the solubility of the peptidomimetic and, in the same time, they represent potential sites for a further functionalization and chemical modification allowing a remarkable peptidomimetic differentiation.

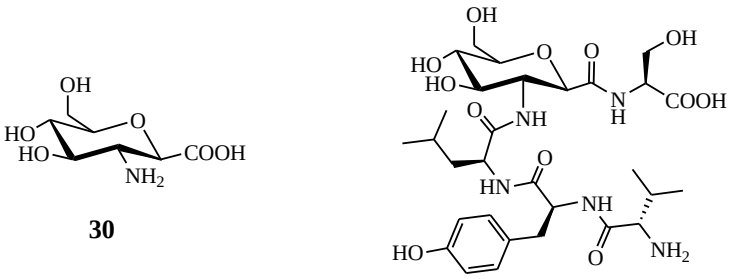

30 **43**

Figure 4. The SAA developed **30** as β-amino acid; its introduction in the linear peptide generates the peptidomimetic **43.**

3.2.1. Synthesis of sugar amino acid

The SAAs synthesis consisted of four steps starting from the commercially available *N*-glucosamine which was converted to 1-cycano-2-tetracholophalimido modifying a reported procedure.[16]

Tetrachlorophthaloyl (NTCP) was used as protecting group of the glucosamine amino moiety, due to its stability towards mild basic and strong acid conditions. Moreover it can be introduced easily in two steps and chemoselectively removed under neutral or mild conditions.

The introduction of the *N*-tetrachlorophalic group (TCP) into glucosamine was readily carried out by Lemieux's classic procedure[17,18] starting from the unprotected amine hydrochloridic salt **29**. The free base is released by treatment with NaOMe in methanol, followed by addition of the tetrachlorophalic anhydride **31**. TEA (1 eq) is also required to increase the reaction yield avoiding the precipitation of the sugar as ammonium salt. After the solvent evaporation *in vacuo*, the crude is redissolved in pyridine with an excess of acetic anhydride allowing the acylation of the hydroxyl groups. The mixed anhydride **33** is formed and, subsequently, undergoes a nucleophilic attack by the weak nucleophilic amidic nitrogen providing the full protected sugar **34**. The purification by a single recrystallization from ethanol afforded the final product in 60% overall yield and with high purity (>95% by ^{1}H-NMR).

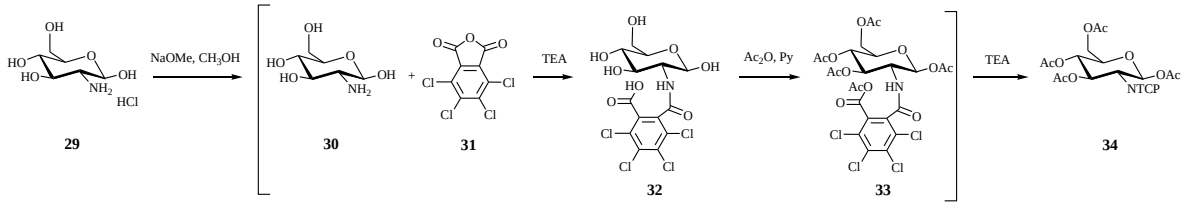

29 **30** **31** **32** **33** **34**

Scheme 1. Synthesis of 1,3,4,6-Tetra-*O*-Acetyl-2-deoxy-2-tetrachlorophalimido-β-D-glucopiranoside.

The acetyl protecting group at C-1 of the glycosyl compound **34** was selectively replaced with bromine by reaction with HBr in acetic acid. The resulting 2,3,4,6-protected glycosyl bromide **35** was used in the next step without further purification because of relative low stability. The conversion of bromine compound to the corresponding cyanide was carried out by treatment with mercuric cyanide in nitrometane under dry condition (to avoid the undesired hydrolysis of bromide to a hydroxyl group). The product **36** was purified by flash chromatography, providing almost quantitative yield (90% over 2 steps).

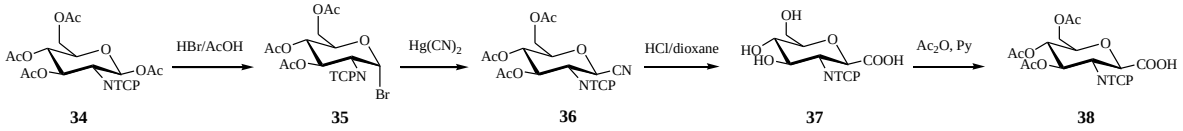

Scheme 2. Synthesis of 3,4,6-Tri-*O*-Acetyl-2-deoxy-2-tetrachlorophalimido-β-D-glucopyranosyl carboxylic acid.

The cyanide group was converted into the corresponding carboxyl group by acidic hydrolysis. Several reaction conditions were tested to obtain the effective cyanide hydrolysis due to the difficulty to follow the reaction evolution by TLC. The best conditions were identified in hydrochloric acid (4M) in dioxane at 60 °C overnight. This treatment not only hydrolyzes the nitrile group but also cleaves the *O*-acetyl protections on the sugar providing a hydrophilic compound **27** which has to be re-acetylated as described before to facilitate the product isolation and purification. The sugar amino acid **38** was obtain in 70% yield and with a purity higher than 95% as detected by ^{1}H-NMR.

3.2.2. Synthesis of a cyclo peptidomimetic

The C1 β-carboxylate group of SAA **38** was condensed with a serine (Ser-O^{t}Bu) previously protected as *tert*-butyl ester on the carboxyl group and as *tert*-butyl ether on the side chain hydroxyl group.

The coupling reaction was performed by an *in situ* activation methodology in DMF solution with HATU/HOAt as condensing reagent and DIEA as a base. The product **39** was purified by silica-gel flash chromatography and completely characterized.

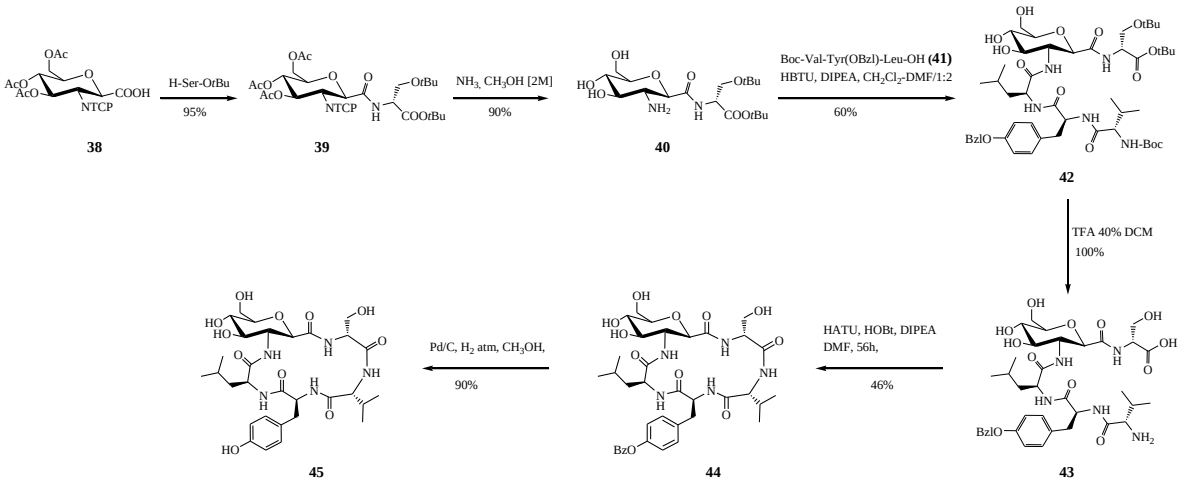

Scheme 3. Synthesis of cyclic peptidomimetic.

The N-TCP cleavage step was extensively investigated in order to obtain a simultaneous cleavage of the hydroxyl protecting groups.
Several cleavage conditions were tested in regard to the amines (ethylendiamine, hydrazine acetate), solvents (ethanol, DMF, acetonitrile) and temperature. Moreover also the Zemplèn reaction was attempted but all these procedures provided complex crude and mixture of partially deprotected products.
The suitable condition to achieve the full deprotection of **39** were found using ammonia (2M) in methanol at room temperature for 18 hours. This cleavage procedure provided the compound **40** which was purified by silica gel chromatography before being used in the next step.

The dipeptide **40** was coupled with a tri-peptide Boc-Val-Tyr(OBzl)-Leu-OH **41** in a mixture DMF-DCM using HBTU as coupling reagent in a basic medium (DIPEA). The crude purification by silica-gel column chromatography afforded the linear peptide in 90% yield. Subsequent cleavage of the Boc and O^{t}Bu in acidic condition provided the fully unprotected linear peptide **43**.
The peptide cyclization was performed in high diluted DMF solution using HATU as coupling reagent, HOBt as racemization suppressant and DIPEA as a base. The reaction was monitored by TLC and after 56 h no more linear peptide was detected. The solvent was removed by distillation and the crude purification by silica gel chromatography afforded the cyclo peptidomimetic **44** which finally was submitted to hydrogenolytic cleavage of the tyrosine *O*-benzyl group with Pd/C as catalyst leading to the formation of **45** as fully deprotected peptidomimetic (8 mg, 95%).
Due to the low amount of the cyclic peptidomimetic **45** it was not attempted a chromatographic purification but it was performed a directly characterization on the reaction crude which show that the final product was obtained with a good purity (90%).

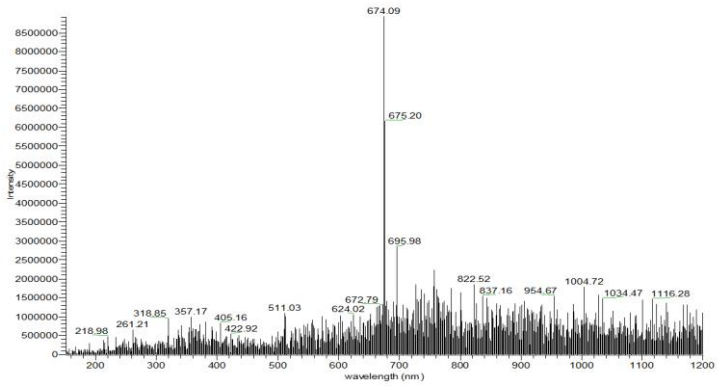

Figure 5. ESI-MS$^+$ of the final cyclic peptidomimetic **35**.

The low overall yield of the multistep synthesis of **45** may be due to a set of several factors such as: the purification after each step by flash chromatography which could lead to product loss; the checking of the reaction progression by TLC, which has a low sensibility for the revelation of compounds in high dilution, poorly UV-visible or by nature barely detectable by the classical TLC stains. Nevertheless, now that the reaction conditions and the purification methodology for each compound are known, the subsequent efforts will be addressed to the optimization of some critical steps (SAA coupling and peptidomimetic cyclization) with the purpose to increase the overall yield.

3.3. Conclusion

A synthetic methodology to achieve a cyclic peptidomimetic with a sugar amino acid in its sequence has been identified and optimized. Despite the final product has been obtained in low amount, this will be enough to perform the preliminary biological test with the p50 NF-κB protein. However, exploiting the synthetic way developed during this stage, the same product as well as some analogues, could be rapidly synthesized; led to the formation of a series of peptidomimetic to test as potential p50 homodimerization inhibitors.

The cyclic peptidomimetic synthesized will be subjected to extensive investigations in order to define how the conformational and chemical properties imposed by the sugar amino acid on the cyclic peptidomimetic can have an affects on the interactions between the peptidic inhibitor and the binding site region of the protein.
Moreover, whether the sugar can influence the solubility and the membrane permeability of the peptidomimetics will be evaluate.

The SAA structure has a huge potential, through an appropriate functionalization of the different hydroxyl groups present in the monosaccharide moiety, a libraries of potentially bioactive compounds for pharmacological screening can be achieved. Therefore the SAA represents an important component to achieve a peptide differentiation.

An alternative approach, always based on sugar peptidomimetics, could be to exploit the sugar as a scaffold for the synthesis of a peptidomimetic in which the amide backbone is substituted with a different skeleton while maintaining the proper orientation of the amino acidic substituents.

References

(1) Hruby, V. J.; al-Obeidi, F.; Kazmierski, W. Emerging approaches in the molecular design of receptor-selective peptide ligands: conformational, topographical and dynamic considerations. *Biochem. J.* **1990**, *268*, 249-262.

(2) Ripka, A. S.; Rich, D. H. Peptidomimetic design. *Curr. Opin. Chem. Biol.* **1998**, *2*, 441-452.

(3) Vagner, J.; Qu, H.; Hruby, V. J. Peptidomimetics, a synthetic tool of drug discovery. *Curr. Opin. Chem. Biol.* **2008**, *12*, 292-296.

(4) Kihlberg, J.; Ahman, J.; Walse, B.; Drakenberg, T.; Nilsson, A.; Soderberg-ahlm, C.; Bengtsson, B.; Olsson, H. Glycosylated peptide hormones: pharmacological properties and conformational studies of analogues of [1-desamino,8-D-arginine]vasopressin. *J. Med. Chem.* **1995**, *38*, 161-169.

(5) Fisher, J. F.; Harrison, A. W.; Bundy, G. L.; Wilkinson, K. F.; Rush, B. D.; Ruwart, M. J. Peptide to glycopeptide: glycosylated oligopeptide renin inhibitors with attenuated in vivo clearance properties. *J. Med. Chem.* **1991**, *34*, 3140-3143.

(6) Seitz, O. Glycopeptide synthesis and the effects of glycosylation on protein structure and activity. *ChemBioChem :* **2000**, *1*, 214-246.

(7) Ingrid Veltera, B. L. F. F. N. Carbohydrate-Based Molecular Scaffolding. *J. Carbohydr. Chem.* **2006**, *25*, 97-138.

(8) Farmer, P. S. Bridging the gap between bioactive peptides and nonpeptides: some perspectives in design. *Med. Chem.* **1980**, 119-143.

(9) Chakraborty, T. K.; Srinivasu, P.; Tapadar, S.; Mohan, B. K. Sugar amino acids in designing new molecules. *Glycoconj. J.* **2005**, *22*, 83-93.

(10) Graf von Roedern, E.; Lohof, E.; Hessler, G.; Hoffmann, M.; Kessler, H. Synthesis and Conformational Analysis of Linear and Cyclic Peptides Containing Sugar Amino Acids. *J. Am. Chem. Soc.* **1996**, *118*, 10156-10167.

(11) Chakraborty, T. K.; Jayaprakash, S.; Ghosh, S. Sugar amino acid based scaffolds--novel peptidomimetics and their potential in combinatorial synthesis. *Comb. Chem. High Throughput Screen* **2002**, *5*, 373-387.

(12) Gruner, S. A.; Locardi, E.; Lohof, E.; Kessler, H. Carbohydrate-based mimetics in drug design: sugar amino acids and carbohydrate scaffolds. *Chem. Rev.* **2002**, *102*, 491-514.

(13) Chakraborty, T. K.; Jayaprakash, S.; Ghosh, S. Sugar amino acid based scaffolds--novel peptidomimetics and their potential in combinatorial synthesis. *Comb. Chem. High Throughput Screen* **2002**, *5*, 373-387.

(14) Hruby, V. J. Conformational restrictions of biologically active peptides via amino acid side chain groups. *Life Sci.* **1982**, *31*, 189-199.

(15) Chery, F.; Murphy, P. V. Synthesis of an iminosugar based peptidomimetic analogue. *Tetrahedron Lett.* **2004**, *45*, 2067-2069.

(16) Myers, R. W.; Lee, Y. C. Synthesis and characterization of some anomeric pairs of per-O-acetylated aldohexopyranosyl cyanides (per-O-acetylated 2,6-anhydroheptononitriles). On the reaction of per-O-acetylaldohexopyranosyl bromides with mercuric cyanide in nitromethane. *Carbohydr. Res.* **1984**, *132*, 61-82.

(17) Lemieux, R. *Synthetic methods for carbohydrates* **1976**.

(18) Debenham, J. S.; Debenham, S. D.; Fraser-Reid, B. N-tetrachlorophthaloyl (TCP) for ready protection/deprotection of amino sugar glycosides. *Bioorg. Med. Chem.* **1996**, *4*, 1909-1918.

Chapter 4

Transmembrane transport

4.1. Introduction

The plasma membrane consists of a lipid bilayer into which proteins and glycoproteins are dispersed. The hydrophobic nature of the inner part of the double layer prevents the hydrophilic compounds to cross it unless specific transport mechanisms are involved. Some small hydrophilic molecules/ions can cross the membrane channels while others, more complex structures, are shuttled from the outer media to the cytoplasm by membrane proteins. In this case, generally, an internalization process, endocytosis, in vesicles is needed to encapsulate the cargo, transfer it through the membrane and finally release it in the cytoplasm.

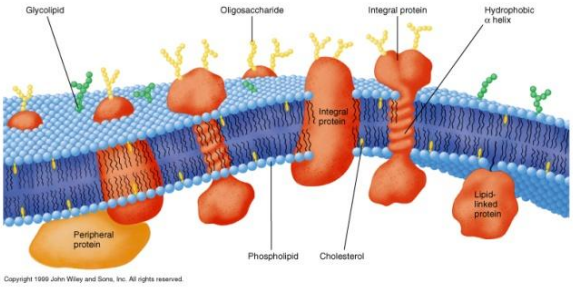

Figure 1. The plasma membrane. (Image from *Fundamentals of Biochemistry* **2006**).

Intracellular transport of different biologically active molecules is one of the key issues in drug delivery. Moreover, many compounds showing a promising activity *in vitro*, cannot be applied *in vivo* owing to bioavailability problems.
Many different pharmaceutical carriers have been developed to increase the stability of administered drugs, improve their efficacy, decrease undesired side effects and, even, promote better intracellular delivery.[1-3]
Nowadays, it is well-known that *nanocarriers*[4,5] had a great potential for a specific delivery of drugs. This approach has been largely exploited to optimize the intracellular delivery of many small molecules as well as of macromolecules like nucleic acids, peptides or proteins, which are unstable in physiological conditions and generally unable to cross the cell membrane. It has be reported that submicronic lipid vesicles known as liposomes,[6] as well as synthetic polymer nanoparticles,[7] were able to deliver into cells, molecules that did not diffuse spontaneously to the cytoplasm.

Liposomes represent the most popular and well-investigated drug carriers.[8,9] They are supramolecular aggregates of natural or artificial phospholipid with the size varying from 50 to 1000 nm, which can be loaded with a variety of drugs. They are biologically inert and completely biocompatible which means that they do not induce toxic or antigenic reactions. Moreover the phospholipid bilayer works as a shield, protecting the internalized drugs from any destructive effect of the external media. The association of the drugs with these carriers results in a delayed drug absorption, restricted drug biodistribution, decreased volume of drug biodistribution, delayed drug clearance and retarded drug metabolism.[10] Finally, liposomes are rapidly eliminated from the blood and captured by the reticuloendothelial system cells (RES), primarily, in the liver and in the spleen, as the result of a rapid opsonization.

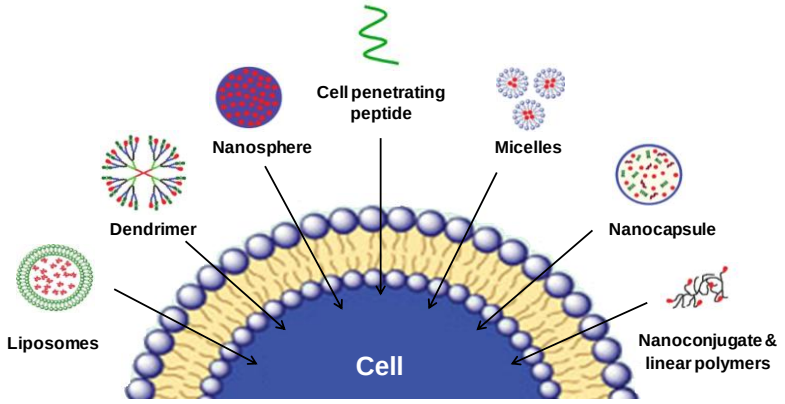

Figure 2. Some examples of drug delivery systems.

Polymeric nanoparticles are generally based either on synthetic biodegradable polymers-like the poly(lactic acid, PLA) and poly(lactic-co-glycolic acid, PLGA) polyesters or the poly(alkylcyanoacrylates, PACA) or natural polymers, like albumin.[5] Nanospheres are matrices in which the drug is dispersed throughout the particles, whereas nanocapsules are vesicular systems in which the drug is confined into a cavity surrounded by a unique polymeric membrane. Other systems based on polymers include polymer micelles, dendritic architectures and polyplexes (formed by the electrostatic interactions of polycations and nucleic acids).[4]

An alternative useful approach to deliver cargo molecules into the cell is represented by the cell-penetrating peptides (CPPs).[3,11,12]
CPPs are short cationic peptide sequences that have been demonstrated to mediate the intracellular delivery of a range of biological molecules. They are able to reach the cytoplasmic and/or nuclear compartments in live cells upon internalization and to deliver the conjugated (or fused) biomolecules.[13,14] These peptides have been used for intracellular delivery of various biological compounds with molecular weights several times higher than their own[15] such as antigenic peptides,[16] peptide nucleic acids,[17] antisense oligonucleotides,[18] full-length proteins,[19-21] or even nanoparticles[22] and liposomes.[23] Conjugation of therapeutic agents with CPPs could become a key-strategy to improve their pharmacological properties.

4.2. Peptide delivery: our approach

Despite the liposome technology and the CCPs method have shown large potential to deliver a wide range of large molecules and potential drugs overcoming the cellular barriers, in this project taking advantage of the great experience in the carbohydrate synthesis in our research group, has been evaluated an alternative approach for the transport of the peptidomimetics into the cells.

The approach proposed is focused on the protein regulating transport of glucose across the plasma membranes (GLUTs).
The idea is based on the functionalization of the cyclopeptide with a glucose-derived carrier which being recognized by the GLUTs, can translocate the cargos through the cellular membranes thereby, enhancing the cyclopeptide delivery inside the cells.

This approach is one of the methods used to promote the drug transport across the BBB.[24] Because, the BBB expresses a number of specific carrier-mediated inward transport mechanisms that ensure an adequate nutrient supply for the brain.[25] These endogenous BBB transporters can be exploited for a drug molecules active transport[26] which can be realized by the conjugation of an endogenous transporter substrate to the active drug molecule according to the prodrug approach.[27]

In this context, GLUT1 transports glucose and other hexoses have the highest transport capacity of the carrier-mediated transporters present at the BBB, being therefore an attractive transporter for prodrug delivery.[28]

In addition, many transporters have been reported to be differentially up-regulated in cancer cells compared to normal tissues, suggesting that the differential expression of transporters in cancer cells may provide good targets for enhancing drug delivery as well as diagnostic markers for cancer therapy.[29] The overexpression of glucose transporter proteins, which facilitate the glucose uptake by cells, was widely observed in tumor tissues,[28] indeed, cancer cells have an increased rates of glucose metabolism compared with healthy one and, this increased GLUT levels and transport activity would contribute significantly to tumor growth.[30]

For instance, GLUT1 is ubiquitously expressed in normal tissue and expressed at high concentrations in some tumors, including hepatic, pancreatic, breast, esophageal, brain, renal, lung, cutaneous, colorectal, endometrial, ovarian, and cervical carcinoma.[31] Thus, GLUT1 expression in tumor tissues is one of the most characteristic biochemical markers for the transformed phenotype.

4.3. Transcellular sugar transport: the mammalian glucose transporter family

Sugars are hydrophilic molecules that are unable to cross lipid cell membranes without a protein-transporter. Two different families of associated membrane carrier proteins are known: the sodium-dependent glucose transporter (SGLT) and the facilitated-diffusion glucose transporter (GLUT) as shown in Table **1**. These proteins mediate the sugars transport with different efficiencies and kinetics.

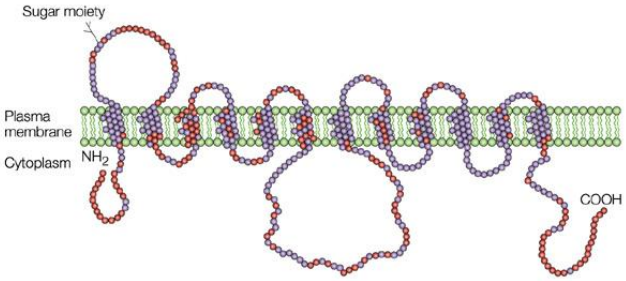

Figure 3. Structure of the GLUT family. (Adapted from *Nature Reviews Molecular Cell Biology* **2002**, 3, 267-277).

GLUTs proteins allow the energy independent transport of glucose across the hydrophobic cell membrane, driven by the concentration gradient.

The GLUT family members have the structural sequence of 12 transmembrane domains with intracellular *N*- and *C*- terminals (Figure **3**).

The human GLUT family consists of 14 members that can be classified in three sub families based on the sequence homology and on the structural similarity.[32-34] The class I

comprises the well characterized GLUTs 1-4 as glucose transporters. The class II comprises the fructose transporter GLUT5 and three proteins, GLUT7, GLUT9, and GLUT11. Finally, the class III comprises five newly described proteins, GLUT6, GLUT8, GLUT10, GLUT12, and the H^+/myoinositol transporter HMIT. These are structurally atypical members of the GLUT family, which are, so far, not clearly defined.
Each member of the GLUT family is different in terms of functional characteristics and, in addition, they exhibit different substrate specificity, kinetic properties and expression profiles.[35]

Transporter	Major site of expression
Na^+-dependent glucose transporter (SGLT)	
SGLT 1	small intestine, kidney
SGLT 2	kidney
Facilitated-diffusion glucose transporter (GLUT)	
GLUT 1	brain, erythrocytes, placenta, fetal tissue
GLUT 2	small intestine, liver, kidney, pancreatic β-cell
GLUT 3	brain
GLUT 4	skeletal muscle, adipose tissue
GLUT 5	small intestine
GLUT 6	pseudogene which is not expressed at the protein level
GLUT 7	intestine, colon, testis (the physiological relevance is being investigated)
GLUT 8	testis
GLUT 9	kidney, liver
GLUT 10	heart, lung, brain, liver
GLUT 11	lung, brain, liver
GLUT 12	heart, muscle, brown adipose tissue
HMIT	brain

Table 1. The family of glucose transporters. (Modified from Blanco et al. *International Journal of Endocrinology* **2010**):

4.4. Development and synthesis of glycosidic carrier

The increased glucose transport and the associated overexpression of GLUT proteins during the tumors progression has been exploited to promote the transmembrane transport of the cyclopeptide inhibitors developed in this project.
The idea was focused on the combination of the peptidomimetic with a sugar moiety which can be recognized by the GLUT transporter protein family.
Based on reported data, a glycosidic carrier, analog of the glucose, was designed. This molecule bears a free hydroxyl in the position 6 which is not primary involved in the GLUTs recognition process.[24] In our synthetic pathway, the 6-hydroxy would be replaced by a carboxylic function able to form a stable covalent bond with the side chain groups of the cyclopeptides. Moreover the introduction of a short aliphatic chain between the sugar moiety and the carboxylic group will prevent any interference from the peptidomimetics in the glucose recognition process.

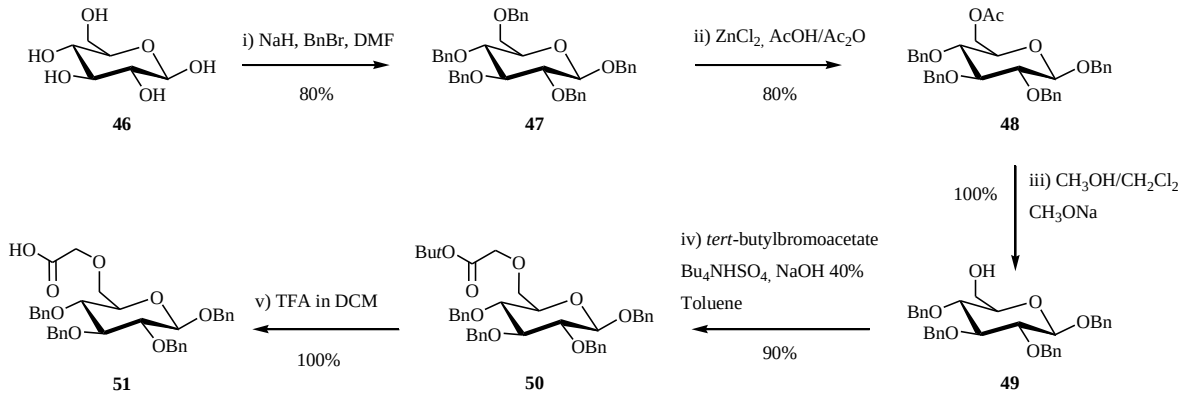

Scheme 1. Synthesis of the glucose-base glycosidic carrier.

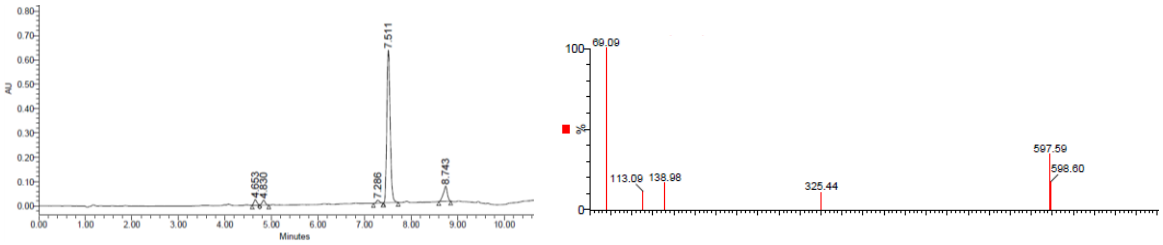

Figure 4. RP-HPLC and RP-HPLC-ESI$^-$ traces of the glycosidic carrier **51**. HPLC were recorded using a 50-100% B gradient in 8 min (A = 0.045% TFA in H_2O, and B = 0.036% TFA in ACN).

4.5. Condensation of cyclic peptides with the glycosidic carrier

The conjugation of the glycosidic carrier with the cyclopeptides containing lysine, Dap and 4-aminophenilalanine, implies the formation of a stable amide bond between the carboxylic group of the carrier and the primary amino group on the cyclopeptide side chain.

To this end, two different approaches were evaluated one based on the coupling of the carrier with the final cyclopeptide and the other one involving the condensation on the carrier on the linear peptide followed by the cyclization reaction.

4.5.1. Coupling reaction with the cyclopeptide in solution

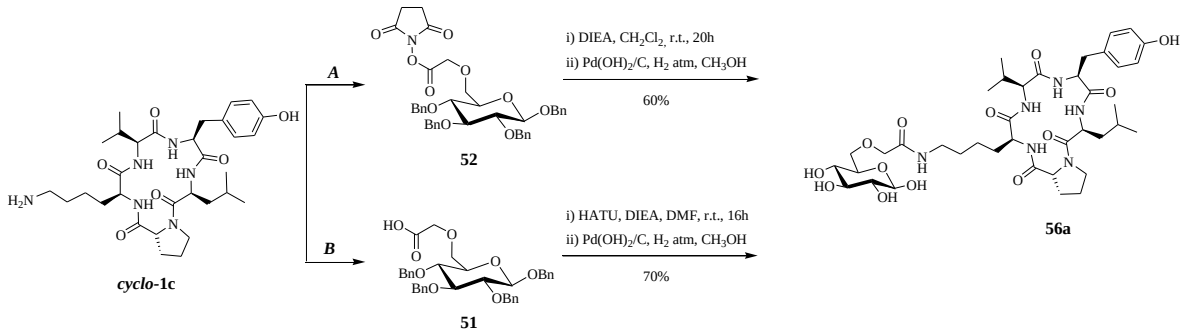

Scheme 2. Condensation of the cyclopeptide with the glycosidic carrier in solution.

The coupling reaction, in two different conditions sets, between the glycosidic carrier and the cyclopeptide was initially performed in solution using the sequence with a lysine as a model.

In the first one **(*A*)**, the pre-activated carboxylic acid as succinimidyl ester was coupled

with the amine in basic (DIEA) dichloromethane. This pathway was justified by the rapid and clean reaction of the *N*-Hydroxysuccinimide esters forming water soluble co-products easy to remove during the work-up.
The second approach (***B***) consisted in the activation of the carboxylic acid by an uronium (HATU) coupling reagent in DMF. The reaction was monitored by TLC and after 16 hours no free carrier was detected.
In both cases, after the formation of the amide bond and the solvent evaporation, the crudes were subjected to the benzyl ester cleavage by a palladium catalyzed hydrogenolysis. After purification by column chromatography the products were isolated, as mixture of α/β anomers, with high purity (>95%) and satisfactory yield (60-70% over 2 steps).

n	*Cyclic peptide*	*Method*	*Yield %*	*Purity %*
56a	&Lys(*carrier*)-Val-Tyr-Leu-D-Pro&	A	60	> 95
56a	&Lys(*carrier*)-Val-Tyr-Leu-D-Pro&	B	70	> 98

Table 2. Results of the coupling reaction between the cyclopeptide and the glycosidic carrier performed in solution. The overall yields are referred to the final products isolated after the purification by flash chromatography. The purities were determined by ^{1}H-NMR.

Both strategies present similarities in terms of mechanism and quality of the final crudes despite the slightly different reactions time. Nevertheless the HATU way gave higher yield, which could be due to higher reactivity of the 7-azabenzotriazol-1-yl esters compared to the succinimidyl one thanks to an intramolecular general base-catalysis.

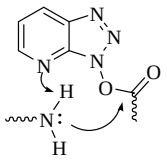

Figure 5. HATU active species

The cyclopeptide conjugated with the sugar moiety shows a remarkable solubility in polar solvents, differently to what observed for its unconjugated analogue (***cyclo*-1c**), indicating that the glucose hydroxyl groups together with the tyrosine one provide an overall hydrophilic character to the peptide promoting its solubility.

4.5.2. Coupling reaction with the linear peptides on solid phase

Solid phase coupling was also tested to conjugate the carrier with the cyclopeptide in order to exploit all the advantages related with the SPPS technique. This methodology was used to condense the carrier with peptides containing primary amino groups on their side chains (Lysine, Dap and 4-amino phenylalanine). It was used an analogue synthetic approach to that employed for the Lys side chain acetylation on solid phase. (Chapter 2, scheme **8**)
The crucial step in this pathway focuses on the proper selection of orthogonal protecting groups that will allow the formation of the free amine without cleaving the protecting groups on the *N*-terminal group or the resin.
We have introduced a Boc protecting group at the *N*-terminal in order to remove it in the same acid condition needed to cleave the resin, while the amino acids side chains were protected with Fmoc.

The synthesis of the linear peptides on solid phase (Scheme **3**) was performed using the standard Fmoc/*t*Bu protocol. The side chains of the resulting linear peptides **52** were deprotected by treatment with piperidine releasing the free amino group. The condensation between the free acid of glycosidic carrier **51** and the amino functionalities on the linear peptide **53**, were performed under the typical activation conditions (PyBOP-HOAt-DIEA). Finally, the peptides were cleaved from the solid support by TFA treatment which removes at the same time also the Boc protecting group on the *N*-terminal giving the unprotected linear peptide 5**4**. The products were isolated and characterized by HPLC, showing high degree of quality without further purifications.

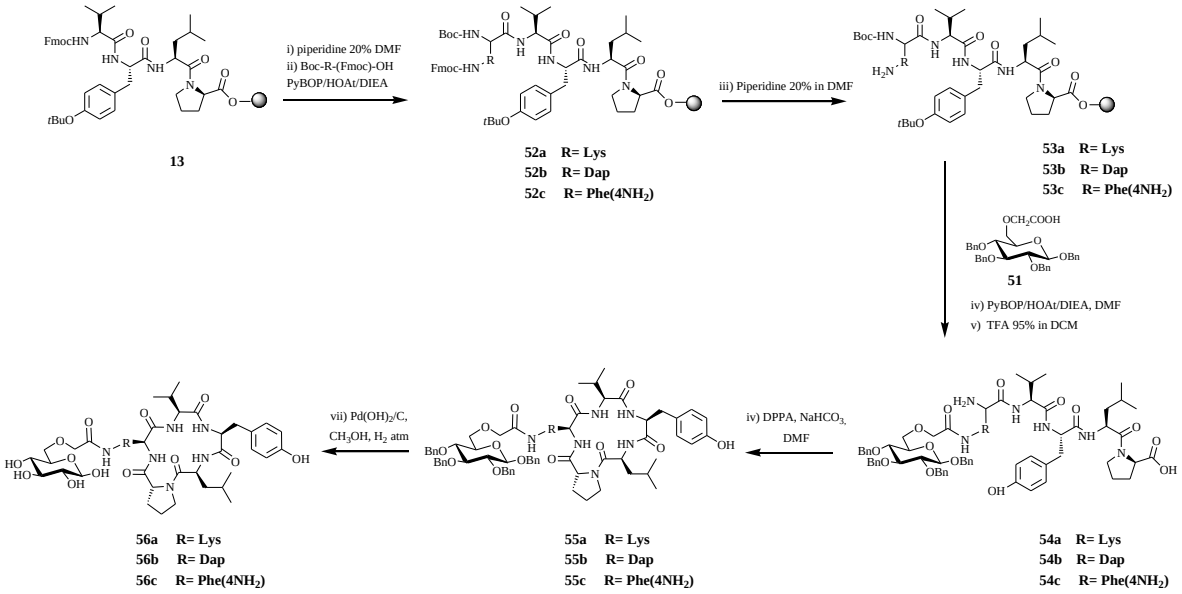

Scheme 3. Synthesis on solid phase of cyclopeptides functionalized with the glycosidic carrier. R represents the residues: Lysine, Dap and 4-aminophenilalanine.

The peptide cyclizations were carried out in high diluted DMF solution using DPPA as condensing agent together with an inorganic base ($NaHCO_3$). The reactions progress was monitored by HPLC and after 48 h the reactions were stopped.

The fully deprotected cyclopeptides **56** were obtained after the cleavage of the benzyl ester groups on the sugar by palladium catalyzed hydrogenolysis in methanol. Finally the products were purified by semipreparative RP-HPLC to provide the desired products with good overall yield and high purity (Table **3**). The experimental data show that the presence of a sugar near the *N*-terminal reactive end of the linear peptide does not affect the peptide cyclization by bulk effect or steric hinderance. Both, the cyclization reactions time and the quality of the final crudes are comparable with the one obtained for the cyclization of the linear peptide without the sugar.

n	*Cyclic peptide*	*Yield %*	*Purity %*
56a	&Lys(*carrier*)-Val-Tyr-Leu-D-Pro&	25	> 95
56b	&Phe(4NH(*carrier*))-Val-Tyr-Leu-D-Pro&	35	> 95
56c	&Dap(*carrier*)-Val-Tyr-Leu-D-Pro&	25	> 95

Table 3. Results of the synthesis of the cyclopeptides functionalized with the glycosidic carrier (*c*) totally performed on solid phase. The overall yields are referred to the final products isolated after the purification by HPLC chromatography. The purities was determined by HPLC.

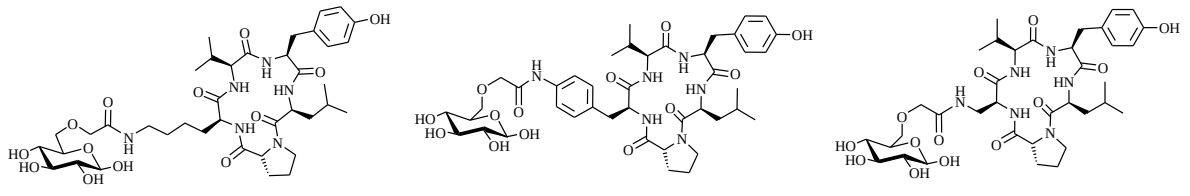

56a **56b** **56c**

Figure 6. Three different cyclic pentapeptides labelled with the glycosidic carrier.

This approach, in which the carrier was attached to the linear peptide on solid support, allows to carry out just a single purification of the final product reducing the overall working time, product loss and material cost.

In addition, the validation of this method offers the ability to attach many different types of labels just before the cyclization, or to modify, again on solid phase, some functional groups on the residues side chain. These aspects are particularly relevant for a rapid develop of a series of cyclic peptides conjugate with different carriers or probes to evaluate the transport of the peptide or to detect its localization during the biological assay giving the opportunity to have access to a large range of different experimental tests.

&Lys(carrier)-Val-Tyr-Leu-D-Pro& **(56a)**

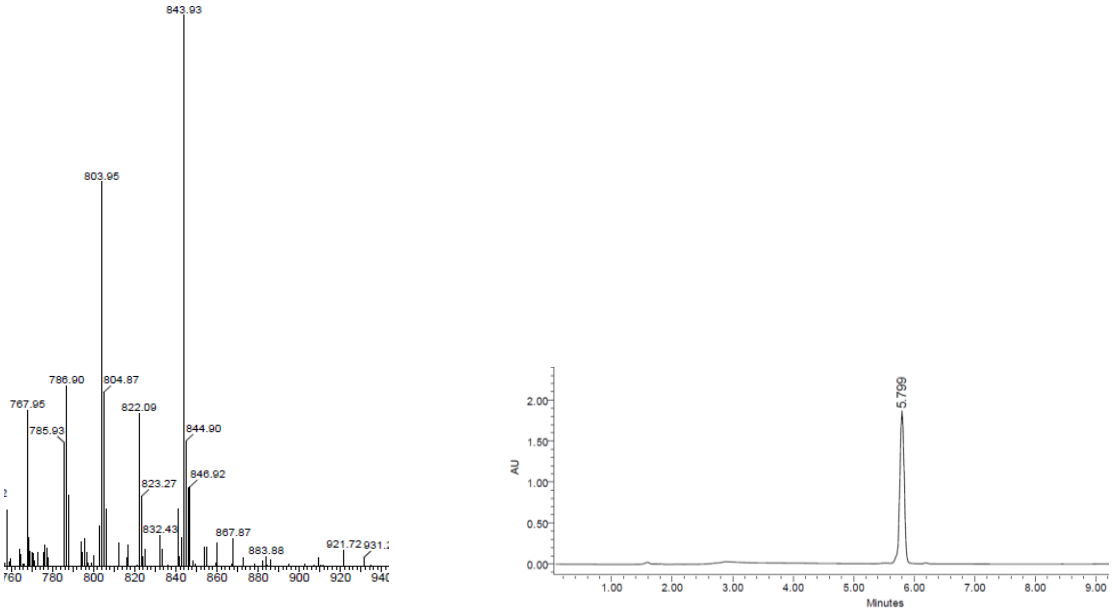

&Phe(4NH-carrier)-Val-Tyr-Leu-D-Pro& **(56b)**

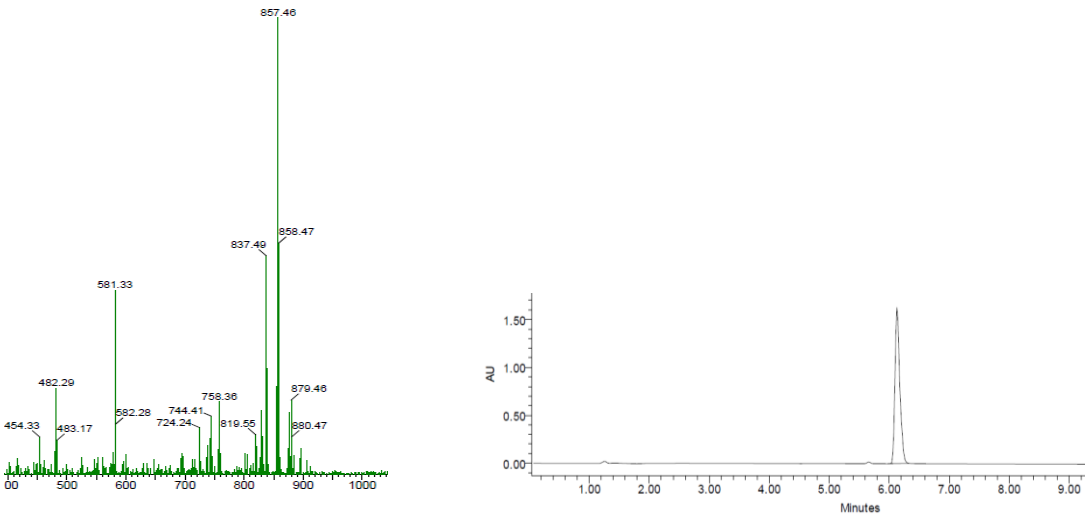

&Dap(carrier)-Val-Tyr-Leu-D-Pro& **(56c)**

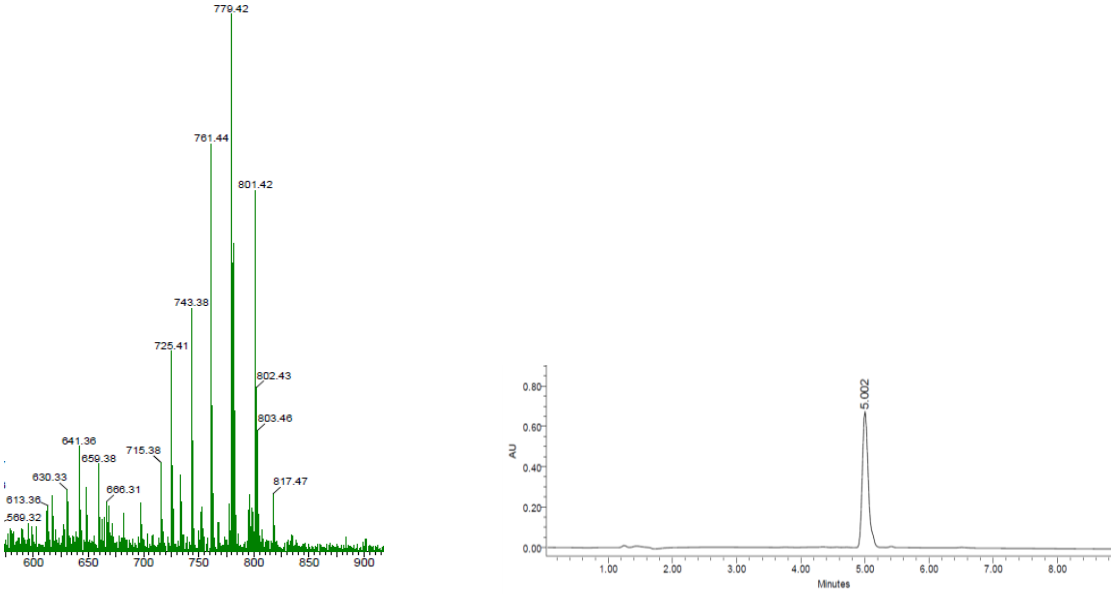

Figure 7: HPLC and HPLS-MS traces of the cyclopeptides conjugate to the glycosidic carrier. HPLC were recorded using a 20-50% B gradient in 8 min (A = 0.045% TFA in H_2O, and B = 0.036% TFA in ACN).

4.6. Conclusion

An alternative approach to the classical drug delivery methods (e.g. liposomes, CCPs) based on the glucose transport protein (GLUTs) was evaluated to shift the cyclopeptides inside the cells. A glucose-based carrier was first synthesized and then linked by an amide bond to the cyclopeptides. The ongoing biological investigation of these compounds will clarify whether the GLUTs mediated transport has the ability to shuttle the peptidomimetic inside the cytoplasm, supporting the original idea of this work, or not. Moreover, based on the biological results, this transport methodology could be further investigated or discharged moving to the classic drug delivery methods.

References

(1) Torchilin, V. Intracellular delivery of protein and peptide therapeutics. *Drug Discov. Today: Technologies* **2008**, *5*, e95-e103.

(2) Torchilin, V. P. Recent approaches to intracellular delivery of drugs and DNA and organelle targeting. *Annu. Rev. Biomed. Eng.* **2006**, *8*, 343-375.

(3) Gupta, B.; Levchenko, T. S.; Torchilin, V. P. Intracellular delivery of large molecules and small particles by cell-penetrating proteins and peptides. *Adv. Drug Deliver Rev.* **2005**, *57*, 637-651.

(4) Hillaireau, H.; Couvreur, P. Nanocarriers' entry into the cell: relevance to drug delivery. *Cell. Mol. life Sci.* **2009**, *66*, 2873-2896.

(5) Wilczewska, A. Z.; Niemirowicz, K.; Markiewicz, K. H.; Car, H. Nanoparticles as drug delivery systems. *Pharmacological reports* **2012**, *64*, 1020-1037.

(6) Varga, C. M.; Wickham, T. J.; Lauffenburger, D. A. Receptor-mediated targeting of gene delivery vectors: insights from molecular mechanisms for improved vehicle design. *Biotechnol. Bioeng.* **2000**, *70*, 593-605.

(7) Chakrabarti, R.; Wylie, D. E.; Schuster, S. M. Transfer of monoclonal antibodies into mammalian cells by electroporation. *J. Biol. Chem.* **1989**, *264*, 15494-15500.

(8) Torchilin, V. P. Recent advances with liposomes as pharmaceutical carriers. *Nat. Rev. Drug Discov.* **2005**, *4*, 145-160.

(9) Lasic, D. D.: *Liposomes : from physics to applications*; Elsevier: Amsterdam; New York, 1993.

(10) Allen, T. M.; Hansen, C. B.; de Menezes, D. E. L. Pharmacokinetics of long-circulating liposomes. *Adv. Drug Deliver. Rev.* **1995**, *16*, 267-284.

(11) Richard, J. P.; Melikov, K.; Vives, E.; Ramos, C.; Verbeure, B.; Gait, M. J.; Chernomordik, L. V.; Lebleu, B. Cell-penetrating peptides. A reevaluation of the mechanism of cellular uptake. *J. Biol. Chem.* **2003**, *278*, 585-590.

(12) Jones, S. W.; Christison, R.; Bundell, K.; Voyce, C. J.; Brockbank, S. M.; Newham, P.; Lindsay, M. A. Characterisation of cell-penetrating peptide-mediated peptide delivery. *Brit. J. Pharmacol.* **2005**, *145*, 1093-1102.

(13) Lindgren, M.; Hallbrink, M.; Prochiantz, A.; Langel, U. Cell-penetrating peptides. *Trends Pharmacol. Sci.* **2000**, *21*, 99-103.

(14) Schwarze, S. R.; Hruska, K. A.; Dowdy, S. F. Protein transduction: unrestricted delivery into all cells? *Trends Cell. Biol.* **2000**, *10*, 290-295.

(15) Schwarze, S. R.; Dowdy, S. F. In vivo protein transduction: intracellular delivery of biologically active proteins, compounds and DNA. *Trends Pharmacol. Sci.* **2000**, *21*, 45-48.

(16) Shibagaki, N.; Udey, M. C. Dendritic cells transduced with protein antigens induce cytotoxic lymphocytes and elicit antitumor immunity. *J. Immunol.* **2002**, *168*, 2393-2401.

(17) Pooga, M.; Soomets, U.; Hallbrink, M.; Valkna, A.; Saar, K.; Rezaei, K.; Kahl, U.; Hao, J. X.; Xu, X. J.; Wiesenfeld-Hallin, Z.; Hokfelt, T.; Bartfai, T.; Langel, U. Cell penetrating PNA constructs regulate galanin receptor levels and modify pain transmission in vivo. *Nat. Biotechnol.* **1998**, *16*, 857-861.

(18) Astriab-Fisher, A.; Sergueev, D.; Fisher, M.; Shaw, B. R.; Juliano, R. L. Conjugates of antisense oligonucleotides with the Tat and antennapedia cell-penetrating peptides: effects on cellular uptake, binding to target sequences, and biologic actions. *Pharm. Res.* **2002**, *19*, 744-754.

(19) Fawell, S.; Seery, J.; Daikh, Y.; Moore, C.; Chen, L. L.; Pepinsky, B.; Barsoum, J. Tat-mediated delivery of heterologous proteins into cells. *PNAS* **1994**, *91*, 664-668.

(20) Nagahara, H.; Vocero-Akbani, A. M.; Snyder, E. L.; Ho, A.; Latham, D. G.; Lissy, N. A.; Becker-Hapak, M.; Ezhevsky, S. A.; Dowdy, S. F. Transduction of full-

length TAT fusion proteins into mammalian cells: TAT-p27Kip1 induces cell migration. *Nat. Med.* **1998**, *4*, 1449-1452.

(21) Schwarze, S. R.; Ho, A.; Vocero-Akbani, A.; Dowdy, S. F. In vivo protein transduction: delivery of a biologically active protein into the mouse. *Science* **1999**, *285*, 1569-1572.

(22) Lewin, M.; Carlesso, N.; Tung, C. H.; Tang, X. W.; Cory, D.; Scadden, D. T.; Weissleder, R. Tat peptide-derivatized magnetic nanoparticles allow in vivo tracking and recovery of progenitor cells. *Nat. Biotechnol.***2000**, *18*, 410-414.

(23) Torchilin, V. P.; Rammohan, R.; Weissig, V.; Levchenko, T. S. TAT peptide on the surface of liposomes affords their efficient intracellular delivery even at low temperature and in the presence of metabolic inhibitors. *PNAS* **2001**, *98*, 8786-8791.

(24) Gynther, M.; Ropponen, J.; Laine, K.; Leppanen, J.; Haapakoski, P.; Peura, L.; Jarvinen, T.; Rautio, J. Glucose promoiety enables glucose transporter mediated brain uptake of ketoprofen and indomethacin prodrugs in rats. *J. Med. Chem.* **2009**, *52*, 3348-3353.

(25) Pardridge, W. M.; Oldendorf, W. H. Transport of metabolic substrates through the blood-brain barrier. *J. Neurochem.* **1977**, *28*, 5-12.

(26) Rautio, J.; Laine, K.; Gynther, M.; Savolainen, J. Prodrug approaches for CNS delivery. *The AAPS journal* **2008**, *10*, 92-102.

(27) Han, H. K.; Amidon, G. L. Targeted prodrug design to optimize drug delivery. *AAPS Pharm. Sci* **2000**, *2*, E6.

(28) Anderson, B. D. Prodrugs for improved CNS delivery. *Adv. Drug Deliv. Rev.* **1996**, *19*, 171-202.

(29) Nakanishi, T. Drug transporters as targets for cancer chemotherapy. *Cancer genomics & proteomics* **2007**, *4*, 241-254.

(30) Brown, R. S.; Wahl, R. L. Overexpression of Glut-1 glucose transporter in human breast cancer. An immunohistochemical study. *Cancer* **1993**, *72*, 2979-2985.

(31) Kannagi, R.; Izawa, M.; Koike, T.; Miyazaki, K.; Kimura, N. Carbohydrate-mediated cell adhesion in cancer metastasis and angiogenesis. *Cancer Sci.* **2004**, *95*, 377-384.

(32) Joost, H. G.; Thorens, B. The extended GLUT-family of sugar/polyol transport facilitators: nomenclature, sequence characteristics, and potential function of its novel members (review). *Mol. Membr. Biol.* **2001**, *18*, 247-256.

(33) Doege, H.; Bocianski, A.; Scheepers, A.; Axer, H.; Eckel, J.; Joost, H. G.; Schurmann, A. Characterization of human glucose transporter (GLUT) 11 (encoded by SLC2A11), a novel sugar-transport facilitator specifically expressed in heart and skeletal muscle. *Biochem. J.* **2001**, *359*, 443-449.

(34) Mueckler, M. Facilitative glucose transporters. *Eur. J. Biochem./ FEBS* **1994**, *219*, 713-725.

(35) Saier, M. H., Jr. Families of transmembrane sugar transport proteins. *Mol. Microbiol.* **2000**, *35*, 699-710.

Chapter 5

Experimental section

5.1. Synthesis linear peptides

5.1.1. Synthesis of linear peptides in solution

All the general procedures are reported in details in the section ***6.6*** of the chapter 6 *General methods and procedures*. The yield of each synthetic step was calculated on the base of pure product recovered after each reaction coupling and subsequent chromatography purification. The purity of each compound was determined through the ^{1}H-NMR spectroscopy.

Fmoc-Val-Tyr(OBzl)-Leu-Pro-Lys(z)-OFm (1a)

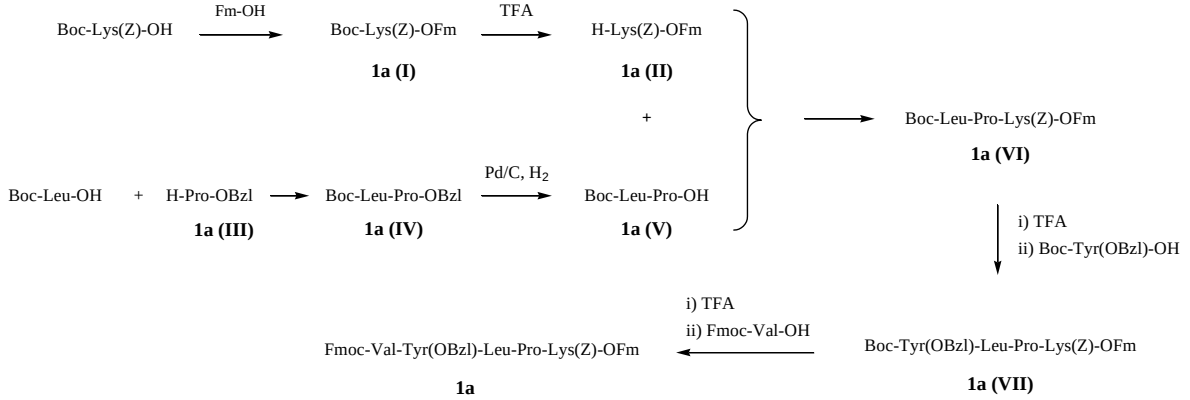

Boc-Lys(Z)-OFm **[1a(I)]**

The reaction was performed according to the methodology reported in the section *6.6.1.1*. Purification of the crude by silica gel chromatography (hexane/Acetone= 85/15) gave the product as a white foam (1.5 g, 85%). Purity> 98%. R_f = 0.2 (hexane-Acetone, 8:2). $[\alpha]_D^{20}$(c 0.5, $CHCl_3$) = - 14.62°

^{1}HNMR (300 MHz, $CDCl_3$): δ 7.77 (d, 2H, J=7.3 Hz, Har-Fm); 7.57 (m, 2H, Har-Fm); 7.35 (m, 9H); 5.09 (s, 2H, CH_2-Cbz); 4.84 (bs, 1H, NH); 4.54 (m, 2H, CH_2-Fm); 4.28 (m, 1H, H^{α}-Lys); 4.22 (t, 1H, J=6.1 Hz, CH-Fm); 3.15 (bd, 2H, J=6.1 Hz, $2H^{\varepsilon}$-Lys); 1.64 (m, 1H, 1H-Lys); 1.47 (m, 12H, 3H-Lys, $3CH_3$-*t*Bu); 1.26 (m, 6H, $2CH_3$-Leu).

^{13}C NMR ($CDCl_3$, 75 MHz): δ 170.53 (1C, s); 154.46 (1C, s); 153.43 (1C, s); 141.13 (2C, s); 139.06 (2C, s); 134.42 (1C, s); 126.24 (2C, d); 125.50 (3C, d); 125.64 (2C, d); 124.94 (2C, d); 122.70 (2C, d); 117.80 (2C, d); 77.67 (1C, s); 64.24 (1C, t), 64.31 (1C, t); 51.29 (1C, d); 48.09 (1C, d); 38.25 (1C, t); 29.66 (1C, t); 27.10 (1C, t); 26.08 (3C, q); 20.07 (1C, t).

H-Pro-OBzl **[1a(III)]**

This compound was synthesized in accordance to the previous reported procedure.[1] The characterization data match with the literature.[1]

Boc-Leu-Pro-OBzl **[1a(IV)]**

The product was synthesized according to the protocol B reported in the section *6.6.2*. Purification by silica gel chromatography: EtOAc/cyclohexane 8:2; gave the product as a colorless syrup (980 mg, 97%). Purity > 98%. R_f = 0.23 (EtOAc/cyclohexane, 2:8). $[\alpha]_D^{20}$ (c 0.25, $CHCl_3$) = - 75.42°

^{1}H NMR ($CDCl_3$, 300 MHz): δ 7.31 (m, 5H, Har-OBzl); 5.19-5.04 (m, 3H, 1NH, CH_2-OBzl); 4.57 (m, 1H, H^{α}-Pro); 4.43 (bm, 1H, H^{α}-Leu); 3.75 (m, 1H, $1H^{\delta}$-Pro); 3.57 (m, 1H, $1H^{\delta}$-Pro); 2.17 (1H, H-Pro); 1.98 (m, 3H, H-Pro); 1.69 (m, 1H, H^{γ}-Leu); 1.38 (m, 11H, $2H^{\beta}$-Leu, 9H-*t*Bu); 0.89 (d, 3H, J=6.7 Hz, $1CH_3$-Leu); 0.85 (d, 3H, J=6.7 Hz, $1CH_3$-Leu).

^{13}C NMR ($CDCl_3$, 75MHz,): δ 172.10; 156.0; 141.6; 135.8; 128.6; 128.5; 127.6; 127.1; 79.7, 67.1; 65.2; 50.5; 46.9; 42.2; 29.2; 25.11; 24.8; 23.6; 21.9.

Boc-Leu-Pro-OH **[1a(V)]**

Boc-Leu–Pro–OBn (420 mg, 2.05 mmol) was dissolved in dry MeOH (8 ml) and 10% (w/w) Pd/C (4 mg) was added. H_2 was introduced with a balloon and the suspension was stirred at room temperature for 12 h. The solution was filtered through a pad of celite and concentrated *in vacuo*. The resulting product was obtained without purification as a white foam (675 mg, 100 %). Purity > 98%. R_f = 0.06 (EtOAc/cyclohexane, 4:6). $[\alpha]_D^{20}$ (c 0.25, $CHCl_3$) = - 73.22°

^{1}H NMR ($CDCl_3$, 300 MHz): δ 5.28 (bd, 1H, J=8.8 Hz, NH); 4.57 (m, 1H, H^{α}-Pro); 4.50 (bm, 1H, H^{α}-Leu); 3.78 (m, 1H, $1H^{\delta}$-Pro); 3.58 (m, 1H, $1H^{\delta}$-Pro); 2.18 (m, 2H, 2H-Pro); 2.03 (m, 2H, 2H-Pro); 1.71 (m, 1H, H^{γ}-Leu); 1.38 (m, 11H, $2H^{\beta}$-Leu, $3CH_3$-*t*Bu); 0.97-0.85 (m, 6H, $2CH_3$-Leu).

^{13}C NMR ($CDCl_3$, 75 MHz): δ 174.08 (1C, s); 173.61 (1C, s); 155.88 (1C, s); 79.90 (1C, s); 59.41 (1C, d); 50.50 (1C, d); 47.27 (1C, t); 41.66 (1C, t); 29.81 (3C, q); 28.46 (1C, t); 24.97 (1C, d); 24.66 (1C, q); 23.46 (1C, q); 21.86 (1C, d).

Boc-Leu-Pro-Lys(Z)-OFm **[1a(VI)]**

The product was synthesized according to the protocol A reported in the section *6.6.2*. Reaction time 12 h. Purification by silica gel chromatography: EtOAc/cyclohexane 7:3; gave the product as a white foam (1.26 g, 92%). Purity > 98%. R_f = 0.1 (EtOAc/cyclohexane, 3:7). $[\alpha]_D^{20}$ (c 0.5, $CHCl_3$) = - 50.81°

^{1}H NMR ($CDCl_3$, 300 MHz): δ 7.75 (d, 2H, J=7.3 Hz, Har-Fm); 7.56 (m, 2H, Har-Fm); 7.35 (m, 9H, 4Har-Fm, 5Har-Bzl); 6.84 (bd, 1H, J= 7.3 Hz, NH); 5.66 (bs, 1H, NH); 5.12 and 5.21 (2 d, 2H, J=12.2Hz, CH_2-Cbz); 4.52 (m, 4H, CH_2-Fm, $1H^{\alpha}$-Lys, $1H^{\alpha}$-Leu); 4.38 (m, 1H, H^{α}-Pro); 4.19 (t, 1H, J=6.12 Hz, CH-Fm); 3.76 (m, 1H, $1H^{\delta}$-Pro); 3.55 (m, 1H, $1H^{\delta}$-Pro); 3.31 (bd, 2H, J= 6.1Hz, H^{ε}-Lys); 2.17 (m, 2H, H-Pro); 1.94 (m, 2H, H-Pro); 1.70 (m, 2H, $1H^{\gamma}$-Leu, 1H-Lys); 1.39 (m, 15H, 4H-Lys, $3CH_3$-*t*Bu, $2H^{\beta}$-Leu); 1.14 (m, 1H, 1H-Lys); 0.95 (d, 3H, J=6.7 Hz, $1CH_3$-Leu); 0.87 (d, 3H, J=6.7 Hz, $1CH_3$-Leu).

^{13}C NMR ($CDCl_3$, 75 MHz): δ 171.05 (1C, s); 169.59 (1C, s); 168.62 (1C, s); 154.19 (1C, s); 141.31 (1C, s); 141.13 (1C, s); 139.19 (1C, s); 139.10 (1C, s); 134.74 (1C, s); 126.13 (2C, d); 125.75 (1C, d); 125.64 (2C, d); 125.58 (2C, d); 124.88 (2C, d); 122.56 (2C, d); 117.74 (2C, d); 77.28 (1C, s); 64.37 (1C, t); 64.15 (1C, t); 59.30 (1C, d); 49.79 (1C, d); 48.22 (1C, d); 45.06 (1C, t); 44.72 (1C, d); 39.56 (1C, t); 38.10 (1C, t); 29.24 (1C, t); 26.71 (1C, t); 26.10 (3C, q); 25.49 (1C, t); 22.89 (1C, t); 22.31 (1C, d); 20.98 (1C, q); 19.51 (1C, t); 19.47 (1C, q).

Boc-Tyr(OBzl)-Leu-Pro-Lys(Z)-OFm **[1a(VII)]**

The product was synthesized according to the protocol A described in the section *6.6.2*. Reaction time 12 h. Purification by silica gel chromatography: EtOAc/*n*-hexane 45:55; gave the product as a white foam (1.22 g, 95%). Purity > 98%. R_f = 0.42 (EtOAc/*n*-hexane, 6:4). $[\alpha]_D^{20}$(c 0.25, $CHCl_3$) = - 29.10°

^{1}H NMR ($CDCl_3$, 300 MHz): δ 7.76 (d, 2H, J=7.3 Hz, Har-Fm); 7.56 (m, 2H, Har-Fm); 7.38-7.25 (m, 14H, 4Har-Fm, 5Har-Cbz, 5Har-OBzl); 7.05 (bd, 2H, J=8.5 Hz, Har-Tyr); 6.84 (d, 2H, J=8.5 Hz, Har-Tyr); 5.23 (bs, 2H, CH_2-OBzl); 4.99 (s, 2H, CH_2-Cbz); 4.82 (m, 1H, H^{α}-Leu); 4.51 (m, 5H, CH_2-Fm, $1H^{\alpha}$-Lys, $1H^{\alpha}$-Pro, $1H^{\alpha}$-Tyr); 4.18 (t, 1H, J=6.1 Hz, CH-Fm); 3.78 (m, 1H, $1H^{\delta}$-Pro); 3.58 (m, 1H, $1H^{\delta}$-Pro); 3.15 (bm, 3H, $2H^{\varepsilon}$-Lys, $1H^{\beta}$-Tyr); 2.85 (m, 1H, $1H^{\beta}$-Tyr); 2.13 (m, 2H, H-Pro); 1.95 (m, 2H, H-Pro); 1.66 (m, 1H, H^{γ}-Leu); 1.49 (m, 2H, H^{β}-Leu); 1.38-1.21 (m, 15H, $3CH_2$-Lys, $3CH_3$-*t*Bu); 0.96 (d, 3H, J=6.1 Hz, $1CH_3$-Leu); 0.88 (d, 3H, J=6.4 Hz; $1CH_3$-Leu).

^{13}C NMR ($CDCl_3$, 75 MHz): δ 169.69 (2C, s); 168.85 (1C, s); 155.49 (1C, s); 153.02 (1C, s); 141.63 (1C, s); 141.36 (1C, s); 141.17 (1C, s); 140.55 (1C, s);139.20 (1C, s); 139.11 (1C, s); 135.00 (1C, s); 134.62 (1C, s); 128.53 (2C, d); 126.23 (4C, d); 125.50 (2C, d); 125.61 (4C, d); 125.07 (2C, d); 124.90 (2C, d); 122.60 (2C, d); 117.77 (2C, d); 112.84 (2C, d); 77.28 (1C, s); 67.90 (2C, t); 64.37 (2C, t); 60.01 (1C, t); 59.80 (1C, t); 58.73 (1C, d); 58.50 (1C, t); 58.10 (1C, d); 49.85 (1C, d); 46.89 (1C, d); 45.23 (1C, t); 44.73 (1C, d); 39.31 (1C, t); 36.06 (1C, t); 29.23 (1C, t); 26.09 (3C, q); 22.94 (1C, t); 22.27 (1C, d); 21.06 (1C, q); 19.61 (1C, q).

Fmoc-Val-Tyr(OBzl)-Leu-Pro-Lys(Z)-OFm **[1a]**

The product was synthesized according to the protocol A described in the section *6.6.2*. Reaction time 12 h. Purification by silica gel chromatography: $CHCl_3$/Acetone, 9:1; gave the product as a white solid (970 mg, 92%). Purity > 98%. R_f = 0.2 ($CHCl_3$/Acetone, 9:1). $[\alpha]_D^{20}$(c 0.25, $CHCl_3$) = - 29.19°

^{1}H NMR ($CDCl_3$, 300 MHz): δ 7.72 (d, 4H, J=6.1 Hz, 2Har-Fm, 2Har-Fmoc); 7.57 (m, 4H, 2Har-Fm, 2Har-Fmoc); 7.31 (m, 18H, 4Har-Fm, 4Har-Fmoc, 5Har-Cbz, 5Har-OBzl); 7.05 (d, 2H, J=8.5 Hz, Har-Tyr); 6.84 (d, 2H, J=8.5 Hz, Har-Tyr); 5.28 (bs, 1H, NH); 5.17 (s, 2H, CH_2-Cbz); 4.91 (s, 2H, CH_2-OBzl); 4.76 (m, 2H, 1NH, $1H^{\alpha}$); 4.54 (m, 5H, $1H^{\alpha}$, CH_2-Fmoc, CH_2-OFm); 4.35 (m, 2H, $2H^{\alpha}$); 4.22 (m, 3H, $1H^{\alpha}$, CH-Fm, CH-Fmoc); 3.95 (bs, 1H, $1H^{\alpha}$); 3.74 (m, 1H, $1H^{\delta}$-Pro); 3.54 (m, 1H, $1H^{\delta}$-Pro); 3.17 (bm, 3H, $2H^{\varepsilon}$-Lys, $1H^{\beta}$-Tyr); 2.87 (m, 1H, $1H^{\beta}$-Tyr); 2.15 (m, 3H, 2H-Pro, $1H^{\beta}$-Val); 1.95 (m, 2H, 2H-Pro); 1.75 (m, 4H,

$2H^{\beta}$-Lys, $2H^{\beta}$-Leu); 1.60 (1H, H^{γ}-Leu); 1.41 (m, 4H, $2H^{\gamma}$-Lys, $2H^{\delta}$-Lys); 0.89-0.80(m, 12H, $2CH_3$-Leu, $2CH_3$-Val).

^{13}C NMR ($CDCl_3$, 75 MHz): δ 172.10 (1C, s); 171.15 (1C, s); 170.99 (1C, s); 170.67 (1C, s); 153.02 (1C, s); 157.90 (1C, s); 157.81 (1C, s); 156.35 (1C, s); 144.10 (1C, s); 144.0 (1C, s); 143.60 (1C, s); 143.4 (1C, s); 143.20 (1C, s); 141.51 (2C, s); 141.36 (2C, s); 137.25 (1C, s); 137.20 (1C, s); 136.76 (1C, s); 130.64 (1C, d); 128.63 (4C, d); 128.27 (1C, d); 127.99 (4C, d); 127.77 (2C, d); 127.51 (4C, d); 127.25 (4C, d); 127.40(2C, d); 125.28 (1C, d);125.10 (1C, d); 124.96 (1C, d); 120.12 (2C, d); 120.05 (2C, d); 114.69 (1C, d); 69.99 (1C, t); 67.08 (1C, t); 67.76 (1C, t); 61.10 (1C, d); 60.82 (1C, d); 54.11 (1C, d), 51.84 (1C, d); 49.10 (1C, d); 48.15 (1C, t); 47.90 (1C, t); 47.37 (1C, d); 46.96 (1C, d); 42.13 (1C, t); 41.95 (1C, t); 41.08 (1C, t); 40.95 (1C, t); 31.50 (1C, d); 31.32 (1C, t); 28.62 (1C, t); 25.42 (1C, t); 25.59 (1C, d); 23.44 (1C, q); 21.93 (1C, q); 21.05 (1C, t); 19.37 (1C, q); 17.74 (1C, q).

Fmoc-Val-Tyr(OBzl)-Leu-Pro-D-Lys(2Cl-Z)-OFm (1b)

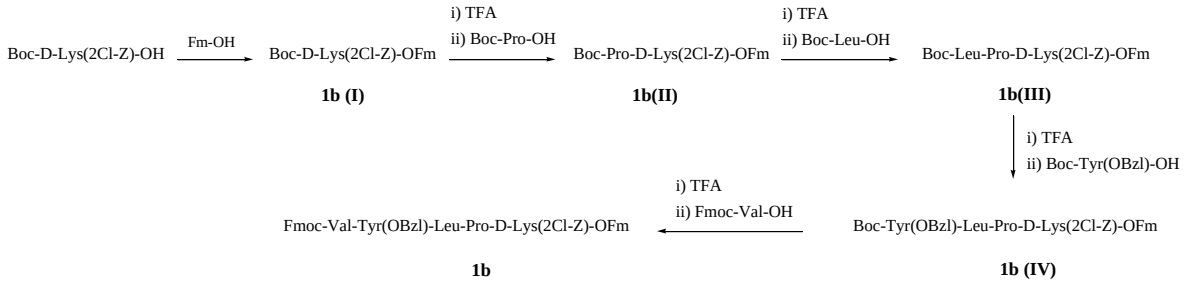

<u>*Boc-D-Lys(2Cl-Z)-OFm*</u> **[1b(I)]**

The reaction was performed according to the methodology reported in the section *6.6.1.1*. Purification of the crude by silica gel chromatography (*n*-hexane/AcOEt= 85/15) gave the product as a pale yellow syrup (2.09 g, 98%). Purity > 98%. R_f = 0.1 (*n*-hexane/AcOEt, 85:15). $[\alpha]_D^{20}$ (c 1, $CHCl_3$) = + 2.67°

^{1}H NMR ($CDCl_3$, 300 MHz): δ 7.76 (d, J=7.3 Hz, 2Har); 7.57 (m, 2H, 2Har); 7.39-7.25 (m, 8Har); 5.20 (s, 2H, CH_2-Cbz); 5.10 (bd, 1H, J= 6.4 Hz, NH); 4.91 (bs, 1H, NH); 4.51 (m, 2H, CH_2-Fm); 4.28 (bm, 1H, H^{α}-Lys); 4.20 (t, 1H, J=6.1 Hz, CH-Fm); 3.15 (bd, 2H, J= 5.8 Hz, $2H^{\varepsilon}$-Lys); 1.64 (bm, 1H, H-Lys); 1.26 (m, 12H, 9H-*t*Bu, 3H-Lys); 1.22 (m, 2H, 2H-Lys).

^{13}C NMR ($CDCl_3$, 75 MHz): δ 172.72 (1C, s); 157.31 (1C, s); 155.54 (1C, s); 143.64 (1C, s), 143.48 (1C, s); 141.49 (1C, s); 141.42 (1C, s); 134.45 (1C, s); 133.64 (1C, s), 129.86 (1C, d); 129.59 (1C, d); 129.42 (1C, d); 12.99 (2C, d); 127.27 (2C, d); 126.94 (1C, d); 125.00 (2C, d), 120.15 (2C, d); 80.05 (1C, s); 66.80 (1C, t); 63.98 (1C, t); 53.32 (1C, d); 46.96 (1C, d); 40.72 (1C, t); 32.29 (1C, t); 29.44 (1C, t); 28.42 (3C, q); 22.35 (1C, t).

<u>*Boc-Pro-D-Lys(2Cl-Z)-OFm*</u> **[1b (II)]**

The reaction was performed according to the protocol C reported in the section *6.6.2*. Purification of the crude by silica gel chromatography (*n*-hexane/AcOEt= 55/45) gave the

product as a white foam (2.3 g, 90%). Purity > 98%. R_f = 0.3 (*n*-hexane/AcOEt, 1:1). $[\alpha]_D^{20}$ (c 0.5, $CHCl_3$) = - 29.60°

^{1}H NMR ($CDCl_3$, 300 MHz): δ 7.75 (d, J= 7.6 Hz, 2Har); 7.55 (m, 2Har); 7.39-720 (m, 8Har); 5.27 (s, 2H, CH_2-Cbz); 4.95 (bs, 1H, NH); 4.53 (m, 3H, CH_2-Fm, 1H$^{\alpha}$-Lys); 4.25 (bm, 1H, H$^{\alpha}$-Pro); 4.18 (t, 1H, J= 6.1 Hz, CH-Fm); 3.99 (bm, 2H, H$^{\delta}$-Pro), 3.11 (m, 2H, H$^{\varepsilon}$-Lys); 2.17 (bm, 1H, H-Pro), 2.01 (bm, 1H, H-Pro), 1.85 (bm, 3H, 1H-Lys, 2H-Pro); 1.43 (m, 12H, 9H-*t*Bu, 5H-Lys).

^{13}C NMR ($CDCl_3$, 75 MHz): δ 172.08 (2C, s); 156.23 (1C, s); 155.54 (1C, s); 143.63(1C, s); 143.44 (1C, s); 141.52 (1C, Cq); 141.41(1C, s); 134.66 (1C, s); 133.53 (1C, s), 129.68 (1C, d); 129.49 (1C, d); 129.23 (1C, d); 127.95 (2C, d); 127.25 (2C, d); 126.85 (1C, d); 124.88 (2C, d), 120.10 (2C, d); 80.56 (1C, s); 66.74 (1C, t); 63.82 (1C, t); 60.70 (1C, d); 51.90 (1C, d); 47.21 (1C, t); 47.03 (1C, d); 40.80 (1C, t); 32.03 (1C, t); 29.32 (1C, t); 28.43 (3C, q); 24.16 (1C, t); 22.25 (1C, t).

Boc-Leu-Pro-D-Lys(2Cl-Z)-OFm **[1b(III)]**

The reaction was performed according to the protocol C reported in the section *6.6.2*. Purification of the crude by silica gel chromatography (cyclohexane/AcOEt= 8/2) gave the product as a white solid (1.7 g, 93%). Purity > 98%. R_f = 0.28 (cyclohexane/AcOEt, 8:2). $[\alpha]_D^{20}$ (c 0.5, $CHCl_3$) = - 46.53°

^{1}H NMR ($CDCl_3$, 300 MHz): δ 7.76 (d, J=7.3 Hz, 2Har); 7.55 (m, 2H, 2Har); 7.40 (m, 8Har); 7.15 (bd, 1H, J= 9.0 Hz, NH); 5.45 (bs, 1H, NH); 5.23 (s, 2H, CH_2-Cbz); 4.60-4.47 (m, 5H, CH_2-Fm, 1H$^{\alpha}$-Lys, 1H$^{\alpha}$-Pro, 1H$^{\alpha}$-Leu); 4.21 (t, 1H, J=6.1 Hz, CH-Fm); 3.37 (bm, 1H, 1H$^{\delta}$-Pro); 3.53 (m, 1H, 1H$^{\delta}$-Pro), 3.16 (m, 2H, 2H$^{\varepsilon}$-Lys); 2.29 (bm, 1H, 1H-Pro), 2.01 (bm, 3H, 3H-Pro), 1.75 (bm, 2H, 1H$^{\gamma}$-Leu, 1H-Lys); 1.46 (m, 13H, 9H-*t*Bu, 2H$^{\beta}$-Leu, 2H-Lys); 1.25 (m, 3H, 3H-Lys); 0.94 (d, 3H, J= 6.4 Hz, 1CH_3-Leu); 0.88 (d, 3H, J= 6.6 Hz, 1CH_3-Leu).

^{13}C NMR ($CDCl_3$, 75 MHz): δ 173.96 (1C, s); 171.88 (1C, s); 170.76 (1C, s); 156.21 (1C, s); 155.79 (1C, s); 143.62 (1C, s); 143.33 (1C, s); 141.49 (1C, s); 141.36 (1C, s); 134.68 (1C, s); 133.82 (1C, s), 129.49 (2C, d); 129.22 (1C, d); 127.97 (2C, d); 127.25 (1C, d); 127.21 (1C, d); 126.90 (1C, d); 124.91 (2C, d); 120.11 (2C, d); 79.76 (1C, s); 66.73 (1C, t); 63.73 (1C, t); 60.10 (1C, d); 51.87 (1C, d); 50.55 (1C, d); 47.29 (1C, t); 46.90 (1C, d); 42.13 (1C, t); 40.43 (1C, t); 31.33 (1C, t); 29.04 (1C, t); 28.39 (3C, q); 27.38 (1C, t); 25.07 (1C, t); 24.71 (1C, d); 23.62 (1C, q); 21.69 (1C, q); 21.50 (1C, t).

Boc-Tyr(OBzl)-Leu-Pro-D-Lys(2Cl-Z)-OFm **[1b (IV)]**

The reaction was performed according to the protocol C reported in the section *6.6*.2. Reaction time 12 h. Purification of the crude by silica gel chromatography (cyclohexane/AcOEt= 1/1) gave the product as a white foam (1.2 g, 94%). Purity > 95%. R_f = 0.18 (cyclohexane/AcOEt, 1:1). $[\alpha]_D^{20}$ (c 0.5, $CHCl_3$) = - 35.10°

^{1}H NMR ($CDCl_3$, 300 MHz): δ 8.44 (bd, 1H, J= 7.6 Hz, NH); 7.76 (dd, J=7.3 Hz, J=3 Hz, 2Har); 7.55 (m, 2Har); 7.39-7.25 (m, 13Har); 7.04 (m, 2Har); 6.86 (m, 2Har); 6.71 (bd, 1H,

J= 8.2 Hz, NH); 6.60 (bs, 1H, NH); 5.35-5.16 (m, 3H); 5.00 (s, 2H, CH_2-OBzl); 4.75 (m, 1H); 4.48 (m, 5H); 4.18 (t, 1H, J=6.1 Hz); 3.81-3.50 (bm, 2H); 3.28 (m, 1H); 3.12 (m, 1H); 2.95 (bm, 2H); 2.24-1.85 (bm, 4H), 1.55-1.25 (bm, 18H); 0.90 (m, 6H).

^{13}C NMR ($CDCl_3$, 75 MHz): δ 174.26 (1C, s); 172.53 (1C, s); 171.90 (1C, s); 157.82 (1C, s); 156.21 (1C, s); 155.32 (1C, s); 143.60 (1C, s); 143.30 (1C, s); 141.64 (1C, s); 141.35 (1C, s); 137.08 (1C, s); 136. 23 (1C, s); 134.60 (1C, s); 130.63 (1C, d); 130.7 (1C, d); 129.77 (1C, d);129.55 (1C, d); 129.28 (1C, s); 129.38 (2C, d); 128.61 (2C, d); 127.97 (3C, d); 127.48 (2C, d); 127.24 (2C, d); 124.89 (1C, d); 124.83 (1C, d); 120.13 (2C, d); 114.91 (1C, d); 114.63 (1C, d); 79.76 (1C, s); 70.04 (1C, t); 66.74 (1C, t); 64.34 (1C, t); 63.85 (1C, t); 60.89 (1C, d); 59.92 (1C, d); 51.88 (1C, d); 51.19 (1C, d); 49.21 (1C, d); 47.35 (1C, t); 41.88 (1C, t); 40.68 (1C, t); 39.51 (1C, t); 31.66 (1C, t); 29.22 (1C, t); 28. 61 (1C, t); 28.12 (3C, q); 24.93 (1C, t); 24.59 (1C, d); 23.28 (1C, q); 20.04 (1C, q).

Fmoc-Val-Tyr (OBzl)-Leu-Pro-D-Lys(2Cl-Z)-OFm **(1b)**

The reaction was performed according to the protocol C reported in the section *6.6.2*. Reaction time 12 h. Purification of the crude by silica gel chromatography (CH_2Cl_2/Acetone= 9/1) gave the product as a white foam (1.2 g, 94%). Purity > 98%. R_f = 0.18 (CH_2Cl_2/Acetone, 9:1). $[\alpha]_D^{20}$ (c 0.5, $CHCl_3$) = - 40.62°

^{1}H NMR ($CDCl_3$, 300 MHz): δ 8.48 (bd, 1H, J= 7.0 Hz, NH); 7.75 (d, J=7.3 Hz, 4Har); 7.57 (m, 4Har); 7.33 (m, 17Har); 7.05 (d, 2H, J= 8.2 Hz, 2Har); 6.79 (d, 2H, J= 8.2 Hz, 2Har); 6.71 (bs, 1H, NH); 6.56 (bs, 1H, NH); 6.42 (bs, 1H, NH); 5.29 (m, 3H); 4.90 (m, 3H); 4.45 (m, 7H); 4.20 (m, 2H); 3.63 (bm, 2H); 3.12 (m, 2H); 2.97 (m, 2H); 2.03 (bm, 4H), 1.68 (bm, 3H); 1.37 (bm, 5H); 1.25 (bm, 2H); 0.88 (bm, 12H).

^{13}C NMR ($CDCl_3$, 75 MHz): δ 172.10 (1C, s); 171.15 (1C, s); 170.99 (1C, s); 170.67 (1C, s); 153.02 (1C, s); 157.90 (1C, s); 157.81 (1C, s); 156.35 (1C, s); 144.10 (1C, s); 144.0 (1C, s); 143.60 (1C, s); 143.4 (1C, s); 143.20 (1C, s); 141.51 (2C, s); 141.39 (2C, s); 137.25 (1C, s); 137.20 (1C, s); 136.76 (1C, s); 136. 68 (1C, s); 130.52 (1C, s); 130.33 (1C, d); 129.67 (1C, d); 129.41 (1C, d); 129.26 (1C, d); 128.41 (2C, d); 127.81 (2C, d); 127.64 (2C, d); 127.38 (2C, d); 127.07 (1C, d); 126.83 (1C, d); 125.12 (1C, d); 124.74 (2C, d); 119.96 (2C, d); 114.56 (1C, d); 69.72 (1C, t); 66.95 (1C, t); 66.76 (1C, t); 61.10 (1C, d); 60.82 (1C, d); 54.11 (1C, d), 51.84 (1C, d); 49.10 (1C, d); 48.15 (1C, t); 47.90 (1C, t); 47.37 (1C, d); 46.96 (1C, d); 42.13 (1C, t); 41.95 (1C, t); 41.08 (1C, t); 40.95 (1C, t); 31.50 (1C, d); 31.32 (1C, t); 28.62 (1C, t); 25.42 (1C, t); 25.59 (1C, d); 23.44 (1C, q); 21.93 (1C, q); 21.05 (1C, t); 19.37 (1C, q); 17.74 (1C, q).

Fmoc-Val-Tyr(OBzl)-Leu-D-Pro-Lys(2Cl-Z)-OFm (1c)

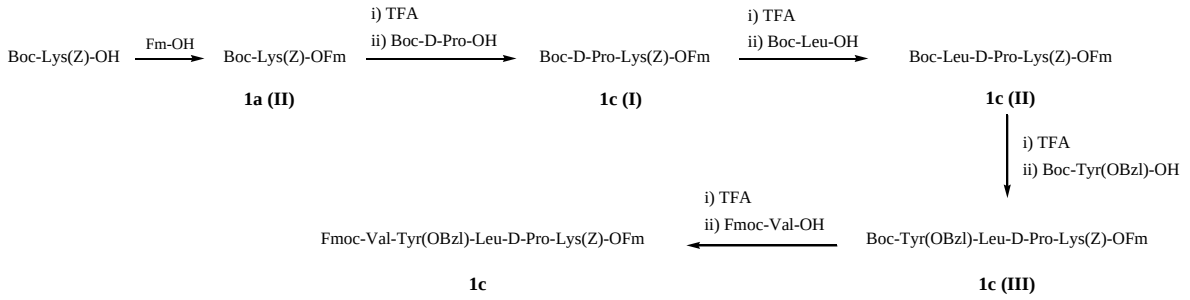

Boc-D-Pro-Lys(Z)-OFm **[1c(I)]**

The reaction was performed according to the methodology A reported in the section *6.6.1*. Purification of the crude by silica gel chromatography (*n*-hexane/Acetone= 75/25) gave the product as a white foam. (970 mg, 85%). Purity > 98%. R_f = 0.16 (*n*-hexane/Acetone, 75:25). $[\alpha]_D^{20}$ (c 0.5, $CHCl_3$) = + 39.61°

^{1}H NMR ($CDCl_3$, 300 MHz): δ 7.75 (d, J= 6 Hz, 2Har); 7.56 (t, 2H, J= 7.5, 2Har); 7.34 (m, 9Har); 5.08 (s, 2H, CH_2-Cbz); 4.56 (m, 3H, CH_2-Fm, 1H$^{\alpha}$-Lys); 4.20 (m, 2H, 1H$^{\alpha}$-Pro, CH-Fm); 3.41 (bm, 2H, H$^{\delta}$-Pro); 3.11 (m, 2H, H$^{\varepsilon}$-Lys), 1.82 (m, 2H, H-Pro), 1.42 (s, 12H, 2H-Pro, 9H-*t*Bu, H-Lys), 1.21 (bm, 4H, H-Lys); 0.88 (t, 1H, J=7.1 Hz, 1H.Lys).

^{13}C NMR ($CDCl_3$, 75 MHz): δ 172.08 (2C, s); 156.23 (1C, s); 155.54 (1C, s); 143.63 (1C, s); 143.44 (1C, s); 141.52 (1C, s); 141.41(1C, s); 134.66 (1C, s); 133.53 (1C, d), 129.68 (1C, d); 129.49 (1C, d); 129.23 (1C, d); 127.95 (2C, d); 127.25 (2C, d); 126.85 (1C, d); 124.88 (2C, d), 120.10 (2C, d); 80.05 (1C, s); 66.80 (1C, t); 63.98 (1C, t); 53.32 (1C, d); 46.96 (1C, d); 40.72 (1C, t); 32.29 (1C, t); 29.44 (1C, t); 28.42 (3C, q); 22.35 (1C, t).

Boc-Leu-D-Pro-Lys(Z)-OFm **[1c(II)]**

The reaction was performed according to the methodology B reported in the section *6.6.2*. Reaction time 16 h. Purification by silica gel chromatography (PE/Acetone= 75/25) gave the product as a white foam. (1.1 g, 90%). Purity > 98%. R_f = 0.20 (PE/Acetone, 75:25). $[\alpha]_D^{20}$ (c 0.5, $CHCl_3$) = + 35.35°

^{1}H NMR ($CDCl_3$, 300 MHz): δ 7.75 (d, 2H, J=7.3 Hz, Har-Fm); 7.56 (m, 2H, Har-Fm); 7.35 (m, 9H, 4Har-Fm, 5Har-Bzl); 6.84 (bd, 1H, J= 7.3 Hz, NH); 5.15 (s, 2H, CH_2-Cbz); 4.52 (m, 4H, CH_2-Fm, 1H$^{\alpha}$-Lys, 1H$^{\alpha}$-Leu); 4.38 (m, 1H, H$^{\alpha}$-Pro); 4.19 (t, 1H, J=6.1 Hz, CH-Fm); 3.76 (m, 1H, 1H$^{\delta}$-Pro); 3.55 (m, 1H, 1H$^{\delta}$-Pro); 3.31 (bd, 2H, J= 6.1, H$^{\varepsilon}$-Lys); 2.17 (m, 2H, H-Pro); 1.94 (m, 2H, H-Pro); 1.70 (m, 2H, 1H$^{\gamma}$-Leu, 1H-Lys); 1.39 (m, 15H, 4H-Lys, 3CH_3-*t*Bu, 2H$^{\beta}$-Leu); 1.14 (m, 1H, 1H-Lys); 0.95 (d, 3H, J=6.7 Hz, 1CH_3-Leu); 0.87 (d, 3H, J=6.7 Hz, 1CH_3-Leu).

^{13}C NMR ($CDCl_3$, 75 MHz): δ 171.05 (1C, s); 169.59 (1C, s); 168.62 (1C, s); 154.19 (1C, s); 141.31 (1C, s); 141.13 (1C, s); 139.19 (1C, s); 139.10 (1C, s); 134.74 (1C, s); 126.13 (2C, d); 125.75 (1C, d); 125.64 (2C, d); 125.58 (2C, d); 124.88 (2C, d); 122.56 (2C, d); 117.74 (2C, d); 77.28 (1C, s); 64.37 (1C, t); 64.15 (1C, t); 59.30 (1C, d); 49.79 (1C, d); 48.22 (1C, d); 45.06 (1C, t); 44.72 (1C, d); 39.56 (1C, t); 38.10 (1C, t); 29.24 (1C, t); 26.71

(1C, t); 26.10 (3C, q); 25.49 (1C, t); 22.89 (1C, t); 22.31 (1C, d); 20.98 (1C, q); 19.51 (1C, t); 19.47 (1C, q).

Boc-Tyr(OBzl)-Leu-D-Pro-Lys(Z)-OFm **[1c(III)]**

The reaction was performed according to the methodology C reported in the section *6.6.2* Purification of the crude by silica gel chromatography (cyclohexane/Acetone= 7/3) gave the product as a white foam (1.1 g, 85%). Purity > 98%. R_f = 0.2 (cyclohexane/Acetone, 7:3). $[\alpha]_D^{20}$ (c 0.25, $CHCl_3$) = + 3.28°

^{1}H NMR ($CDCl_3$, 300 MHz): δ 7.76 (d, 2H, J=7.3 Hz, Har-Fm); 7.56 (m, 2H, Har-Fm); 7.38-7.25 (m, 14H, 4Har-Fm, 5Har-Cbz, 5Har-OBzl); 7.05 (bd, 2H, J=8.5 Hz, Har-Tyr); 6.84 (d, 2H, J=8.5 Hz, Har-Tyr); 5.14 (s, 2H, CH_2-OBzl); 5.00 (s, 2H, CH_2-Cbz); 4.80 (m, 1H, H^{α}-Leu); 4.51 (m, 5H, CH_2-Fm, $1H^{\alpha}$-Lys, $1H^{\alpha}$-Pro, $1H^{\alpha}$-Tyr); 4.17 (t, 1H, J=6.1 Hz, CH-Fm); 3.79 (m, 1H, $1H^{\delta}$-Pro); 3.55 (m, 1H, $1H^{\delta}$-Pro); 3.13 (bm, 3H, $2H^{\varepsilon}$-Lys, $1H^{\beta}$-Tyr); 2.89 (bm, 1H, $1H^{\beta}$-Tyr); 2.15 (m, 2H, H-Pro); 1.97 (m, 2H, H-Pro); 1.44-1.58 (m, 3H, $1H^{\gamma}$-Leu, $2H^{\beta}$-Leu); 1.38-1.21 (m, 15H, $3CH_2$-Lys, $3CH_3$-*t*Bu); 0.96 (d, 3H, J=6.1 Hz, $1CH_3$-Leu); 0.88 (d, 3H, J=6.4 Hz; $1CH_3$-Leu).

^{13}C NMR ($CDCl_3$, 75 MHz): δ 169.69 (2C, s); 168.85 (1C, s); 155.49 (1C, s); 153.02 (1C, s); 141.63 (1C, s); 141.36 (1C, s); 141.17 (1C, s); 140.55 (1C, s);139.20 (1C, s); 139.11 (1C, s); 135.00 (1C, s); 134.62 (1C, s); 128.53 (2C, d); 126.23 (4C, d); 125.50 (2C, d); 125.61 (4C, d); 125.07 (2C, d); 124.90 (2C, d); 122.60 (2C, d); 117.77 (2C, d); 112.84 (2C, d); 77.28 (1C, s); 67.90 (2C, t); 64.37 (2C, t); 60.01 (1C, t); 59.80 (1C, t); 58.73 (1C, d); 58.50 (1C, t); 58.10 (1C, d); 49.85 (1C, d); 46.89 (1C, d); 45.23 (1C, t); 44.73 (1C, d); 39.31 (1C, t); 36.06 (1C, t); 29.23 (1C, t); 26.09 (3C, q); 22.94 (1C, t); 22.27 (1C, d); 21.06 (1C, q); 19.61 (1C, q).

Fmoc-Val-Tyr(OBzl)-Leu-D-Pro-Lys(Z)-OFm **(1c)**

The reaction was performed according to the methodology C reported in the section *6.6.2.* Purification of the crude by silica gel chromatography (cyclohexane/Acetone= 7/3) gave the product as a white foam. (1.2 g, 98%). Purity > 98%. R_f = 0.12 (cyclohexane/Acetone, 7:3). $[\alpha]_D^{20}$ (c 0.5, $CHCl_3$) = + 18.14°

^{1}H NMR ($CDCl_3$, 300 MHz): δ 7.89 (m, 4H, 2Har-Fm, 2Har-Fmoc); 7.75 (m, 4H, 2Har-Fm, 2Har-Fmoc); 7.31 (m, 18H, 4Har-Fm, 4Har-Fmoc, 5Har-Cbz, 5Har-OBzl); 7.10 (d, 2H, J=8.5 Hz, Har-Tyr); 6.84 (d, 2H, J=8.5 Hz, Har-Tyr); 6.60 (bd, 1H, J= 4.8 Hz, NH); 6.49 (bs, 1H, NH); 5.31 (bs, 1H, NH); 5.09 (s, 2H, CH_2-Cbz); 4.91 (s, 2H, CH_2-OBzl); 4.58 (m, 2H, $1H^{\alpha}$-Tyr, $1H^{\alpha}$-Pro); 4.45 (m, 5H, $1H^{\alpha}$-Lys, $1H^{\alpha}$-Leu, CH_2-Fmoc, CH-Fmoc); 4.30 (m, 1H, CH-Fm); 4.17 (m, 2H, CH_2-Fm); 3.94 (bm, 1H, H^{α}-Val); 3.79 (bm, 1H, $1H^{\delta}$-Pro); 3.34 (bm, 1H, $1H^{\delta}$-Pro); 3.14 (m, 2H, $2H^{\varepsilon}$-Lys); 2.99 (d, 2H, J=6.4 Hz, $2H^{\beta}$-Tyr); 2.30 (bm, 1H, 1H-Pro), 1.95 (m, 4H, 3H-Pro, $1H^{\beta}$-Val); 1.73 (m, 1H, H-Lys); 1.48 (m, 5H, 2H-Lys, $2H^{\beta}$-Leu, $1H^{\gamma}$-Leu); 1.27 (m, 2H, 2H-Lys); 0.88 (d, 6H, J=6.1 Hz, $2CH_3$). 0.80 (d, 6H, J=6.7 Hz, $2CH_3$).

^{13}C NMR ($CDCl_3$, 75 MHz): δ 172.57 (1C, s); 171.50 (1C, s); 170.13 (1C, s); 157.97 (1C, s); 156.72 (1C, s); 156.50 (1C, s); 157.81 (1C, s); 156.35 (1C, s); 143.92 (1C, s); 143.83 (1C, s); 143.73 (1C, s); 143.47 (1C, s); 143.20 (1C, s); 141.46 (2C, s); 141.38 (3C, s); 136.99 (1C, s); 136.89 (1C, s); 130.48 (1C, d); 128.68 (2C, s); 128.60 (4C, d); 128.55 (2C, d); 128.11 (2C, d); 128.03 (1C, d); 127.91 (4C, d); 127.82 (4C, d); 127.53 (2C, d); 127.24 (1C, d); 127.17 (1C, d); 125.15 (2C, d); 125.00 (1C, d); 120.09 (2C, d); 115.05 (1C, d); 69.94 (1C, t); 67.08 (1C, t); 66.89 (1C, t); 66.60 (1C, t); 60.67 (1C, d); 60.56 (1C, d); 54.30 (1C, d), 52.14 (1C, d); 50.66 (1C, d); 47.51 (1C, t); 47.26 (1C, d); 46.86 (1C, d); 40.73 (1C, t); 40.04 (1C, t); 36.85 (1C, t); 31.01 (1C, t); 30.95 (1C, d); 29.33 (1C, t); 28.96 (1C, t); 24.70 (1C, d); 24.46 (1C, t); 23.36 (1C, q); 22.30 (1C, t); 21.85 (1C, q); 19.27 (1C, q); 17.71 (1C, q).

Fmoc-Ser-D-Pro-Val-Tyr(OBzl)-Leu-OFm (2)

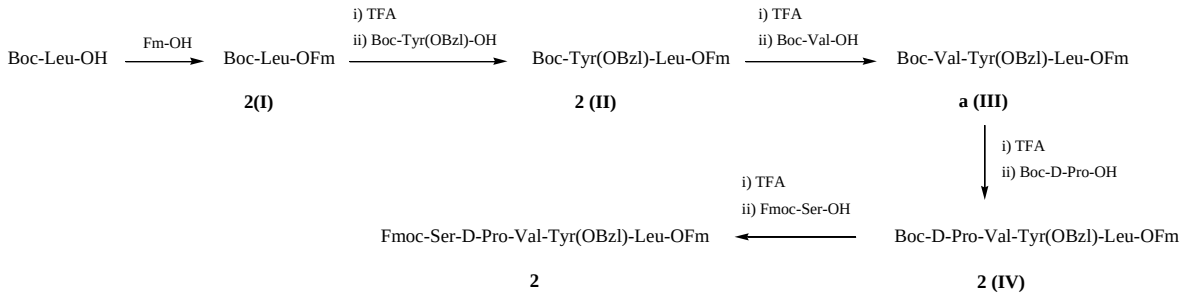

<u>*Boc-Leu-OFm*</u> **[2 (I)]**

The reaction was performed according to the methodology reported in the section *6.6.1.1*. Reaction time 3 h. Purification by silica gel chromatography (cyclohexane/AcOEt= 9/1) gave the product as a colorless syrup. (1.5 g, 85%). Purity > 98%. R_f = 0.45 (cyclohexane/AcOEt, 8:2). $[\alpha]_D^{20}$ (c 0.5, $CHCl_3$) = - 24.27°

^{1}H NMR ($CDCl_3$, 300 MHz): δ 7.77 (d, 2H, J=7.6 Hz, 2H, Har-Fm); 7.62 (m, 2H, Har-Fm); 7.41 (m, 4H, Har-Fm); 4.91 (bd, 1H, J= 8.2 Hz, NH); 4.50 (d, 2H, J= 6.1 Hz, CH_2-Fm); 4.35 (m, 1H, H^{α}-Leu); 4.42 (t, 1H, J=6.1 Hz, CH-Fm); 1.57 (m, 12H, $2H^{\beta}$-Leu, $1H^{\gamma}$-Leu, $3CH_3$-*t*Bu); 0.89 (m, 6H, $2CH_3$-Leu).

^{13}C NMR ($CDCl_3$, 75 MHz): δ 171.28 (1C, s); 156.08 (1C, s); 145.55 (2C, s); 141.65 (2C, s); 128.15 (2C, d); 127.45 (2C, d); 125.32 (2C, d); 120.32 (2C, d), 80.17 (1C, s); 67.01 (1C, t); 52.63 (1C, d); 47.18 (1C, d); 42.08 (1C, t); 28.64 (3C, q); 25.04 (1C, d); 23.09 (1C, q); 22.23 (1C, q).

<u>*Boc-Tyr(OBzl)-Leu-OFm*</u> **[2 (II)]**

The product was synthesized according to the protocol A reported in the section *6.6.2*. Reaction time 4 h. Purification by silica gel flash chromatography (EtOAc/cyclohexane, 2:8) yielded the final product (1.5 g, 92%). Purity > 98%. R_f = 0.3 (EtOAc/cyclohexane, 2:8). $[\alpha]_D^{20}$ (c 0.5, $CHCl_3$) = -9.54°

^{1}H NMR ($CDCl_3$, 300 MHz): δ 7.75 (d, 2H, J=7.6 Hz, Har-Fm); 7.62 (m, 2H, Har-Fm); 7.42 (m, 9H, 4Har-Fm, 5Har-OBzl); 7.13 (d, 2H, J=8.5 Hz, Har-Tyr); 6.87 (d, 2H, J= 8.5 Hz, Har-Tyr); 5.15 (bd, 1H, J= 9.0 Hz, NH); 4.95 (s, 2H, CH_2-OBzl); 4.51 (m, 1H, H^{α}-Tyr); 4.49 (m, 2H, CH_2-Fm); 4.33 (m, 1H, H^{α}-Leu); 4.20 (t, 1H, J= 6.1 Hz, CH-Fm); 3.01 (d, 2H, J=8.2 Hz, CH^{β}-Tyr); 1.43 (bm, 12H, $2H^{\beta}$-Leu, CH^{γ}-Leu, 9H-*t*Bu); 0.87 (m, 6H, $2CH_3$-Leu).

^{13}C NMR ($CDCl_3$, 75 MHz): δ 172.72 (1C, s); 171.44 (1C, s); 158.14 (1C, s); 155.76 (1C, s); 145.95 (1C, s); 143.68 (1C, s); 141.73 (1C, s); 141.66 (1C, s); 137. 32 (1C, s); 130.74 (2C, d); 129.50 (1C, s); 128.50 (3C, d); 128.10 (2C, d); 128.0 (3C, d); 127.80 (2C, d); 125. 27 (1C, d), 120.36 (2C, d), 115.27 (2C, d); 80.46 (1C, s); 70.27 (1C, t); 67.06 (1C, t); 56.07 (1C, d); 52.63 (1C, d); 47.13 (1C, d); 42.88 (1C, t); 37.62 (1C, t); 28.60 (3C, q); 24.96 (1C, d); 23.03 (1C, q), 22.31 (1C, q).

Boc-Val-Tyr(OBzl)-Leu-OFm **[2 (III)]**

The product was synthesized according to the protocol A reported in the section *6.6.2.* Reaction time 4 h. Purification by silica gel flash chromatography (EtOAc/cyclohexane, 25:75) gave the final product as a white solid (1.60 g, 97%). Purity >98%. R_f = 0.33 (EtOAc/cyclohexane, 3:7). $[\alpha]_D^{20}$ (c 0.5, $CHCl_3$) = - 23.84°

^{1}H NMR ($CDCl_3$, 300 MHz): δ 7.76 (d, 2H, J=7.6 Hz, Har-Fm); 7.60 (m, 2H, Har-Fm); 7.36 (m, 9H, 4Har-Fm, 5Har-OBzl); 7.10 (d, 2H, J=8.5 Hz, Har-Tyr); 6.85 (d, 2H, J=8.5 Hz, Har-Tyr); 6.52 (bd, 1H, J= 5.8 Hz, NH); 6.29 (bs, 1H, NH); 5.03 (bd, 1H, NH); 4.97 (s, 2H, CH_2-OBzl); 4.51 (m, 4H, $1H^{\alpha}$-Tyr, $1H^{\alpha}$-Leu, CH_2-Fm); 4.20 (t, 1H, J=6.1 Hz, CH-Fm); 3.92 (m, 1H, H^{α}-Val); 3.04 (m, 2H, $2H^{\beta}$-Tyr); 1.15 (m, 1H, H^{β}-Val); 1.42 (bm, 12H, $2H^{\beta}$-Leu, $1H^{\gamma}$-Leu, 9H-*t*Bu); 0.91 (d, 6H, J=6.7 Hz, $2CH_3$-Leu); 0.85 (d, 6H, J=6.4 Hz, $2CH_3$-Val).

^{13}C NMR ($CDCl_3$, 75 MHz): δ 172.27 (1C, s) 171.51 (1C, s); 170.59 (1C, s); 157.37 (1C, s); 156.03 (1C, s); 143.74 (1C, s); 143.55 (1C, s); 141.48 (1C, s); 141.41 (1C, s); 136.90 (1C, s); 130.47 (2C, d); 128.65 (2C, d); 128.61 (1C, s); 128.03 (2C, d); 127.95 (2C, d); 127.53 (2C, d); 127.26 (2C, d); 125.16 (1C, d); 120.11 (2C, d); 115.06 (2C, d); 80.46 (1C, s); 69.97 (1C, t); 66.85 (1C, t); 60.21 (1C, d); 54.26 (1C, d); 51.07 (1C, d); 46.86 (1C, d); 41.38 (1C, t); 37.24 (1C, t); 30.65 (1C, d); 28.39 (3C, q); 24.70 (1C, d); 22.77 (1C, q); 20.05 (1C, q); 19.36 (1C, q); 17.53 (1C, q).

Boc-D-Pro-Val-Tyr(OBzl)-Leu-OFm **[2 (IV)]**

The product was synthesized according to the protocol A reported in the section *6.6.2.* Reaction time 2 h. Purification by silica gel flash chromatography (EtOAc/cyclohexane, 4:6) gave the final product as a white solid (1.2 g, 97%). Purity > 98%. R_f = 0.3 (EtOAc/cyclohexane, 1:1). $[\alpha]_D^{20}$ (c 0.5, $CHCl_3$) = + 0.59°

^{1}H NMR ($CDCl_3$, 300 MHz): δ 7.71 (d, 2H, J=7.6 Hz, Har-Fm); 7.60 (d, 2H, J=7.3 Hz, Har-Fm); 7.30 (m, 9H, 4Har-Fm, 5Har-OBzl); 7.09 (bd, 2H, J= 7.3 Hz, Har-Tyr); 6.79 (d, 2H, J=7.3 Hz, Har-Tyr); 4.95 (bs, 2H, CH_2-OBzl); 4.61 (bs, 1H, H^{α}); 4.41 (m, 3H, $1H^{\alpha}$, CH_2-Fm); 4.17 (m, 3H, $2H^{\alpha}$, CH-Fm); 3.42 (bm, 2H, H^{β}-Tyr), 3.15 (bm, 1H, $1H^{\delta}$-Pro); 2.86 (m,

1H, 1H$^{\delta}$-Pro); 2.20-1.68 (m, 5H, 1H$^{\beta}$-Val, 4H-Pro); 1.42 (bm, 12H, 2H$^{\beta}$-Leu, 1H$^{\gamma}$-Leu, 9H-*t*Bu); 0.87 (m, 12H, 2CH_3-Leu, 2CH_3-Val).

^{13}C NMR ($CDCl_3$, 75 MHz): δ 172.61 (2C, s); 171.33 (2C, s), 157.91 (1C, s); 156.03 (1C, s); 144.00 (1C, s); 141.64 (2C, s); 141.58 (1C, s); 137.27 (1C, s); 132.74 (2C, d); 130.74 (1C, s); 129.10 (2C, d); 128.80 (2C, d); 128.60 (2C, d), 127.50 (2C, d), 127.0 (2C, d);125.0 (1C, d); 120.23 (2C, d); 115.06 (2C, d); 80.98 (1C, s); 70.23 (1C, t); 67.04 (1C, t); 61.94 (1C, d); 60.17 (1C, d); 54.74 (1C, d); 52.40 (1C, d); 47.59 (1C, t); 47.07 (1C, d); 41.06 (1C, t); 37.24 (1C, t); 31.15 (1C, t); 31.25 (1C, t); 28.69 (3C, q); 24.87 (1C, d), 22.94 (2C, q); 22.36 (1C, d); 19.44 (1C, q); 17.53 (1C, d).

Fmoc-Ser-D-Pro-Val-Tyr(OBzl)-Leu-OFm **(2)**

The product was synthesized according to the protocol B reported in the section *6.6.2.* The purification was done in two steps: after the first silica gel flash chromatography (EtOAc/PE, 9:1) the product was triturated with diethyl ether to remove the residues of tetramethyl urea (TMU). The final product was recovered as a white solid (350 mg, 64%). Purity > 98%. R_f = 0.28 (EtOAc/PE, 9:1). $[\alpha]_D^{20}$ (c 0.25, $CHCl_3$) = -26.80°

^{1}H NMR ($CDCl_3$, 300 MHz): δ 7.75 (d, 4H, J=7.3 Hz, Har); 7.56 (m, 4H, Har); 7.30 (m, 13H, 4Har-Fm, 5Har-OBzl); 7.09 (d, 2H, J=8.5 Hz, Har-Tyr); 6.81 (d, 2H, J=8.5 Hz, Har-Tyr); 5.82 (d, 1H, J=8.2 Hz, NH); 4.89 (s, 2H, CH_2-OBzl); 4.76 (m, 1H, H$^{\alpha}$); 4.62 (m, 2H); 4.54 (m, 1H); 4.42 (m, 5H); 4.19 (m, 2H); 3.93 (m, 2H); 3.71 (m, 2H,); 3.03 (m, 2H); 2.19 (m, 1H, H$^{\beta}$-Val); 2.98 (m, 4H, H-Pro); 1.44 (m, 3H, 2H$^{\beta}$-Leu, 1H$^{\gamma}$-Leu); 0.84 (m, 12H, 2CH_3-Leu, 2CH_3-Val).

^{13}C NMR ($CDCl_3$, 75 MHz): δ 172.42 (1C, s); 172.29 (1C, s); 172.17 (1C, s); 171.55 (1C, s); 170.71 (1C, s); 157.96 (1C, s); 156.75 (1C, s); 144.03 (1C, s); 143.92 (1C, s); 143.73 (1C, s); 143.48 (1C, s); 141.45 (2C, s); 141.33 (2C, s); 137.20 (1C, s); 130.45 (1C, d); 129.38 (1C, s); 128.82 (1C, d); 128.57 (2C, d); 127.86 (1C, d); 127.87 (2C, d); 127.77 (2C, d); 127.44 (2C, d); 127.23 (2C, d); 127.14 (2C, d); 126.74 (2C, d); 125.46 (1C, d); 125.29 (1C, d); 125.02 (1C, d); 119.97 (2C, d); 119.82 (1C, d); 115.05 (1C, d); 70.06 (1C, t); 67.55 (1C, t); 66.57 (1C, t); 62.71 (1C, t); 60.98 (1C, d); 59.37 (1C, d); 54.48 (1C, d); 54.25 (1C, d); 51.18 (1C, d); 47.72 (1C, t); 47.20 (1C, d); 46.89 (1C, d); 41.08 (1C, t); 36.28 (1C, t); 29.42 (1C, d); 28.65 (1C, t); 25.26 (1C, t); 24.47 (1C, d); 22.74 (1C, q); 21.96 (1C, q); 19.42 (1C, q); 17.15 (1C, q).

Fmoc-Val-Tyr(OBzl)-Leu-Pro-Lys(z)-SFm (1a')

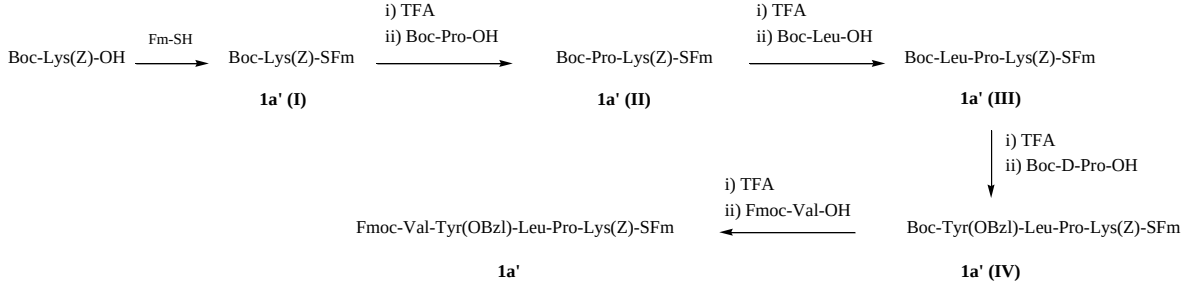

Boc-Lys(Z)-OFm **[1a'(I)]**

The product was synthesized according to the procedure described in the section *6.6.1.2*. Purification of the residue by silica gel chromatography (cyclohexane/EtOAc= 8/2 to 4/6) gave the product as a yellow foam (990 mg, 93%). Purity > 95%. R_f = 0.16 (cyclohexane/AcOEt= 8/2). $[\alpha]_D^{20}$ (c 0.5, $CHCl_3$) = − 29.0°

^{1}H NMR ($CDCl_3$, 300 MHz): δ 7.73 (d, J=7.3 Hz, 2H); 7.62 (d, J=7.3 Hz, 2H); 7.37 (m, 9H); 5.09 (s, 2H, CH_2-Cbz); 5.01 (bs, 1H, NH); 4.76 (bm, 1H, HN); 4.19 (m, 2H, CH-SFm, $1H^{\alpha}$-Lys); 3.56 (m, 2H, CH_2-SFm); 3.14 (bm, 2H, $2H^{\varepsilon}$-Lys); 1.68 (m, 2H, H-Lys); 1.41 (bm, 12H, 9H-*t*Bu, 2H-Lys), 1.24 (m, 2H, H-Lys).

Boc-Pro-Lys(Z)-OFm **[1a'(II)]**

The product was synthesized according to the protocol A reported in the section *6.6.2*. Reaction time 2 h. The purification by silica gel flash chromatography (Toluene/Acetone, 9:1) gave the product as a white foam (572 mg, 92%). Purity >95%. R_f = 0.46 (Toluene/Acetone= 8/2. $[\alpha]_D^{20}$ (c 0.5, $CHCl_3$) = − 61.5°

^{1}H NMR ($CDCl_3$, 300 MHz): δ 7.73 (d, J=7.3 Hz, 2H); 7.57 (d, J=7.3 Hz, 2H); 7.31 (m, 9H); 5.07 (s, 2H, CH_2-Cbz); 4.94 (bs, 1H, NH); 4.50 (bm, 1H, $1H^{\alpha}$-Pro); 4.26 (bs, 1H, H^{α}-Lys); 4.16 (t, 1H, J= 6.1 Hz, CH-SFm); 3.53 (m, 2H, CH_2-SFm); 3.40 (bm, 2H, H^{δ}-Pro); 3.09 (bd, 2H, J= 6.1 Hz, $2H^{\varepsilon}$-Lys); 2.32 (bm, 1H, H-Pro); 1.83 (bm, 3H, H-Pro); 1.63 (bm, 1H, H-Lys); 1.42 (bm, 12H, 9H-*t*Bu, 3H-Lys), 1.24 (m, 2H, H-Lys).

^{13}C NMR ($CDCl_3$, 75 MHz): δ 200.10 (1C, s); 173.20 (1C, s); 171.50 (1C, s); 156.35 (1C, s); 156.47 (1C, s), 145.13 (1C, s); 141.15 (1C, s); 141.12 (1C, s); 137.71 (1C, s); 136.82 (1C, s); 129.01 (1C, d); 128.42 (2C, d); 128.21 (1C, d); 128.00 (1C, d); 127.94 (1C, d); 127.70 (2C, d); 127.02 (2C, d); 125.30 (1C, d); 124.62 (1C, d); 124.57 (1C, d); 119.82 (1C, d); 79.80 (1C, s); 80.48 (1C, t); 66.37 (1C, t); 58.92 (1C, d); 47.06 (1C, t); 46.41 (1C, d); 40.53 (1C, t); 32.83 (1C, t); 21.66 (1C, t); 29.20 (1C, t); 28.32 (3C, q); 24.33 (1C, t); 22.17 (1C, t); 21.43 (1C, d).

Boc-Leu-Pro-Lys(Z)-SFm **[1a'(III)]**

The product was synthesized according to the protocol A reported in the section *6.6.2*. Reaction time 12 h. The purification by silica gel flash chromatography (cyclohexane/AcOEt, 1:1) gave the product as a white foam (530 mg, 80%). Purity >98 %. R_f = 0.36 (cyclohexane/AcOEt = 1/1). $[\alpha]_D^{20}$ (c 0.5, $CHCl_3$) = − 68.33°

^{1}H NMR ($CDCl_3$, 300 MHz): δ 7.73 (d, J=7.3 Hz, 2H); 7.57 (d, J=7.3 Hz, 2H); 7.31 (m, 9H); 6.95 (bd, 2H, J= 7.6 Hz, NH); 5.05 and 4.94 (2d, 2H, J=12.2 Hz, CH_2-Cbz); 4.45 (bm, 3H, $1H^{\alpha}$-Pro, $1H^{\alpha}$-Lys, $1H^{\alpha}$-Leu); 4.15 (t, 1H, J=6.1 Hz, CH-SFm); 3.76 (m, 1H, $1H^{\delta}$-Pro); 3.55 (m, 3H, CH_2-SFm, $1H^{\delta}$-Pro); 3.13 (m, 2H, $2H^{\varepsilon}$-Lys); 2.18 (bm, 2H, H-Pro); 1.94 (m, 2H, H-Pro); 1.64 (m, 2H, H-Lys); 1.43 (m, 16H, 4H-Lys, $2H^{\beta}$-Leu, $1H^{\gamma}$-Leu, 9H-*t*Bu); 0.94 (d, 3H, J=6.4 Hz, $1CH_3$-Leu); 0.88 (d, 3H, J=6.4 Hz, $1CH_3$-Leu).

^{13}C NMR ($CDCl_3$, 75 MHz): δ 200.27 (1C, s); 173.08 (1C, s); 171.30 (1C, s); 156.43 (1C, s); 156.14 (1C, s); 145.33 (1C, s), 145.29 (1C, s); 141.09 (1C, s); 141.01 (1C, s); 136.64 (1C, s); 128.43 (2C, d); 128.23 (2C, d); 127.99 (1C, d); 127.64 (2C, d); 127.03 (1C, d); 124.78 (2C, d); 124.71 (2C, d); 119.79 (1C, d); 79.86 (1C, s); 66.49 (1C, t); 61.05 (1C, d); 60.31 (1C, t); 58.34 (1C, d); 50.75 (1C, d); 47.27 (1C, t); 46.51 (1C, d); 40.68 (1C, t); 31.88 (1C, t); 30.63 (1C, t); 28.88 (1C, t); 28.43 (3C, q); 27.95 (1C, t); 25.50 (1C, t); 23.30 (1C, q); 21.97 (1C, t); 21.59 (1C, d).

Boc-Tyr(OBzl)-Leu-Pro-Lys(Z)-SFm **[1a'(IV)]**

The product was synthesized according to the protocol A reported in the section *6.6.2.* Reaction time 2 h. The purification by silica gel flash chromatography (cyclohexane/AcOEt, 1:1 to 3:7) gave the product as a white foam (600 mg, 88%). Purity >98%. R_f = 0.45 (cyclohexane/AcOEt = 4/6). $[\alpha]_D^{20}$ (c 0.25, $CHCl_3$) = − 64.87°

^{1}H NMR ($CDCl_3$, 300 MHz): δ 7.72 (d, 2H, J=7.3 Hz); 7.57 (m, 2H); 7.31 (m, 14H); 7.04 (d, 2H, J=8.5 Hz, Har-Tyr); 6.76 (d, 2H, J=8.5 Hz, Har-Tyr); 4.99 (bs, 2H, CH_2-OBzl); 4.91 (s, 2H, CH_2-CBz); 4.63 (bm, 1H, H^{α}-Leu); 4.25 (bm, 3H, $1H^{\alpha}$-Pro, $1H^{\alpha}$-Lys, $1H^{\alpha}$-Tyr); 4.06 (t, J=6.1 Hz, 1H, CH-SFm); 3.65 (bm, 1H, $1H^{\delta}$-Pro); 3.47 (bm, 1H, $1H^{\delta}$-Pro); 3.44 (d, 2H, J=6.1 Hz, CH_2-SFm); 3.01 (m, 3H, $2H^{\varepsilon}$-Lys, $1H^{\beta}$-Tyr); 2.72 (bm, 1H $1H^{\beta}$-Tyr); 2.25-1.93 (bm, 4H, H-Pro); 1.69 (m, 1H, $1H^{\gamma}$-Leu); 1.25 (m, 17H, 6H-Lys, $2H^{\beta}$-Leu, 9H-*t*Bu); 0.91 (d, 3H, J=6.4 Hz, $1CH_3$-Leu); 0.85 (d, 3H, J=6.4 Hz, $1CH_3$-Leu).

^{13}C NMR ($CDCl_3$, 75 MHz): δ 199.95 (1C, s); 172.10 (1C, s); 171.30 (1C, s); 171 (1C, s); 158.12 (1C, s); 157.98 (1C, s); 156.88 (1C, s); 145.61 (1C, s), 145.40 (1C, s); 141.29 (2C, s); 137.08 (2C, s); 130.59 (1C, d); 128.80 (1C, s); 128.71(2C, d); 128.58 (2C, d); 128.30 (1C, d); 128.20 (2C, d); 128.10 (2C, d); 127.77 (2C, d); 127.50 (2C, d); 127.21 (2C, d); 124.90 (2C, d); 119.92 (2C, d); 115.11 (2C, d); 82.00 (1C, s); 70.11 (1C, t); 66.58 (1C, t); 60.83 (1C, d); 50.58 (1C, d); 55.0 (1C, d); 50.58 (1C, d); 47.30 (1C, t); 46.69 (1C, d); 40.80 (1C, t); 40.66 (1C, t); 37.40 (1C, t); 32.10 1C, t); 31.10 (1C, t); 29.08 (2C, t); 28.96 (3C, q); 24.76 (1C, d); 24.50 (1C, t); 24.45 (1C, q); 23.43 (1C, t); 21.84 (1C, q).

Fmoc-Val-Tyr(OBzl)-Leu-Pro-Lys(Z)-SFm **[1a']**

The product was synthesized according to the protocol A reported in the section *6.6.2.* Reaction time 16 h. The purification by silica gel flash chromatography (cyclohexane/AcOEt, 6:4 to 3:7) gave the product as a white foam (564 mg, 80%). Purity >98%. R_f = 0.33 (cyclohexane/AcOEt = 4/6). $[\alpha]_D^{20}$ (c 0.25, $CHCl_3$) = − 43.74°

^{1}H NMR ($CDCl_3$, 300 MHz): δ 7.65 (m, 4H, 2Har-SFm, 2Har-Fmoc); 7.57 (m, 4H, 2Har-SFm, 2Har-Fmoc); 7.24 (m, 18H, 4Har-SFm, 4Har-Fmoc, 5Har-Cbz, 5Har-OBzl); 6.98 (d, 2H, J=8.5 Hz, Har-Tyr); 6.71 (d, 2H, J=8.5 Hz, Har-Tyr); 5.06 (bs, 2H, CH_2-Cbz); 4.2 (s, 2H, CH_2-OBzl); 4.58 (bm, 2H); 4.35 (m, 3H); 4.25 (m, 1H); 4.12 (m, 3H); 3.80 (bm, 1H, $1H^{\delta}$-Pro); 3.59 (bm, 1H, $1H^{\delta}$-Pro); 3.46 (d, 2H, J=6.1 Hz, CH_2-SFm); 3.03 (bm, 3H, $2H^{\varepsilon}$-Lys, $1H^{\beta}$-Tyr); 2.81 (bm, 1H, $1H^{\beta}$-Tyr); 1.97 (m, 5H, 4H-Pro, $1H^{\beta}$-Val); 1.33 (m, 9H, 6H-Lys, $2H^{\beta}$-Leu, $1H^{\gamma}$-Leu); 0.79 (bm, 12H, $2CH_3$-Leu, $2CH_3$-Val).

^{13}C NMR ($CDCl_3$, 75 MHz): δ 200.31 (1C, s); 171.76 (2C, s); 171.63 (2C, s); 171.42 (1C, s); 157.88 (1C, s); 156.55 (1C, s); 145.46 (1C, s); 145.26 (1C, s); 143.89 (1C, s); 143.75 (1C, s); 141.30 (2C, s); 141.17 (1C, s); 141.13 (1C, s); 136.91 (1C, s); 136.81 (1C, s); 130.39 (1C, d); 128.51 (1C, s); 128.47 (4C, d); 127.96 (4C, d); 127.75 (4C, d); 127.46 (4C, d); 127.12 (2C, d); 125.11 (2C, d); 124.82 (2C, d); 124.76 (2C, d); 120.02 (2C, d); 119.85 (2C; d); 114.97 (1C, d); 69.84 (1C, t); 67.06 (1C, t); 66.60 (1C, t); 60.80 (2C, d); 59.22 (1C, d); 54.31 (1C, d), 50.66 (1C, d); 47.18 (1C, d); 46.52 (1C, d); 40.85 (2C, t); 39.88 (1C, t); 36.72 (1C, t); 31.95 (2C, t); 31.14 (1C, t); 30.91 (1C, d); 29.17 (1C, t); 24.66 (1C, d); 24.40 (1C, t); 23.38 (1C, q); 22.26 (1C, t); 21.72 (1C, q); 19.23 (1C, q); 17.84 (1C, q).

Fmoc-Val-Tyr(OBzl)-Leu-Pro-Lys(z)-SFm (1c')

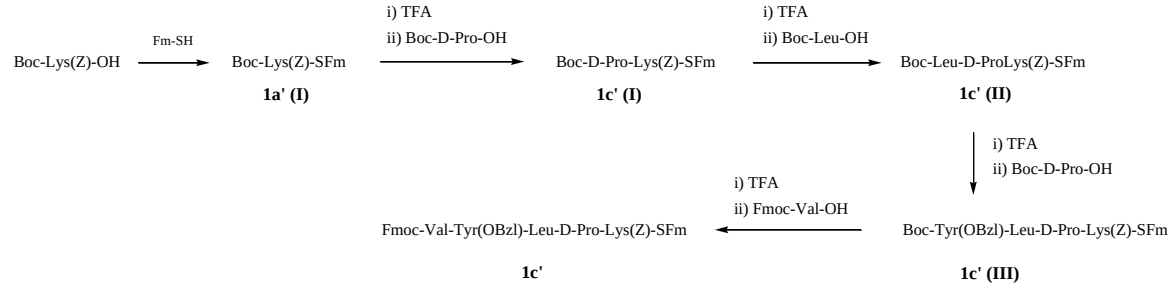

<u>*Boc-D-Pro-Lys(Z)-SFm*</u> **[1c'(I)]**

The reaction was performed according to the methodology A reported in the section *6.6.1.2*. Purification of the crude by silica gel chromatography (Toluene/Acetone= 9/1) gave the product as a white foam. (555 mg, 89%). Purity > 98%. R_f = 0.20 (Toluene/Acetone, 9:1). $[\alpha]_D^{20}$ (c 0.5, $CHCl_3$) = + 58.29°

^{1}H NMR ($CDCl_3$, 300 MHz): δ 7.75 (d, 2H, J=7.3 Hz, 2Har); 7.56 (m, 2H, 2Har); 7.29 (m, 9Har); 5.08 (s, 2H, CH_2-Cbz); 4.50 (bm, 1H, H^{α}-Lys); 4,26 (bm, 1H, H^{α}-Pro); 4.16 (t, 1H, J=6.1 Hz, CH-SFm); 3.53 (bm, 3H, CH_2-SFm, 1 H^{δ}-Pro); 3.20 (bm, 1H, 1H^{δ}-Pro); 3.10 (m, 2H, H^{ε}-Lys), 2.01 (m, 2H, H-Pro), 1.81 (m, 2H, H-Pro), 1.60 (m, 1H, 1H-Lys); 1.42 (m, 14H, 9H-*t*Bu, 5H-Lys).

^{13}C NMR $CDCl_3$, 75 MHz): δ 200.31 (1C, s); 171.70 (1C, s); 171.63 (1C, s); 171.42 (1C, s); 156.47 (1C, s); 145.13 (1C, s); 141.15 (1C, s); 137.71 (1C, s); 136.82 (1C, s); 129.01 (1C, d); 128.42 (2C, d); 128.21 (1C, d); 128.00 (1C, d); 127.94 (1C, d); 127.70 (1C, d); 127.06 (2C, d); 125.30 (1C, d); 124.62 (1C, d); 124.47 (1C; d); 119.82 (1C, d); 80.48 (1C, s); 66.37 (1C, t); 58.92 (1C, t); 47.06 (1C, t); 46.41 (1C, d); 40.57 (1C, t); 31.83 (1C, t); 31.66 (1C, t); 29.20 (1C, t); 28.32 (3C, q); 24,33 (1C, t); 22.17 (1C, t); 21.44 (1C, d).

<u>*Boc-Leu-D-Pro-Lys(Z)-SFm*</u> **[1c'(II)]**

The reaction was performed according to the methodology A reported in the section *6.6.2.* Reaction time 12 h. Purification of the crude by silica gel chromatography (cyclohexane/AcOEt= 1/1) gave the product as a white foam. (550 mg, 97%). Purity > 98%. R_f = 0.35 (AcOEt/petroleum ether, 7:3). $[\alpha]_D^{20}$ (c 0.5, $CHCl_3$) = + 38.15°

^{1}H NMR ($CDCl_3$, 300 MHz): δ 7.73 (d, 2H, J= 7.3 Hz); 7.57 (m, 2H); 7.34 (m, 9H); 7.05 (bd, 1H, J=8.2 Hz, NH); 6.04 (bs, 1H, NH); 5.08 (s, 2H, CH_2-Cbz); 4.59 (bm, 1H, $1H^{\alpha}$-Leu); 4.46 (m, 1H, $1H^{\alpha}$-Pro); 4.31 (bm, 1H, H^{α}-Lys); 4.14 (t, 1H, J=6.1 Hz, CH-SFm); 3.84 (bm, 1H, $1H^{\delta}$-Pro); 3.41 (m, 3H, CH_2-SFm, $1H^{\delta}$-Pro); 3.19 (m, 2H, $2H^{\varepsilon}$-Lys); 2.22 (bm, 1H, H-Pro); 1.94 (m, 3H, H-Pro); 1.80 (m, 1H, $1H^{\gamma}$-Leu); 1.43 (m, 17H, 6H-Lys, $2H^{\beta}$-Leu, 9H-*t*Bu); 0.86 (m, 6H, $2CH_3$-Leu).

^{13}C NMR ($CDCl_3$, 75 MHz): δ 200.27 (1C, s); 173.08 (1C, s); 171.30 (1C, s); 156.43 (1C, s); 156.14 (1C, s); 145.33 (2C, s), 141.07 (2C, s); 136.64 (1C, s); 128.43 (2C, d); 128.23 (2C, d); 127.99 (1C, d); 127.64 (2C, d); 127.03 (1C, d); 124.78 (2C, d); 124.71 (2C, d); 119.79 (1C, d); 79.86 (1C, s); 66.49 (1C, t); 61.05 (1C, d); 60.31 (1C, t); 58.34 (1C, d); 50.75 (1C, d); 47.27 (1C, t); 46.51 (1C, d); 40.68 (1C, t); 31.88 (1C, t); 30.63 (1C, t); 28.88 (1C, t); 28.43 (3C, q); 27.95 (1C, t); 25.50 (1C, t); 23.30 (1C, q); 21.97 (1C, t); 21.59 (1C, d).

Boc-Tyr(OBzl)-Leu-Pro-Lys(Z)-SFm **[1c'(III)]**

The product was synthesized according to the protocol A reported in the section *6.6.2*. Reaction time 12 h. The purification by silica gel flash chromatography (cyclohexane/AcOEt, 4:6) gave the product as a white foam (460 mg, 75%). Purity > 98%. R_f = 0.35 (cyclohexane/AcOEt, 4:6). $[\alpha]_D^{20}$ (c 0.25, $CHCl_3$) = + 1.95°

^{1}H NMR ($CDCl_3$, 300 MHz): δ 7.72 (d, 2H, J=7.3 Hz); 7.57 (m, 2H); 7.33 (m, 14H); 7.07 (d, 2H, J=8.5 Hz, Har-Tyr); 6.88 (d, 2H, J=8.5 Hz, Har-Tyr); 5.08 (bs, 2H, CH_2-OBzl); 4.98 (s, 2H, CH_2-Z); 4.58 (bm, 2H, $1H^{\alpha}$-Leu, $1H^{\alpha}$-Pro); 4.40 (bm, 1H, H^{α}-Lys); 4.24 (bm, 1H, H^{α}-Tyr); 4.14 (t, 1H, J=6.1 Hz, CH-SFm); 3.84 (bm, 1H, $1H^{\delta}$-Pro); 3.53 (m, 1H, 1H-CH_2-SFm); 3.43 (bm, 2H, $1H^{\delta}$-Pro, 1H-CH_2-SFm); 3.14 (m, 2H, $2H^{\varepsilon}$-Lys); 2.98 (bm, 2H, $2H^{\beta}$-Tyr); 2.30 (bm, 1H, H-Pro); 1.97 (bm, 3H, H-Pro); 1.76 (m, 1H, $1H^{\gamma}$-Leu); 1.41 (bm, 16H, 6H-Lys, $2H^{\beta}$-Leu, 9H-*t*Bu); 1.25 (m, 1H, H-Lys); 0.89 (bd, 6H, J=6.7 Hz, $2CH_3$-Leu).

^{13}C NMR ($CDCl_3$, 75 MHz): δ 200.01 (1C, s); 172.10 (1C, s); 171.30 (1C, s); 171 (1C, s); 158.12 (1C, s); 157.98 (1C, s); 156.88 (1C, s); 145.61 (1C, s), 145.40 (1C, s); 141.29 (2C, s); 137.08 (2C, s); 130.59 (1C, d); 128.80 (1C, s); 128.71(2C, d); 128.58 (2C, d); 128.30 (1C, d); 128.20 (2C, d); 128.10 (2C, d); 127.77 (2C, d); 127.50 (2C, d); 127.21 (2C, d); 124.90 (2C, d); 119.92 (2C, d); 115.11 (2C, d); 82.00 (1C, s); 70.11 (1C, t); 66.58 (1C, t); 60.83 (1C, d); 50.58 (1C, d); 55.0 (1C, d); 50.58 (1C, d); 47.30 (1C, t); 46.69 (1C, d); 40.80 (1C, t); 40.66 (1C, t); 37.40 (1C, t); 32.10 1C, t); 31.10 (1C, t); 29.08 (2C, t); 28.96 (3C, q); 24.76 (1C, d); 24.50 (1C, t); 24.45 (1C, q); 23.43 (1C, t); 21.84 (1C, q).

Fmoc-Val-Tyr(OBzl)-Leu-D-Pro-Lys(Z)-SFm **(1c')**

The product was synthesized according to the protocol A reported in the section *6.6.2*. Reaction time 12 h. The purification by silica gel flash chromatography (cyclohexane/AcOEt, 6:4 to 2:8) gave the product as a white foam (550 mg, 98%). Purity > 98%. R_f = 0.45 (cyclohexane/AcOEt, 2:8). $[\alpha]_D^{20}$ (c 0.25, $CHCl_3$) = − 24.06°

^{1}H NMR ($CDCl_3$, 300 MHz): δ 7.75 (m, 4H, 2Har-SFm, 2Har-Fmoc); 7.54 (m, 4H, 2Har-SFm, 2Har-Fmoc); 7.30 (m, 18H, 4Har-SFm, 4Har-Fmoc, 5Har-Cbz, 5Har-OBzl); 7.09 (d, 2H, J=8.5 Hz, Har-Tyr); 6.82 (d, 2H, J=8.5 Hz, Har-Tyr); 6.71 (bs, 1H, NH); 5.35 (bs, 1H, NH); 5.06 (s, 2H, CH_2-Cbz); 4.89 (s, 2H, CH_2-OBzl); 4.56 (bm, 3H, $2H^{\alpha}$, 1H-CH_2-Fmoc); 4.40 (m, 3H, $2H^{\alpha}$, 1H-CH_2-Fmoc); 4.17 (m, 2H, 1CH-SFm, 1CH-Fmoc); 3.94 (bm, H^{α}-Leu); 3.79 (bm, 1H, $1H^{\delta}$-Pro); 3.54 (m, 2H, $1H^{\delta}$-Pro, 1H-CH_2-SFm); 3.13 (m, 2H, $2H^{\varepsilon}$-Lys); 2.97 (bm, 2H, $2H^{\beta}$-Tyr); 2.29 (m, 1H, $1H^{\beta}$-Val); 1.94 (m, 4H, 4H-Pro,); 1.44 (m, 9H, 6H-Lys, $2H^{\beta}$-Leu, $1H^{\gamma}$-Leu); 0.79 (bm, 12H, $2CH_3$-Leu, $2CH_3$-Val).

^{13}C NMR ($CDCl_3$, 75 MHz): δ 200.31 (1C, s); 171.83 (3C, s); 157.90 (2C, s); 156.61 (2C, s); 145.46 (1C, s); 145.33 (1C, s); 143.70 (1C, s); 143.75 (1C, s); 141.30 (3C, s); 141.23 (1C, s); 136.94 (1C, s); 136.88 (1C, s); 130.44 (1C, d); 128.62 (1C, s); 128.52 (2C, d); 128.47 (2C, d); 127.97 (2C, d); 127.93 (1C, d); 127.91 (2C, d); 127.76 (2C, d); 127. 71 (1C; d); 127.47 (4C, d); 127.12 (2C, d); 125.11 (2C, d); 124.83 (2C, d); 124.76 (2C, d); 120.03 (2C, d); 119.86 (2C; d); 114.95 (1C, d); 69.85 (1C, t); 67.10 (1C, t); 66.65 (1C, t); 60.87 (2C, d); 59.31 (1C, d); 54.31 (1C, d), 50.66 (1C, d); 47.25 (1C, d); 46.21 (1C, d); 40.85 (2C, t); 39.88 (1C, t); 36.72 (1C, t); 31.97 (2C, t); 31.09 (1C, t); 30.91 (1C, d); 29.17 (1C, t); 24.66 (1C, d); 24.40 (1C, t); 23.38 (1C, q); 22.26 (1C, t); 21.72 (1C, q); 19.23 (1C, q); 17.84 (1C, q).

Fmoc-Ser-D-Pro-Val-Tyr(OBzl)-Leu-SFm (2')

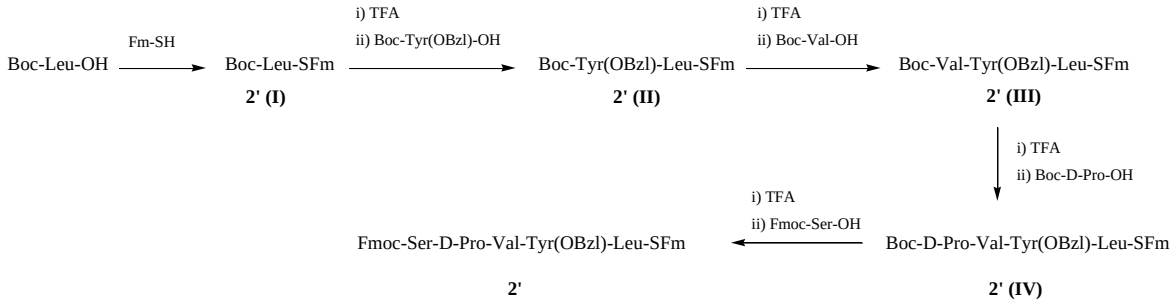

<u>*Boc-Leu-SFm*</u> **[2'(I)]**

The product was synthesized according to the protocol A reported in the section *6.6.1.2.* Purification of the residue by silica gel chromatography (cyclohexane/EtOAc = 98/2 to 95/5) gave the product as a white foam (1.16 g, 85%). Purity >95%. R_f = 0.26 (cyclohexane/AcOEt= 9/1). $[\alpha]_D^{20}$ (c 0.5, $CHCl_3$) = − 79.62°

^{1}H NMR ($CDCl_3$, 300 MHz): δ 7.77 (d, 2H, J=7.3 Hz, 2H, Har-SFm); 7.64 (d, 2H, J=7.3 Hz, Har-SFm); 7.35 (m, 4H, Har-SFm); 4.79 (bd, 1H, J=8.2 Hz, NH); 4.26 (bm, 1H, H^{α}-Leu); 4.16 (t, 1H, J=5.8 Hz, CH-Fm); 3,53 (d, 2H, J=5.8 Hz, CH_2-SFm); 1.57 (m, 2H, $2H^{\beta}$-Leu) 1.43 (m, 9H, 9H-*t*Bu); 1.25 (m, 1H, $1H^{\gamma}$-Leu); 0.88 (d, 6H, J=6.7 Hz, $2CH_3$-Leu).

^{13}C NMR ($CDCl_3$, 75 MHz): δ 202 (1C, s); 155.42 (1C, s); 145.65 (2C, s); 141.37 (2C, s); 130.03 (2C, d); 128.88 (2C, d); 125.60 (2C, d); 120.03 (2C, d); 80.25 (1C, s); 59.53 (1C, d); 46.96 (1C, d); 41.57 (1C, d); 32.11 (1C, t); 28.60 (3C, q); 24.86 (1C, d); 23.86 (1C, q); 21.62 (1C, q).

Boc-Tyr(OBzl)-Leu-SFm ***[2'(II)]***

The product was synthesized according to the protocol A reported in the section *6.6.2*. Reaction time 2 h. The purification by silica gel flash chromatography (cyclohexane/EtOAc, 9:1 to 8:2) gave the product as a white foam (1.50 g, 97%). Purity >98%. R_f = 0.28 (cyclohexane/AcOEt, 8:2). $[\alpha]_D^{20}$ (c 0.5, $CHCl_3$) = - 37.67°

^{1}H NMR ($CDCl_3$, 300 MHz): δ 7.72 (d, 2H, J =7.3 Hz, Har-SFm); 7.59 (dd, 2H, J=7.3 Hz, J=2 Hz, Har-SFm); 7.38 (m, 9H, 4Har-SFm, 5Har-OBzl); 7.10 (d, 2H, J =8.5 Hz, Har-Tyr); 6.85 (d, 2H, J= 8.5 Hz, Har-Tyr); 6.24 (bd, 1H, J=8.5 Hz, NH); 4.99 (bs, 2H, CH_2-OBzl); 4.56 (m, 1H, H^{α}-Tyr); 4.26 (m, 1H, H^{α}-Leu); 4.12 (t, 2H, J =5.8 Hz, CH-SFm); 3.48 (d, 1H, J= 5.8 Hz, CH_2-SFm); 2.98 (d, 2H, J=7 Hz, 2H^{β}-Tyr); 1.67 (bm, 1H, CH^{γ}-Leu); 1.42 (m, 11H, 2H^{β}-Leu, 9H-*t*Bu); 0.82 (d, 6H, J=6.7 Hz, 2CH_3-Leu).

^{13}C NMR ($CDCl_3$, 75 MHz): δ 200.21 (1C, s); 171.62 (1C, s); 158.03 (1C, s), 155.78 (1C, s); 145.48 (2C, s); 141.36 (2C, s); 137.20 (1C, s); 130.67 (2C, d), 129.03 (1C, s); 80.41 (1C, s); 70.15 (1C, t); 58.01 (1C, d); 55.95 (1C, d); 46.91 (1C, d); 41.66 (1C, t); 37.14 (1C, t); 32.17 (1C, t); 28.49 (3C, q); 24.71 (1C, d); 24.74 (1C, q); 21.98 (1C, q).

Boc-Val-Tyr(OBzl)-Leu-SFm **[2'(III)]**

The product was synthesized according to the protocol A reported in the section *6.6.2*. Reaction time 2 h. The purification by silica gel flash chromatography (cyclohexane/EtOAc, 7:3) gave the product as a white solid (1.45 g, 90%). Purity > 98%. R_f = 0.25 (cyclohexane/AcOEt, 7:3). $[\alpha]_D^{20}$ (c 0.5, $CHCl_3$) = −56.85 °

^{1}H NMR ($CDCl_3$, 300 MHz): δ 7.72 (d, 2H, J=7.3 Hz, Har-Fm); 7.60 (dd, 2H, J=7Hz, J= 3Hz, Har-Fm); 7.36 (m, 9H, 4Har-Fm, 5Har-OBzl); 7.10 (d, 2H, J= 8.5 Hz, Har-Tyr); 6.85 (d, 2H, J= 8.5 Hz, Har-Tyr); 6.49 (bd, 1H, J= 7.6 Hz, NH); 6.38 (bd, 1H, J= 5.5 Hz, NH); 4.96 (s, 2H, CH_2-OBzl); 4.83 4.85 (bd, 1H, J= 6.1 Hz, NH); 4.62 (bm, 1H, H^{α}-Leu); 4.45 (m, 1H, H^{α}-Tyr); 4.12 (t, 2H, J= 5.8 Hz, CH-SFm); 3.88 (m, 1H, H^{α}-Val); 3.47 (d, 1H, J= 5.8 Hz, CH_2-SFm); 3.01 (m, 2H, 2H^{β}-Tyr); 1.14 (m, 1H, H^{β}-Val); 1.78 (bm, 1H, H^{γ}-Leu); 1.36 (bm, 9H, 9H-*t*Bu); 1.25 (m, 2H, 2H^{β}-Leu); 0.91 (d, 6H, J=6.7 Hz, 2CH_3-Val); 0.81 (d, 6H, J=6.1 Hz, 2CH_3-Leu).

^{13}C NMR ($CDCl_3$, 75 MHz): δ 200.45 (1C, s); 172.50 (2C, s); 157.89 (1C, s), 156.08 (1C, s); 145.83 (2C, s); 145.78 (2C, s); 137.51 (1C, s); 130.84 (1C, d), 129.14 (1C, s); 128.49 (2C, d), 127.87 (2C, d), 127.68 (1C, d), 127.54 (2C, d), 127.34 (1C, d), 127.34 (1C, d), 127.23 (1C, d), 125.11 (1C, d), 24.97 (1C, d), 120.03 (2C, d); 115.16 (2C, d); 79.38 (1C, s); 69.74 (1C, t); 54.56 (1C, d); 47.14 (1C, d); 41.15 (1C, t); 38.04 (1C, t); 32.42 (1C, t); 31.17 (1C, d); 28.91 (3C, q); 24.91 (1C, d); 23.18 (1C, q); 22.11 (1C, q); 19.47 (1C, q); 18.79 (1C, q).

Boc-D-Pro-Val-Tyr(OBzl)-Leu-SFm **[2a'(IV)]**

The product was synthesized according to the protocol A reported in the section *6.6.2*. Reaction time 12 h. The purification by silica gel flash chromatography (Toluene/Acetone,

90:10 to 85:15) gave the product as a white solid (1.45 g, 93%). Purity > 98%. R_f = 0.32 (Toluene/Acetone, 85:15). $[\alpha]_D^{20}$ (c 0.25, $CHCl_3$) = − 15.74°

^{1}H NMR ($CDCl_3$, 300 MHz): δ 7.71 (m, 4H, Har-SFm); 7.37 (m, 9H, 4Har-SFm, 5CHar-OBzl); 7.10 (d, 2H, J = 8.5 Hz, Har-Tyr); 6.87 (d, 2H, J= 8.5 Hz, Har-Tyr); 6.43 (bd, 1H, J= 6.4 Hz, NH); 4.99 (s, 2H, CH_2-OBzl); 4.71 (m, 1H, H^{α}); 4.51 (m, 1H, H^{α}); 4.15 (m, 3H, 1CH-SFm, $2H^{\alpha}$); 3.43 (bm, 5H, 2H-SFm, $2H^{\delta}$-Pro, $1H^{\beta}$-Tyr); 2.98 (m, 1H, $1H^{\beta}$-Tyr); 2.08 (bm, 5H, $1H^{\beta}$-Val, 4H-Pro); 1.41 (bs, 12H, $2H^{\beta}$-Leu, $1H^{\gamma}$-Leu, $3CH_3$-*t*Bu); 0.90 (m, 12H, $2CH_3$-Leu, $2CH_3$-Val).

^{13}C NMR ($CDCl_3$, 75 MHz): δ 202.07 (1C, s); 171.28 (3C, s); 157.89 (1C, s), 156.08 (1C, s); 145.55 (2C, s); 145.78 (2C, s); 141.18 (1C, s); 130.35 (2C, d); 129.14 (1C, s); 128.57 (2C, d); 127.4 (2C, d); 127.71 (2C, d); 127.42 (2C, d); 127.16(2C, d); 119.81 (2C, d); 115.16 (2C, d); 80.71 (1C, s); 70.10 (1C, t); 62.08 (1C, d); 61.14 (1C, d); 58.11 (1C, d); 54.56 (1C, d); 47.33 (1C, t); 46.83 (1C, d); 41.11 (1C, t); 36.84 (1C, t); 32.27 (1C, t); 28.85 (1C, t); 28.59 (3C, q); 24.59 (1C, t); 24.50 (1C, q); 23.01 (1C, d); 22.10 (1C, q); 19.34 (1C, q); 16.92 (1C, q).

Fmoc-Ser-D-Pro-Val-Tyr(OBzl)-Leu-SFm **(2')**

The product was synthesized according to the protocol A reported in the section *6.6.2*. Reaction time 2 h. The purification by silica gel flash chromatography (AcOEt/PE, 8:2) gave the product as a white solid (870 mg, 70%). Purity > 98%. R_f = 0.3 (AcOEt/PE = 9/1). $[\alpha]_D^{20}$ (c 0.5, $CHCl_3$) = − 36.15°
MS-HPLC calcd for: $C_{64}H_{69}N_5O_9S$, expected: 1083.48, found: 1106.55 $[M+Na]^+$

^{1}H NMR ($CDCl_3$, 300 MHz): δ 7.68 (m, 9H, Har); 7.35 (m, 18H, Har); 6.80 (d, 2H, J= 8.5 Hz, Har-Tyr); 6.80 (d, 2H, J= 8.5 Hz, Har-Tyr); 6.51 (d, 1H, J=7.8 Hz, NH); 6.38 (d, 1H, J=8.1 Hz, NH); 4.93 (s, 2H, CH_2-OBzl); 4.62 (m, 2H, $1H^{\alpha}$-Ser, $1H^{\alpha}$-Tyr); 4.55 (m, 1H, H^{α}-Leu); 4.3 (m, 5H, CH_2-Fmoc, CH-Fmoc, $1H^{\alpha}$-Val, $1H^{\alpha}$-Pro); 4.01 (m, 3H, CH-SFm, $2H^{\beta}$-Ser); 3.66 (m, 2H, H^{δ}-Pro); 3.30 (d, 2H, J=5.8 Hz, CH_2-SFm); 3.06 (m, 2H, H^{β}-Tyr); 2.20 (5H, $1H^{\beta}$-Val, 4H-Pro); 1.33 (m, 3H, $2H^{\beta}$-Leu, $1H^{\gamma}$-Leu), 0.88 (d, 6H, J= 6.7 Hz, $1CH_3$-Val), 0.77 (m, 6H, $2CH_3$-Leu); 0.61 (d, 3H, J= 6.7 Hz, $1CH_3$-Val).

^{13}C NMR ($CDCl_3$, 75 MHz): δ 202.07 (1C, s); 172.27 (1C, s); 171.49 (1C, s); 171.39 (1C, s); 170.60 (2C, s); 157.79 (1C, s), 156.67 (1C, s); 145.39 (2C, s); 144.02 (1C, s); 143.77 (1C, s); 141.29 (1C, s); 141,21 (1C, s); 141.04 (1C, s); 137.03 (1C, s); 134.77 (1C, d); 130.39 (2C, d); 129.35 (1C, s); 129.10 (2C, d); 127.89 (2C, d); 127.63 (2C, d); 127.40 (2C, d); 127.14 (2C, d); 127.06 (2C, d); 125.49 (2C, d); 125.22 (2C, d); 124.75 (1C, d); 119.90 (1C, d); 119.77 (2C, d); 115.03 (2C, d); 69.90 (1C, t); 67.53 (1C, t); 62.63 (1C, t); 62.80 (1C; d); 59.24 (1C; d); 58.05 (1C; d); 54.03 (1C; d); 53.50 (1C; d); 47.66 (1C, t); 47.03 (1C, d); 46.63 (1C; d); 40.01 (1C, t); 35.85 (1C, t); 31.97 (1C, t); 29.25 (1C, d); 28.63 (1C, t); 25.21 (1C, t); 24.45 (1C, d); 22.80 (1C, q); 21.69 (1C, q); 19.34 (1C, q); 16.87 (1C, q).

5.1.2. Synthesis of linear peptides on solid phase

Linear peptides (16-25)

All the linear peptides were synthesized by SPPS using the Fmoc/*t*Bu strategy and Cl-Trt resin (f=1.60 mmol/g) in accordance to the experimental procedures reported in the section *6.5* of the chapter 6 *General methods and procedures*. Synthesis of a common tetra-peptide **13** was performed at 800 µmol scale, then the peptide-resin was split in 10 equal portions and the coupling with the fifth amino acid was performed.
Each coupling was carried out using PyBOP, HOAt and DIEA (3:3:6) as coupling reagents. Solvents and soluble reagents were removed by suction. Washings between synthetic steps were done with DMF (5 x 30 s) and DCM (5 x 30 s). During couplings the mixture was left to react with intermittent manual stirring and the good outcome of each coupling was verified by ninhydrin, chloranil or *p*-nitrophenyl ester test. The Fmoc group were removed by treatment with 20% of piperidine in DMF, the Leu Alloc protecting group was removed by treatment with $Pd(PPh_3)_4$ as described in the section *6.5.15*. The cleavage of the peptide from the resin was accomplished by treatment with a solution of 2% TFA in DCM (5x 1 min). Crude products were analyzed by RP-HPLC and MS-HPLC. HPLC chromatograms were recorded on a Waters Alliance 2695 separation module using a Sunfire C18 column flow 1ml/min, solvents H_2O (0.045% TFA) and ACN (0.036% TFA). The gradient (G) is expressed as % of ACN in H_2O.
The initial resin loading was determined by UV spectroscopy as reported in the section *6.5.6.* The overall yields of each linear peptide synthesis was estimated by Fmoc UV detection related to the last cleavage step, whereas the purity of the crudes were determined through analytical HPLC analysis (peak detected at λ=220 nm).

Linear peptide 28

This compound was synthesized using the same experimental conditions described before until the intermediate **13**. Then a mixture of Boc-Lys(Fmoc)-OH (3eq), PyBOP (3eq), and HOAt (3eq) was dissolved in the minimum volume of DMF and pre-activated by adding DIEA (6 eq). After 1 min the mixture was added to the peptide-resin **13** and the couplings were performed at r.t. with intermittent manual stirring. Treatment with piperidine (20% in DMF, 2x10 min) removed the Fmoc pretecting group on the Lys-side chain amino group. Amine acetylation was accomplished with treatment with Ac_2O/DIEA according to the conditions reported in the section *6.5.14*. The peptide resin **27** was treated with a solution of TFA-H_2O-TIS/95:2.5:2.5 (5 ml) at r.t. for 30 min obtaining the linear peptide **28**.

Linear peptides characterization

H-Lys(Boc) Val-Tyr(tBu)-Leu-D-Pro-OH ***(16)***

Initial loading: 0.72 mmol/g
HPLC: t_R (min, G0100 ACN in 8 min)= 5.44
MS-HPLC calcd for: $C_{40}H_{66}N_6O_9$, expected: 774,49, found: 775.24 $[M+1]^+$
Yield: 95 %
Purity: 95 %

H-Phe(4-NH-Boc)-Val-Tyr(tBu)-Leu-D-Pro-OH ***(17)***

Initial loading: 0.75 mmol/g
HPLC: t_R (min, G0100 ACN in 8 min)= 5.78
MS-HPLC calcd for: $C_{43}H_{64}N_6O_9$, expected: 808,47, found: 809.0 = $[M+H]^+$
Yield: 94 %
Purity: 85 %

H-Cys(Trt)-Val-Tyr(tBu)-Leu-D-Pro-OH ***(18)***

Initial loading: 0.75 mmol/g
HPLC: t_R (min, G0100 ACN in 8 min)= 6.49
MS-HPLC calcd for: $C_{51}H_{65}N_5O_7S$, expected: 891,46, found: 892.45 = $[M+H]^+$
Yield: 97 %
Purity: 95 %

H-Glu(OtBu)-Val-Tyr(tBu)-Leu-D-Pro-OH ***(19)***

Initial loading: 0.75 mmol/g
HPLC: t_R (min, G0100 ACN in 8 min)= 6.38
MS-HPLC calcd for: $C_{38}H_{61}N_5O_9$, expected: 731,45, found: 732.43 = $[M+H]^+$
Yield: 80 %
Purity: 95 %

H-Gln(Trt)-Val-Tyr(tBu)-Leu-D-Pro-OH ***(20)***

Initial loading: 0.75 mmol/g
HPLC: t_R (min, G0100 ACN in 8 min)= 6.28
MS-HPLC calcd for: $C_{53}H_{68}N_6O_8$, expected: 916,51, found: 917.50 = $[M+H]^+$
Yield: 85 %
Purity: 98 %

H-Arg(Pbf)-Val-Tyr(tBu)-Leu-D-Pro-OH ***(21)***

Initial loading: 0.75 mmol/g
HPLC: t_R (min, G0100 ACN in 8 min)= 6.02
MS-HPLC calcd for: $C_{48}H_{74}N_8O_{10}S$, expected: 954,52, found: 955.53 = $[M+H]^+$
Yield: 93 %
Purity: 90 %

H-Trp(Boc)-Val-Tyr(tBu)-Leu-D-Pro-OH ***(22)***

Initial loading: 0.75 mmol/g
HPLC: t_R (min, G0100 ACN in 8 min)= 6.19
MS-HPLC calcd for: $C_{45}H_{64}N_6O_9$, expected: 832,47, found: 833.50 = $[M+H]^+$
Yield: 92 %
Purity: 90 %

H-Ser(tBu)-Val-Tyr(tBu)-Leu-D-Pro-OH ***(23)***

Initial loading: 0.75 mmol/g
HPLC: t_R (min, G0100 ACN in 8 min)= 5.28
MS-HPLC calcd for: $C_{36}H_{59}N_5O_8$, expected: 689,44, found: 690.86 = $[M+H]^+$
Yield: 82 %
Purity: 90 %

H-Dap(Boc)-Val-Tyr(tBu)-Leu-D-Pro-OH ***(24)***

Initial loading: 0.75 mmol/g
HPLC: t_R (min, G0100 ACN in 8 min)= 5.52
MS-HPLC calcd for: $C_{37}H_{60}N_6O_9$, expected: 732,44, found: 733.38 = $[M+H]^+$
Yield: 66 %
Purity: 93 %

H-Ala-Val-Tyr(tBu)-Leu-D-Pro-OH ***(25)***

Initial loading: 0.75 mmol/g
HPLC: t_R (min, G0100 ACN in 8 min)= 4.88
MS-HPLC calcd for: $C_{32}H_{51}N_5O_7$, expected: 617,38, found: 661.42 = $[M-t\text{Bu})]^+$
Yield: 74 %
Purity: 95%

H-Lys(NHAc)-Val-Tyr-Leu-D-Pro-OH ***(28)***

Initial loading: 0.75 mmol/g
HPLC: t_R (min, G0100 ACN in 8 min)= 4.43
MS-HPLC calcd for: $C_{33}H_{52}N_6O_8$, expected: 660,38, found: 661.28 = $[M+H]^+$
Yield: 90 %
Purity: 98 %

5.2. Synthesis of cyclic peptides

All the experimental conditions are reported in the section *6.7* of the chapter **6** *General methods and procedures*.

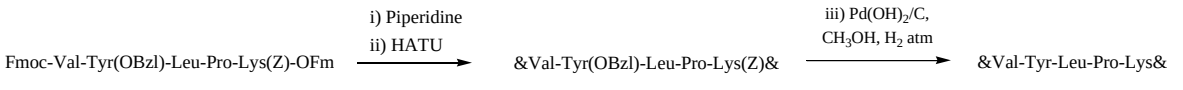

1a= Pro, Lys — **cyclo-1a= Pro, Lys** — **cyclo-1A= Pro, Lys**
1b= Pro, D-Lys — **cyclo-1b= Pro, D-Lys** — **cyclo-1B= Pro, D-Lys**
1c= D-Pro, Lys — **cyclo-1c= D-Pro, Lys** — **cyclo-1C= D-Pro, Lys**

&Val-Tyr-Leu-Pro-Lys& (cyclo-1A)

The Fmoc and OFm protecting groups of the linear pentapeptide **1a** (600 mg, 0,48 mmol) were removed by treatment with piperidine (20% in DMF, 2 ml) at r.t. under stirring for 1

h. The solvent was evaporated and the remaining residue was triturated with diethyl ether, filtrated and dried under vacuum to yield the product as a white solid (400 mg, 97%). Purity > 95%. R_f= 0.3 (ACN/MeOH/H_2O, 8:1:1)

HATU mediated cyclization.The linear peptide cyclization (100 mg, 0.12 mmol) was performed in accordance to the protocol E. Reaction time 72 h. Purification by silica gel flash chromatography (AcOEt/*i*PrOH, 95:5) gave the title compound ***cyclo*-1a** as a white solid (20 mg, 20%). Purity = 95%.

PyBOP mediated cyclization.The linear peptide cyclization (100 mg, 0.12 mmol) was performed in accordance to the procedure described in the protocol F. Reaction time 72 h. Purification by silica gel flash chromatography (AcOEt/*i*PrOH, 95:5) gave the title compound ***cyclo*-1a** as a white solid (12 mg, 12%). Purity= 95%.

PPAA mediated cyclization The linear peptide cyclization (100 mg, 0.12 mmol) was performed in accordance to that described in protocol G. Reaction time 56 h. Purification by silica gel flash chromatography (AcOEt/*i*PrOH, 95:5) gave the title compound ***cyclo*-1a** as a white solid (54 mg, 56%). Purity=95%.

R_f = 0.25 (AcOEt/*i*PrOH, 95:5). $[\alpha]_D^{20}$ (c 0.5, $CHCl_3$) = − 40.15°
MS-HPLC calcd for: $C_{46}H_{60}N_6O_8$, expected: 824,45, found: 825.90 =$[M+H]^+$, 848.08 = $[M+Na]^+$, 823.76 $[M-H]^-$.

^{1}H NMR (CD_3OD, 300 MHz): δ 7.3 (m, 9H); 7.13 (d, 2H, J=8.5 Hz, 2H-Tyr); 6.9 (d, 2H, J=8.5 Hz, 2H-Tyr); 5.13 (s, 4H, CH_2-OBzl, CH_2-(Cbz); 4.66 (m, 1H); 4.43 (m, 1H); 4.15-4.03 (m, 2H); 3.96, (d, 1H, J= 9.1 Hz); 3.71 (m, 1H); 3.56 (m, 1H); 3.34- 3.10 (m, 4H); 2.31-1.85 (m, 6H), 1.75- 1.4 (m, 8H); 0.98 (m, 6H); 0.88 (d, 3H, J= 6.6 Hz); 0.78 (d, 3H, J= 6.4 Hz).

To a solution of a Z/OBzl-protected peptide ***cyclo-1a*** (30 mg, 0.036 mmol) in dry MeOH (4 ml) was added $Pd(OH)_2$/C (4mg) on activated charcoal) and the mixture was hydrogenated overnight under atmospheric pressure using an H_2-filled balloon. The catalyst was removed by filtration through a pad of celite and the solvent evaporated under reduced pressure yielding the final product ***cyclo-1A*** as a white solid (20 mg, 97%). R_f = 0.1 (ACN/MeOH/H_2O, 7:2:1).

MS-HPLC calcd for: $C_{31}H_{48}N_6O_6$, expected: 600,36, found: 601.32 $[M+H]^+$ 623.31 $[M+Na]^+$

&Val-Tyr-Leu-Pro-D-Lys& (*cyclo*-1B)

The Fmoc and OFm protecting groups of the linear pentapeptide **1b** (230 mg, 0,18 mmol) were removed by treatment with piperidine (20% in DMF, 2 ml) at r.t. under stirring for 1 h. The solvent was evaporated and the remaining residue was triturated with diethyl ether, filtrated and dried under vacuum to yield the product as a white solid (157 mg, 100%). Purity > 95%. R_f= 0.27 (ACN/MeOH/H_2O, 8:1:1)

The peptide cyclization (150 mg, 0.17 mmol) was performed with HATU in accordance to the procedure described in the protocol E. Reaction time 56 h. Purification by silica gel flash chromatography (DCM/ACN/*i*PrOH, 8:1.5:0.5) gave the title compound ***cyclo*-1b** as a

white solid (39 mg, 25%). Purity >95%. R_f = 0.25 (DCM/ACN/*i*PrOH, 8:1.5:0.5). $[\alpha]_D^{20}$ (c 0.5, $CHCl_3$) = − 36.10°
MS-HPLC calcd for: $C_{46}H_{59}ClN_6O_8$, expected: 858,41, found: 859.33 = $[M+H]^+$.

^{1}H NMR (CD_3OD, 300 MHz): δ 7.25 (m, 9H); 7.57 (m, 4H); 7.09 (d, 2H, J=8.5 Hz, 2H-Tyr); 6.78 (d, 2H, J=8.5 Hz, 2H-Tyr); 5.13 (s, 2H, CH_2-OBzl); 4.90 (m, 4H, CH_2-(2Cl-Z), $2H^{\alpha}$); 4.17 (m, 2H, $2H^{\alpha}$); 4.10 (d, 1H, J=9.6 Hz, H^{α}-Val); 3.68 (bm, 1H, H^{δ}-Pro); 3.53 (bm, 1H, H^{δ}-Pro); 3.08 (m, 3H, $1H^{\beta}$-Tyr, $2H^{\varepsilon}$-Lys); 2.01 (m, 5H, 4H-Pro, $1H^{\beta}$-Val); 1.38 (bm, 9H, $1H^{\gamma}$-Leu, $2H^{\beta}$-Leu, 6H-Lys), 1.02 (d, 3H, J=6.7 Hz, $1CH_3$-Leu); 0.88 (m, 9H, $1CH_3$-Leu, $2CH_3$-Val).

To a solution of a Z/OBzl-protected peptide ***cyclo-1b*** (30 mg, 0.035 mmol) in dry MeOH (3ml) was added $Pd(OH)_2$/C (3 mg) and the mixture was hydrogenated overnight under atmospheric pressure using an H_2-filled balloon. The catalyst was removed by filtration through a pad of celite and the solvent evaporated under reduced pressure yielding the final product ***cyclo-1B*** as a white solid (27 mg, 95%). R_f = 0.1 (ACN/MeOH/H_2O, 7:2:1).

MS-HPLC calcd for: $C_{31}H_{48}N_6O_6$, expected: 600.36, found: 601.32 $[M+H]^+$, 623.31 $[M+Na]^+$

&Val-Tyr-Leu-D-Pro-Lys& (*cyclo*-1C)

The Fmoc and OFm protecting groups of the linear pentapeptide **1c** (150 mg, 0,12 mmol) were removed by treatment with piperidine (20% in DMF, 2 ml) at r.t. under stirring for 1 h. The solvent was evaporated and the remaining residue was triturated with diethyl ether, filtrated and dried under vacuum to yield the product as a white solid (100 mg, 100%). Purity > 95%. R_f= 0.3 (ACN/MeOH/H_2O, 8:1:1)

The peptide cyclization (100 mg, 0.12 mmol) was performed with HATU in accordance to the procedure described in the protocol E. Reaction time 56 h. Purification by silica gel flash chromatography (DCM/ACN/*i*PrOH, 8:1.5:0.5) gave the title compound ***cyclo*-1c** as a white solids (60 mg, 45%). Purity > 95%. R_f = 0.25 (DCM/ACN/*i*PrOH, 8:1.5:0.51/1). $[\alpha]_D^{20}$ (c 0.5, MeOH) = -125.84

MS-HPLC calcd for: $C_{46}H_{60}N_6O_8$, expected: 824.45, found: 847.49 = $[M+Na]^+$, 823.26 = $[M-H]^-$.

^{1}H NMR (CD_3OD, 300 MHz): δ 7.32 (m, 9H); 7.12 (d, 2H, J=8.5 Hz, 2H-Tyr); 6.87 (d, 2H, J=8.5 Hz, 2H-Tyr); 5.04 (s, 4H, CH_2-OBzl, CH_2-(Cbz)); 4.68 (bm, 1H, H^{α}-Lys); 4.42 (bm, 1H, H^{α}-Leu); 4.15 (m, 1H, H^{α}-Pro); 4.03 (m, 1H, H^{α}-Tyr); 3.90 (d, 1H, J=9.6 Hz, $1H^{\alpha}$-Val); 3.71 (m, 1H, $1H^{\delta}$-Pro); 3.54 (m, 1H, $1H^{\delta}$-Pro); 3.30 (m, 2H, $2H^{\beta}$-Tyr); 3.09 (t, 2H, J=7.0 Hz, $2H^{\varepsilon}$-Lys); 2.17 (m, 5H, 4H-Pro, $1H^{\beta}$-Val); 1.50 (bm, 9H, $1H^{\gamma}$-Leu, $2H^{\beta}$-Leu, 6H-Lys), 0.97 (m, 12H, $2CH_3$-Leu, $2CH_3$-Val).

^{13}C NMR (CD_3OD, 75 MHz): δ 173.04 (1C, s); 172.90 (1C, s); 172.82 (1C, s); 172.68 (1C, s); 172.17 (1C, s); 158.0 (1C, s); 157.85 (1C, s), 137.49 (1C, s); 137.39 (1C, s); 129.85 (1C, d); 129.26 (1C, d); 128.17 (2C, d); 128.14 (1C, s); 127.62 (2C, d); 127.48 (2C, d); 127.45 (2C, d); 127.13 (2C, d); 114.73 (2C, d); 69.62 (1C, t); 66.53 (1C, t); 62.39 (1C, t); 60.92 (1C; d); 59.11 (1C; d); 52.68 (1C; d); 50.42 (1C; d); 40.68 (1C; t); 40.54 (1C, t); 39.98 (1C,

t); 30.69 (1C, t); 29.35 (1C, t); 29.23 (1C, t); 29.25 (1C, t); 28.83 (1C, d); 24.67 (1C, d); 24.56 (1C, t); 22.77 (1C, d); 22.44 (1C, q); 20.71 (1C, q); 18.41 (1C, q); 18.00 (1C, q).

To a solution of a Z/OBzl-protected peptide ***cyclo-1c*** (50 mg, 0.06 mmol) in dry MeOH (5ml) was added $Pd(OH)_2/C$ (5 mg) and the mixture was hydrogenated overnight under atmospheric pressure using an H_2-filled balloon. The catalyst was removed by filtration through a pad of celite and the solvent evaporated under reduced pressure. The purification by silica gel flash chromatography (ACN/H_2O, 7:3) gave the final product ***cyclo*-1C** as a white solids (34 mg, 95%). Purity >95%. R_f = 0.15 (ACN/H_2O, 7:3). $[\alpha]_D^{20}$ (c 0.5, MeOH) = -120.22

MS-HPLC calcd for: $C_{31}H_{48}N_6O_6$, expected: 600,36, found: 601.13 = $[M+H]^+$

&Val-Tyr(OBzl)-Leu-D-Pro-Lys(Cbz)& (*cyclo*-1c')

To a solution of **1c'** (100 mg, 79 μmol) in DMF (700 μl) was added piperidine (155 μl, 1.58 μmol) at 0 °C. The reaction mixture was stirred for 15 min, then the volatiles were removed under high vacuum. The residual piperidine was removed by azeotropic distillation with toluene *in vacuo*. The residue was dissolved in DMF (15.8 ml) and 2,4-dinitrofluorobenzene (11.6 μl, 90 μmol) was added to it and the reaction mixture was stirred for 5 min at r.t. DMF was removed under high vacuum, obtaining a yellow oil as a crude. The purification was done in two steps: a first silica gel flash chromatography (Toluene/AcOEt, 50:50 to 0:100) to remove the non-polar by-products, then a second silica gel flash chromatography (AcOEt/*i*PrOH= 98:2 to 95:5) yielded the final product as a white solid (25 mg, 30%). Purity =90%. R_f = 0.45 (AcOEt/*i*PrOH, 9:1). $[\alpha]_D^{20}$ (c 0.5, $CHCl_3$) = − 34.33°

MS-HPLC calcd for: $C_{46}H_{60}N_6O_8$, expected: 824.45, found: 825.90 =$[M+H]^+$, 848.08 = $[M+Na]^+$, 823.76 $[M-H]^-$.

^{1}H NMR (CD_3OD, 300 MHz): 7.34 (m, 10H, 5Har-OBzl, 5Har-Cbz); 7.16 (d, 2H, J= 8.5 Hz, Har-Tyr), 6.90 (d, 2H, J= 8.5 Hz, Har-Tyr); 5.05 (s, 4H, 2H-CH_2-OBzl, 2H-CH_2-Cbz); 4.66 (m, 1H, H^{α}); 4.41 (1H, H^{α}); 4.10 (m, 2H, $2H^{\alpha}$); 3.95 (d, 1H, J= 9.6 Hz, H^{α}-Val); 3.72 (m, 1H, $1H^{\delta}$–Pro); 3.56 (m, 1H, $1H^{\delta}$–Pro); 3.20 (d, 2H, $2H^{\beta}$-Tyr); 3.10 (t, J= 7.0 Hz, $2H^{\varepsilon}$-Lys), 2.01 (m, 7H, 4H-Pro, $1H^{\beta}$-Val, $2H^{\beta}$ Leu); 1.70 (m, 7H, 6H-Lys, $1H^{\gamma}$-Leu); 0.98 (m, $2CH_3$-Leu); 0.88 (d, J=6.4 Hz, 3H, $1CH_3$-Val); 0.78 (d, 3H, J=6.4 Hz, $1CH_3$-Val).

^{13}C NMR spectrum is in agreement with that obtained for the analogue product titled ***cyclo*-1c**.

&Ser-Pro-Val-Tyr-Leu& (*cyclo*-2a)

The Fmoc and OFm groups of the linear pentapeptide **2** (80 mg, 0,075 mmol) were removed by treatment with piperidine (20% in DMF, 2 ml) at r.t. under stirring for 1 h. The solvent was evaporated and the remaining residue was triturated with diethyl ether, filtrated and dried under vacuum to yield the product as a white solid (45 mg, 90%). Purity > 95%. R_f= 0.1 (DCM/MeOH, 9:1).

The peptide cyclization was performed with HATU, in accordance to the procedure described in the protocol E. Reaction time 48 h. The crude residue was purified by silica gel flash chromatography (DCM/cyclohexane/*i*PrOH, 7:2:1), then the resulting oil was crystallized from diethyl ether/DCM yielding the title compound ***cyclo*-a** as a white solid (28.5 mg, 65%). Purity >95%. R_f = 0.25 (DCM/ACN/*i*PrOH, 8:1:1). $[\alpha]_D^{20}$ (c 0.5, MeOH) = − 32.85

MS-HPLC calcd for: $C_{35}H_{47}N_5O_7$, expected: 649.35, found: 673.08= $[M+Na]^+$, 823.26 = $[M-H]^-$

^{1}H NMR ($CDCl_3$, 300 MHz): 8.02 (bd, 1H, J=6.6 Hz; NH), 8,06 (bd, 1H, J=8.7 Hz; NH), 7.60 (bd, 1H, J= 8.5 Hz; NH),7.39 (m, 5H, 5Har-OBzl); 7.13 (d, 2H, J= 8.5 Hz, Har-Tyr), 6.89 (d, 2H, J= 8.5 Hz, Har-Tyr); 6.14 (bd, 1H, J=6.7 Hz; NH), 4.99 (s, 4H, CH_2-OBzl); 4.84 (m, 2H, H^{α}); 4.29 (1H, H^{α}); 4.18 (m, 2H, $2H^{\alpha}$); 3.90 (dd, 1H, J= 8.2, J= 3Hz, $1H^{\beta}$-Ser); 3.74 (dd, 1H, J= 8.2, J= 3Hz, $1H^{\beta}$-Ser); 3.46 (m, 1H, $1H^{\delta}$-Pro); 3.32 (m, 2H, $1H^{\delta}$-Pro, $1H^{\beta}$-Tyr); 3.18 (m, 2H, $1H^{\beta}$-Tyr); 1.87 (m, 5H, 4H-Pro, $1H^{\beta}$-Val,); 1.21 (m, 2H, $2H^{\beta}$-Leu); 1.50 (m, 1H, H^{γ}-Leu); 0.99 (d, 3H, J= 6.7 Hz, CH_3); 0.94 (d, 3H, J= 6.4 Hz, CH_3); 0-78 (d, 3H, J= 6.4 Hz, CH_3);0.67 (d, 3H, J= 6.4 Hz, CH_3).

To a solution of ***cyclo-2*** (28 mg, 44 μmol) in dry MeOH (2 ml), was added Pd(OH)/C (3 mg, 10% on activated charcoal) and the mixture was hydrogenated overnight under atmospheric pressure using an H_2-filled balloon. The catalyst was removed by filtration through a pad of celite and the solvent evaporated under reduced pressure. The residue purification by silica gel chromatography ($CHCl_3$/ACN/*i*PrOH= 8:1.5:0.5 to 8:1:1) yielded the product ***cyclo*-2a** as a white solid (22 mg, 90%). Purity >95%. R_f = 0.28 (DCM/ACN/*i*PrOH, 7:1:2). $[\alpha]_D^{20}$ (c 0.5, MeOH) = −28.63

MS-HPLC calcd for: $C_{28}H_{41}N_5O_7$, expected: 559.3, found: 560.60 $[M+H]^+$, 582.81 $[M-Na]^+$.

^{1}H-NMR (CD_3OD, 300 MHz): δ 7.06 (d, 2H, J=8.2 Hz, Har-Tyr); 6.71 (d, 2H, J=8.2 Hz, Har-Tyr); 4.77 (t, 1H, J=7.5 Hz, H^{α}-Ser); 4.41 (t, 1H, J=8.0 Hz, H^{α}-Tyr); 4.04 (d, 1H, J=5.8 Hz, H^{α}-Val); 3.83 (m , 1H, $1H^{\alpha}$-Pro); 3.72 (m, 3H, $1H^{\alpha}$-Leu, $2H^{\beta}$-Ser); 3.65 (m, 1H, $1H^{\delta}$-Pro); 3.34 (m, 1H, $1H^{\delta}$-Pro); 3.04 (d, 2H, J=8Hz, $2H^{\beta}$-Tyr); 2.09 (m, 4H, $1H^{\beta}$-Val, 3H-Pro); 1.56 (m, 1H, 1H-Pro); 1.28 (m, 1H, $1H^{\gamma}$-Leu, $2H^{\beta}$-Leu); 0.99 (m, 9H, $2CH_3$-Val, $1CH_3$-Leu); 0.77 (d, 3H, J=6.3 Hz, $1CH_3$-Leu).

&Ser-Pro-Val-Tyr-Leu& (*cyclo*-2a')

To a solution of linear peptide **2'** (200 mg, 184 μmol) in 1.8 ml of DMF was added piperidine (360 μl, 3.6 mmol) at 0 °C. The reaction mixture was stirred for 15 min, then the volatiles were removed under high vacuum. The residual piperidine was removed by azeotropic distillation with toluene *in vacuo*. The residue was dissolved DMF (36.8 ml) and 2,4-Dinitrofluorobenzene (27 μl, 215 μmol) was added to it, and the reaction mixture was stirred for 5 min. DMF was removed under high vacuum, and the residue was purified by silica gel chromatography ($CHCl_3$/*i*PrOH= 95/5) to give ***cyclo-2'*** as yellow solid (59 mg, 50%). Purity >95%. R_f = 0.43 ($CHCl_3$/*i*PrOH, 9:1).

MS-HPLC calcd for: $C_{35}H_{47}N_5O_7$, expected: 649.35, found: 672.69 $[M+Na]^+$, 648.26 $[M-H]^-$.

^{1}H-NMR (CD_3OD, 300 MHz): δ 7.06 (d, 2H, J=8.5 Hz, Har-Tyr); 6.71 (d, 2H, J=8.5 Hz, Har-Tyr); 4.77 (t, 1H, J= 7.5 Hz, H^{α}-Ser); 4.37 (m, 3H, $1H^{\alpha}$-Tyr, $1H^{\alpha}$-Pro, $1H^{\alpha}$-Leu); 4.03 (d, 1H, J=5.8 Hz, H^{α}-Val); 3.74 (m, 3H, $2H^{\beta}$-Ser, $1H^{\delta}$-Pro); 3.65 (m, 1H, $1H^{\delta}$-Pro); 3.04 (d, 2H, J=8.0 Hz, $2H^{\beta}$-Tyr); 2.09 (m, 5H, $1H^{\beta}$-Val, 4H-Pro); 1.53 (m, 1H, $1H^{\gamma}$-Leu); 1.28 (m, 2H, $2H^{\beta}$-Leu); 0.99 (d, 6H, J=6.7 Hz, $2CH_3$-Val); 0.85(d, 3H, J=6.4, $1CH_3$-Leu); 0.73 (d, 3H, J=6.4, $1CH_3$-Leu).

To a solution of ***cyclo-2'*** (40 mg, 60 μmol) in dry MeOH (2 ml), was added $Pd(OH)_2$/C (4 mg, 10% on activated charcoal) and the mixture was hydrogenated overnight under atmospheric pressure using an H_2-filled balloon. The catalyst was removed by filtration through a pad of celite and the solvent evaporated under reduced pressure. The titled ***cyclo*-2a'** product was obtained as a pale yellow solid (31 mg, 90%). Purity >95%. The physical and spectroscopic data are the same to those obtained for its analogue ***cyclo*-2a**

&Lys-Val-Tyr-Leu-D-Pro& *(cyclo-16)*

The cyclization of the linear peptide **16** was performed in accordance to the protocol G. Reaction time 48 h. The crude cyclopeptide was dissolved in TFA-TIS-H_2O/95:2.5:2.5 (10 ml), at r.t. and stirred for 1 h. Excess TFA was removed under a stream of nitrogen. The residue was dissolved in ACN/H_2O and lyophilized. The purification was performed by automated flash chromatography with RediSepC18 (0:20 to 20:50 H_2O/ACN + 0.1% TFA, linear gradient over 30 min) yielding the product as a white solid (104 mg, 40%). Purity > 98%.

HPLC: t_R (min, G0100 ACN in 8 min) = 4.623

MS-HPLC calcd for: $C_{31}H_{48}N_6O_6$, expected: 600.36, found: 601.32 $[M+H]^+$

^{1}H-NMR (CD_3OD, 400MHz): 7.06 (d, 2H, J=8.5 Hz, 2H-Tyr), 6.69 (d, 2H, J=8.5 Hz, 2H-Tyr), 4.64 (m, 1H, H^{α}-Leu), 4.43 (m, 1H, H^{α}-Pro), 4.20 (m, 2H, H^{α}-Lys), 4.09 (m, 1H, H^{α}-Tyr), 3.95 (t, 1H, J= 9.1 Hz, H^{α}-Val), 3.71 (m, 1H, $1H^{\delta}$-Pro); 3.55 (m, 1H, $1H^{\delta}$-Pro); 3.17 (m, 2H, H^{β}-Tyr); 2.91 (t, 2H, J= 7.3 Hz, H^{ε}-Lys), 2.22 (m, 2H, $1H^{\beta}$-Val, 1H-Pro); 2.00 (m, 4H, 3H-Pro, 1H-Lys), 1.77- 1.39 (m, 8H, $1H^{\gamma}$-Leu, $2H^{\beta}$-Leu, 5H-Lys), 0.99 (m, 6H, $2CH_3$-Leu); 0.91 (d, 3H, J=6.7 Hz, $1CH_3$-Val); 0.85 (d, 3H, J= 6.7 Hz, $1CH_3$-Val).

&Phe(4-NH_2)-Val-Tyr-Leu-D-Pro& (*cyclo*-17)

The cyclization of the linear peptide **17** was performed in accordance to the protocol G. Reaction time 24 h. The crude cyclopeptide was dissolved in TFA-TIS-H_2O/95:2.5:2.5 (10 ml), at r.t. and stirred for 30 min. Excess TFA was removed under a stream of nitrogen. The residue was dissolved in ACN/H_2O and lyophilized. The purification by HPLC-semi-preparative (SunFirePrepC18, 25:50 H_2O/ACN + 0.1% TFA, linear gradient over 25 min) gave the product as a white solid (30 mg, 35%). Purity > 98%.

HPLC: t_R (min, G2550 ACN in 8 min) = 3.57

MS-HPLC calcd for: $C_{34}H_{46}N_6O_6$, expected: 634.35, found: 635.42 $[M+H]^+$

^{1}H-NMR (CD_3OD, 400MHz): 7.40 (d, 2H, J=6.4 Hz, 2H-Phe(4-NH_2)); 7.25 (d, 2H, J=8.4 Hz, 2H-Phe(4-NH_2)); 7.07 (d, 2H, J=8.5 Hz, 2H-Tyr); 6.70 (d, 2H, J=8.5 Hz, 2H-Tyr); 4.61 (m, 1H, H^{α}-Leu); 4.51 (m, 1H, H^{α}-Phe(4-NH_2)); 4.36 (m, 1H, H^{α}-Pro); 4.17 (m, 1H, H^{α}-Tyr); 3.93 (d, 1H, J=9.6 Hz, H^{α}-Val); 3.63 (m, 1H, $1H^{\delta}$-Pro); 3.53 (m, 1H, $1H^{\delta}$-Pro); 3.30 (m, 1H, $1H^{\beta}$-Phe(4-NH_2)); 3.16 (d, 2H, J=8.1 Hz, $2H^{\beta}$-Tyr); 2.88 (m, 1H, $1H^{\beta}$-Phe(4-NH_2)); 2.20-2.11 (m, 2H, $1H^{\beta}$-Val, 1H Pro); 1.93 (m, 2H, 2H-Pro); 1.83-1.49 (m, 5H, $1H^{\gamma}$-Leu, $2H^{\beta}$-Leu, 1H-Pro); 1.00 (m, 6H, $2CH_3$-Leu); 0.90 (d, 3H, J=6.7 Hz, $1CH_3$-Val); 0.85 (d, 3H, J=6.7 Hz, $1CH_3$-Val).

&Cys-Val-Tyr-Leu-D-Pro& (*cyclo*-18)

The cyclization of the linear peptide **18** was performed in accordance to the protocol G. Reaction time 24 h. The crude cyclopeptide was dissolved in TFA-TIS-H_2O/95:2.5:2.5 (10 ml), at r.t. and stirred for 30 min. Excess TFA was removed under a stream of nitrogen. The residue was dissolved in ACN/H_2O and lyophilized. The purification by HPLC-semi-preparative (SunFirePrepC18, 20:80 H_2O/ACN + 0.1% TFA, linear gradient over 30 min) yielded the product as a white solid (30 mg, 15%). Purity > 98%.

HPLC: t_R (min, G2080 ACN in 8 min) = 5,48

MS-HPLC calcd for: $C_{28}H_{41}N_5O_6S$, expected: 575.28, found: 576.27 $[M+H]^+$

^{1}H-NMR (CD_3OD, 400MHz): δ 7.07 (d, 2H, J= 8.5 Hz, 2H-Tyr); 6.70 (d, 2H, J=8.5 Hz, 2H-Tyr); 4.64 (dd, 1H, J= 9.8 Hz, J= 4.2 Hz); 4.47 (t, 1H, J= 7.1 Hz); 4.30-4.21 (m, 2H); 3.95 (m, 2H); 3.58 (m, 1H); 3.19 (dd, 2H, J=9.7 Hz, J= 4.2 Hz); 2.93 (dd, 1H, J= 13.4 Hz, J= 7.3 Hz); 2.71 (dd, 1H, J= 7.1, Hz, J= 2.4 Hz); 2.32 (m, 1H), 2.08- 2.97 (m, 4H); 1.62 (m, 2H), 1.48 (m, 1H), 0.99 (d, 6H, J=6.4 Hz), 0.93 (d, 3H, J=6.6 Hz), 0.87 (d, 3H, J=6.6 Hz).

&Glu-Val-Tyr-Leu-D-Pro& (*cyclo*-19)

The cyclization of the linear peptide **19** was performed in accordance to the protocol G. Reaction time 24 h. The crude cyclopeptide was dissolved in TFA-TIS-H_2O/95:2.5:2.5 (10 ml), at r.t. and stirred for 30 min. Excess TFA was removed under a stream of nitrogen. The residue was dissolved in ACN/H_2O and lyophilized. This compound was synthesized following the protocol G reported in the section *6.7*. Reaction time 24 h. The purification was performed by automated flash chromatography with RediSepC18 (0:25 to 25:50 H_2O/ACN + 0.1% TFA, linear gradient over 30 min) yielding the product as white solid. (37 mg, 45%). Purity > 98%.

HPLC: t_R (min, G0100 ACN in 8 min) = 5.69 min

MS-HPLC calcd for: $C_{30}H_{43}N_5O_8$, expected: 601.31, found: 602.25 $[M+H]^+$

^{1}H-NMR (CD_3OD, 400MHz): δ 7.06 (d, 2H, J=8.5 Hz, H-Tyr); 6.70 (d, 2H, J=8.5 Hz, 2H-Tyr); 4.67 (dd, 1H, J= 10.5 Hz, J= 3.9 Hz, H^{α}); 4.41(dd, 1H, J= 7.1 Hz, J= 4.4 Hz, H^{α}); 4.22 (dd, 1H, J= 9.1 Hz, J= 4.8 Hz, H^{α}); 4.04 (t, 1H, J=7.6 Hz, H^{α}-Tyr); 3.97 (d, 1H, J=9.4

Hz, H^{α}-Val); 3.71 (m, 1H, $1H^{\delta}$-Pro); 3.56 (m, 1H, $1H^{\delta}$-Pro); 3.22 (m, 2H, $2H^{\beta}$-Tyr); 2.42 (m, 2H); 2.23-1.87 (m, 7H); 1.69 m, 1H); 1.59 (m, 1H); 1.51 (m, 1H); 1.00 (m, 6H); 0.91(d, 3H, J=6.6 Hz), 0.81 (d, 3H, J=6.6 Hz).

&Gln-Val-Tyr-Leu-D-Pro& (*cyclo*-20)

The cyclization of the linear peptide **20** was performed in accordance to the protocol G. Reaction time 24 h. The purification by HPLC-semi-preparative (SunFirePrepC18, 20:50 H_2O/ACN + 0.1% TFA, linear gradient over 25 min) yielded the product as a white solid (35 mg, 54%). Purity > 98%.

HPLC: t_R (min, G2050 ACN in 8 min) = 6,35

MS-HPLC calcd for: $C_{30}H_{44}N_6O_7$, expected: 600.33, found: 601.32 $[M+H]^+$

^{1}H-NMR (CD_3OD, 400MHz): 7.07 (d, 2H, J=8.5 Hz, 2H-Tyr); 6.70 (d, 2H, J=8.5 Hz, 2H-Tyr); 4.67 (m, 1H, H^{α}-Leu); 4.0 (dd, 1H, J= 10.4 Hz, J=4.0 Hz, H^{α}-Gln); 4.21 (m, 1H, H^{α}-Pro); 4.07 (t, 1H, J=7.6 Hz, H^{α}-Tyr), 3.98 (d, 1H, J=9.4 Hz, H^{α}-Val), 3.71 (m, 1H, $1H^{\delta}$-Pro), 3.57 (m, 1H, $1H^{\delta}$-Pro), 3.19 (dd, 2H, J= 7.6 Hz, J=4.7 Hz, $2H^{\beta}$-Tyr), 2.34 (m, 2H, $2H^{\gamma}$-Gln), 2.18-1.93 (m, 7H, $1H^{\beta}$-Val, 4H-Pro, $2H^{\beta}$-Gln), 1.72 (m, 1H, CH^{γ}-Leu), 1.61-1.49(m, 2H, $2H^{\beta}$-Leu), 0.99 (m, 6H, $2CH_3$-Leu), 0.92 (d, 3H, J=6.6 Hz, $1CH_3$-Val), 0.85 (d, 3H, J=6.6 Hz, $1CH_3$-Val).

&Arg-Val-Tyr-Leu-D-Pro& (*cyclo*-21)

The cyclization of the linear peptide **21** was performed in accordance to the protocol G. Reaction time 16 h. The purification by HPLC-semi-preparative (SunFirePrepC18, 30:40 H_2O/ACN + 0.1% TFA, linear gradient over 25 min) yielded the product as a white solid (15 mg, 16%). Purity > 99%.

HPLC: t_R (min, G2050 ACN in 8 min) = 4,34

MS-HPLC calcd for: $C_{31}H_{48}N_8O_6$, expected: 628.37, found: 629.33 $[M+H]^+$

^{1}H-NMR (CD_3OD, 400MHz): δ 7.07 (d, 2H, J=8.5 Hz, H-Tyr); 6.70 (d, 2H, J=8.5 Hz, H-Tyr); 4.6 (dd, 1H, J= 10.6 Hz, J= 4.0 Hz, H^{α}-Leu); 4.44 (dd, 1H, J= 7.5 Hz, J= 4.4 Hz); 4.22 (dd, 1H, J= 9.0 Hz, J= 4.8 Hz); 4.12 (t, 1H, J= 7.6 Hz, H^{α}-Tyr); 3.96 (d, 1H, J=9.4 Hz, H^{α}-Val); 3.69 (m, 1H, $1H^{\delta}$-Pro); 3.55 (m, 1H, $1H^{\delta}$-Pro); 3.30 (m, 4H, $2H^{\beta}$-Trp, $2H^{\delta}$-Arg); 2.20 (m, 6H, $1H^{\gamma}$-Leu, $2H^{\beta}$-Leu, 3H-Arg); 1.71 (m, 5H, 4H-Pro, 1H-Arg); 1.58 (m, 1H, $1H^{\beta}$-Val); 0.99 (m, 6H, $2CH_3$-Val); 0.91 (d, 3H, J=6.6 Hz, $1CH_3$-Leu); 0.85 (d, 3H, J=6.6 Hz, $1CH_3$-Leu).

&Trp-Val-Tyr-Leu-D-Pro& *(cyclo-22)*

The cyclization of the linear peptide **22** was performed in accordance to the protocol G. Reaction time 48 h. The purification was performed by automated flash chromatography with RediSepC18 (0:25 to 20:50 H_2O/ACN + 0.1% TFA, linear gradient over 30 min) yielding the product as a white solid (30 mg, 30%). Purity > 95%.

HPLC: t_R (min, G4070 ACN in 8 min) = 4,71 min

MS-HPLC calcd for: $C_{36}H_{46}N_6O_6$, expected: 658.35, found: 659.25 $[M+H]^+$

^{1}H-NMR (CD_3OD, 400MHz): δ 7.62 (d, 1H, J=7.7 Hz, H-Trp), 7.33 (d, 1H, J=7.9 Hz, H-Trp), 7.10 (m, 4H, 2H-Trp, 2H-Tyr), 6.70 (d, 2H, J=8.5 Hz, 2H-Tyr), 4.66-4.57 (m, 2H, H^{α}-Trp, H^{α}-Leu), 4.41 (m, 1H, H^{α}-Pro), 4.14 (t, 1H, J=8.4 Hz, H^{α}-Tyr), 3.90 (d, 1H, J=9.5 Hz, H^{α}-Val), 3.64 (m, 1H, $1H^{\delta}$-Pro), 3.52 (m, 1H, $1H^{\delta}$-Pro), 3.42-3.36 (dd, 1H, J= 14.7 Hz, J=4.3 Hz, $1H^{\beta}$-Trp), 3.19 (dd, 2H, J= 8.4 Hz, J= 2.6 Hz, H^{β}-Tyr), 3.07 (dd, 1H, J= 14.7 Hz, J=4.8 Hz, $1H^{\beta}$-Trp), 2.15 (m, 2H, $1H^{\beta}$-Val, 1H-Pro), 1.92 (m, 3H, 3H-Pro), 1.71-1.50 (m, 4H, H^{γ}-Leu, $2H^{\beta}$-Leu, $1H^{\delta}$-Trp), 1.00 (m, 6H, $2CH_3$-Leu), 0.81 (t, 6H, J=6.4 Hz, $2CH_3$-Val).

& Ser-Val-Tyr-Leu-D-Pro& (*cyclo*-23)

The cyclization of the linear peptide **23** was performed in accordance to the protocol G. Reaction time 48 h. The purification by HPLC-semi-preparative (SunFirePrepC18, 20:50 H_2O/ACN + 0.1% TFA, linear gradient over 25 min) yielded the product as a white solid (22 mg, 20%). Purity > 99%.

HPLC: t_R (min, G0100 ACN in 8 min) = 5,38

MS-HPLC calcd for: $C_{28}H_{41}N_5O_7$, expected: 559.30, found: 560.14 $[M+H]^+$

^{1}H-NMR (CD_3OD, 400MHz): δ 7.07 (d, 2H, J=8.5 Hz, H-Tyr); 6.70 (d, 2H, J=8.5 Hz, H-Tyr); 4.67 (dd, 1H, J= 10.5 Hz, J= 4.0 Hz, H^{α}-Leu); 4.46 (dd, 1H, J= 7.4 Hz, 4.8 Hz, $1H^{\alpha}$-Pro); 4.29 (t, 1H, J=4.2 Hz, H^{α}-Ser); 4.07 (t, 1H, J= 7.6 Hz, H^{α}-Tyr); 4.03 (d, 1H, J=9.4 Hz, H^{α}-Val); 3.87 (m, 2H, H^{β}-Ser), 7.73 (m, 1H, $1H^{\delta}$-Pro); 3.58 (m, 1H, $1H^{\delta}$-Pro); 3.18 (m, 2H, $2H^{\beta}$-Tyr), 2.16-1.99 (m, 5H, 2H-Pro, $1H^{\beta}$-Val), 1,72 (m, 1H, $1H^{\gamma}$-Leu), 1.62 (m, 2H, $2H^{\beta}$-Leu), 1.01 (m, 6H, $2CH_3$-Leu), 0.93 (d, 3H, J=6.7 Hz, $1CH_3$-Val), 0.86 (d, 3H, J=6.7 Hz, $1CH_3$-Val).

&Dap-Val-Tyr-Leu-D-Pro& (*cyclo*-24)

The cyclization of the linear peptide **24** was performed in accordance to the protocol G. Reaction time 24 h. The purification by HPLC-semi-preparative (SunFirePrepC18, 20:80 H_2O/ACN + 0.1% TFA, linear gradient over 25 min) yielded the product as a white solid (10 mg, 15%). Purity > 99%.

HPLC: t_R (min, G0100 ACN in 8 min) = 4.70

MS-HPLC calcd for: $C_{28}H_{42}N_6O_6$, expected: 558.32, found: 559.37 $[M+H]^+$

^{1}H-NMR (CD_3OD, 400MHz): δ 7.07 (d, 2H, J= 8.5 Hz, H-Tyr); 6.71 (d, 2H, J=8.5 Hz, H-Tyr); 4.71 (dd, 1H, J= 8.3 Hz, J= 5.2 Hz, H^{α}-Dap); 4.45 (m, 2H, $1H^{\alpha}$-Pro, $1H^{\alpha}$-Leu); 4.30 (t, 1H, J=8.1 Hz, H^{α}-Tyr); 3.76 (d, 1H, J=9.8 Hz, H^{α}-Val), 3.65 (m, 1H, $1H^{\delta}$-Pro), 3.55 (m, 1H, $1H^{\delta}$-Pro); 3.41 (dd, 1H, J=13.1 Hz, J= 5.2 Hz, $1H^{\beta}$-Dap); 3.19 (dd, 1H, J=13.1 Hz, J= 8.3 Hz, $1H^{\beta}$-Dap); 3.40 (d, 2H, J=8.1 Hz, H^{β}-Tyr), 2.35 (m, 1H, H^{β}-Val), 2.11-1.96 (m, 4H,

H-Pro), 1,60 (m, 3H, 1H$^{\gamma}$-Leu, 2H$^{\beta}$-Leu), 0.98 (m, 9H, 1CH_3-Val, 2CH_3-Leu), 0.87 (d, 3H, J=6.6 Hz, 1CH_3-Val).

&Ala-Val-Tyr-Leu-D-Pro& (*cyclo*-25)

The cyclization of the linear peptide **25** was performed in accordance to the protocol G. Reaction time 48 h. The purification was performed by automated flash chromatography with RediSepC18 (0:25 to 20:50 H_2O/ACN + 0.1% TFA, linear gradient over 30 min) yielding the product as white solid (40 mg, 46%). Purity > 99%.

HPLC: t_R (min, G30100 ACN in 8 min) = 3.58

MS-HPLC calcd for: $C_{28}H_{41}N_5O_6$, expected: 543.31, found: 544.30 $[M+H]^+$

^{1}H-NMR ($CDCl_3$, 300 MHz): δ 7.90 (d, 1H, J= 9.1 Hz, NH); 7.38 (d, 1H, J= 8.4 Hz, NH); 7.16 (d, 1H, J= 7.0Hz, NH); 7.09 (d, 1H, d, J=7.4 Hz, NH-Ala); 7.02 (d, 2H, J=8.5 Hz, H-Tyr); 6.72 (d, 2H, J=8.5 Hz, H-Tyr); 4.77 (q, 1H, J= 7.2 Hz, H$^{\alpha}$-Ala); 4.42 (m, 1H, H$^{\alpha}$-Pro); 4.33 (t, 1H, J= 7.4 Hz, H$^{\alpha}$-Leu); 4.07 (m, 1H, H$^{\alpha}$-Tyr); 3.82 (m, 1H, 1H$^{\delta}$-Pro); 3,72 (t, 1H, J= 9.1 Hz, H$^{\alpha}$-Val); 3.50 (m, 1H, 1H$^{\delta}$-Pro); 3.29 (m, 2H, H$^{\beta}$-Tyr); 2.20 (m, 3H, 3H-Pro); 1,95 (m, 2H, 1H$^{\gamma}$-Leu, 1H-Pro); 1.59 (m 3H, 1H$^{\beta}$-Val, 2H$^{\beta}$-Leu); 1.40 (d, 3H, J=7.2 Hz, CH_3-Ala); 0.96 (m, 6H, 2CH_3-Val); 0.84 (d, 3H, J=6.6 Hz, 1CH_3-Leu); 0.76 (d, 3H, J=6.6 Hz, 1CH_3-Leu).

&Lys(NHAc)-Val-Tyr-Leu-D-Pro& (*cyclo*-28)

The cyclization of the linear peptide **28** was performed in accordance to the protocol G. Reaction time 48 h. The crude cyclopeptide was dissolved in TFA-TIS-H_2O/95:2.5:2.5 (10 ml), at r.t. and stirred for 30 min. Excess TFA was removed under a stream of nitrogen. The residue was dissolved in ACN/H_2O and lyophilized
The purification by HPLC-semi-preparative (SunFirePrepC18, 20:50 H_2O/ACN + 0.1% TFA, linear gradient over 25 min) yielded the product as a white solid (15 mg, 26%). Purity > 98%.

HPLC: t_R (min, G2050 MeCN in 8 min) = 6,53

MS-HPLC calcd for: $C_{33}H_{50}N_6O_7$, expected: 642.37, found: 643.27 $[M+H]^+$

^{1}H-NMR (CD_3OD, 400MHz): 7.06 (d, 2H, J=8.5 Hz, 2H-Tyr), 6.69 (d, 2H, J=8.5 Hz, 2H-Tyr), 4.71 (m, 1H, H$^{\alpha}$-Leu), 4.42 (m, 1H, H$^{\alpha}$-Pro), 4.13 (m, 2H, H$^{\alpha}$-Lys), 3.96 (m, 2H, H$^{\alpha}$-Tyr, H$^{\alpha}$-Val), 3.72 (m, 1H, 1H$^{\delta}$-Pro); 3.57 (m, 1H, 1H$^{\delta}$-Pro); 3.20-3.13 (m, 4H, 2H$^{\beta}$-Tyr, 2H$^{\varepsilon}$-Lys), 2.24-1.98 (m, 6H, 1H$^{\beta}$-Val, 4H-Pro, 1H-Lys), 1.90 (s, 3H, NH-Ac), 1.71- 1.46 (m, 8H, 1H$^{\gamma}$-Leu, 2H$^{\beta}$-Leu, 5H-Lys), 0.99 (m, 2CH_3-Leu); 0.91 (d, 3H, J=6.7 Hz, 1CH_3-Val); 0.85 (d, 3H, J= 6.4 Hz, 1CH_3-Val).

5.3. Synthesis peptidomimetic

1,3,4,6-Tetra-O-acetyl-2-deoxy-2-tetrachlorophthalimido-α-D-glucopyranoside (34).

This compound was synthesized following previous reported procedure. The characterization data match with the literature.[2]

3,4,6-tri-O-acetyl-2-deoxy-2-tetrachlorophthalimido-α-D-glucopyranosyl cyanide. (36)

To a solution of **34** (300 mg, 0.488 mmol) in DCM (3 ml) was added HBr (33 wt. % in AcOH, 1.8 ml, 8.5 mmol). After stirring in darkness for 12 h, the reaction mixture was diluted with CH_2C1_2 and poured onto ice cold H_2O. The layers were separated and the organic portion was washed with H_2O and with a saturated solution of $NaHCO_3$, dried and concentrated to a syrup **35** which was used without any further purification for the subsequent reaction. To a solution of **35** in dry nitromethane (3 ml) was added mercuric cyanide (135.6 mg, 0.537 mol) at 0°C and the reaction was allowed to proceed under stirring at r.t. for 2 h, according to the method reported in literature.[3] The mixture was filtrated on a pad of celite and the filtrate was concentrated in *vacuo*. The residue was diluted in CH_2Cl_2 and washed with an aqueous solution of KBr 1M (2x50 ml). The organic layers was combined, washed with brine, dried over Na_2SO_4, filtered and concentrated *in vacuo.*

Purification by silica gel column chromatography (PE/EtOAc, 7/3) furnished the compound **36** as a white solid (255 mg, 90% over 2 steps). Purity =98%. R_f= 0.3 (*n*-hexane/EtOAc, 7:3)

^{1}HNMR (CD_3OD, 300MHz): δ 5.64 (dd, 1H, $J_{3,4}$=9.2 Hz; $J_{2,3}$=10.1 Hz, H_3); 5.36 (d, 1H, J=10.7 Hz, H_1); 5.24 (dd, 1H, $J_{3,4}$=9.2 Hz; $J_{4,5}$=10.1 Hz, H_4); 4.64 (dd, 1H, $J_{1,2}$=10.7 Hz; $J_{2,3}$=10.1, H_2); 4.28 (dd, 1H, $J_{5,6}$=4.6 Hz, $J_{6,6'}$=12.5 Hz, 1H_6); 4.19 (dd, 1H, $J_{5,6'}$=2.2 Hz, $J_{6,6'}$=12.5 Hz, 1H_6); 3.84 (m, 1H, H_5); 2.13 (s, 3H, OAc); 2.04 (s, 3H, OAc); 1,90(s, 3H, OAc).

^{13}C NMR (CD_3OD, 75 MHz): 170.50 (3C, s); 170.46 (2C, s); 141.17 (2C, s); 130.45 (2C, s); 126.78 (2C, s); 114.08 (1C, s); 76.78 (1C, d); 70.47 (1C, d); 67.56 (1C, d); 61.50 (1C, t); 53.11 (1C, d); 20.72 (3C, q).

2,6,-anhydro-3,4,7-tri-O-acetyl-2-tetrachlorophthalimido-2-deoxy-D-glycero-D-gulo-Heptonic acid (38)

The solution of **36** (250 mg, 0,43 mmol) in HCl/dioxane [4M] (4.5 ml) was heated to 60°C and stirred overnight. The solvent were removed *in vacuo*, then the residue was treated with acetic anhydride (0.5 ml, 6.88 mmol) in pyridine (1.4 ml, 13.76 mol) for 12 h at room temperature. The mixture was concentrate *in vacuo*, the residue was dissolved in CH_2Cl_2 and washed with HCl (1N), aqueous saturated $NaHCO_3$ (20 ml) and brine (20 ml), dried over sodium sulfate (Na_2SO_4), and concentrated *in vacuo.* The purification by silica flash chromatography (PE/AcOEt, 75:35) yielded the title compound **38** as a white solid (180 mg, 70%). R_f= 0.28 (PE/EtOAc, 7:3).

MS-HPLC calcd for: $C_{21}H_{17}Cl_4NO_{11}$, expected: 598.96, found: 597.67 = $[M-H]^-$

^{1}HNMR (CD_3OD, 300MHz): δ 5.83 (t, 1H, J= 9.1 Hz, H_3); 5.13 (t, 1H, J= 9.1 Hz, H_4); 4.93 (d, 1H, J= 9.0 Hz, H_1); 4.51 (t, 1H, J= 9.1 Hz, H_2); 4.32 (dd, 1H, J=12.5 Hz, J=4.8 Hz, $1H_6$); 4.20 (dd, 1H, J=12.5 Hz, J=4.8 Hz, $1H_6$); 4.01 (m, 1H, H_5); 2,93 (s, 3H, OAc); 2.04 (s, 3H, OAc); 1.87(s, 3H OAc).

^{13}C NMR (CD_3OD, 75 mHz): 171.48 (1C, s); 170.80 (1C, s); 170.04 (C, s); 163.33 (1C, s), 139.16 (1C, s); 129.39 (2C, s); 127.84 (2C, s); 75.60 (1C, d); 71.70 (1C, d); 68.91 (1C, d); 62.43 (1C, t); 53.13 (1C, d); 29.40 (1C, d); 20.72 (1C, q); 19.43 (1C, q); 19.29 (1C, q); 19.17 (1C, q).

Compound (39)

To a stirred solution of **38** (150 mg, 0.25 mmol) in dry CH_2Cl_2/DMF (2:1 v/v, 3 ml) was added sequentially HBTU (113.7 mg, 0.3 mmol) and DIPEA (130.6 μl, 0.75 mmol). After 15 min, serine(*t*Bu)-t*ert*-butyl ester (65.15 mg, 0.3 mmol); in dry CH_2Cl_2/DMF (2:1 v/v, 2 ml). The reaction mixture was allowed to proceed at room temperature under stirring for 2.5 h. Then it was diluted with CH_2Cl_2 (20 ml), washed with HCl 1N (20 ml), water (10 ml), saturated aqueous $NaHCO_3$ solution (20 ml) and brine (20 ml). The combined organic layers were dried over Na_2SO_4 and concentrated *in vacuo*. Purification by silica gel column chromatography (*n*-hexanes/EtOAc, 8:2 to 7:3) yielded the compound **39** (192 mg, 96%). Purity = 98%. R*f*= 0.3 (*n*-hexanes/AcOEt, 7:3)**.**

^{1}HNMR ($CDCl_3$, 300MHz,): δ 7.30 (d, 1H, J= 7.9 Hz, NH); 5.85 (t, 1H, J= 9.0 Hz, H_3); 5.18 (t, 1H, J= 9.0 Hz, H_4); 4.90 (d, 1H, J= 10.7 Hz, H_1,); 4.44 (t, 1H, J= 10.4 Hz, H_2); 4.32 (m, 1H, H^{α}-Ser); 4.29 (dd, 1H, J=8.8 Hz, J=3.0 Hz, $1H_6$); 4.12 (dd, 1H, J=8.8 Hz, J=3.0 Hz, $1H_6$); 3.92 (m, 1H, H_5); 3.68 (dd, 1H, J= 8.8 Hz, J= 3 Hz, $1H^{\beta}$-Ser); 3.46 (dd, 1H, J= 8.8 Hz, J= 3Hz, $1H^{\beta}$-Ser); 2.11 (s, 3H, OAc), 2.04 (s, 3H, OAc); 1.91 (s, 3H, OAc); 1.46 (s, 3H, O*t*Bu); 1.10 (s, 3H, O*t*Bu).

Compound (40)

Compound **49** (192 mg, 0,240 mmol), was dissolved in a solution of NH_3 in MeOH [2M] (4ml), the mixture was allowed to react under stirring at room temperature for 18 h, then the solution was concentrated *in vacuo*. The residue was triturated first with toluene, then with cold ethyl ether affording **40** as a white solid. (93 mg, 96%). Purity 98%. R_f = 0.44 (ACN/MeOH/H_2O, 7:2:1).

^{1}HNMR (CD_3OD, 300 MHz): δ 4.45 (t, 1H, J= 3.9 Hz, H^{α}-Ser,); 4.14 (d, 1H, J= 10.1 Hz, H_1); 4.02 (t, 1H, J= 9.7 Hz, H_2); 3.85 (dd, 1H, J= 11.9 Hz; J= 2.1Hz, $1H_6$); 3.76 (m, 3H, H_3, $1H_6$, $1H^{\beta}$-Ser); 3.58 (m, 1H, $1H^{\beta}$-Ser); 3.45 (t, 1H, J= 9.4 Hz, H_4,); 3.89 (m, 1H, H_5); 1.87 (3H, s, O*t*Bu); 1.18 (s, 3H, O*t*Bu).

^{13}CNMR (CD_3OD, 75 MHz): δ 169.53 (1C, s); 169.17 (1C, s); 81.81 (1C, s); 80.57 (1C, d); 76.80 (1C, d); 76.03 (1C, d); 73.28 (1C, s); 69.42 (1C, d); 61.72 (1C, t); 61.34 (1C, t); 55.01 (1C, d); 53.5 (1C, d); 27.01 (3C, q); 26.33 (3C, q).

Boc-Val-Tyr(OBzl)-Leu-SAA-Ser-(OtBu) (42)

Boc-Val-Tyr(OBzl)-Leu-OH **41** (134 mg, 0.23 mmol) and HBTU (87.3 mg, 0.23 mmol) were dissolved in dry DCM/DMF (2:1 v/v, 3 ml), and the reaction mixture was stirred for 3 h at r.t. under nitrogen atmosphere. DIPEA (100μl, 0.57 mmol) was added, followed by a solution of **40** (85 mg, 0.21 mmol) in DCM/DMF (2:1 v/v, 3 ml). The reaction mixture was stirred for further 12 h, and then the mixture was diluted with CH_2Cl_2, and washed with 1 N aqueous HCl solution (2 x 20ml), aqueous saturated solution of $NaHCO_3$ (2 x 20ml) and brine (1 x 20 ml). The combined organic layer was dried over Na_2SO_4 and concentrated *in vacuo*. Purification of the residue by silica gel chromatography (DCM/MeOH = 95/5) gave the product **42** as a yellow solid (111 mg, 60%). Purity =95%. R_f = 0.44 (DCM/MeOH, 9:1).

MS-HPLC calcd for: $C_{50}H_{77}N_5O_{14}$, expected: 971.55, found: 972.14 = $[M+H]^+$, 994.31 = $[M+Na]^+$

^{1}H NMR ($CDCl_3$, 300 MHz): δ 7.60 (bs, 1H, NH); 7.35 (m, 5H); 7.01 (d, 2H, J= 8.5 Hz); 6.88 (d, 2H, J= 8.5 Hz); 4.98 (d, 2H); 4.49 (bm, 2H); 4.32 (bm, 1H); 3.87 (m, 8H); 3.51 (m, 1H); 3.40 (m, 1H); 3.00 (bm, 2H); 3.64 (bm, 1H, OH); 2.08 (bm, 1H); 1.51 (m, 18H); 1.6 (s, 3H); 1.12 (d, 9H, J= 6.9 Hz); 0.86 (m, 12H).

^{13}C NMR ($CDCl_3$, 75 MHz): 173.49 (1C, s); 173.07 (1C, s); 172.32 (1C, s); 169.75 (1C, s); 168.81 (1C, s); 158.12(1C, s); 156.70 (1C, s); 137.16 (1C, s); 137.0 (1C, s); 130.39 (1C, d); 128.69 (1C, d); 128,29 (2C, d); 128.22 (1C, s); 127.62 (2C, d); 115.38 (1C, d); 115.10 (1C, d); 82.36 (1C, s); 82.27 (1C, s); 75.99 (1C, d); 73.56 (1C, t); 70.05 (1C, t); 62.29 (1C, t); 61.71 (1C, t); 61.14 (1C, d); 55.24 (1C, d); 54.75 (1C, d); 54.47 (1C, d); 53.30 (1C, d); 53.17 (1C, d); 30.13 (1C, d); 29.83 (1C, t); 28.36 (9C, q); 27.17 (9C, q); 27.45 (9C, q); 24.63 (1C, d); 23.32 (1C, q); 21.34 (1C, q); 19.45 (1C, q); 17.78 (1C, q).

Cyclo-(Val-Tyr(OBzl)-Leu-SAA-Ser) (44)

The compound **42** (54 mg, 55 μmol) was dissolved in 40% TFA/CH_2Cl_2 (800 μl), and the solution was stirred for 15 min. The volatiles were removed *in vacuo*, and the residual TFA was removed by azeotropic distillation with toluene *in vacuo* yielding the product **43** which was not purified but used directly in the next reaction.
To a solution of HATU (67.8 mg, 0.22 mmol), HOBt (29.7 mg, 0.22 mmol), and DIPEA (76.6 μl, 0.44 mmol) in dry DMF was added dropwise, in an ice bath, a solution of **43** in dry DMF (final concentration $8\cdot10^{-4}$ M). The reaction mixture was stirred for 56 h at r.t., then was concentrate *in vacuo.* Purification of the residue by silica gel chromatography (ACN/MeOH= 93:7) gave the title compound **44** as a white solid (18 mg, 46%). Purity =90%. R_f= 0.18 (ACN/MeOH, 90:10).

MS-HPLC calcd for: $C_{37}H_{51}N_5O_{11}$, expected: 741.36, found: 764.04 = $[M+Na]^+$, 739.86 = $[M-H]^-$

^{1}H NMR (CD_3OD, 300 MHz): δ 7.36 (m, 5H); 7.07 (d, 2H, J=8.5 Hz); 6.88 (d, 2H, J=8.5 Hz); 5.06 (s, 2H); 4.70 (m, 1H); 4.50 (bm, 3H); 4.26 (d, 1H, J=4.5 Hz); 4.03 (m, 2H); 3.86 (m, 4H); 3.45 (m, 2H); 3.00 (bm, 2H); 1.70 (m, 3H); 0.89 (m, 6H); 0.77 (m, 6H).

Cyclo-(Val-Tyr-Leu-SAA-Ser) (45)

Cyclo-(Val-Tyr(OBzl)-Leu-SAA-Ser) **44** (10 mg, 0.013 mmol) was dissolved in dry MeOH (2 ml) and 10% $Pd(OH)_2/C$ (2 mg) was added to it. The suspension was stirred for 12 h under H_2 atmosphere (balloon). The reaction mixture was filtrated through a pad of celite, and the filtrate was concentrated *in vacuo* giving **45** (8.8 mg, 100%) as a white solid. Purity 90%. R_f= 0.10 (ACN/MeOH, 90:10).

MS-HPLC calcd for: $C_{30}H_{45}N_5O_{11}$, expected: 651.31, found: 674.09 = $[M+Na]^+$, 649.86 = $[M-H]^-$

^{1}H NMR (300 MHz, CD_3OD): δ 6.88 (d, 2H, J=8.4 Hz); 6.72 (d, 2H, J=8.4 Hz); 4.50 (s, 4H); 4.28 (m, 1H); 4.03 (bm, 2H); 4.85 (m, 6H,); 3.30 (m, 2H); 3.06 (bm, 2H); 2.01 (m, 1H) 1.65 (m, 3H); 0.93 (m, 12H).

5.4. Synthesis glycosidic carrier

β-D-glucose pentabenzoate (37)

This compound was synthesized following previous reported procedure. The characterization data match with the literature.[4]

Benzyl 6-O-acetyl-2,3,4-tri-O-benzyl-β-D-glucopyranoside (38)

This compound was synthesized following previous reported procedure.[4] The crude was recrystallized from MeOH affording **38** as a white solid (856 mg, 78%). Purity= 98% R_f= 0.41 (toluene/AcOEt, 8:2). $[\alpha]_D^{20}$ (c 1, $CHCl_3$) = -2.9°

^{1}H-NMR ($CDCl_3$, 300MHz,) δ: 7.32 (m, 20H); 4.96-4.49 (m, 9H); 4.35 (dd, 1H, J= 4.5 Hz, J= 1.8 Hz); 4.27 (dd, 1H, J= 4.5 Hz, J=1.8 Hz); 3.67 (d, 1H, J= 9 Hz); 3.54 (m, 3H); 2.08 (s, 3H).

^{13}C NMR spectrum is in agreement with those published.[4]

Benzyl 2,3,4-tri-O-benzyl-β-D-glucopyranoside (39)

To a solution of **38** (4.2g, 7.21 mmol) in CH_2Cl_2/MeOH (2:1 v/v, 50ml) was added dropwise sodium methoxide (freshly prepared 1.0 M solution in MeOH, 2.16 ml) at r.t and left to stir for 3 h. The solution was acidified to pH 7 by the addition of Dowex 50 (H^+), then the mixture was filtrated and the solvent removed *in vacuo*.
Purification by silica gel chromatography (*n*-hexane/AcOEt= 8/2) affording **39** as a white solid (2.6g, 67%). Purity= 98%. R_f= 0.17 (*n*-hexane/AcOEt, 8:2). $[\alpha]_D^{20}$ (c 1, $CHCl_3$) = -9.2°

^{1}H-NMR ($CDCl_3$, 300MHz,) δ: 7.32 (m, 20H); 4.96-4.49 (m, 9H); 3.86 (m, 1H); 3.71-3.49 (m, 4H); 3.38 (m, 1H); 1.86 (m, 1H).

Benzyl 2,3,4-tri-O-benzyl-6-O-(t-butylcarboxymethyl)-β-D-glucopyranoside (40)

To a solution of **39** (1.30 g, 2.4 mmol) in toluene (13 ml) were added NaOH (40% aqueous solution, 13 ml) and Bu_4NHSO_4 (981 mg, 2.89 mmol) and left to stir for 10 min, then *tert*-Butyl bromoacetate (1.07 ml, 7.22 mmol) was added and the reaction mixture was stirred at r.t. for 5 h. The mixture was diluted with H_2O and the product extracted with CH_2Cl_2. The organic layers were combined, washed with brine, dried over Na_2SO_4, filtered and evaporated to give a yellow oil. Crystallization from MeOH gave **40** as a white solid (1.44 g, 91%). Purity= 99%. R_f= 0.46 (*n*-hexane/AcOEt, 8:2).

^{1}H-NMR ($CDCl_3$, 300MHz,) δ: 7.29 (m, 20H); 4.96-4.48 (m, 8H); 4.5 (d, 1H, J= 11.7 Hz) 4.04 (s, 2H); 3.84 (m, 2H); 3.63 (m, 2H); 3.51 (m, 2H); 1.47 (s, 9H).

^{13}CNMR ($CDCl_3$, 75 MHz,) δ: 169.87 (1C, s); 139.01 (1C, s); 138.78 (1C, s); 138.64 (2C, s); 137.83 (1C, s); 128.74-128.18 (20C, d); 130.0 (1C, d); 85. 06 (1C, d); 82.59 (1C, d); 81.76 (1C, t); 77.99 (1C, d); 77.09 (1C, t); 75.41 (1C, d); 71.53 (1C, t); 70.59 (1C, t); 69.93 (1C, d); 28.50 (3C, q).

Benzyl 2,3,4-tri-O-benzyl-6-O-(carboxymethyl)-β-D-glucopyranoside (41)

The title compound **40** (800 mg, 1.22 mmol) was dissolved in 40% TFA/CH_2Cl_2 (5 ml), and the solution was stirred for 2 h at r.t. The volatiles were removed *in vacuo*, and the residual TFA was removed by azeotropic distillation with toluene *in vacuo* to give the product as a white solid (730 mg, 100%). Purity 95%. R_f = 0.54 (DCM/MeOH, 9:1).

HPLC: t_R (min, G0100 ACN in 8 min) = 9.39

MS-HPLC calcd for: $C_{36}H_{38}O_8$, expected: 598.26, found: 621.26 $[M+Na]^+$

^{1}H-NMR ($CDCl_3$, 300MHz,) δ: 7.39 (m, 20H); 5.03-4.16 (m, 9H); 4.16 (s, 2H); 3.88-3.60 (m, 6H).

5.5. Synthesis of cyclic peptides functionalized with the glycosidic carrier

5.5.1. Condensation in solution

***&Lys(carrier)-Val-Tyr-Leu-D-Pro&* (56a)**

Method A: carboxylic acid pre-activation as succinimidyl ester.
To a solution of **51** (100 mg, 0.167 mmol) and NHS (76.0 mg, 0.668 mmol) in a 2:1 mixture of CH_2Cl_2/DMF (3 ml), EDC (35 mg, 0.184 mmol) was added and the mixture was stirred for 12 h at r.t. The reaction mixture was diluted with CH_2Cl_2 and washed with H_2O. The organic layers were combined, dried over Na_2SO_4, filtered and evaporated to give a colorless syrup **52** which has greater than 95% purity and was used directly for the next coupling reaction. R_f= 0.16 (cyclohexane/Acetone, 1:1)

To a solution of **52** (35 mg, 0.5 mmol), ***cyclo*-1c** (25 mg, 0.042 mmol) in CH_2Cl_2 (5 ml) was added DIPEA (36.5 μl, 0.21 mmol). The reaction was left to stir at r.t. for 20 h, then the mixture was washed with a 5% solution of citric acid, saturated aqueous solution of

$NaHCO_3$ and brine. The organic phase was dried over Na_2SO_4, filtered and the solvent was removed *in vacuo*.
Purification by silica gel flash chromatography (toluene/*i*PrOH= 9:1) yielded **55a** as a white solid (29 mg, 60%). Purity =98%. R_f= 0.4 (toluene/*i*PrOH, 9:1).
MS-HPLC calcd for: $C_{67}H_{84}N_6O_{13}$, expected: 1180.61, found: 1203.73 = $[M+Na]^+$

To a solution of a **55a** (29 mg, 0.025 mmol) in dry MeOH (2 ml) was added $Pd(OH)_2/C$ (3 mg, 10% on activated charcoal) and the mixture was hydrogenated overnight under atmospheric pressure using an H_2-filled balloon. The catalyst was removed by filtration through a pad of celite and the solvent was evaporated under reduced pressure. The product **56a** was recovered as a white solid (18 mg, 90%). Purity 98%.

Method b: HATU mediated condensation

To a solution of **51** (15 mg, 0.025 mmol), in DMF (1ml) is added HATU (11.40 mg, 0.030 mmol), DIEA (10.45 µl, 0.06 mmol) and ***cyclo*-1c** (18 mg, 0.030 mmol). The reaction was allowed to stir at r.t. for 16 h. The mixture was diluted with CH_2Cl_2, washed with HCl 1N, a saturated aqueous solution of $NaHCO_3$ and brine. The organic phase was dried over Na_2SO_4, filtered and the solvent was removed in *vacuo*. The product was directly underwent to hydrogenolysis according to the procedure describe before.
Purification by HPLC-semi-preparative (SunFirePrepC18, 0:80 H_2O/ACN + 0.1% TFA, linear gradient over 25 min) yielded the product **56a** as white solid (14 mg, 70%, over two steps). Purity = 99%.

5.5.2. Synthesis of peptides functionalized with a glycosidic carrier on solid phase

Peptide (13)

The linear peptide was synthesized manually by SPPS using the Fmoc/*t*Bu strategy and Cl-Trt resin following the experimental conditions reported in the section *6.5* of the chapter **6** *General methods and procedures.* The synthesis was performed at a 400 µmol scale. Peptide chain elongation was carried out using PyBOP, HOAt and DIEA as coupling reagents, according to the conditions reported in the section *6.6*. During couplings the mixture was left to react (45 min) with intermittent manual stirring and the good outcome of each coupling was verify by ninhydrin or chloranil test. The Fmoc groups were removed by treatment with 20% of piperidine in DMF and the Leucine Alloc protecting group was removed by treatment with $Pd(PPh_3)_4$ as described in the section *6.5.15*. After the synthesis, the peptide-resin **13** was splitted in 3 different polypropylene syringes.

Peptide (54a)

The peptide-resin **13** was subjected to a standard treatment with piperidine (20% in DMF, 1x1 min, 2x10 min). Then the coupling with the Boc-Lys-(Fmoc)-OH, carried out under the same conditions described before (PyBOP/HOAt/DIEA), gave the pentapeptide **52a**. Treatment with piperidine (20% in DMF) removed the Fmoc protecting group on the Lys side chain amino group providing the intermediate **53.** Subsequently, a mixture of **51** (45mg), PyBOP (39 mg) and HOAt (10.4 mg) was dissolved in DMF (400 µl) and pre-

activated by adding DIEA (26 μl). After 1 min the mixture was added to the peptide-resin **53**. The coupling was performed at r.t. with intermittent manual stirring, for 1.5 h. Treatment with the cocktail cleavage solution TFA/TIS/H_2O-94:3:3 (1h) provided the peptide complete deprotection and cleavage from the resin, yielding the product **47a**.
Crude products were analyzed by RP-HPLC and MS-HPLC.

HPLC: t_R (min, G0100 ACN in 8 min) = 7.06
MS-calcd for: $C_{67}H_{86}N_6O_{14}$, expected: 1198.62, found: 1199.71 $[M+H]^+$

Peptide (54b)
This compound was synthesized following the previous reported procedure for **54a.** The coupling was performed with Phe(4NH-Fmoc)-OH instead of with Boc-Lys-(Fmoc)-OH.

HPLC: t_R (min, G0100 MeCN in 8 min) = 7.06
MS-calcd for: $C_{70}H_{84}N_6O_{14}$, expected: 1232.60, found: 233.68 $[M+H]^+$; 1255.81 $[M+Na]^+$

Peptide (54c)

This compound was synthesized following the previous reported procedure for **54a**. The coupling was performed with Dap(4NH-Fmoc)-OH instead of with Boc-Lys-(Fmoc)-OH.

HPLC: t_R (min, G0100 MeCN in 8 min) = 7.06
MS-calcd for: $C_{64}H_{80}N_6O_{14}$, expected: 1156.57, found: 1157.69 $[M+H]^+$

Synthesis cyclic peptides 54 (a-c)

The *head-to-tail* peptide cyclizations of linear peptide **54 (a-c)** were performed with DPPA according to the protocol G described in the section *6.7.* The linear peptides were dissolved in DMF (5 mM solution) and to the solution were added $NaHCO_3$ (8 eq) and DPPA (1.5 eq). The reaction was left to proceed at r.t. under stirring and monitored by analytical HPLC. $NaHCO_3$ was removed by filtration e the solvent was evaporated under reduced pressure**.**

Complete deprotection of each cyclopeptide was performed by treatment with $Pd(OH)_2/C$ (10% w/w) under hydrogen atmosphere in MeOH according to the conditions described in the section *6.6.5.* The cyclopeptides were purified by semi-preparative-HPLC. Peaks of interest were analyzed by analytical HPLC, combined and lyophilized.

The final products were analyzed and fully characterized by RP-HPLC, HPLS-MS and ^{1}H-NMR. CD_3OD was used for the analysis of the compounds because of the hydrofilic character of the carrier induced by the hydroxyl groups. Nevertheless, the solvent peak overlapped with some molecule patterns preventing a complete assignation of the protons.

***Cyclo*-(Lys(*carrier*)-D-Pro-Leu-Tyr-Val) (56a)**

Cyclization reaction time 48 h. Purification by HPLC-semi-preparative (SunFirePrepC18, 0:80 H_2O/ACN + 0.1% TFA, linear gradient over 25 min) yielded the product as white solid. (10 mg, 25%). Purity: 98%.

HPLC: t_R (min, G080 ACN in 8 min) = 5.79

MS-HPLC calcd for: $C_{39}H_{60}N_6O_{13}$, expected: 820.42, found: 821.88 $[M+H]^+$; 843,89 $[M+Na]^+$

^{1}H-NMR (CD_3OD, 300 MHz): 7.06 (d, 2H, d, J=8.5 Hz), 6.69 (d, 2H, J=8.5 Hz), 5.12 (d, 0.5 H, J= 3.7 Hz, H_1); 4.70 (m, 1H); 4.51 (d, 0.5 H, J= 7.6 Hz, H_1); 4.45 (m, 1H), 4.15 (m, 1H); 4.02-3.92 (m, 4H), 3.78-3.66 (m, 3H), 3.57 (m, 1H); 3.40-3.15 (m, 8H); 2.21-1.87 (m, 6H); 1.74 (m, 2H); 1.60- 1.45 (m, 6H); 0.99 (m, 6H); 0.91 (d, 3H, J=6.7 Hz); 0.85 (d, 3H, J= 6.7 Hz).

Cyclo-(Phe(4-NH-*carrier*)-D-Pro-Leu-Tyr-Val) (56b)

Cyclization reaction time 48 h. Purification by HPLC-semi-preparative (SunFirePrepC18, 20:35 H_2O/ACN + 0.1% TFA, linear gradient over 25 min) yielded the product as white solid. (8 mg, 35%). Purity: 98%

HPLC: t_R (min, G2050 ACN in 8 min) = 6.13

MS-HPLC calcd for: $C_{42}H_{58}N_6O_{13}$, expected: 854.41, found: 858 $[M+H]^+$

^{1}H-NMR (CD_3OD, 300 MHz): 7.55 (m, 2d); 7,24 (d, 2H, J= 8.5 Hz); 7.07 (2H, d, J=8.5 Hz); 6.70 (d, 2H, J= 8.5 Hz); 5.18 (d, 0.3H, J= 3.5 Hz, H_1); 4.52 (d, 0.7 H, J= 7.6 Hz, H_1); 4.75 (m, 1H); 4.52 (m, 1H); 4.37 (m, 1H); 4.11 (m, 3H); 3.88 (m, 2H); 3.81 (m, 2H); 3.64 (m, 2H); 3.52 (m, 2H); 3.33 (m, 4H); 3.15 (m, 3H); 2.88 (dd, 1H, J= 10.7, J= 3.6 Hz); 2.14 (m, 2H); 1.2 (m, 3H); 1.57 (m, 3H); 0.98 (t, 6H, J= 7.1 Hz); 0.85 (t, 6H, J=7.1 Hz).

Cyclo-(Dap(NH-*carrier*)-D-Pro-Leu-Tyr-Val) (56c)

Cyclization reaction time 48 h. Purification by HPLC-semi-preparative (SunFirePrepC18, 20:35 H_2O/ACN + 0.1% TFA, linear gradient over 25 min) yielded the product as white solid. (8 mg, 25%). Purity: 98%

HPLC: t_R (min, G2050 ACN in 8 min) = 5.0

MS-HPLC calcd for: $C_{36}H_{54}N_6O_{13}$, expected: 778.37, found: 779.48 $[M+H]^+$

^{1}H-NMR (CD_3OD, 300 MHz): δ 7.05 (2H, d, J= 8.5 Hz), 6.70 (2H, d, J= 8.5 Hz), 5.18 (d, 0.3H, J= 3.5 Hz, H_1); 4.70 (m, 1H); 4.47 (m, 2H), 4.13 (m, 1H); 3.85 (m, 5H); 3.66 (m, 8H); 3.15 (d, 2H, J= 6.4 Hz); 2.06 (m, 5H); 1.71 (m, 1H); 1.62 (m, 2H); 1.00 (m, 9H); 0.86 (3H, d, J=6.7 Hz).

5.6. Synthesis of other products

Alloc-Leu (9).

This compound was synthesized in one step following previous reported procedure. The characterization data match with the literature.[5]

9-fluorenylmethanethiol (6).

This compound was synthesized in three steps following previous reported procedure. The characterization data match with the literature.[6]

References

(1) Dai, N.; Etzkorn, F. A. Cis−Trans Proline Isomerization Effects on Collagen Triple-Helix Stability Are Limited. *J. Am. Chem. Soc.* **2009**, *131*, 13728-13732.

(2) Debenham, J. S.; Debenham, S. D.; Fraser-Reid, B. N-tetrachlorophthaloyl (TCP) for ready protection/deprotection of amino sugar glycosides. *Bioorg. Med. Chem.* **1996**, *4*, 1909-1918.

(3) Myers, R. W.; Lee, Y. C. Synthesis and characterization of some anomeric pairs of per-O-acetylated aldohexopyranosyl cyanides (per-O-acetylated 2,6-anhydroheptononitriles). On the reaction of per-O-acetylaldohexopyranosyl bromides with mercuric cyanide in nitromethane. *Carbohydr. Res.* **1984**, *132*, 61-82.

(4) Lu, W.; Navidpour, L.; Taylor, S. D. An expedient synthesis of benzyl 2,3,4-tri-O-benzyl-beta-D-glucopyranoside and benzyl 2,3,4-tri-O-benzyl-beta-D-mannopyranoside. *Carbohydr. Res.* **2005**, *340*, 1213-1217.

(5) Cruz, L. J.; Beteta, N. G.; Ewenson, A.; Albericio, F. "One-Pot" Preparation of N-Carbamate Protected Amino Acids via the Azide. *Org. Process Res. Dev.* **2004**, *8*, 920-924.

(6) Crich, D.; Sana, K.; Guo, S. Amino acid and peptide synthesis and functionalization by the reaction of thioacids with 2,4-dinitrobenzenesulfonamides. *Org. Lett.* **2007**, *9*, 4423-4426.

Chapter 6

General methods and procedures

6.1. Solvents and reagents

Reagents for synthesis, if not otherwise specified, were purchased from Aldrich, Fluka and Acros. Amino acid derivatives, condensing reagents and additives were purchased from Albatros Chem Inc, Iris Biotech, and Luxemburg Industries. PPAA was purchase from Archimica. Linker AB and PyBOP was from Novabiochem. Aminomethyl-ChemMatrix was purchase from PCAS BioMatrix Inc whereas the 2-Chlorotrityl chloride resin was from CBL Patras. D-glucose and *N*-glucosamine were from A.C.E.F

Solvents, acid and base, were purchased from Aldrich and Fluka. Acetonitrile and methanol used for products purification and characterization were HPLC grade purity. Buffer solutions were prepared with deionized water over a milli-Q plus system. Dry solvents were prepared over molecular sieves (3 or 4 Å) and stored under nitrogen atmosphere.

6.2. General equipments

Balances	Mettler Toledo0020 (3 decimal)
	Precisa Balances (3 decimal)
pH-meter	GLP21, Crison
Centrifuge	Allegra 21R, Beckmann Coulter
Lyophilizer	Vitris; Freezemobil 12EL; Edwards RV12 pump
Rotavapors	Laborota, 4003, Heidolph
Agitator orbital	Unimax 1010, Heidolph
Eppendorf	5415 benchtop
Fluorescence plate	Reader Bio-Tek Instruments; Bio-Tek FL600
Magnetic stirrer	IKA; Werke
Micropipete Gilson	P2, P20, P200 and P1000
MilliQ system Millipore	MilliQ gradient A10;
Ovens	Mettler Toledo; PB303-S, AB204
Rotator stirrer	Labnet; labroller
UV	Shimadzu UV mini 1240 UV-Vis spectrophotometer

6.3. Chromatography

6.3.1. Thin layer chromatography (TLC)

Analytical thin layer chromatography (TLC) was performed on aluminum sheets (20 x 20 cm) covered with silica gel 60 (Merck® K 60 F_{254}) using a specific mixture of eluent for each compound. The revelation of the TLC was performed using different methods in relation to the nature of the compound to detect. Direct revelation under UV-lamp was used to detect compounds with aromatic and chromophore groups. Specific TLC stains were employed for the revelation of compounds with specifying functional groups.

6.3.1.1. TLC stains

Ninhydrin: detection of primary and secondary amines. Spray plates and heat gently, the development of blue spots correspond to primary amine, whereas, brown spots are related

to Boc protected amines or secondary amines. Preparation: 200 mg ninhydrin, 95 ml 2-propanol, 5 ml 10% AcOH.

Dragendorff Reagent: detection of primary and secondary amines. Spray plates, orange spots develop. Spots intensify if sprayed later with HCl, or 50% water-phosphoric acid. Preparation: solution A: 1.7 g basic bismuth nitrate in 100 ml water/acetic acid (4:1). Solution B: 40 g potassium iodide in 100 ml of water. Mix reagents together as follows: 5 ml A + 5 ml B + 20 ml acetic acid + 70 ml water.

Cerium Molybdate: detection of all functional groups (multifunctional group stain). Spray plates and heat vigorously, blue spots develop on light background. Preparation: solution A: ammonium molibdate (21g) in 450 ml water. Solution B: 40 g cerium sulfate (1g) in 31 ml of H_2SO_4 + and 20 ml water . Mix reagents together.

Sulfuric Acid: general detection method for most oxidable compounds such as carbohydrates. After dipping with the reagent the TLC plate is heated and many compounds are charred to give grey or black spots. Preparation: 5% sulfuric acid in methanol.

Permanganate ($KMnO_4$): detection method for functional groups which are sensitive to oxidation. Alkenes and alkynes will appear readily on a TLC plate following immersion into the stain and will appear as a bright yellow spot on a bright purple background. Alcohols, amines, sulfides, mercaptans and other oxidizable functional groups may also be visualized, however it will be necessary to gently heat the TLC plate following immersion into the stain. These spots will appear as either yellow or light brown on a light purple or pink background. Preparation: dissolve 1.5g of $KMnO_4$, 10g K_2CO_3, and 1.25mL 10% NaOH in 200mL water.

6.3.2. Column chromatography

Column chromatography was carried out on silica gel 60 (Fluka, 40-63 μm). Samples were loaded dissolved in the eluent mixture or loaded as a solid (by dissolving the sample in a strong solvent followed by adsorbing the sample onto silica by removing the solvent). Purifications were run using linear gradients. Fraction detected by TLC, spots of interest were combined and concentrated *in vacuo*.

6.3.3. Analytical HPLC

HPLC chromatograms were recorded on a Waters Alliance 2695 separation module equipped with a Waters 2998 photodiode array detector and Empower software (Waters) using a Sunfire C18 column (100 mm x 4.6 mm, 3.5 μm; Waters); flow 1ml/min, solvents H_2O (0.045% TFA) and ACN (0.036% TFA). The gradient (G) is expressed as % of ACN in H_2O.

6.3.4. Semi-preparative HPLC

The cyclopeptides were purified using reverse phase semi-preparative HPLC. Samples were dissolved in the appropriate solvent (low percentage ACN-aqueous solutions are preferred), filtered through a 0.45 μm nylon filter and injected onto the semi-preparative HPLC system provided with a loading loop of 10 ml. Purifications were run using 20 min linear gradients

of ACN in H_2O. Flow = 15 ml/min. Detection λ= 220 nm. Peaks of interest were analyzed by analytical HPLC, combined and lyophilized.

6.3.5. Isco Combi Flash Chromatography

The cyclopeptides were purified using automated flash chromatography. Samples were dissolved in the appropriate solvent (low percentage ACN-aqueous solutions are preferred), filtered through a 0.45 µm nylon filter and injected onto the Isco system. Purifications were run using 30 min linear gradients of ACN (0.1% TFA) in H_2O (0.1% TFA), C18 Reversed-phase RediSep Rf columns. Flow= 30 ml/min. Detection λ= 220 nm. Peaks of interest were analyzed by analytical HPLC, combined and lyophilized.

6.4. Methods for structural determination e product characterization

6.4.1. Mass Spectroscopy

6.4.1.1. HPLC-MS

HPLC-MS were recorded using a Waters Alliance 2695 equipped with a Waters 2998 photodiode array detector, ESI-MS micromass ZQ (Waters) and Masslynx software (Waters) using a Sunfire C18 column (100mm x 2.1 mm, 3.5 µm, Waters); flow rate = 0.3 ml/min, solvents H_2O (0.1% formic acid) and ACN (0.07% formic acid).

6.4.1.2. ESI-HRMS

ESI-HRMS (Electron Spray Ionization High Resolution Mass Spectroscopy) were performed, respectively, on a QSTAR Pulsar (AB/MDS Sciex) and DFS- Thermofischer and are reported as mass-per-charge ratio m/z calculated and observed.

6.4.1.3. MALDI-TOF

Mass spectra were obtained using a MALDI-TOF Applied Biosystem 4700 with a N_2 laser of 337 nm. Sample preparation: a mix of peptide solution (1 µl) and matrix (1 µl) was placed on a MALDI-TOF plate and dried by air.

Matrices:

20 mg/ml ACH in 50%/ 49.9% H_2O/ 0.1% TFA
20 mg/ml DHB in 50%/ 49.9% H_2O/ 0.1% TFA

6.4.2. Nuclear magnetic resonance

^{1}H and ^{13}C spectra were recorded either on a Bruker 400 MHz, or Jeol 300 MHz spectrometer and were processed by Mestrenova software. Chemical shift are reported in ppm downfield relative to TMS (δ = 0) internal reference in the solvents. Spin multiplicities are reported as singlet (s), doublet (d), triplet (t) and quartet (q) with coupling constants (*J*) given in Hz or multiplet (m). ^{1}H and ^{13}C resonances were assigned with the aid of additional 1D and 2D NMR spectra (H,H-COSY, DEPT 135 and HSQC).

6.4.3. Optical rotation

The optical rotation values [α] were determined using a Perkin-Elmer Model 241 polarimeter and were recorded at room temperature. Optical rotation was determined according to equation 1:

$$[\alpha]_D = \frac{\alpha}{l \cdot c} \qquad \textbf{(1)}$$

α Observed rotation in degrees.
l Cell path length in decimeters.
c Concentration in g ml^{-1}

6.5. Solid-Phase Peptide Synthesis (SPPS)

6.5.1. General considerations for SPPS

All peptides were synthesized by SPPS using mostly the 9-fluorenylmethoxycarbonyl/*tert*-butyl (Fmoc/*t*Bu) strategy.[1] Syntheses were performed at a 200-μmol scale. Solid-phase peptide elongation and other solid-phase manipulations were done manually in polypropylene syringes, each fitted with a polyethylene porous disk. Solvents and soluble reagents were removed by suction. Washings between synthetic steps were done with DMF (5 x 30 s) and DCM (5 x 30 s) using 5 ml of solvent/g resin each time. During couplings the mixture was allowed to react with intermittent manual stirring.

6.5.2. Colorimetric tests

6.5.2.1. Kaiser test[2]

The Kaiser test, also known as ninhydrin test, allows the detection of primary amines and is used during solid-phase peptide chain assembly to monitor deprotection and coupling steps. The peptide-resin is washed with DCM and vacuum dried. A few peptide-resin beads are transferred to a small glass tube. Six drops of reagent solution A and 2 drops of reagent solution B are added to the tube and the mixture is heated at 110 ºC for 3 min. The formation of a blue color on the beads or the supernatant is indicative of the presence of free amines and thus of an incomplete coupling, while a yellow coloration is characteristic of a negative test. The method is highly sensitive and a negative test assures a coupling rate higher than 99%.

<u>*Reagent solution A*</u>: 400 g of phenol are dissolved in 100 ml of absolute EtOH and the mixture is heated until complete dissolution of the phenol. 20 ml of 10 mM KCN (65 mg in 100 ml of H_2O) are added to 1000 mL of freshly distilled pyridine over ninhydrin. Both solutions are stirred for 45 min with 40 g of Amberlite MB-3 resin ion exchange resin, filtered, and combined.

<u>*Reagent solution B*</u>: 2.5 g of ninhydrin are dissolved in 50 ml of absolute EtOH; the resulting solution is kept in flask protect from light.

6.5.2.2. Chloranil test[3]

Chloranil test detects secondary amines during solid-phase chain assembly and is used to evaluate couplings onto proline or *N*-methylated residues.
The peptide-resin is washed with DCM and vacuum dried. A small portion of peptide resin beads is transferred to a small glass tub and 20 µl of a saturated chloranil solution (0.75 mg of 2,3,5,6-tetrachloro-1,4-benzoquinone in 25 ml of toluene) and 200 µl of acetone are added and mixed for 5 min at room temperature. The solution is shaken at room temperature for 5 min. A blue-greenish color is indicative of the presence of free secondary amines and is thus considered a positive test.

6.5.2.3. p-Nitrophenyl ester test[4]

p-Nitrophenyl ester test is used to detect secondary amines or hindered amines, with higher sensitivity than chloranil test.
After washing the peptide-resin beads with DCM and dry it with vacuum a few beads are transferred to a small glass tube; 0.3 ml of 2 mM *p*-nitrophenyl ester in ACN are added and the suspension is heated at 70ºC for 8 min. Resin beads are washed with MeOH (3 times), DMF (3 times), and DCM (3 times). The presence of free amines is indicated by red-colored beads whereas a negative test yield naturally colored beads.
Reagent synthesis: the *p*-nitrophenyl ester is readily accessible from commercial disperse red 1 by a high-yielding three-step procedure. (A) To a solution of 20 mmol of disperse red 1 (6.28 mg) and 0.34 mmol of $Rh_2(OAc)_4$ (150 mg) in a mixture of DCM (100 mL) and toluene (100 ml) is added at 40ºC a solution of 80 mmol of ethyl diazoacetate (8.4 ml) in toluene (40 ml) over 1h period. The reaction mixture is stirred overnight at room temperature and purified by chromatography. (B) 62.5 mmol of KOH (4.062 g) are added to a solution of the product obtained in step (a) 12.5 mmol (5 g) in MeOH (300 ml) and toluene (70 ml) and refluxed under N_2 for 1.5h. The product is purified by a series of extractions. (C) To a solution of 6 mmol of the product obtained in step (b) (2.322 g) and 6 mmol of *p*-nitrophenol (0.834 g) in pyridine (100 ml) and DCM (120 ml) at -15ºC 10.8 mmol of $POCl_3$ (1.006 mL in 10 mL DCM) are added over 1h period. The product is purified by a series of extractions. The *p*-nitrophenyl ester of disperse red 1 is used at a concentration of 0.02 M in ACN.

6.5.3. Analysis of amino acids

A known volume of sample in solution was transferred to an analysis tube. Sample was lyophilized and the solid was hydrolyzed with HCl 6 N at 110ºC for 8 h. The resulting solution was evaporated under vacuum and derivatized according to the derivatization protocol provided with the derivatization kit (AccQ-Tag™, Waters). Amino acid concentration was determined by HPLC.

6.5.4. Initial conditioning of resin and coupling of the first amino acid

The initial conditioning of the resins and the coupling of the first amino acid were performed as follows:

- 2-chlorotrityl chloride resin (Cl-Trt):

Step	Treatment	Reagents
1	Wash	1x DCM (15 min)
2	Coupling	0.8 eq Fmoc-AA-OH
		8 eq DIEA, DCM (1 h)
3	Capping (without filtration)	1x MeOH (1ml/g resin, 15 min)
4	Wash	5 x DCM (1 min)

- Aminomethyl-ChemMatrix functionalized with the Fmoc-Rink linker:

Step	Treatment	Reagents
1	Wash	3x DMF (1 min)
2	Wash	3x DCM (1 min)
3	Wash	3x DIEA/DCM (1:19, 1 min)
4	Wash	3x DCM (1 min)
5	Wash	3x DMF (1 min)
6	Linker coupling	3 eq Fmoc-Rink linker
		3 eq TBTU
		9 eq DIEA, DMF (60 min)
7	Wash	3x DMF (1 min)
8	Wash	3x DCM (1 min)
9	Wash	3x DMF (1 min)
10	Capping	10 eq Ac_2O
		10 eq DIEA, DMF (15 min)
11	Wash	3x DMF (1 min)
12	Deprotection	piperidine 20% in DMF (1x1, 2x10 min)

- Aminomethyl-ChemMatrix functionalized with the AB linker:

Step	Treatment	Reagents
1	Wash	3x DMF (1 min)
2	Wash	3x DCM (1 min)
3	Wash	3x DIEA/DCM (1:19, 1 min)
4	Wash	3x DCM (1 min)
5	Wash	3x DMF (1 min)
6	Linker coupling	3 eq AB linker
		3 eq DIPCDI, 3 eq HOBt
		9 eq DIEA, DMF (15 min)
7	Capping	10 eq Ac_2O
		10 eq DIEA, DMF (15 min)
8	Wash	3x DMF (1 min)
9	Wash	3x DCM (1 min)
10	Coupling	5 eq Fmoc-AA, 5 eq DIPCDI

		0.5 eq DMAP, DCM (1x2 h, overnight)
11	Wash	1 x DCM (1 min)
12	Wash	1 x DMF (1 min)
13	Deprotection	piperidine 20% in DMF (1x1, 2x10 min)

6.5.5. Fmoc group removal

The Fmoc group was removed by treating the resin with 20% piperidine in DMF (3-4 ml/g resin, 2 x 1 min and 1 x 10 min). In order to remove the Fmoc group from Fmoc-Pro-OH and additional treatment with DBU, toluene, piperidine and DMF (5:5:20:70, 2 x 3 min) was performed.

6.5.6. Fmoc group quantification and resin loading capacity

Piperidine washes were collected and measured by UV spectroscopy (λ= 290 nm) to determine the loading capacity of the resin after the coupling of the first amino acid and the yield of the linear peptide syntheses after the last coupling. Loading capacity was determined according to equation 2:

$$Z = \frac{A \cdot X}{\varepsilon \cdot Y \cdot l} \qquad \textbf{(2)}$$

A Absorbance
X Volume of solvent (ml)
ε Molar absorbance coefficient (5800 L mol^{-1} cm^{-1})
Y Resin weight (g)
l Length of the cell (cm)
Z Loading of the resin

6.5.7. Peptide chain elongation

The amino acid couplings were performed according to the following protocol: a mixture of Fmoc-AA-OH (3eq), PyBOP (3eq), and HOAt (3eq) was dissolved in the minimum volume of DMF and pre-activated by adding DIEA (6 eq). After 1 min the mixture was added to the peptide-resin.

Step	Treatment	Reagents
1	Wash	5x DCM (1 min)
2	Deprotection	1 x 20% piperidine in DMD (1 min)
3	Deprotection	2 x 20% piperidine in DMD (10 min)
4	Coupling	3 eq Fmoc-Aa-OH 6 eq HOAt, 3 eq PyBOB, 6 eq DIEA (1 h)
5	Wash	5 x DCM (1 min)

Couplings were performed at room temperature with intermittent manual stirring. The extent of the coupling reaction was controlled by the ninhydrin, or chloranil test and re-couplings were judiciously performed. Fmoc deprotection from proline residues was carried out using an extra treatment of DBU, toluene, piperidine and DMF as described in point *6.5.5*.

6.5.8. Coupling with Fmoc-8-amino-3,6-dioxaoctanoic acid

Fmoc-O_2O–OH (3 eq), HBTU (3 eq) were sequentially added to the peptide-resin in DMF, followed by DIEA (6 eq). The mixture was allowed to react with intermittent manual stirring for 1 h. The solvent was removed by filtration, and the resin was washed with DMF (5 x 30 s) and DCM (5 x 30 s). The extent of coupling was checked by the Kaiser an chloranil test.

6.5.9. Coupling with 5(6)-carboxyfluorescein

A mixture of 5(6)-carboxyfluorescein (3 eq), PyBOP (3eq) and HOAt (3 eq) was dissolved in the minimum volume of DMF and pre-activated by adding DIEA (6 eq). After 1 min the mixture was added to the peptide-resin. The mixture was allowed to react with intermittent manual stirring overnight. The solvent was removed by filtration and the resin was washed with DMF (5 x 30 s) and DCM (5 x 30 s). The extent of coupling was checked by the ninhydrin, and chloranil test.

6.5.10. Coupling with 4,4,4-Trifluoro-3-(trifluoromethyl)butanoic acid

A mixture of 4,4,4-Trifluoro-3-(trifluoromethyl)butanoic acid (20 eq), PyBOP (20 eq) and HOAt (60 eq), was dissolved in the minimum volume of DMF and pre-activated by adding DIEA (60 eq). After 1 min the mixture was added to the peptide-resin. The mixture was allowed to react with intermittent manual stirring 1.5 h. The solvent was removed by filtration and the resin was washed with DMF (5 x 30 s) and DCM (5 x 30 s). The extent of coupling was checked by the ninhydrin, and chloranil test.

6.5.11. Coupling with glycosidic carrier on solid phase

The coupling whit the carrier was performed as followed reported: a mixture of **41** (1.5 eq), PyBOP (1.5 eq), and HOAt (1.5 eq) was dissolved in the minimum volume of DMF and pre-activated by adding DIEA (3 eq). After 1 min the mixture was added to the peptide-resin. Couplings were performed at room temperature with intermittent manual stirring. The extent of the coupling reaction was controlled by the ninhydrin, or chloranil test.

6.5.12. Disulfide bond formation between Cys(Trt) on Cl-Trt resin

To the peptide-resin in DMF was added iodine (2.5 eq for each Trt group). The mixture was left to react with intermittent manual stirring for 15 min. Then the solvent was removed by suction and the treatment was repeat again. The solvent was removed by filtration and the resin was washed with DMF (5 x 30 s), a saturated solution of $NaHSO_4$ (5x1 min) and $CHCl_3$ (5x1 min). The reaction was checked by Ellman's test.

6.5.13. Peptide synthesis using microwave assisted technology

Aminomethyl ChemMatrix resin was used as solid support. It was swelled and functionalized with the linker as describe in the procedure reported in the section *6.5.4*. The peptide chain elongation was performed through coupling–deprotection cycle performed by

automated microwaves assisted heating technology, using TBTU/DIEA for the amino acid coupling reaction and piperidine 20% in DMF for the Fmoc deprotection.

Microwaves conditions:

Treatment	Reagents
Deprotection	3min, 28W, 78ºC Piperidine/DMF
Coupling	5min, 15W, 75ºC (0.2M aa/0.5M TBTU/2M DIEA)
Arg Coupling	1° cycle 30 min, 0W, 75ºC (0.2M Arg/0.5M TBTU/2M DIEA
	2º cycle 5 min, 18W, 75ºC (0.2M Arg/0.5M TBTU/2M DIEA)
Cys/His Coupling	5min, 15W, 50ºC (0.2M His/0.5M TBTU/2M DIEA)

6.5.14. Amine acetylation on 2-Cl-Trt resin

The peptide-resin in DMF was treated with Ac_2O (15 eq) then DIEA was added (30 eq).The mixture was allowed to react with intermittent manual stirring for 1h. The solvent was removed by suction and the resin washed with DMF (5 x 1 min), and DCM (5x1 min). The reaction was checked by Ninhydrin test.

6.5.15. Alloc removal group

The peptide-resin protect with an Allyl group was solvated in DCM, then $Pd(PPh_3)_4$ (0.1 eq) was added in presence of $PhSiH_3$ (10 eq). The mixture was allowed to react with intermittent manual stirring for 15 min. The solvent was removed by suction and the treatment was repeated twice more. The resin was washed with DMF (5x1 min), and DCM (5x1 min). The reaction was checked by Ninhydrin test.

6.5.16. Cleavage of the peptides from the resin

The peptide cleavage from the resin was accomplished by treatment with a 2% of TFA DCM solution (5 x 1 min), or with a 25% Hexafluoro-2-propanol solution in DCM (2 x 15 min) both treatments ensure do not remove the side chain acid labile protecting group.

6.5.17. Complete peptide deprotection

Complete deprotection of the peptide was performed by acidolytic treatment with a TFA solution containing the appropriate scavengers in order to minimize the unwanted side reactions.

The peptide was transferred to a 50 ml centrifuge tube. The freshly made cleavage cocktail solution (3 ml) was added and the reaction was carried out at room temperature for 1 h with gentle agitation. As an exception, in the cleavage of peptides containing Arginine, reaction time was increased up to 3 h in order to ensure the complete removal of all Arg side-chain protecting group (Pbf). The corresponding peptide was precipitated through addition of cold *tert*-butyl methyl ether. The suspension was centrifuged at 4000 rpm and 4ºC during 10 min. The ether fraction was discarded and the process repeated up to 3 times, in order to remove all scavengers and by-products from cleavage of side-chain protecting groups. The peptide residue thus obtained was dried by means of a N_2 flow stream, resuspended in a mixture of H_2O and ACN (1:1) and lyophilized.

Election of the cleavage cocktail is crucial and highly dependent on the presence of sensitive residues within the peptide sequence. The following flow-chart was used as a general selection guide:

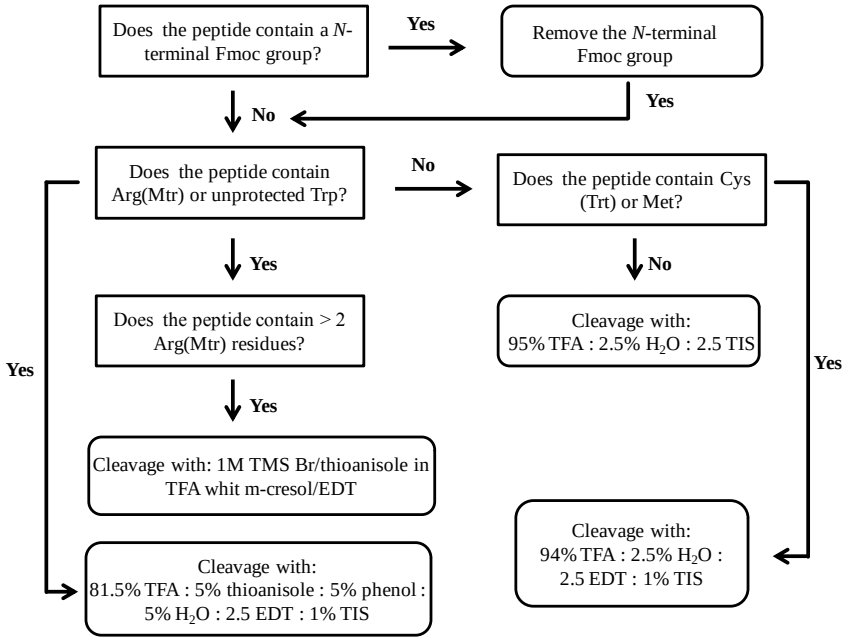

6.5.18. Split resin

To the peptide-resin was added a properly volume of DMF and with the aid of a micropipette was generated a homogeneous suspension. A known volume of the suspension was withdrawn with the pipette and divided among the various polypropylene syringes, each fitted with a polyethylene porous disk. The procedure is repeated until the peptide resin on the initial syringe has been completely transferred.

6.6. Solution-phase peptide synthesis

6.6.1. Introduction carboxylic protecting groups

6.6.1.1. 9-Fluorenylmethyl esters (OFm)

Nα -protected amino acid was treated with 9-fluorenylmethyl methanol (0.8 eq), EDCI (1 eq) and catalytic amount of DMAP (0.04 eq) in DCM/DMF (5:1) at room temperature for 3 h. The reaction was quenched by adding water (50 ml). The reaction mixture was added to a separation funnel and the product was extracted with DCM (3 x 100 ml). Dichloromethane layers were combined, washed with brine (3 x 100 ml) and dried over Na_2SO_4. Solvent was removed under vacuum and the crude was purify by silica gel column chromatography to give the Boc-AA-OFm.

6.6.1.2. 9-Fluorenylmethyl thioesters (SFm)

S-(9-Fluorenylmethyl) *N-tert*-butoxycarbonyl-AA was prepared according to the procedure described by Sasaki et al.[5] To a solution of Boc-AA-OH and 9-fluorenylmethylthiol (0.8 eq) in DCM/DMF (5/1) were added EDCI (1eq) and DMAP (0.04 eq), and the reaction

mixture was stirred for 1 h. The reaction was quenched with water (100 ml) and the mixture was extracted with CH_2Cl_2 (3 x 50 ml). The combined organic layer was washed with brine (100 ml), dried over Na_2SO_4, and concentrated *in vacuo*. Purification of the residue by silica gel chromatography give the final product.

6.6.2. Peptide chain elongation

The amino acid couplings were performed according to three different protocols. Protocol A was used for couplings onto primary amines, Protocol B was used for coupling onto secondary amines, (proline), while the Protocol C was used to test the efficiency of the PPAA as condensing coupling reagent.

Protocol A

In a reaction flask, Boc-AA-OH (1.2 eq) and HOBt (1.5 eq) were suspended in DCM/DMF (5/1) and EDCI (1.2 eq) was added. The reaction mixture was stirred for 15 min, and DIPEA (1eq) was added, followed by a solution containing the *N*-deprotected residue in DCM/DMF (5/1). The reaction mixture was stirred for further 1 h, and then poured to water (100 ml). The mixture was extracted with EtOAc, and the combined organic layer was washed with brine (100 ml), dried over Na_2SO_4, and concentrated *in vacuo*. Purification of the residue by silica gel chromatography gave the desired product.

Protocol B

In a reaction flask, Boc-AA-OH (1.2 eq) and HBTU (1.3 eq) were dissolved in DMF. The reaction mixture was stirred at room temperature for 1 h to obtain the activate ester. DIEA (2 eq) was added, followed by a solution containing the *N*-deprotected peptide in DMF. The reaction mixture was stirred at room temperature overnight. The reaction mixture was diluted with DCM, added to a separation funnel and washed with HCl 1N, saturated solution of $NaHCO_3$ and brine. The combined organic layer was dried over Na_2SO_4 and the solvent was removed under *vacuo*. Purification of the peptide by silica gel chromatography gave the product.

Protocol C

A suspension of *N*-Boc-AA-OH and the *N*-deprotected peptide in DCM is cooled in a ice bath before addition of DIEA. A solution of PPAA (50wt% in DCM) is then added slowly. The mixture is removed from the cooling bath and allowed to stir overnight at room temperature. Water is added and the mixture was stirred vigorously for 1 h. The reaction mixture was added to a separation funnel, the two phases were separated and the aqueous phase washed with Et_2O (2 x 50 ml). The combined organic layer were washed with brine and dried with anhydrous Na_2SO_4. Solvent was removed under *vacuo* and purification of the peptide by silica gel chromatography gave the product.

6.6.3. Boc-deprotection

The Boc-AA-OFm (or Boc-AA-SFm) was dissolved in 40% TFA/DCM and the solution was stirred for 15 min at room temperature. The volatiles were removed *in vacuo*, and the residual TFA was removed by azeotropic distillation with toluene *in vacuo*.

6.6.4. Fmoc/OFm – deprotection

To a solution of Fmoc-AA-OFm (or Fmoc-AA-SFm) in DMF [5 mM] was added piperidine (20 eq). The reaction mixture was stirred for 1 h, then the volatiles were removed under high vacuum. The residual piperidine was removed by azeotropic distillation.

6.6.5. Hydrogenolytic deprotection

To a solution of a Z-protected peptide in dry MeOH was added $Pd(OH)_2/C$ (w/w 10% on activated charcoal) and the mixture was hydrogenated overnight under atmospheric pressure using an H_2-filled balloon. The catalyst was removed by filtration through a pad of celite and the solvent evaporated under reduced pressure.

6.7. Peptide cyclization

The *head-to-tail* peptide cyclizations were performed according to four different condensing reagents and relatives protocols.

Protocol D: PPAA mediated cyclization

To a solution of the *C*- and *N*-terminal un-protected linear peptide in DCM [5 mM] is added DMAP (6 eq) and then cooled in a ice bath. Then maintaining the reaction mixture under vigorous agitation, a solution of PPAA (50wt% in DCM, 1.5 eq) is added dropwise. The reaction flask is removed from the cooling bath and the mixture was stirred at r.t. until the starting material was consumed. (TLC).
The volume of the reaction mixture is concentrated by distillation *in vacuo*, then water is added and the mixture was stirred vigorously for 1 h. The reaction mixture was added to a separation funnel, the two phases were separated and the aqueous phase washed with Et_2O (2 x 50 ml). The combined organic layer were washed with brine and dried over Na_2SO_4 and the solvent was removed under *vacuo*. Purification of the peptide by silica gel chromatography gave the product.

Protocol E: HATU mediated cyclization

To a stirred solution of the *C*- and *N*-terminal un-protected linear peptide in dry DMF under N_2, was added dropwise at 0°C a solution of HATU (1.5 eq), HOAt (1.5 eq) and DIPEA (4 eq) in dry DMF (final peptide concentration [5 mM]). The reaction was allowed to proceed at r.t. under nitrogen atmosphere monitoring its evolution by TLC. The solvent was removed under reduced pressure and the crude residue was purified by silica gel flash chromatography to give the pure cyclic peptide.

Protocol F: PyBOP mediated cyclization

To an ice-cold solution of PyBOP (3 eq) and DIEA (4 eq) in dry DMF [3 mM] was added dropwise a solution of *C*- and *N*-terminal un-protected linear peptide (1 eq) in DMF to reach a final peptide concentration of [5 mM]. The reaction evolution was followed by TLC. The solvent was removed under reduced pressure and the crude was purified by silica gel flash chromatography.

Protocol G: DPPA mediated cyclization

The *C*- and *N*-terminal un-protected linear peptide was dissolved in DMF [5 mM] and to the solution were added $NaHCO_3$ (8 eq) and DPPA (1.5 eq for the cyclic peptides of the part I of this thesis and 2 eq for the cyclopeptides of the part II) under stirring. The reaction was allowed to proceed at r.t. and monitored by analytical HPLC. The sodium bicarbonate was removed by filtration, then the solvent was evaporated under reduced pressure. The crude cyclopeptide was completely deprotected by treatment with a solution TFA-TIS-H_2O/ 95:2.5:2.5 and then purified by semi-preparative HPLC or automated flash chromatography.

Protocol H: Sanger's reagent mediated cyclization

The *C*- and *N*-terminal un-protected linear peptide was dissolved in DMF [5 mM], 2,4-Dinitrofluorobenzene (1.2 eq) was added to it, and the reaction mixture was stirred for 5 min at r.t. DMF was removed under high vacuum, and the residue was purified by silica gel chromatography.

6.8. Parallel artificial membrane permeability assay (PAMPA)

Parallel artificial membrane permeability assay (PAMPA) was used to determine the capacity of compounds to cross the BBB by passive diffusion. The effective permeability (*Pe*) of the compounds was measured at an initial concentration of 200 µM.
The buffer solution was prepared from a concentrate one, commercialized by pION, and following manufacturer's instructions. pH was adjusted to 7.4 using 0.5 M NaOH solution. The compound of interest was dissolved in buffer solution to the desired concentration. The PAMPA sandwich was separated and each acceptor well was filled with 200 µl of buffer solution. The donor plate was then placed into the acceptor plate ensuring that the underside of the membrane was in contact with buffer. 4 µl of a mixture of phospholipids (20 mg/ml) in dodecane was added to each well filter and 200 µl of the compound of interest in buffer solution was added to each acceptor well. The plate was covered and incubated at room temperature in a saturated humidity atmosphere for 4 h under orbital agitation (100 rpm). After 4h the content of the acceptors and donors compartments was analyzed by HPLC.

6.9. Fluorescence polarization (FP)

Direct binding FP assays

Wells of a black Corning 384-well polystyrene plate (*384 Flat Bottom Black Polystyrol*) contained fluorescent peptide tracer (67 nM for tracers) and increasing concentrations (from 57.6 µM to 0.49 nM) of VEGF protein in FP buffer (50 mM NaCl, 16.2 mM Na_2HPO_4, 3.8 mM KH_2PO_4, 0.15 mM NaN_3, 0.15 mM EDTA, and 0.5 mg/ml Pluronic, pH 7.4). Plates were read after a 2 h incubation at room temperature using an PerkinElmer EnVision multilabel plate reader (PerkinElmer, Wellesley, MA, USA) with polarized filters and optical modules for fluorescein (λex = 480 nm, λem = 535 nm) mP values were calculated from raw parallel and perpendicular fluorescence intensities.[6] GraphPad Prism 4.03 (GraphPad, San Diego, CA, USA) was used to plot mP versus VEGF concentration, and the

curve was fit to a single-site binding model to extract a binding dissociation constant (Kd value).[7] Experiments were performed in duplicate.

Competition binding FP assays

Wells of a 384-well plate contained 67 nM tracer peptide, 1 μM VEGF protein, and tested inhibitor (v107) dissolved in DMSO (final concentration from 160 μM to 0.02 nM) in a final volume of 50 μl in FP buffer. Plates were read after a 2 h incubation at room temperature, the time necessary for complete equilibration. Experiments were performed in duplicate. The equilibrium dissociation constant (Ki)[8] was calculated, and the error was given as the 95% confidence interval as calculated by GraphPad Prism.

6.10. Molecular modeling

The experimental structures entries as pdb files were built using Maestro 6.0. The input files were created whit the program LEaP which reads in force field, topology and coordinate information and produces the files necessary for production calculations (*i.e.* minimization, molecular dynamics, analysis). In particular, it has been used the graphical versions of this program called *xleap.*

The structures were solvated in an explicit truncated octahedral box of water and TIP3P water model was used for simulations of each structures. The net charge of the structures were neutralized with sodium ions as explicit counterions.

Each structures were subject to energy minimization before the molecular dynamics analysis using Sander module of the Amber software suite. The minimization was run using the most commonly steepest descent minimization algorithms, with 500 steps with a 1 fs time step giving simulation lengths of 100 ps. In this simulation the non-bonded cut off was fixed to 12 angstroms as a reasonable tradeoff, given that a larger cut off introduces less error in the non-bonded force evaluation but increases the computational complexity and thus calculation time system error and long process time. The temperature of the system has been set at 300 K.

MD simulations of each cyclopeptide was performed using Amber11 and its FF03 force fields which is recommended for the simulation of proteins and nucleic acids in explicit solvent. The obtained trajectory were analyzed and seen as a movie using VMD as methods of visualization, whereas the energy profile was plotted using GRACE. The analysis of the results was performed by plotting temperature, total energy, kinetic energy and potential energy from the output file.

References

(1) Lloyd-Williams, P. A., F.; Giralt, E. . Chemical Approaches to the Synthesis of Peptides and Proteinss *CRC Press: Boca Raton, FL* **1997**.

(2) Kaiser, E.; Colescott, R. L.; Bossinger, C. D.; Cook, P. I. Color test for detection of free terminal amino groups in the solid-phase synthesis of peptides. *Anal. Biochem.* **1970**, *34*, 595-598.

(3) Christensen, T. Qualitative test for monitoring coupling completeness in solid-phase peptide-synthesis using chloranil. *Acta Chem. Scand. B* **1979**, *33*, 763-766.

(4) Madder, A.; Farcy, N.; Hosten, N. G. C.; De Muynck, H.; De Clercq, P. J.; Barry, J.; Davis, A. P. A Novel Sensitive Colorimetric Assay for Visual Detection of Solid-Phase Bound Amines. *Eur. J. Org. Chem.* **1999**, *1999*, 2787-2791.

(5) Sasaki, K.; Crich, D. Cyclic peptide synthesis with thioacids. *Org. Lett.* **2010**, *12*, 3254-3257.

(6) Banks, P.; Harvey, M. Considerations for using fluorescence polarization in the screening of G protein-coupled receptors. *J. Biomol. Screen.* **2002**, *7*, 111-117.

(7) Zhang, R.; Mayhood, T.; Lipari, P.; Wang, Y.; Durkin, J.; Syto, R.; Gesell, J.; McNemar, C.; Windsor, W. Fluorescence polarization assay and inhibitor design for MDM2/p53 interaction. *Anal. Biochem.* **2004**, *331*, 138-146.

(8) Roehrl, M. H.; Wang, J. Y.; Wagner, G. A general framework for development and data analysis of competitive high-throughput screens for small-molecule inhibitors of protein-protein interactions by fluorescence polarization. *Biochemistry* **2004**, *43*, 16056-16066.

Part II

Development of a cyclic peptides library to modulate EGF-EGFR and VEGF-VEGFR interactions

Chapter 1

Introduction

Introduction

Gliomas are the most frequent tumours of the brain. Glioma can be classified into four clinical grades on the basis of their histology and prognosis. Grade IV gliomas (glioblastoma multiforme, GBM) is one of the most malignant human tumors affecting approximately 13,000 people/year in the EUs.[1]

GBMs are highly malignant tumours, usually resistant to radio- and chemotherapy and affected patients have a median survival of 1-2 years. GBMs are extremely invasive resulting in the failure of surgery to completely eradicate the tumor. Radiation therapy improves overall survival for each tumour grade, yet no patients are median survival by 2.5 months compared with radiation therapy alone. Thus temozolamide has become a standard adjuvant therapy for gliomas although it offers modest clinical benefit.

Many different compounds have been tested as anti-glioma agents during the last 10 years with barely any success. Among many different reasons, the presence of the blood-brain-barrier (BBB) and the intra-tumoral heterogeneity are the two characteristics of brain tumours that make them especially recalcitrant to the treatments.

Indeed, cerebral vessels have a physiological barrier (BBB) that prevents the proper delivery of compounds to the tumours and, cell within a tumour are different and have different sensitivities to treatments. Among the different cell subpopulations present in a tumour, cancer stem cells are the most malignant, being responsible for recurrence and therapeutic resistance.

Many efforts have been directed to the identification of novel molecular-targeted therapies against these kinds of tumours and to the development of novel pharmacological compounds that would cross the BBB and target glioma.

1.1. The selected target protein-protein interactions

A variety of environmental, genetic and epigenetic factors induce the reprogramming of cancer-initiating cells and the acquisition of physical and molecular features that promote tumorigenesis and provide resistance to therapeutics. These characteristics, including sustained proliferative signaling and evasion of growth suppressors, permit the development and progression of cancer and have been recognized as distinctive hallmarks of cancer. Importantly, PPIs represent the basic units within such vital networks. In cancer, PPIs form signalling nodes and hubs that transmit pathophysiological cues along molecular networks to achieve an integrated biological output, thereby promoting tumorigenesis, tumor progression, invasion, and/or metastasis. Thus, disruption of PPIs critical for cancer, offers a novel and effective strategy for curtailing the transmission of oncogenic signals. EGF-EGFR and VEGF-VEGFR are two of the important cancer-enabling PPIs.

1.1.1. VEGF and VEGFR complex

Angiogenesis plays an essential role in the growth of most primary tumors as well as their subsequent metastasis. Sufficient nutrients and oxygen are needed by tumors, and growth beyond a certain size requires the elaboration of vascular supply. This is usually done by

recruiting neighbouring mature vasculature and sprouting of new capillaries that eventually infiltrate the tumor mass.[2,3]
Angiogenesis has become an attractive drug target, since Folkman[4] proposed that antiangiogenesis would be a novel antitumor strategy,[5,6] especially, Vascular Endothelial Growth Factor (VEGF) and its receptors (VEGFR).

VEGF is a 45 KDa homodimeric glycoprotein.[7] Each monomer has a central antiparallel four-stranded β-sheet core and a characteristic cysteine knot motif, fixed by a network of three disulfide bonds. VEGF is overexpressed in most tumors and its activity is mediate by binding to specific VEGF receptors, leading to receptor dimerization and activation of the receptor's kinase activity through autophosphorilation. This in turn induces phosphorylation on a variety of protein substrates, activating a series of intracellular signalling pathways and unchaining several processes common to other growth factors: cell migration, survival and proliferation.

VEGF is a member of the platelet-derived growth factor (PDGF)/vascular endothelial growth factor (VEGF) family, which comprises seven members (VEGF-A, VEGF-B, VEGF-C, VEGF-D, VEGF-E, VEGF-F and PIGF), each one binding to their receptor/s. VEGF-A is expressed in the human body in at least seven isoforms, containing 121, 145, 148, 165, 183, 189 and 206 residues per monomer.[8]

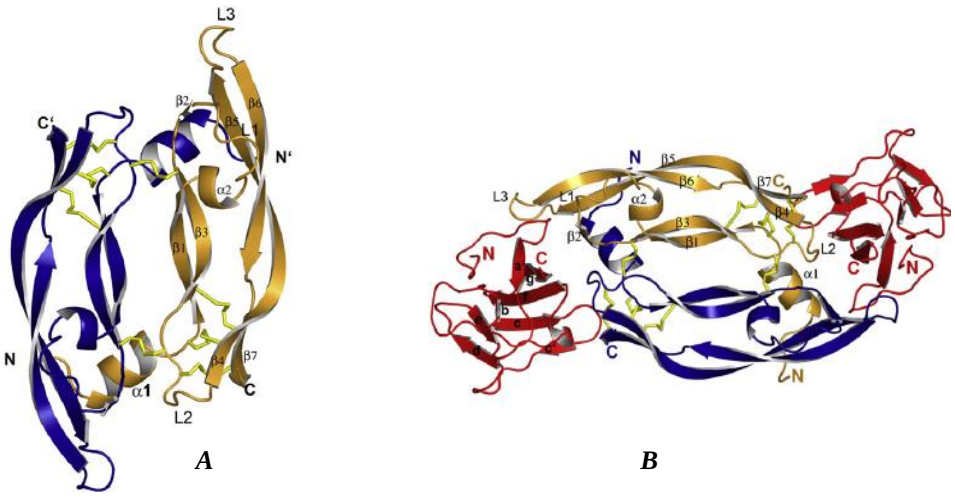

Figure 1. Structures of VEGF-A and VEGFR-1 domain 2. Ribbon representations of (A) the non-liganded VEGF-A_{109} (bottom view looking up from the cell membrane) and (B) the complex between VEGF-A_{109} and VEGFR-1 domain 2 (bottom view). The two VEGF monomers are shown in blue and light orange, respectively; the VEGFR-1 domain 2 in red. Disulfide bonds are shown as yellow sticks. The secondary structure elements are labeled according to the original references. (Adapted from *Biochimica et Biophysica Acta* **2010**, *1804*, 567–580).

VEGF gene expression is triggered by several host stimuli such as estrogen, nitric oxide and other growth factors (e.g., bFGF, TNF-α, EGF); but its production is particularly sensitive to oxygen tension, for instance the hypoxic conditions typically found in tumors rapidly upregulate VEGF. As a result, VEGF is overexpressed in most tumours and has a direct effect on their development by relieving tumor masses from stress conditions through oxygen and nutrients recruitment, but also acting as a survival factor by enhancing the expression of anti-apoptotic factors such as Bcl-2.

VEGF activity is mediated by binding to specific VEGF receptors, leading to receptor dimerization and activation of the receptor's kinase activity through autophosphorilation.

This in turn induces phosphorylation on a variety of protein substrates, activating a series of intracellular signalling pathways and unchaining several processes common to other growth factors: cell migration, survival and proliferation.

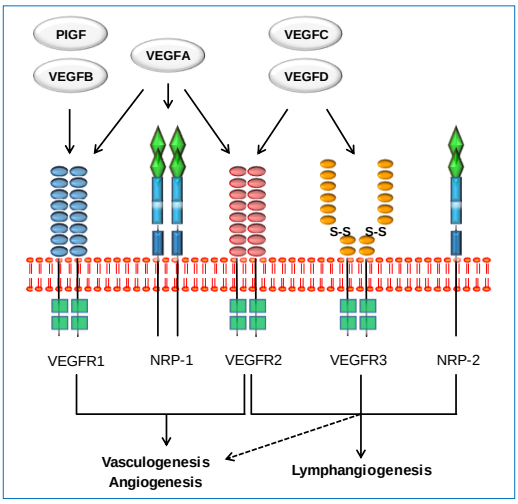

Figure 2. Schematic representation of VEGF family ligands and their receptors. (Adapted from Nature Reviews Cancer **2008**, *8*, 579-591).

The role of VEGF-A as therapeutic target has been extensively described[8] because it is a major regulator of normal and abnormal angiogenesis, including that associated with tumors and several intraocular syndromes. It binds to two receptors tyrosine kinases (RTK), VEGFR-1 (flt-1), and VEGFR-2 (KDR, flk-1). In particular, VEGFR-2 is the major mediator to the mitogenic, angiogenic and permeability-enhancing effects of VEGF-A.
Generally, VEGF-A up regulation is associated with tumours growth, facilitating the spread of blood vessels and blood supply of the tumour. Inhibition of VEGF-induce angiogenesis hinders this growth[10] and increase the tumor response to radiotherapy.[11] In addition to tumor growth VEGF-A is involved in a number of pathological conditions, including cardiovascular diseases, diabetic retinopathy, rheumatoid arthritis and psoriasis. Furthermore, VEGF-A is required for the normal functioning and development of mammals, thus making it an attractive target for both antiangiogenic and proangiogenic therapy.

In the field of peptide ligands, peptides that inhibit binding of VEGF to its receptors were produced using phage display.[12] Libraries of short disulfide-constrained peptides yielded three distinct classes of peptides that bind to the receptor-binding domain of VEGF with micromolar affinities.

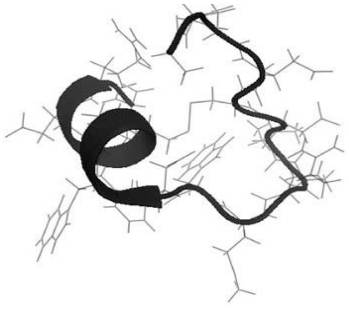

Figure 3. The most remarkable peptidic ligands v107, identified by a phage display strategy (K_d = 0.2 µM).

In the field of biologics, the monoclonal antibody bevacizumab (selective for VEGF-A) is used for the treatment of certain cancer types; however its cost-benefit ratio is high. In the case of small organic molecules, orally available inhibitors lapatinib, sunitinib, sorafenib, axitinib and pazopanib target multiple kinases, including VEGFRs are used for treatment. Serious side effects of these inhibitors include gastrointestinal perforation, wound healing complications and hemorrhage.

Currently, there are three Food and Drug Administration-approved drugs for treatment of diseases related to overexpression of VEGF: Bevacizumab (Avastin),[13] Ranibizumab (Lucentis),[14] and Pegaptanib (Macugen).[15] Each of these drugs blocks the signalling by binding to VEGF and thereby preventing interaction with cell surface receptors.
In addition, a number of small molecules that inhibit the kinase activity of VEGFR-1 and/or VEGFR-2 are currently in clinical trials.[16] Despite the success of the therapeutic antibodies inhibitors of the VEGF–VEGFR interaction with lower molecular weight (e.g., peptides or small molecules) might offer advantages in terms of production, stability, and/or administration.[17] It is very challenging to identify small molecules that bind tightly and specifically to a given protein surface.[18,19] In principle, steric inhibition of VEGF–VEGFR interaction could be accomplished via a molecule that binds to the recognition surface on VEGF or a molecule that binds to the recognition surface on a receptor. All steric inhibitors in the clinic or in clinical trials function by binding to VEGF rather than a receptor.[16] An agent that binds to VEGF can be specific for one type of biological response, whereas an agent that binds to a VEGF receptor may block interaction of this receptor with other natural ligands (other members of the VEGF superfamily), thereby affecting processes other than angiogenesis.[20]

1.1.2. EGF and EGFR complex

Human epidermal growth factor (EGF) is a small protein consisting of 53 amino acid residues including six Cys residues that form three disulfide bonds. The solution structure of monomeric EGF consists of one antiparallel β-sheet and two α-helices that adopt a αβα-fold that is stabilized by the three disulfide bridges. EGF performs its biological function by binding to a specific transmembrane receptor (EGFR) of the receptor tyrosine kinase (RTK) family. The EGFR family of RTK comprises four members collectively referred to as the ErbB family: EGFR itself, ErbB2, ErbB3 and ErbB4.
ErbR receptors are composed of an extracellular region (~620 amino acids), a single transmembrane helix, an intracellular tyrosine kinase domain (~270 amino acids) and a ~200 amino acids *C*-terminal tail. The extracellular region of EGFR, containing two ligand binding-domains (domains I and III) and two cysteine-rich domains (domains II and IV), is thought to exist in a dynamic equilibrium sampling multiple conformations. Binding to EGF shifts the equilibrium to a dimerization-competent extended configuration, driving the system towards the active dimeric form.[21] EGFR dimerization is achieved only by receptor-receptor interactions. In the dimeric EGF-EGFR complexes (2:2), each EGF molecule binds simultaneously to the domains I and III of the same receptor molecule and is distant from the dimer interface.[22]

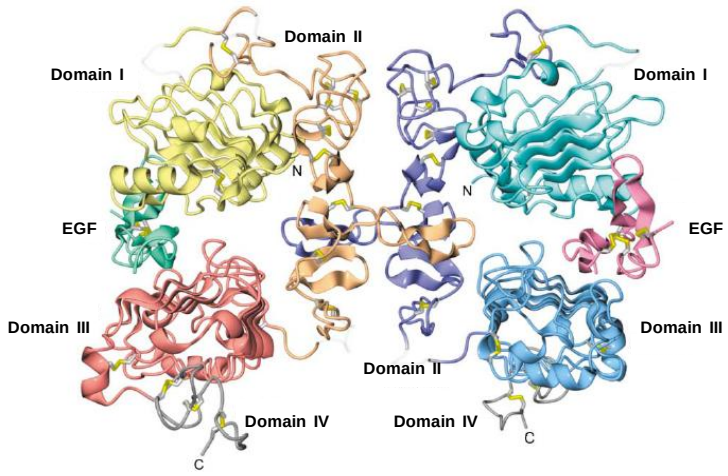

Figure 4. Crystal structure of the 2:2 EGF-EGFR complexes. Ribbon diagram with the approximate two-fold axis oriented vertically. One EGF chain in the 2:2 EGF•EGFR complex is pale green, and the other EGF chain is pink. Domains I, II, III, and IV in one receptor in the dimer are colored yellow, orange, red, and gray, respectively. Domains I, II, III, and IV in the other receptor are colored cyan, dark blue, pale blue, and gray, respectively. Most of domain IV is disordered. The disulfide bonds are shown in yellow. The intervening parts that were not assigned are transparent. (Extract from *Cell* **2002**, *110*, 775-787)

The receptor dimerization interface is centred on a β-hairpin arm (residues 242-259) that projects from domain II in each of the two EGFR molecules in the dimer. In the inactive, ligand-free tethered configuration of EGFR (Figure **4**), this β-hairpin arm is buried by intramolecular interactions with the domain IV inhibiting receptor dimerization. However, simply exposing the dimerization arm in the absence of EGF is not sufficient to promote EGFR dimerization.[23] EGF binding is accompanied by a drastic conformational change that remodels the entire dimerization interface. EGF binding promotes a domain reorientation that leads to an extended receptor configuration, but also imposes a precise bend on the domain II that defines the optimal trajectory of the β-hairpin arm allowing multiple weak contacts outside this arm which can cooperate effectively in driving high-affinity dimerization.

Ligand-induced homo- and/or heterodimerization is essential for the activation of the intracellular kinase domain and the subsequent receptor autophosphorylation. EGFR activation initiates a signalling pathway that regulates many cellular processes including proliferation, cell motility and differentiation. Aberrant EGFR signalling, caused by overexpression of the EGFR protein or by the presence of activating mutations, is associated with a wide range of epithelial cancers, including those of the breast, colon, head and neck, kidney, lung, pancreas and prostate.[24,25]

Therapies that target EGFR are of major clinical importance in the treatment of cancer.[25] Current clinical therapeutics either target the extracellular region of EGFR with monoclonal antibodies (mAbs) or interfere with the intracellular EGFR tyrosine kinase activity with small molecule defined as tyrosine kinase inhibitors (TKIs).[25,26] Small molecule TKIs, such as erlotinib and gefitinib, compete with ATP to bind to the intracellular tyrosine kinase catalytic domain inhibiting EGFR autophosphorylation. The most important antibodies targeting the extracellular domain of EGFR are cetuximab and panitumumab.[27] On binding to the domain III of EGFR, these antibodies compete with EGF binding, prevent EGFR activation and therefore inhibit proliferation of tumor cells.[28,29]

Although those mAbs and TKIs are an effective treatment for patients, their use has several drawbacks including exorbitant costs, severe side effects[30] and a considerable incidence of primary or acquired drug resistance, which support the need for development of additional inhibitors for the EGFR signalling.[31] Peptides that mimic the dimerization arm of ErbB receptors[32,33] and small molecules targeting the dimerization of EGFR[34] have been recently described as inhibitors of EGFR activity. As an alternative approach, an EGFR-directed fusion protein composed of human EGF and the catalytic and translocation domains of diphteric toxin has been tested for antitumor activity with promising results.[35]

In the field of the small molecules has been demonstrate that Suramin can prevent the interaction between hEGF and EGFR by interacting to the receptor binding region on hEGF. Consequently to the binding, Suramin blocks the conformational change of hEGF.[36] This blocking ability is one of the reasons for which Suramin has antiproliferative activity against cancer cells that overexpress EGFR on their cell surfaces.[37] Nowadays, Suramin is in the Phase II of clinic trials for glioblastoma.[38]

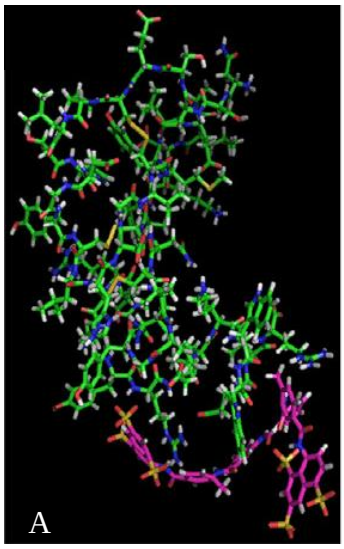

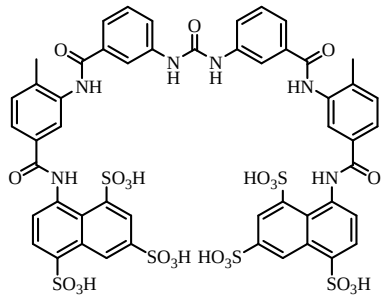

Suramin

Figure 5. A. Stereo representation of the interaction between hEGF (in green) and Suramin (in pink). On the left the Suramin structure.

Suramin, a symmetrical polysulfonated naphthylurea, is a growth factor blocker with anti-cancer activity.[39] Several investigators have reported that Suramin has an antiproliferative activity against cancer cells by inhibiting the binding of growth factors to their receptors.[40] It has also been employed therapeutically in a variety of disorders, including HIV, with limited success.[41] Most recently, it has been evaluated as an anti-tumor agent.[42] The mechanism by which Suramin disrupts the activity of growth factors is not fully understood yet but it is supposed to involve a direct binding of the drug to the growth factor itself rather than its complementary receptor.[43]

Targeting the EGF molecule itself could represent an effective way to prevent the binding of the growth factor to the receptor and thus, inhibit the EGFR activation and downstream events. Peptide ligands directed to the individual sites observed in the crystal structure may be active in preventing EGFR binding, representing a new therapeutic approach against cancer.

The X-ray structure of the complex of human EGF and the extracellular region of EGFR has revealed the EGF-EGFR interactions.[22] The protein-receptor interface on each receptor consists of three sites, designated as site 1 to 3, involving domains I and III. The residues 20-31 of EGF interact with the site 1 in the domain I, the EGF region containing residues 6-19 and Arg41 interacts with the site 2 in the domain III, and the *C*-terminal region around Arg45 interacts with site 3 in domain III. Mutagenesis studies have identified that Ile23[44] and Arg41[45] in EGF are critical determinants for receptor binding. EGF binds much more strongly to the domain III of EGFR than to the domain I, although the interaction with the domain III is sensitive to pH and can be disrupted at low pH.[46] This observation suggests that the EGF binding ability of some interaction sites may be easily modulated.

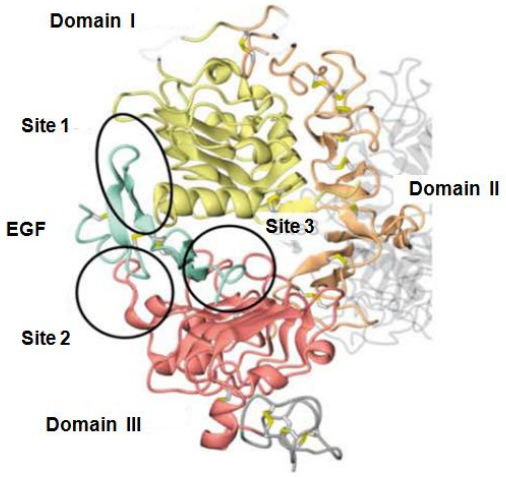

Figure 6. Mapping the interaction sites onto ribbon representations of EGFR and EGF. Three binding sites in the interface are outlined. (Extract from *Cell* **2002**, *110*, 775-787)

1.2. Transport through the BBB

The blood-brain barrier (BBB) is located in brain capillaries and is considered the most important barrier to tackle in order to achieve drug delivery to the brain. This barrier is composed of a continuous layer of highly specialized vascular endothelial cells whose primary function is to maintain the brain homeostasis. The BBB is a highly efficient physical and enzymatic barrier, restricting and regulating the flow of substances from the blood to the brain, thus providing an optimal environment for the function of this organ. The barrier effect is achieved in part by a complex network of tight junctions between endothelial cells[47-49] that hinders paracellular transport.[50-54]

Furthermore, transcellular transport from blood to brain is also limited as a result of low vesicular transport, high metabolic activity, lack of fenestrae and the expression of a variety of enzymes.

Most central nervous system (CNS) drugs enter the brain by transcellular passive diffusion, due to the tight junction structure and limited transport pathways. There are also two active processes in the BBB that influence penetration[55,56] active influx transporters (e.g. amino acid, peptide) and active efflux transporters (e.g. P-glycoprotein, multi-drug resistant proteins). In addition, partial or complete metabolism of a compound will limit its penetration into the brain.

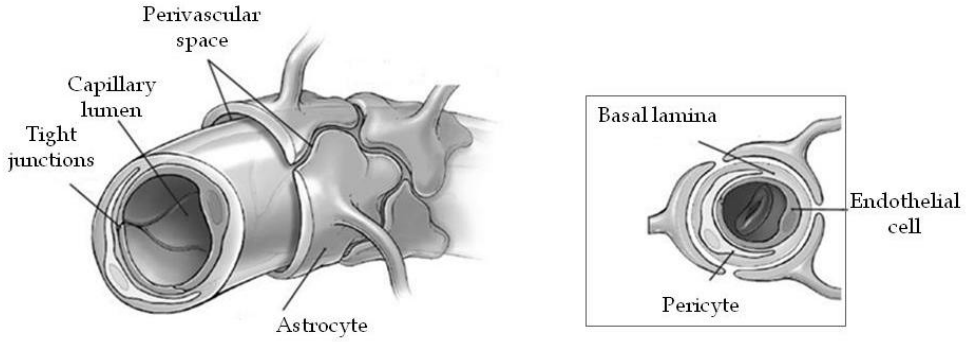

Figure 7. Schematic representation of a brain capillary. The BBB is formed by capillary endothelial cells, surrounded by a basal membrane and astrocytic perivascular end-feet. Tight junctions between the cerebral endothelial cells form a diffusion barrier, which severely restricts the penetration of water soluble compounds, including polar drugs, into the brain. Astrocytic end-feet appear to be critical for the induction and maintenance of the endothelial barrier. Furthermore, pericytes intimately embrace the brain capillaries and seem to contribute to the development, maintenance, and regulation of the BBB. The tightness of the endothelial barrier results in the paracellular transport of substances being negligible under physiological conditions. (Adapted from *J. Pharm. Pharmaceut. Sci.* **2003**, 6(*2*), 252-273.)

To bypass the BBB and deliver drugs to the brain, several strategies have been used: temporarily opening the BBB, administration of very high doses of a drug and direct injection of a drug into the spinal cord. However, these approaches imply risks of infection and toxicity. Other strategies have been developed such as modifying the structure of a drug to increase its permeability by passive diffusion. Another option is to couple a drug to a "Trojan horse", a compound that passes the BBB by receptor-mediated transcytosis (RMT) and can carry the drug across the barrier.[50,54,57-59]

There are several *in vitro* methods and computational models that have been used in drug discovery to predict the BBB penetration potential of test compounds. *In vitro* methods include log P /log D,[60] D log P,[61] immobilized artificial membrane (IAM),[62] polar surface area (PSA),[63] linear free energy equations,[64,65] surface tension,[66,67] and membrane permeability across cell culture systems.[68] These methods are useful, but the reliability of prediction and resources required may be limiting.

There are also numerous cell-based assays to predict the permeability of compounds across the BBB, such as bovine brain microvessel endothelial cells (BBMEC),[69,70] porcine brain microvessel endothelial cells (PBMEC),[71,72] rat brain microvascular endothelial cells (rBMEC)[73] and Madin Darby canine kidney cells (MDCK).[74] Despite these cell methods have the advantage to incorporate both passive transport and active transporters, their application, as a high throughput screening tool, is limited by the elaborate membrane preparation and cost of resources.

1.2.1. BBB permeability by passive diffusion

This is a non-saturable and spontaneous transport process. It has been reported that some small lipophilic molecules (< 400 Da) cross the BBB by this mechanism, but most molecules do not. The classical approach of medicinal chemistry to bypass this limitation is the modification of the molecules in order to increase their lipid solubility by blocking hydrogen bond-forming groups on the parent drug molecule. A gain in lipid solubility increases permeation across all biological membranes of the body, including the BBB, thus

potentially leading to side effects. Moreover, lipidization may enhance binding to plasma proteins, which could offset the increase in membrane permeation caused by greater lipid solubility. Nevertheless, many plasma protein-bound drugs are available for transport across the BBB *in vivo* via a mechanism of enhanced dissociation at the brain capillary endothelial surface.[75]

Recent years have witnessed several key advances in the development of peptides as therapeutic agents and drug carriers for brain disorders. Although from a classical point of view passive diffusion has been considered probable only for small molecules, peptides are no longer considered too large to cross the BBB. Many large peptides cross this barrier by simple diffusion;[76-80] therefore molecular weight does not appear to be the only key point for peptide penetration into the brain. Indeed, some peptides have already been used to shuttle drugs into the CNS.[76,81,82] In general, shuttles with the ability to cross the BBB by passive diffusion do so because of its unique physicochemical properties. If the cargo linked to the BBB-shuttle is a small molecule that does not affect the properties of the shuttle, then the latter will be able to transport the cargo into the CNS. In contrast, if the cargo affects the physical and/or chemical properties of the shuttle, which is likely to happen with nanoparticles, proteins or peptides, the cargo will not penetrate the BBB.

1.2.2. BBB permeability by active transport: *carried-mediated transport (CMT)*

This is a saturable and energy-dependent mechanism. Endothelial membranes contain several specific transport (carrier) proteins that provide essential nutrients and endogenous compounds to the brain. These transport systems include the glucose transporters, large neutral and cationic amino acid transporters and nucleoside transporters, to mention a few.[83] CMT systems are potential points of drug entry to the brain, but these are highly stereospecific pore-based transporters and there are significant structural requirements for transport affinity. The medicinal chemistry approach to achieve drug delivery to the brain by means of CMT has been the modification of the structure of drugs to resemble the native substrate of the transporter. The challenge is to preserve the activity of the drug after these modifications.[84] An alternative approach is to link a cargo to a substrate of a given endogenous transporter system. Since CMT is highly substrate structure-specific, it is difficult to make a drug that is normally not transported across the BBB transportable by the simple coupling to a substrate of a given transporter. However, there are some examples of drug delivery into the CNS that include linking the drug to a substrate of a CMT system.[85,86]

Glycosylation of the linear opioid peptide H-Tyr-D-Thr-Gly-Phe-Leu-Ser-NH_2 on Ser6 or the attachment of various sugar moieties to the cyclic opioid peptide enkephalin increases their penetration and allows the resulting glycopeptide analogs to function as analgesic drugs. This finding could be attributed, at least in part, to the transport of the analogs by the glucose transporter GLUT-1 and to the organic anion-transporting polypeptide transporter (OATP).[87,88]

CMT requires high affinity consequently, the cargo conjugated to a BBB-shuttle that crosses the barrier by this mechanism should preserve substrate ability to be recognized by the receptor. Even when recognition is preserved, the drug-BBB shuttle construct might

have insufficient affinity for a BBB transporter to achieve significant uptake and/or transport across the BBB. In addition, it might be limited by competition with endogenous substrates. Since CMT is highly stereospecific, it is not particularly amenable for the transport of large-molecule therapeutics.

1.2.3. Receptor-mediated transcytosis (RMT)

Although CMT is a highly selective way to overcome the BBB is limited to small cargos, whereas the RMT is not limited for the size of the cargos and represents one of the most promising mechanisms to transport cargos across the BBB. This system enables large molecules such as peptides, proteins and nucleic acids to specifically enter the brain, since this approach uses vesicle-based transport rather than a stereoselective carrier. Three types of receptors are present on brain endothelial cells: bi-directional receptors, reverse receptors and receptor-mediated endocytosis systems.[84] In terms of the delivery of compounds to the brain, the most interesting are the bi-directional receptors. Some of these receptors are well known and have been used for the delivery of various types of cargo into the CNS. The most important receptors are represented by: transferrin receptor, insulin receptor, low-density lipoprotein receptor, nicotinic acetylcholine receptor, membrane-bound precursor heparin binding epidermal growth factor, lactotransferrin receptor and leptin receptor. Among all of them, transferrin receptor (TfR) is one of the most widely studied receptor for drug targeting. TfR is expressed in practically all the cells of the body, including brain capillaries and it mediates the delivery of iron to the brain.[89] Despite its expression differs depending on the cell type,[90] in general, highly proliferating cells, such as cancer cells, overexpress TfR because of their increased metabolism.[91] This makes TfR very attractive for drug targeting and explains why it has received so much attention for drug delivery.

References

(1) http://WWW.cancerhelp.org.uk.

(2) Ferrara, N.; Kerbel, R. S. Angiogenesis as a therapeutic target. *Nature* **2005**, *438*, 967-974.

(3) Ferrara, N. Vascular Endothelial Growth Factor as a Target for Anticancer Therapy. *The Oncologist* **2004**, *9*, 2-10.

(4) Folkman, J. Tumor angiogenesis: therapeutic implications. *New Eng. J. Med.* **971**, *285*, 1182-1186.

(5) Folkman, J. Angiogenesis: an organizing principle for drug discovery? *Nat. Rev. Drug Discov.* **2007**, *6*, 273-286.

(6) Grothey, A.; Galanis, E. Targeting angiogenesis: progress with anti-VEGF treatment with large molecules. *Nat. Rev. Clin. Oncol.* **2009**, *6*, 507-518.

(7) Ferrara, N.; Gerber, H.-P.; Le Couter, J. The biology of VEGF and its receptors. *Nat. Med.* **2003**, *9*, 669-676.

(8) Hoeben, A.; Landuyt, B.; Highley, M. S.; Wildiers, H.; Van Oosterom, A. T.; De Bruijn, E. A. Vascular Endothelial Growth Factor and Angiogenesis. *Pharmacol. Rev.* **2004**, *56*, 549-580.

(9) Ellis, L. M.; Hicklin, D. J. VEGF-targeted therapy: mechanisms of anti-tumour activity. *Nature Rev. Cancer* **2008**, *8*, 579-591.

(10) Lu, N.; Gao, Y.; Ling, Y.; Chen, Y.; Yang, Y.; Gu, H.-Y.; Qi, Q.; Liu, W.; Wang, X.-T.; You, Q.-D.; Guo, Q.-L. Wogonin suppresses tumor growth in vivo and VEGF-induced angiogenesis through inhibiting tyrosine phosphorylation of VEGFR2. *Life Sci.* **2008**, *82*, 956-963.

(11) Brazelle, W. D.; Shi, W.; Siemann, D. W. VEGF-associated tyrosine kinase inhibition increases the tumor response to single and fractionated dose radiotherapy. *Int. J. Radiat. Onc. Biol. Phys.* **2006**, *65*, 836-841.

(12) Fairbrother, W. J.; Christinger, H. W.; Cochran, A. G.; Fuh, G.; Keenan, C. J.; Quan, C.; Shriver, S. K.; Tom, J. Y. K.; Wells, J. A.; Cunningham, B. C. Novel Peptides Selected to Bind Vascular Endothelial Growth Factor Target the Receptor-Binding Site. *Biochemistry* **1998**, *37*, 17754-17764.

(13) Muhsin, M.; Graham, J.; Kirkpatrick, P. Bevacizumab. *Nat. Rev. Drug Discov.* **2004**, *3*, 995-996.

(14) Narayanan, R.; Kuppermann, B. D.; Jones, C.; Kirkpatrick, P. Ranibizumab. *Nat. Rev. Drug Discov.* **2006**, *5*, 815-816.

(15) Ng, E. W. M.; Shima, D. T.; Calias, P.; Cunningham, E. T.; Guyer, D. R.; Adamis, A. P. Pegaptanib, a targeted anti-VEGF aptamer for ocular vascular disease. *Nat. Rev. Drug Discov.* **2006**, *5*, 123-132.

(16) Andreoli, C. M.; Miller, J. W. Anti-vascular endothelial growth factor therapy for ocular neovascular disease. *Curr. Opin. Ophthalmol.* **2007**, *18*, 502-508.

(17) Arkin, M. R.; Wells, J. A. Small-molecule inhibitors of protein-protein interactions: progressing towards the dream. *Nat. Rev. Drug Discov.* **2004**, *3*, 301-317.

(18) Fry, D. C. Protein–protein interactions as targets for small molecule drug discovery. *Peptide Sci.* **2006**, *84*, 535-552.

(19) Whitty, A.; Kumaravel, G. Between a rock and a hard place? *Nat. Chem. Biol.* **2006**, *2*, 112-118.

(20) Ferrara, N. VEGF as a therapeutic target in cancer. *Oncology* **2005**, *69 Suppl 3*, 11-16.

(21) Lemmon, M. A. Ligand-induced ErbB receptor dimerization. *Exp. Cell Res.* **2009**, *315*, 638-648.
(22) Ogiso, H.; Ishitani, R.; Nureki, O.; Fukai, S.; Yamanaka, M.; Kim, J. H.; Saito, K.; Sakamoto, A.; Inoue, M.; Shirouzu, M.; Yokoyama, S. Crystal structure of the complex of human epidermal growth factor and receptor extracellular domains. *Cell* **2002**, *110*, 775-787.
(23) Dawson, J. P.; Berger, M. B.; Lin, C. C.; Schlessinger, J.; Lemmon, M. A.; Ferguson, K. M. Epidermal growth factor receptor dimerization and activation require ligand-induced conformational changes in the dimer interface. *Mol. Cell. Biol.* **2005**, *25*, 7734-7742.
(24) Holbro, T.; Civenni, G.; Hynes, N. E. The ErbB receptors and their role in cancer progression. *Exp. Cell Res.* **2003**, *284*, 99-110.
(25) Desai, M. D.; Saroya, B. S.; Lockhart, A. C. Investigational therapies targeting the ErbB (EGFR, HER2, HER3, HER4) family in GI cancers. *Expert opinion on investigational drugs* **2013**, *22*, 341-356.
(26) Mendelsohn, J.; Baselga, J. Epidermal growth factor receptor targeting in cancer. *Seminars in oncology* **2006**, *33*, 369-385.
(27) Galizia, G.; Lieto, E.; De Vita, F.; Orditura, M.; Castellano, P.; Troiani, T.; Imperatore, V.; Ciardiello, F. Cetuximab, a chimeric human mouse anti-epidermal growth factor receptor monoclonal antibody, in the treatment of human colorectal cancer. *Oncogene* **2007**, *26*, 3654-3660.
(28) Li, S.; Schmitz, K. R.; Jeffrey, P. D.; Wiltzius, J. J.; Kussie, P.; Ferguson, K. M. Structural basis for inhibition of the epidermal growth factor receptor by cetuximab. *Cancer cell* **2005**, *7*, 301-311.
(29) Voigt, M.; Braig, F.; Gothel, M.; Schulte, A.; Lamszus, K.; Bokemeyer, C.; Binder, M. Functional dissection of the epidermal growth factor receptor epitopes targeted by panitumumab and cetuximab. *Neoplasia* **2012**, *14*, 1023-1031.
(30) Inoue, A.; Saijo, Y.; Maemondo, M.; Gomi, K.; Tokue, Y.; Kimura, Y.; Ebina, M.; Kikuchi, T.; Moriya, T.; Nukiwa, T. Severe acute interstitial pneumonia and gefitinib. *Lancet* **2003**, *361*, 137-139.
(31) Mendez, M.; Custodio, A.; Provencio, M. New molecular targeted therapies for advanced non-small-cell lung cancer. *J. Thoracic Disease* **2011**, *3*, 30-56.
(32) Xu, R.; Povlsen, G. K.; Soroka, V.; Bock, E.; Berezin, V. A peptide antagonist of the ErbB1 receptor inhibits receptor activation, tumor cell growth and migration in vitro and xenograft tumor growth in vivo. *Cellular oncology* **2010**, *32*, 259-274.
(33) Mizuguchi, T.; Ohara, N.; Iida, M.; Ninomiya, R.; Wada, S.; Kiso, Y.; Saito, K.; Akaji, K. Evaluation of dimerization-inhibitory activities of cyclic peptides containing a beta-hairpin loop sequence of the EGF receptor. *Bioorg. Med. Chem:* **2012**, *20*, 5730-5737.
(34) Yang, R. Y.; Yang, K. S.; Pike, L. J.; Marshall, G. R. Targeting the dimerization of epidermal growth factor receptors with small-molecule inhibitors. *Chem. Biol. Drug Design* **2010**, *76*, 1-9.
(35) Yang, X.; Kessler, E.; Su, L. J.; Thorburn, A.; Frankel, A. E.; Li, Y.; La Rosa, F. G.; Shen, J.; Li, C. Y.; Varella-Garcia, M.; Glode, L. M.; Flaig, T. W. Diphtheria toxin-epidermal growth factor fusion protein DAB389EGF for the treatment of bladder cancer. *Clin. Cancer Res.* **2013**, *19*, 148-157.
(36) Huang, H. W.; Mohan, S. K.; Yu, C. The NMR solution structure of human epidermal growth factor (hEGF) at physiological pH and its interactions with suramin. *Biochem. Biophysic. Res. Comm.* **2010**, *402*, 705-710.

(37) Fujiuchi, S.; Ohsaki, Y.; Kikuchi, K. Suramin inhibits the growth of non-small-cell lung cancer cells that express the epidermal growth factor receptor. *Oncology* **1997**, *54*, 134-140.
(38) Alexander, B. M.; Lee, E. Q.; Reardon, D. A.; Wen, P. Y. Current and future directions for Phase II trials in high-grade glioma. *Expert Rev. of neurotherapeutics* **2013**, *13*, 369-387.
(39) Middaugh, C. R.; Mach, H.; Burke, C. J.; Volkin, D. B.; Dabora, J. M.; Tsai, P. K.; Bruner, M. W.; Ryan, J. A.; Marfia, K. E. Nature of the interaction of growth factors with suramin. *Biochemistry* **1992**, *31*, 9016-9024.
(40) Coffey, R. J., Jr.; Leof, E. B.; Shipley, G. D.; Moses, H. L. Suramin inhibition of growth factor receptor binding and mitogenicity in AKR-2B cells. *J. Cell. Physiol.* **1987**, *132*, 143-148.
(41) Cheson, B. D.; Levine, A. M.; Mildvan, D.; Kaplan, L. D.; Wolfe, P.; Rios, A.; Groopman, J. E.; Gill, P.; Volberding, P. A.; Poiesz, B. J.; et al. Suramin therapy in AIDS and related disorders. Report of the US Suramin Working Group. *J. Am. Med. Ass.* **1987**, *258*, 1347-1351.
(42) La Rocca, R. V.; Stein, C. A.; Danesi, R.; Myers, C. E. Suramin, a novel antitumor compound. *J. Steroid. Biochem.* **1990**, *37*, 893-898.
(43) Hosang, M. Suramin binds to platelet-derived growth factor and inhibits its biological activity. *J. Cell. Biochem.* **1985**, *29*, 265-273.
(44) Koide, H.; Muto, Y.; Kasai, H.; Kohri, K.; Hoshi, K.; Takahashi, S.; Tsukumo, K.; Sasaki, T.; Oka, T.; Miyake, T.; et al. A site-directed mutagenesis study on the role of isoleucine-23 of human epidermal growth factor in the receptor binding. *Biochim. Biophys. Acta* **1992**, *1120*, 257-261.
(45) Engler, D. A.; Campion, S. R.; Hauser, M. R.; Cook, J. S.; Niyogi, S. K. Critical functional requirement for the guanidinium group of the arginine 41 side chain of human epidermal growth factor as revealed by mutagenic inactivation and chemical reactivation. *J. Biol. Chem.* **1992**, *267*, 2274-2281.
(46) Ferguson, K. M.; Berger, M. B.; Mendrola, J. M.; Cho, H. S.; Leahy, D. J.; Lemmon, M. A. EGF activates its receptor by removing interactions that autoinhibit ectodomain dimerization. *Mol. Cell* **2003**, *11*, 507-517.
(47) Rubin, L. L.; Staddon, J. M. The cell biology of the blood-brain barrier. *Annual review of neuroscience* **1999**, *22*, 11-28.
(48) Brightman, M. W.; Reese, T. S. Junctions between intimately apposed cell membranes in the vertebrate brain. *J. Cell Bio.* **1969**, *40*, 648-677.
(49) Reese, T. S.; Karnovsky, M. J. Fine structural localization of a blood-brain barrier to exogenous peroxidase. *J. Cell Bio.* **1967**, *34*, 207-217.
(50) Temsamani, J.; Scherrmann, J. M.; Rees, A. R.; Kaczorek, M. Brain drug delivery technologies: novel approaches for transporting therapeutics. *Pharm. Sci. Tech. Today* **2000**, *3*, 155-162.
(51) Witt, K. A.; Gillespie, T. J.; Huber, J. D.; Egleton, R. D.; Davis, T. P. Peptide drug modifications to enhance bioavailability and blood-brain barrier permeability. *Peptides* **2001**, *22*, 2329-2343.
(52) Alavijeh, M. S.; Chishty, M.; Qaiser, M. Z.; Palmer, A. M. Drug metabolism and pharmacokinetics, the blood-brain barrier, and central nervous system drug discovery. *NeuroRx: J. Am. Soc. Exp. NeuroTherapeutics* **2005**, *2*, 554-571.
(53) Pardridge, W. M. Blood-brain barrier delivery. *Drug Discov. Today* **2007**, *12*, 54-61.
(54) Egleton, R. D.; Davis, T. P. Bioavailability and transport of peptides and peptide drugs into the brain. *Peptides* **1997**, *18*, 1431-1439.

(55) Pardridge, W. M. CNS drug design based on principles of blood-brain barrier transport. *J. Neurochem.* **1998**, *70*, 1781-1792.
(56) Tamai, I.; Tsuji, A. Transporter-mediated permeation of drugs across the blood-brain barrier. *J. Pharm. Sci.* **2000**, *89*, 1371-1388.
(57) Scherrmann, J. M. Drug delivery to brain via the blood–brain barrier. *Vascular Pharmacology* **2002**, *38*, 349-354.
(58) Abbott, N. J.; Romero, I. A. Transporting therapeutics across the blood-brain barrier. *Mol. Med. Today* **1996**, *2*, 106-113.
(59) Rousselle, C.; Clair, P.; Lefauconnier, J. M.; Kaczorek, M.; Scherrmann, J. M.; Temsamani, J. New advances in the transport of doxorubicin through the blood-brain barrier by a peptide vector-mediated strategy. *Mol. Pharmacol.* **2000**, *57*, 679-686.
(60) Levin, V. A. Relationship of octanol/water partition coefficient and molecular weight to rat brain capillary permeability. *J. Med. Chem.* **1980**, *23*, 682-684.
(61) Young, R. C.; Mitchell, R. C.; Brown, T. H.; Ganellin, C. R.; Griffiths, R.; Jones, M.; Rana, K. K.; Saunders, D.; Smith, I. R.; Sore, N. E.; et al. Development of a new physicochemical model for brain penetration and its application to the design of centrally acting H2 receptor histamine antagonists. *J. Med. Chem.* **1988**, *31*, 656-671.
(62) Reichel, A.; Begley, D. J. Potential of immobilized artificial membranes for predicting drug penetration across the blood-brain barrier. *Pharmaceut. Res.* **1998**, *15*, 1270-1274.
(63) Clark, D. E. Rapid calculation of polar molecular surface area and its application to the prediction of transport phenomena. 2. Prediction of blood-brain barrier penetration. *J. Pharm. Sci.* **1999**, *88*, 815-821.
(64) Platts, J. A.; Abraham, M. H.; Zhao, Y. H.; Hersey, A.; Ijaz, L.; Butina, D. Correlation and prediction of a large blood-brain distribution data set-an LFER study. *Eur. J. Med. Chem.* **2001**, *36*, 719-730.
(65) Gratton, J. A.; Abraham, M. H.; Bradbury, M. W.; Chadha, H. S. Molecular factors influencing drug transfer across the blood-brain barrier. *J. Pharm. Pharmacol.* **1997**, *49*, 1211-1216.
(66) Fischer, H.; Gottschlich, R.; Seelig, A. Blood-brain barrier permeation: molecular parameters governing passive diffusion. *J. Membr.Biol.* **1998**, *165*, 201-211.
(67) Seelig, A.; Gottschlich, R.; Devant, R. M. A method to determine the ability of drugs to diffuse through the blood-brain barrier. *PNAS* **1994**, *91*, 68-72.
(68) Audus, K. L.; Ng, L.; Wang, W.; Borchardt, R. T. Brain microvessel endothelial cell culture systems. *Pharm. Biotech.* **1996**, *8*, 239-258.
(69) Otis, K. W.; Avery, M. L.; Broward-Partin, S. M.; Hansen, D. K.; Behlow, H. W., Jr.; Scott, D. O.; Thompson, T. N. Evaluation of the BBMEC model for screening the CNS permeability of drugs. *J. Pharmacol. Toxicol. Methods* **2001**, *45*, 71-77.
(70) Hansen, D. K.; Scott, D. O.; Otis, K. W.; Lunte, S. M. Comparison of in vitro BBMEC permeability and in vivo CNS uptake by microdialysis sampling. *J. Pharm. Biomed. Anal.* **2002**, *27*, 945-958.
(71) Franke, H.; Galla, H. J.; Beuckmann, C. T. An improved low-permeability in vitro-model of the blood-brain barrier: transport studies on retinoids, sucrose, haloperidol, caffeine and mannitol. *Brain Res.* **1999**, *818*, 65-71.
(72) Zhang, Y.; Li, C. S.; Ye, Y.; Johnson, K.; Poe, J.; Johnson, S.; Bobrowski, W.; Garrido, R.; Madhu, C. Porcine brain microvessel endothelial cells as an in vitro model to predict in vivo blood-brain barrier permeability. *Drug metab. Disp.* **2006**, *34*, 1935-1943.

(73) Sun, J. J.; Xie, L.; Liu, X. D. Transport of carbamazepine and drug interactions at blood-brain barrier. *Acta Pharm. Sinic.* **2006**, *27*, 249-253.
(74) Mahar Doan, K. M.; Humphreys, J. E.; Webster, L. O.; Wring, S. A.; Shampine, L. J.; Serabjit-Singh, C. J.; Adkison, K. K.; Polli, J. W. Passive permeability and P-glycoprotein-mediated efflux differentiate central nervous system (CNS) and non-CNS marketed drugs. *J. Pharmacol. Exp. Ther.* **2002**, *303*, 1029-1037.
(75) Pardridge, W. M. Brain Drug Targeting: The Future of Brain Drug Development. *Cambridge University Press, Cambridge, U.K., 1-12.* **2001**.
(76) Teixido, M.; Zurita, E.; Malakoutikhah, M.; Tarrago, T.; Giralt, E. Diketopiperazines as a tool for the study of transport across the blood-brain barrier (BBB) and their potential use as BBB-shuttles. *J. Am. Chem. Soc.* **2007**, *129*, 11802-11813.
(77) Gray, R. A.; Vander Velde, D. G.; Burke, C. J.; Manning, M. C.; Middaugh, C. R.; Borchardt, R. T. Delta-sleep-inducing peptide: solution conformational studies of a membrane-permeable peptide. *Biochemistry* **1994**, *33*, 1323-1331.
(78) Abbruscato, T. J.; Thomas, S. A.; Hruby, V. J.; Davis, T. P. Blood-brain barrier permeability and bioavailability of a highly potent and mu-selective opioid receptor antagonist, CTAP: comparison with morphine. *J. Pharmacol. Exp. Ther.* **1997**, *280*, 402-409.
(79) Banks, W. A.; Schally, A. V.; Barrera, C. M.; Fasold, M. B.; Durham, D. A.; Csernus, V. J.; Groot, K.; Kastin, A. J. Permeability of the murine blood-brain barrier to some octapeptide analogs of somatostatin. *PNAS* **1990**, *87*, 6762-6766.
(80) Dogrukol-Ak, D.; Banks, W. A.; Tuncel, N.; Tuncel, M. Passage of vasoactive intestinal peptide across the blood-brain barrier. *Peptides* **2003**, *24*, 437-444.
(81) Malakoutikhah, M.; Teixido, M.; Giralt, E. Toward an optimal blood-brain barrier shuttle by synthesis and evaluation of peptide libraries. *J. Med. Chem.* **2008**, *51*, 4881-4889.
(82) Malakoutikhah, M.; Prades, R.; Teixido, M.; Giralt, E. N-methyl phenylalanine-rich peptides as highly versatile blood-brain barrier shuttles. *J. Med. Chem.* **2010**, *53*, 2354-2363.
(83) Tsuji, A.; Tamai, I. I. Carrier-mediated or specialized transport of drugs across the blood-brain barrier. *Adv. Drug Deliv. Rev.* **1999**, *36*, 277-290.
(84) Pardridge, W. M. The blood-brain barrier: bottleneck in brain drug development. *NeuroRx : J. Am. Soc. Exp. NeuroTherapeutics* **2005**, *2*, 3-14.
(85) Bonina, F. P.; Arenare, L.; Palagiano, F.; Saija, A.; Nava, F.; Trombetta, D.; de Caprariis, P. Synthesis, stability, and pharmacological evaluation of nipecotic acid prodrugs. *J. Pharm. Sci* **1999**, *88*, 561-567.
(86) Gynther, M.; Laine, K.; Ropponen, J.; Leppanen, J.; Mannila, A.; Nevalainen, T.; Savolainen, J.; Jarvinen, T.; Rautio, J. Large neutral amino acid transporter enables brain drug delivery via prodrugs. *J. Med. Chem.* **2008**, *51*, 932-936.
(87) Egleton, R. D.; Mitchell, S. A.; Huber, J. D.; Janders, J.; Stropova, D.; Polt, R.; Yamamura, H. I.; Hruby, V. J.; Davis, T. P. Improved bioavailability to the brain of glycosylated Met-enkephalin analogs. *Brain Res.* **2000**, *881*, 37-46.
(88) Egleton, R. D.; Mitchell, S. A.; Huber, J. D.; Palian, M. M.; Polt, R.; Davis, T. P. Improved blood-brain barrier penetration and enhanced analgesia of an opioid peptide by glycosylation. *J. Pharmacol. Exp. Ther.* **2001**, *299*, 967-972.
(89) Skarlatos, S.; Yoshikawa, T.; Pardridge, W. M. Transport of [125I]transferrin through the rat blood-brain barrier. *Brain Res.* **1995**, *683*, 164-171.
(90) Qian, Z. M.; Li, H.; Sun, H.; Ho, K. Targeted drug delivery via the transferrin receptor-mediated endocytosis pathway. *Pharmacol. Rev.* **2002**, *54*, 561-587.

(91) Miyamoto, T.; Tanaka, N.; Eishi, Y.; Amagasa, T. Transferrin receptor in oral tumors. *Int. J. Oral Max. Surg.* **1994**, *23*, 430-433.

Chapter 2

Results and discussion

2.1 Aim of the work

Peptides are considered excellent candidates for the recognition of proteins surface; indeed, over the last few years, many examples showing the ability of peptides to recognize efficiently the surface regions on relevant proteins have been reported.[1-3]

Inspired by those works, we have focussed our attention on this class of molecules to develop novel pharmacological compounds able to selectively bind the proteins surface of EGF and VEGF. This competitive interaction will prevent the proteins to bind with the respective receptor and, as a consequence, will affect the protein activity towards the glioma progression.

We have designed an explorative library of cyclic hexapeptides, named "EXORIS", as rigid scaffolds bearing the functional groups involved in the protein interaction. These small cyclohexapeptides could act as ligand traps binding to EGF or VEGF.

Cyclic peptides present well-known advantages compared to the linear one. Among them, the cyclization enables to reduce the conformational space, to increase the binding affinity and selectivity to a receptor and enhances the stability of the peptide toward the proteases.

We have been focussed on symmetric cyclic hexapeptides because of their straightforward synthesis and also due to the reduced conformational space required starting from the C_2 symmetry.

The insertion of prolines and D-amino acids as β-turn motifs was also evaluated to confer structural rigidity and to promote the cyclization. In addition, D-amino acids provide resistance towards proteases and proline promotes the transport and BBB permeability.

The library has been developed considering a representative reduce dataset composed by seven different amino acids (Trp, Glu, Ile, Arg, Ser, Val, Pro) that were chosen to represent all the proteinogenic amino acids. Based on these residues, it was possible to identify 36 different cyclic peptides and, in addition, one epimer was synthesized for each combination. The epimer allows the detection of side-reactions during the cyclization step (*C*-terminal epimerization) and the exploration of the protein binding interaction when the symmetry is broken.

2.2. Reaction set up

2.2.1. Diketopiperazine (DKP) evaluation

A preliminary investigation was performed to evaluate the more efficient way to start the synthesis of the linear peptide, taking into account that using a proline as *C*-terminal prevents the epimerization but, on the other hand, could lead to the formation of diketopiperazine (DKP). This side reaction is more relevant especially when D and L amino acids are alternate as first and second residues along the peptide sequence (D-Pro-L-XXa or L-XXa-D-Pro).[4]

The studies on the DKP formations were performed with different peptide sequences and the amount of DKP was quantified by UV intensities of the Fmoc group. The obtained results (Table **1**) show that when Fmoc group is removed under standard conditions (**a)** the DKP amount reaches 50%. The DKP formation is lowered but not prevented using the same conditions with shorter cleavage time (**b**) followed by a subsequent coupling with a

large excess (6 eq) of the third amino acid. These results evidenced that the use of D-proline as *C*-terminal was not a suitable choice.

Peptide Sequence	Fmoc cleavage	% DKP
H-Arg-**D**-Trp-Pro-OH	a	50
H-Ala-Ser(*t*Bu)-Pro-OH	b	9
H-Ala-**D**-Ser(*t*Bu)-Pro-OH	b	8
H-Gly-Ala-**D**-Pro–OH	b	21
H-Ser(*t*Bu)-Ala-**D**-Pro-OH	b	42

Table 1. Linear peptides subjected to investigation of DKP formation. Cleavage conditions: ***a***: 20% piperidine in DMF: 2 cycles of 10 minutes followed by coupling with 3 eq of the third amino acid. ***b*** 20% piperidine in DMF, 2 cycles of 2 minutes followed by coupling with 6 eq of the third amino acid.

2.2.2. Investigation of D-amino acids position along the sequence

Additional studies were performed to evaluate the best relative position along the peptide chain in which the D-amino acids and the proline can promote the peptide cyclization, considering that these residues will be common elements in within the cyclic hexapeptides library.

Keeping the C_2 symmetry, peptide analogues, characterized by the same amino acid composition but shifting the D-residues position along the chain, were synthesized. Moreover, the sequence with all natural amino acids was also synthesized as negative control to evaluate the real efficiency of the D-amino acid to induce the cyclization.

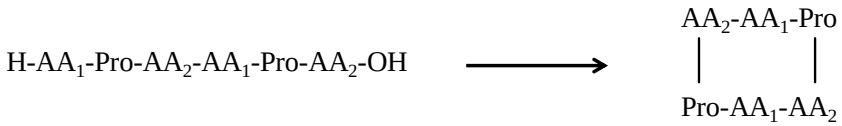

Figure 1. General scheme of the investigated peptide sequences.

The cyclization of the different analogues, were performed using two different coupling reagents system: DPPA (Diphenylphosphoryl azide) and PS-DCC (N'-methyl polystyrene supported N-Cyclohexylcarbodiimide) in order to identify the synthetic procedure that maximize the cyclo peptide yield and purity.

The polymer-supported activating reagent, PS-DCC, was chosen due to the possibility to remove both the coupling reagent and its related by-products bound to the polymer support by easy filtration. This allows a fast recovery of the final product and an easier purification.

DPPA (Diphenylphosphonic azide) was selected as an efficient condensing reagent for peptide cyclization because it allows the use of an inorganic base ($NaHCO_3$) which can be removed by filtration and does not interfere in the following side chain deprotection step, avoiding the formation of undesired by-products.

n	Peptide sequence	PS-DCC (h)	DPPA (h)
1a	H-Trp(Boc)-Pro-Arg(Pbf)-Trp(Boc)-Pro-Arg(Pbf)-OH	> 96	36
1b	H-**D**-Trp(Boc)-Pro-Arg(Pbf)-**D**-Trp(Boc)-Pro-Arg(Pbf)-OH	48	24
1c	H-Trp(Boc)-**D**-Pro-Arg(Pbf)-Trp(Boc)-**D**-Pro-Arg(Pbf)-OH	-	4
1d	H-Trp(Boc)-Pro-**D**-Arg(Pbf)-Trp(Boc)-Pro-**D**-Arg(Pbf)-OH	-	18
2a	H-Arg(Pbf)-Pro-Trp(Boc)-Arg(Pbf)-Pro-Trp(Boc)-OH	> 96	36
2b	H-**D**-Arg(Pbf)-Pro-Trp(Boc)-**D**-Arg(Pbf)-Pro-Trp(Boc)-OH	48	24
2c	H-Arg(Pbf)-**D**-Pro-Trp(Boc)-Arg(Pbf)-**D**-Pro-Trp(Boc)-OH	-	4
2d	H-Arg(Pbf)-Pro-**D**-Trp(Boc)-Arg(Pbf)-Pro-**D**-Trp(Boc)-OH	-	18

Table 2. Cyclization results relative to the D-amino acids position along the sequence. **PS-DCC**: cyclization reaction time (h) using PS-DCC (18 eq), DIPEA(18 eq), DCM-DMF/4:1 [50 mM], 37°C. **DPPA**: cyclization reaction time (h) using DPPA (2 eq), $NaHCO_3$ (8 eq), DMF [5 mM], r.t.

2.2.3. N'-methyl polystyrene supported N-Cyclohexylcarbodiimide PS-DCC

The cyclization reaction with the polystirene supported *N*-Cyclohexylcarbodiimide was performed initially using a large excess (18 eq) of condensing agent, in high diluted DCM solution [5 mM] at room temperature. The reaction progress was monitored by HLPC and after 96 hours the reactions were not yet completed. Thus has been evaluated to change the reaction conditions in order to push the cyclization. A second trial was performed using the same equivalents of condensing agent together with a basic medium DIEA (18 eq), in a more concentrated solution (DCM-DMF/4:1) [50 mM] at 37°C. The obtained results show that, under these last conditions, the reactions involving the linear peptides with a D-amino acid were completed in 48 h, whereas the sequences with all natural amino acids required more than 96 hours to achieve a complete cyclization.
These data underline how the presence of a D-amino acid in the sequence is essential in promoting the peptide cyclization.

2.2.4. Diphenylphosphonic azide (DPPA)

The cyclization using DPPA was carried out in high DMF dilution [5 mM], using 2 eq of condensing agent associate with $NaHCO_3$ (8 eq) as an inorganic base.
The experimental results show that, as expected, the introduction of a D-amino acid speed up the reaction. Whereas related to the position of D-amino acid respected to the proline, the data revealed that the linear peptide containing a D-amino acid in the position (*i*+1) leads to the cyclic peptide with a reaction time slightly lower than those with a D-amino acid shifted in position (*i*+2).
However, the best results were obtained when a D-proline was present along the sequence, obtaining the desired product in just 4 h.

Based on the experimental results, the DPPA method was selected for the synthesis of the cyclic hexapeptide library due to the fact that, in association with two D-prolines in the peptide sequence, reduces the cyclization time and produces fairly pure crudes.

2.2.5. The role of protecting groups on the cyclization

The side chain bulky effect of the protecting groups on the peptide reactivity was also investigated during the preliminary investigation.
Some unprotected linear peptides, were subjected to cyclization under the same reaction conditions shown before using both PS-DCC and DPPA. The obtained results show that, independently of the peptide sequence, the cyclization of unprotected linear peptides, lead to the formation of many by-products and crudes with low quality, suggesting that the functional groups on the peptide side chain could be involved in side reactions. The side chain reactions may compete with the cyclization, extending the reaction time and promoting the by-products formation.

n	**Peptide sequence**	**PS-DCC**		**DPPA**	
		Time (h)	**Purity %**	**Time (h)**	**Purity %**
1a'	H-Trp-Pro-Arg-Trp-Pro-Arg-OH	> 96	< 50	24	40
1b'	H-**D**-Trp-Pro-Arg-**D**-Trp-Pro-Arg-OH	> 96	< 50	36	70
2a'	H-Arg-Pro-Trp-Arg-Pro-Trp-OH	> 96	< 50	24	45
2b'	H-**D**-Arg-Pro-Trp-**D**-Arg-Pro-Trp-OH	> 96	< 50	24	70

Table 3. Side chain protecting groups effect on peptide cyclization yield. **PS-DCC**: Time (h) is the cyclization reaction time expressed in hours using PS-DCC (18 eq), DIPEA (18 eq), DCM-DMF/4:1 [50 mM], 37°C. **DPPA**: Time (h) is the cyclization reaction time expressed in hours, using DPPA (2 eq), $NaHCO_3$ (8 eq), DMF [5 mM]. The purities for both methodologies were determined by analytical HPLC analysis (peaks detected at λ=220 nm).

The best conditions and the definition of the synthetic approach for the development of the hexacyclic peptide library were identified based on the data obtained during this first stage. The key points of the optimized synthetic procedure are represented by the introduction of D-proline as D-residues along the sequence (but not as first amino acid to avoid the DKP formation) and to performed the cyclization in solution, on protected linear peptides, using DPPA as coupling reagent.

2.3. Peptide synthesis

2.3.1. Synthesis of the linear peptides

The synthesis of the linear peptides were performed by solid-phase peptide synthesis (SPPS) following the Fmoc/*t*Bu strategy and using all the advantages of solid-phase chemistry.[5] The 2-chlorotrityl chloride resin was chosen as a polymeric support to obtain the side-chain protected linear precursors. The synthesis of the linear peptides started with the *C*-terminal residues loaded on the solid support, then, all the peptide couplings were performed using PyBOP, HOAt and DIPEA in DMF followed by Fmoc deprotection under the standard conditions.
The amino acid couplings and the deprotection steps were monitored by the ninhydrin Kaiser test,[6] the chloranil test[7] or De Clercq,[8] according to the type of amine which should be detected. The cleavage of the peptide from the resin was accomplished by acidolytic treatment with a 2% TFA solution, which retains the protecting groups on the residues side chain.

The HPLC analyses of the crude linear peptides show the high quality of all the crudes which were subjected to the cyclization without any further purification.

n	Linear peptide	Yield %	Purity %
1a	H-Trp(Boc)-Pro-Arg(Pbf)-Trp(Boc)-Pro-Arg(Pbf)-OH	82	83
1a'	H-Trp-Pro-Arg-Trp-Pro-Arg-OH	86	80
1b	H-**D**-Trp(Boc)-Pro-Arg(Pbf)-**D**-Trp(Boc)-Pro-Arg(Pbf)-OH	70	94
1b'	H-**D**-Trp-Pro-Arg-**D**-Trp-Pro-Arg-OH	90	70
1c	H-Trp(Boc)-**D**-Pro-Arg(Pbf)-Trp(Boc)-**D**-Pro-Arg(Pbf)-OH	75	83
1d	H-Trp(Boc)-Pro-**D**-Arg(Pbf)-Trp(Boc)-Pro-**D**-Arg(Pbf)-OH	70	92
2a	H-Arg(Pbf)-Pro-Trp(Boc)-Arg(Pbf)-Pro-Trp(Boc)-OH	77	88
2a'	H-Arg-Pro-Trp-Arg-Pro-Trp-OH	90	83
2b	H-**D**-Arg(Pbf)-Pro-Trp(Boc)-**D**-Arg(Pbf)-Pro-Trp(Boc)-OH	91	90
2b'	H-**D**-Arg-Pro-Trp-**D**-Arg-Pro-Trp-OH	85	70
2c	H-Arg(Pbf)-**D**-Pro-Trp(Boc)-Arg(Pbf)-**D**-Pro-Trp(Boc)-OH	75	90
2d	H-Arg(Pbf)-Pro-**D**-Trp(Boc)-Arg(Pbf)-Pro-**D**-Trp(Boc)-OH	89	73
3a	H-Ser(*t*Bu)-**D**-Pro-Trp(Boc)-Ser(*t*Bu)-**D**-Pro-Trp(Boc)-OH	80	91
3b	H-Ser(*t*Bu)-**D**-Pro-Trp(Boc)-Ser(*t*Bu)-**D**-Pro-**D**-Trp(Boc)-OH	80	90
4a	H-Glu(O*t*Bu)-**D**-Pro-Trp(Boc)-Glu(O*t*Bu)-**D**-Pro-Trp(Boc)-OH	89	87
4b	H-Glu(O*t*Bu)-**D**-Pro-Trp(Boc)-Glu(O*t*Bu)-**D**-Pro-**D**-Trp(Boc)-OH	85	83
5a	H-Ile-**D**-Pro-Trp(Boc)-Ile-**D**-Pro-Trp(Boc)-OH	84	95
5b	H-Ile-**D**-Pro-Trp(Boc)-Ile-**D**-Pro-**D**-Trp(Boc)-OH	78	97
6a	H-Ser(*t*Bu)-**D**-Pro-Glu(O*t*Bu)-Ser(*t*Bu)-**D**-Pro-Glu(O*t*Bu)-OH	88	80
6b	H-Ser(*t*Bu)-**D**-Pro-Glu(O*t*Bu)-Ser(*t*Bu)-**D**-Pro-**D**-Glu(O*t*Bu)-OH	80	80
7a	H-Ser(*t*Bu)-**D**-Pro-Ile-Ser(*t*Bu)-**D**-Pro-Ile-OH	80	94
8a	H-Glu(O*t*Bu)-**D**-Pro-Ile-Glu(O*t*Bu)-**D**-Pro-Ile-OH	77	95

Table 4. Linear peptides synthesized for the *Exoris* library. The overall yields of the linear peptides synthesis were calculated by Fmoc UV detection related to the last cleavage step, whereas the purities of the crudes were determined through analytical HPLC analysis (peaks detected at λ=220 nm).

2.3.2. Peptides cyclization

Cyclic peptides have been synthesized by *head-to-tail* approach; the reactions were performed in solution using DPPA as coupling reagent, with $NaHCO_3$ as base under high DMF dilution [5 mM]. The progress of each synthesis was checked by HPLC, and the cyclizations were completed within 4 to 24 h (according to the specific peptide sequence). The base was removed by filtration and the DMF was evaporated *in vacuo*. Finally, the complete removal of the side chain protecting groups was accomplished by acidolytic treatment with a TFA solution containing appropriate scavengers.

The final cyclic hexapeptides were obtained after the purification by automated flash chromatography.

The pure products were fully characterized by HPLC, HRMS, MALDI-TOF and amino acids analysis. All the cyclo peptides were obtained with excellent yields and purity (Table **5**).

The differences in the yields of the final products could be reasonably related to the purification step and not to the linear peptide synthesis or to the cyclization efficiency, as evidenced by the comparable yields obtained for the linear peptides and the few amounts of by-products detected during the cyclization of each sequence.

The two cyclic peptides (*cyclo*-1a, *cyclo*-2a) containing all L-amino acids present crudes more complex and it was decided to perform their purification further in case of positive results in terms of protein binding affinity of their analogues. These results underline the importance of the introduction along the peptide sequence of elements able to promote the cyclization. If the peptide is not properly preorganized to cyclize the ring closure will be slow and could favour the side reactions, leading to the formation of many by-products that affect the isolation of the final product.

n	Cyclic peptide	Purity %	Yield %
***cyclo*-1a**	&Trp-Pro-Arg-Trp-Pro-Arg&	< 60	-
***cyclo*-1b**	&**D**-Trp-Pro-Arg-**D**-Trp-Pro-Arg&	> 90	75
***cyclo*-1c**	&Trp-**D**-Pro-Arg-Trp-**D**-Pro-Arg&	> 90	80
***cyclo*-1d**	&Trp-Pro-**D**-Arg-Trp-Pro-**D**-Arg&	> 95	20
***cyclo*-2a**	&Arg-Pro-Trp-Arg-Pro-Trp–OH	< 50	-
***cyclo*-2b**	&**D**-Arg-Pro-Trp-**D**-Arg-Pro-Trp&	> 95	84
***cyclo*-2c**	&Arg-**D**-Pro-Trp-Arg-**D**-Pro-Trp&	> 95	80
***cyclo*-2d**	&Arg-Pro-**D**-Trp-Arg-Pro-**D**-Trp&	> 95	30
***cyclo*-3a**	&Ser-**D**-Pro-Trp-Ser-**D**-Pro-Trp&	> 98	69
***cyclo*-3b**	&Ser-**D**-Pro-Trp-Ser-**D**-Pro-**D**-Trp&	> 95	58
***cyclo*-4a**	&Glu-**D**-Pro-Trp-Glu-**D**-Pro-Trp&	> 97	50
***cyclo*-4b**	&Glu-**D**-Pro-Trp-Glu-**D**-Pro-**D**-Trp&	> 90	60
***cyclo*-5a**	&Ile-**D**-Pro-Trp-Ile-**D**-Pro-Trp&	> 94	75
***cyclo*-5b**	&Ile-**D**-Pro-Trp-Ile-**D**-Pro-**D**-Trp&	> 96	68
***cyclo*-6a**	&Ser-**D**-Pro-Glu-Ser-**D**-Pro-Glu&	> 95	15
***cyclo*-6b**	&Ser-**D**-Pro-Glu-Ser-**D**-Pro-**D**-Glu&	> 95	41
***cyclo*-7a**	&Ser-**D**-Pro-Ile-Ser-**D**-Pro-Ile&	> 98	47
***cyclo*-8a**	&Glu-**D**-Pro-Ile-Glu-**D**-Pro-Ile&	> 90	70

Table 5. Cyclic peptides synthesized for the *Exoris* library. The yields are referred to the recovered products after the chromatography purification. The purities were determined by analytical HPLC analysis (peaks detected at λ=220 nm).

&D-Trp-Pro-Arg-D-Trp-Pro-Arg& ***(cyclo-1b)***

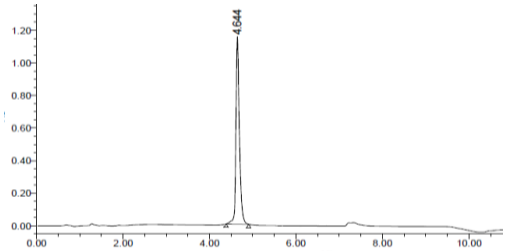

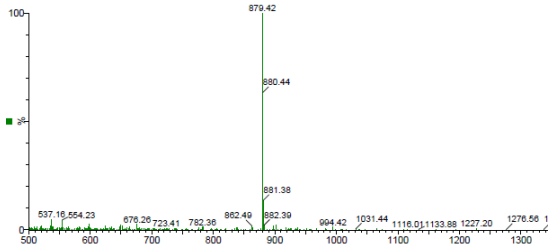

&Trp-D-Pro-Arg- Trp-D-Pro-Arg& ***(cyclo-1c)***

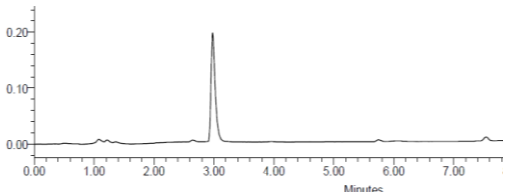

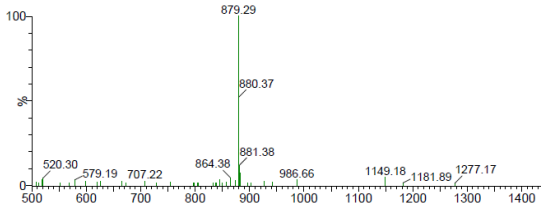

&Trp-Pro-D-Arg- Trp-Pro-D-Arg& ***(cyclo-1d)***

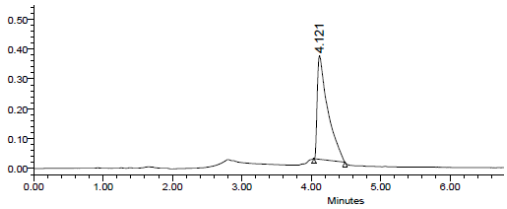

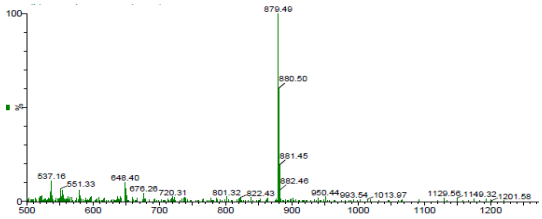

&D-Arg-Pro-Trp-D-Arg-Pro-Trp& ***(cyclo-2b)***

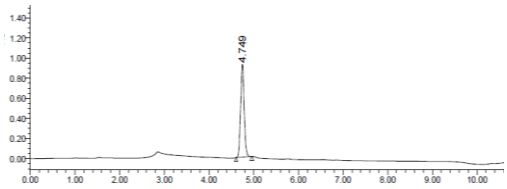

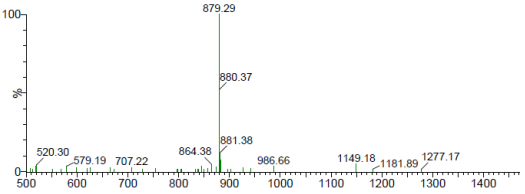

&Arg-D-Pro-Trp-Arg-D-Pro-Trp& ***(cyclo-2c)***

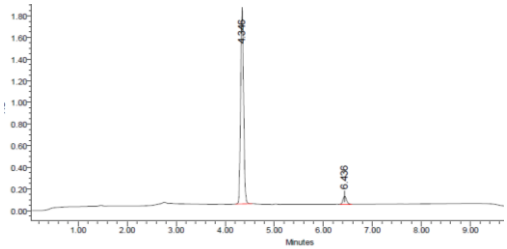

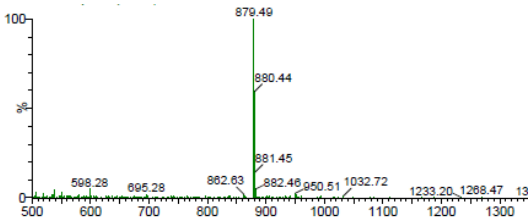

&Arg-Pro-D-Trp-Arg-Pro-D-Trp& ***(cyclo-2d)***

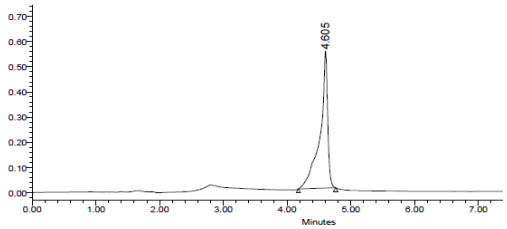

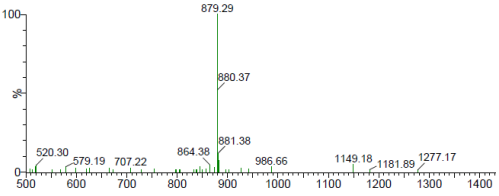

&Ser-D-Pro-Trp-Ser-D-Pro-Trp& ***(cyclo-3a)***

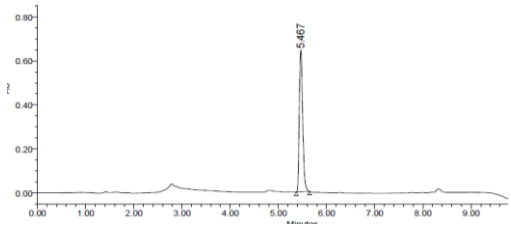

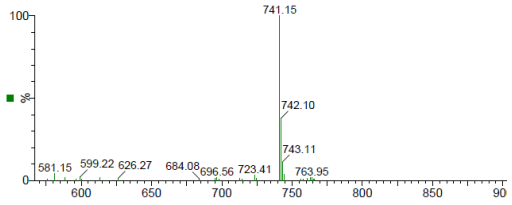

&Ser-D-Pro-Trp-Ser-D-Pro-Trp& ***(cyclo-3b)***

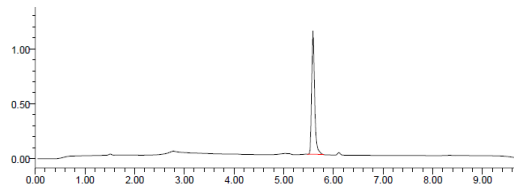

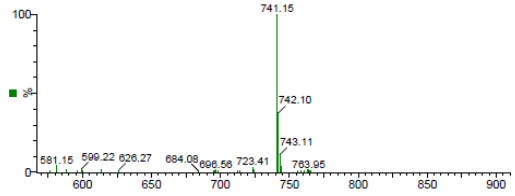

&Glu-D-Pro-Trp-Glu-D-Pro-Trp& ***(cyclo-4a)***

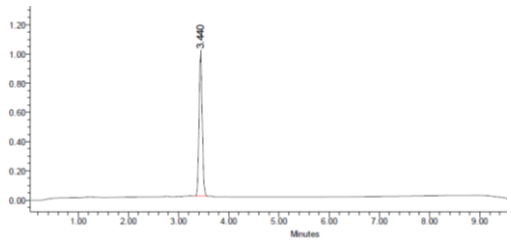

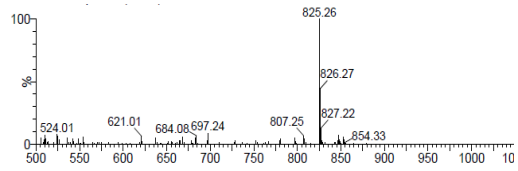

&Glu-D-Pro-Trp-Glu-D-Pro-D-Trp& ***(cyclo-4b)***

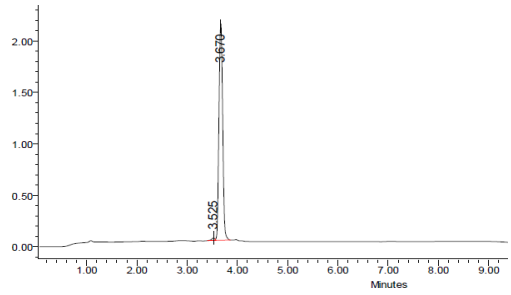

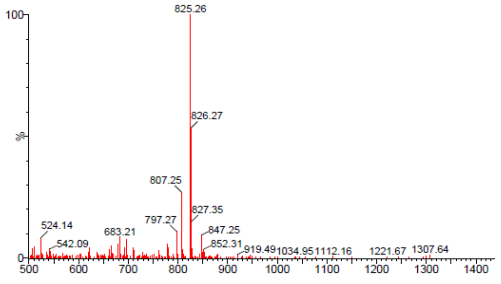

&Ile-D-Pro-Trp-Ile-D-Pro-Trp& ***(cyclo-5a)***

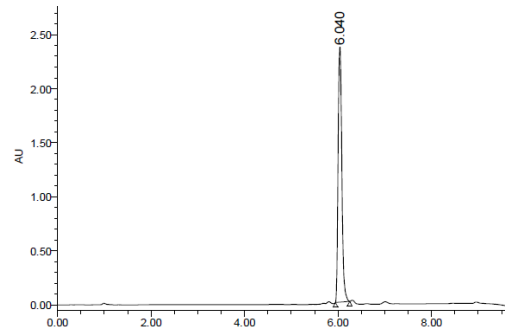

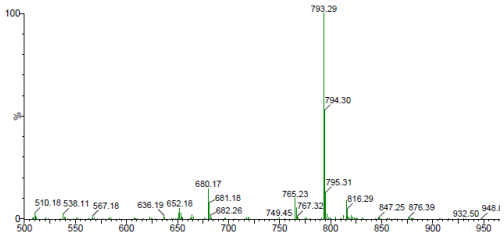

&Ile-D-Pro-Trp-Ile-D-Pro-D-Trp& ***(cyclo-5b)***

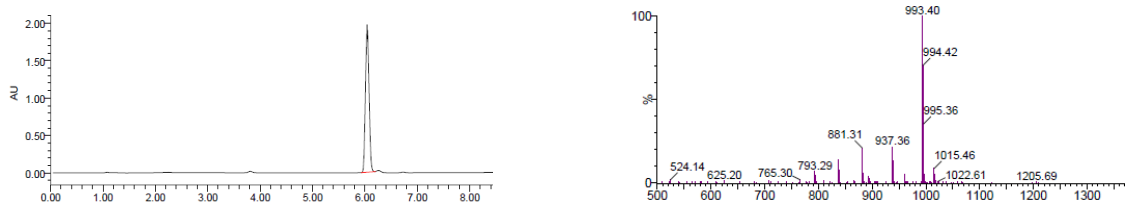

&Ser-D-Pro-Glu-Ser-D-Pro-Glu& ***(cyclo-6a)***

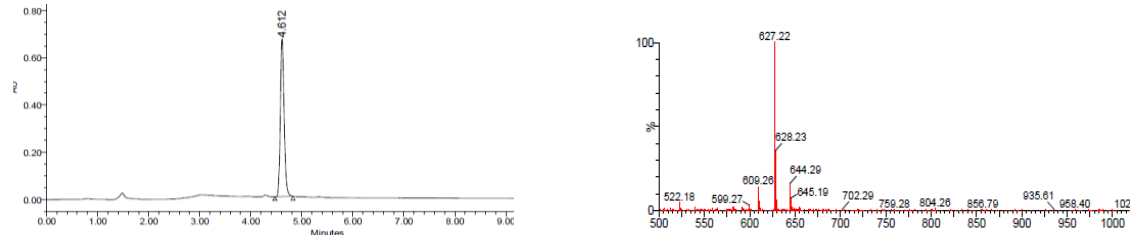

&Ser-D-Pro-Glu-Ser-D-Pro-D-Glu& ***(cyclo-6b)***

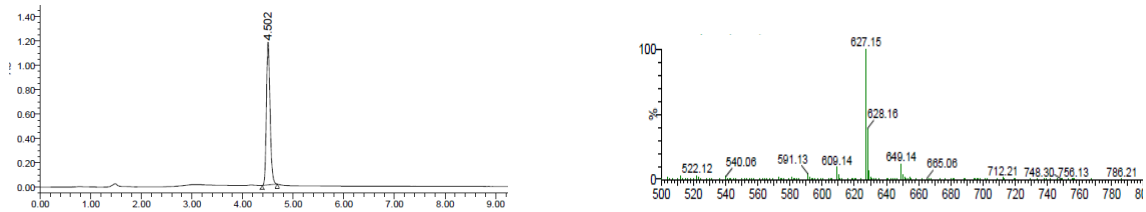

&Ser-D-Pro-Ile-Ser-D-Pro-Ile& ***(cyclo-7a)***

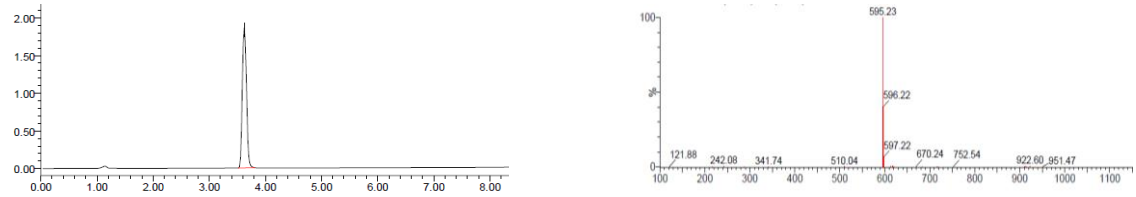

&Glu-D-Pro-Ile-Glu-D-Pro-Ile& ***(cyclo-8a)***

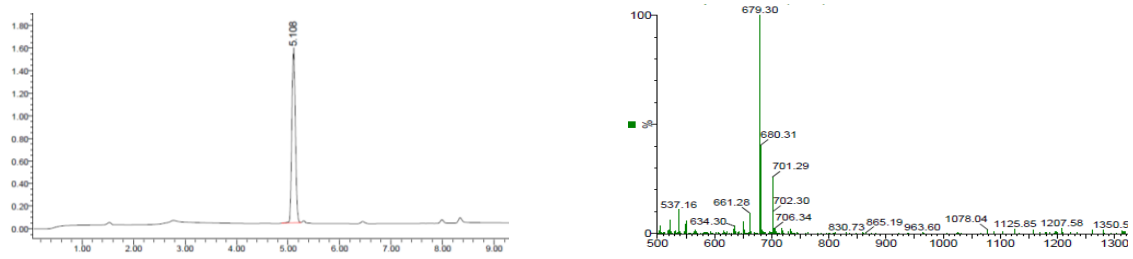

Figure 2. HPLC traces and MS-HPLC of cyclic hexapeptides. HPLC were recorded using a 0-100% B gradient in 8 min (A = 0.045% TFA in H_2O and B = 0.036% TFA in ACN).

Once a set of cyclohexapeptides of the library have been prepared, different NMR studies have been done to characterize the cyclic peptide structures and to perform a primary screening for the identification of possible candidates able to interact with the target proteins.

2.4. NMR characterization and binding studies

Different NMR studies have been done (in collaboration with Sonia Ciudad and Jesus Garcia) to characterize the structure of the cyclic peptides. ^{1}H-NMR spectra at different temperatures showed the presence of only one defined conformation per each peptide, which is in accordance with rigid structures.

The conformation of *trans*-proline has been determined by using the chemical shift difference between $^{13}C_{\beta}$ and $^{13}C_{\gamma}$ of the proline residues and by looking at the NOE's patters.[9]

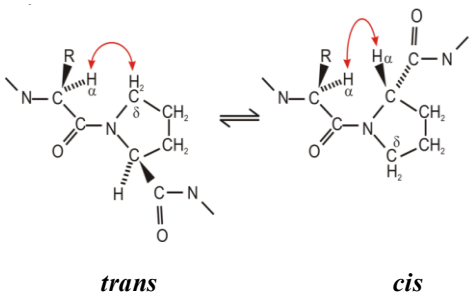

Figure 3. All the studied peptides showed the same pattern of NOEs, confirming that the Xaa-D-Pro bonds are in the *trans* conformation.

Temperature coefficients ($-\Delta\delta_{NH}/\Delta T$) were used as an indication of solvent accessibility to amide protons and to explore the presence of hydrogen bonds in the cyclic hexapeptides. Considering that small temperature coefficients ($0 < -\Delta\delta_{NH}/\Delta T < 5$ ppb/K) are related to low accessibility and are often interpreted as evidence for intramolecular hydrogen bonding, compared to grater values ($6 < -\Delta\delta_{NH}/\Delta T < 10$ ppb/K) for amide groups in a random coil conformation.[10] It has been observed that the NH of the residue preceding the D-proline is more solvent shielded independently on the amino acid present in this position, probably due to the formation of an hydrogen bond in this position. These results are compatible with the presence of two consistent β-turn motives.

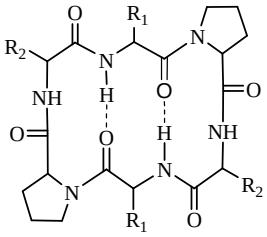

Figure 4. The NMR results suggest that the cyclic hexapeptides form hydrogen bonds between the residues preceding the prolines, which is totally consistent with a conformation containing two β-turns.

2.5. Binding evaluation by Nuclear Magnetic Resonance

NMR spectroscopy has been used as initial screening method to test the different binding behaviors of the cyclic peptides towards ^{13}CMet VEGF protein. The cyclohexapeptides binding evaluation was initially performed using VEGF as target protein, because it was previously expressed (as labelled protein by overexpression in E. coli.)[11] and already available in the laboratory at the time of this screening.

The Chemical Shift Perturbation (CSP) has been used for a primary screening to identify the binding site of the ligands to the protein target. This assay is based on the variation of

the chemical shifts of both ligand and protein proton resonances upon binding, especially for the nuclei located within the binding site.[12] Once the protein has been enriched with ^{15}N (or ^{13}C) and the chemical shift assignments are known, the protein is titrated with a ligand and the chemical shift changes are monitored. 2D ^{1}H-^{15}N (or ^{1}H-^{13}C) heteronuclear single quantum coherence (HSQC) spectroscopy is the most common method to monitor the backbone chemical shifts. Only the protein resonances are visible in such spectra and, therefore, the ligand can be included at a high concentration.[13] Information on where the ligand is bound can be obtained by comparing the HSQC spectra with and without ligand. Moreover, binding constants and stoichiometry can be obtained through the titration of the protein with the ligand observing the chemical shifts of selected residues.

Two cyclopeptides as candidates that showed a promising binding affinity with the VEGF have been identified by this preliminary assay (performed by Sonia Ciudad). Small changes in the chemical shift in some residues of the protein (e.g. Met18 and Met81 that are known to be in the binding site of VEGF with its receptors) were observed in the presence of different equivalents of these cyclopeptides. An estimated Kd was obtained by the titration assay, which reveals that two peptides are VEGF binders in a low-mM range (Table **6**).

n	Cyclic peptide	Kd (mM)
***cyclo*-4a**	&Glu-**D**-Pro-Trp-Glu-**D**-Pro-Trp&	2.9
***cyclo*-4b**	&Glu-**D**-Pro-Trp-Glu-**D**-Pro-**D**-Trp&	14.8

Table 6. NMR titration assay results.

It is worth to notice that the two identified candidates are epimers. They have the same peptide sequence but differ one for another only in the chirality of the *C*-terminal amino acid (Trp). This observation, in addition to provide information about the key-residues for the protein binding interaction, suggests that breaking the symmetry in the cyclopeptide might have a role to modulate the affinity and to increase the specificity towards the protein.

Moreover, based on NMR investigation, it seems that the presence of aromatic residues (Trp) in the cyclopeptide is important to induce small but detectable chemical shift perturbation in the VEGF signals. On the other hand, non-Trp containing peptides, show negligible changes in the chemical shifts of all the protein methionines.

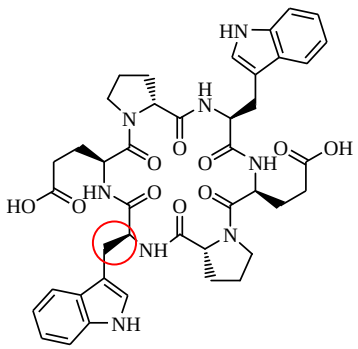

***cyclo*-4a**

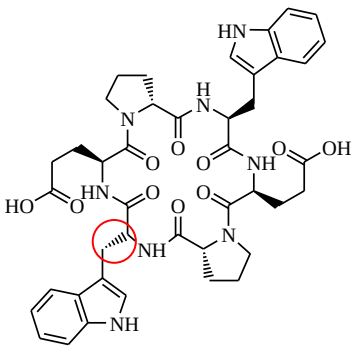

***cyclo*-4b**

Figure 5. The two cyclic hexapeptides that show better affinity for VEGF.

2.6. Evaluation of BBB-permeability

The next step in the characterization of the cyclohexapeptides of the EXORIS library focused on the evaluation of their ability to overcome the cellular membrane.

These assays were initially performed on the two cyclic hexapeptides identified as the best candidates for the interaction with VEGF (compounds *cyclo*-4a and *cyclo*-4b, Table **6**). In parallel, the same cyclopeptides were tested as conjugated with a well-known BBB shuttle (THRre) able to cross the BBB using the active transport via transferrin receptor.[14]

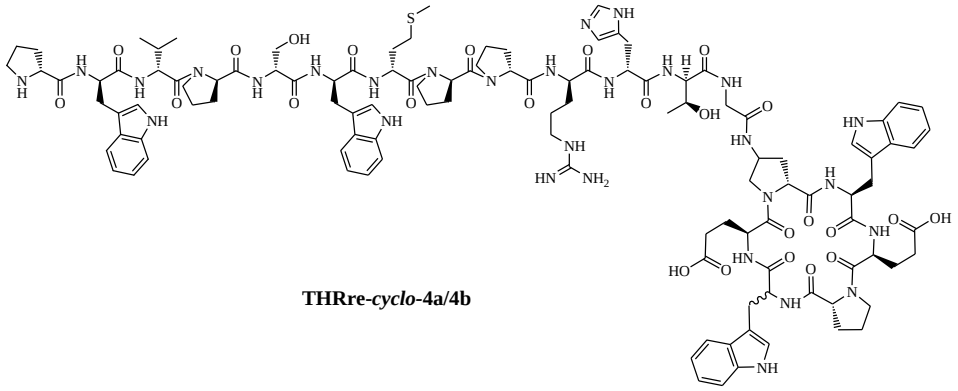

THRre-*cyclo*-4a/4b

Figure 6. Cyclic peptides (*cyclo*-4a and *cyclo*-4b) conjugated with the THRre underwent to BBB permeability evaluation.

2.6.1. Evaluation of BBB permeability by passive diffusion

2.6.1.1. Parallel artificial membrane permeability assay (PAMPA)

The parallel artificial membrane permeability assay (PAMPA), is a phospholipid-based transport assay, widely used in the pharmaceutical industry as a high throughput permeability method to predict oral absorption.[15-17]

Since its introduction,[18] several variants of the experimental conditions have been proposed to improve the correlation between this artificial membrane model system and human absorption data.[19] This technique is utilized as an evaluation tool to determine whether a compound can cross a biological barrier, such as the BBB, the gastro-intestinal barrier or skin,[20-22] depending on the mixture of phospholipids used or not. In addition, numerous statements have been made about the utility of the PAMPA also as a tool for medicinal chemists to elucidate structure–permeability relationships.[23]

The PAMPA phospholipidid membrane mimics the cell membrane, but it has no means for active or paracellular transport of drug molecules. So, it models only the passive transport system.

The parallel artificial membrane permeability assay for the blood−brain barrier (PAMPA-BBB),[20] is a very simple, rapid and inexpensive technique compared to cell-based assay[24] or chromatography-based approaches[25]. Due to these reasons, it is considered one of the most powerful and versatile physicochemical screening tools in early stage CNS targeted drug discovery practice.[26,15]

It has been also demonstrated that PAMPA correlated with *in situ* brain diffusion remarkably better than MDR1-MDCKII for a broad range of CNS drugs with diverse physicochemical properties available on the market.[27]

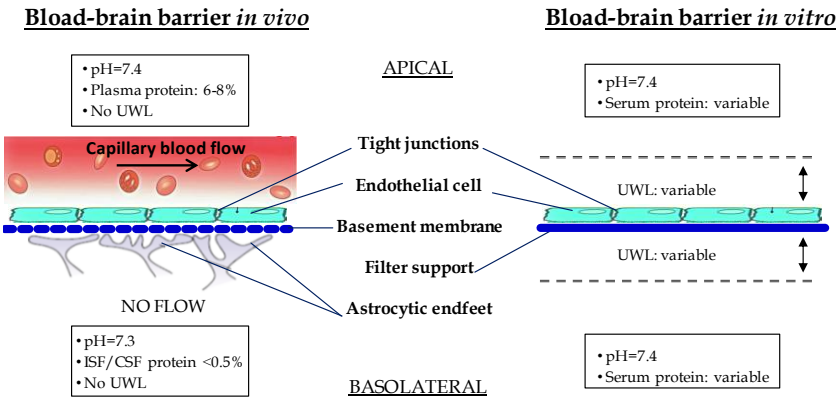

Figure 7. The differences between the properties at the endothelial surface of blood-brain barrier capillaries *in vivo* and those generated by *in vitro* cell monolayer systems. UWL: unstirred water layer. ISF: iron-sulfur proteins, CFS: cerebrospinal fluid. (Adapted from *Drug Discovery Today*, **2003**, 8 (*21*), 997-1003**)**.

The transport across an artificial membrane barrier is a combination of diffusion through the membrane and diffusion through the aqueous boundary layers (ABL) (also called the unstirred water layer UWL) at the two sides of the membrane. Convective forces (e.g. from stirring) and diffusion quickly translocate solute molecules in the bulk aqueous phase. However, their transport through the ABL is driven mainly by diffusion, which can be very slow if the ABL is very thick or if the solute molecules are very large. If the thickness of the ABL is greater than the thickness of the phospholipid membrane barrier, the water layer becomes the rate-limiting component in the transport of lipophilic molecules hiding the membrane contributions to transport. If the assays ignore the ABL effect with lipophilic test compounds, the resulting permeability values will not correctly indicate the *in vivo* conditions of permeability and will merely reveal properties of water rather than membrane permeation. However, it has been demonstrated that stirring the sample in the wells displays the *in vivo* relevant ABL and in some cases also reduces the assay time because the excessive ABL resistance is lessened.

2.6.1.2. PAMPA experimental results

The first investigation was performed by a PAMPA assay to figure out whether the cyclopeptides alone and conjugated with the BBB-shuttle are able to cross the BBB membrane by a passive diffusion process or not.

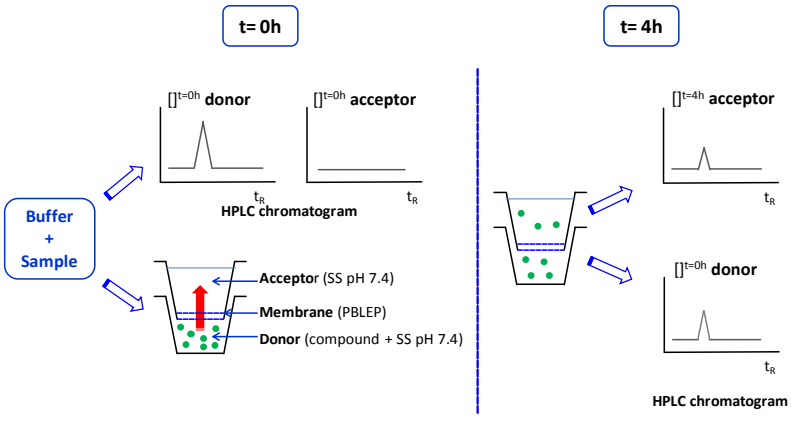

Figure 8. Schematic representation of the PAMPA assay. PBLEP: polar brain lipid extract porcine. SS: system solution **(**buffer solution and 20% 1-propanol as cosolvent).

The assay was carried out using a porcine polar brain lipid extract which better mimics the lipid composition of the endothelial cells of the BBB. The candidates were placed in the donor compartment at a concentration of 220 µM and the polycarbonate filters of the PAMPA plate was coated with a lipid extract, then the peptides were incubated at room temperature for 4 hours under stirring in a gut box. Propranolol has been used as positive control compound in this assay due to its known ability to cross the BBB by passive diffusion (P_e in the high permeability range).[28] After 4 hours the apical and basal solution in the wells were analyzed by RP-HPLC and MALDI-TOF in order to obtain the effective permeability (P_e) of each compound.

The HPLC analysis showed that it was possible to detect the compound in the acceptor compartments only for the unconjugated cyclopeptides, indicating that these candidates crossed the cellular barrier by passive diffusion mechanism transport. Whereas, as expected, their analogues, conjugated with the BBB-shuttle, have not crossed the membrane. The effective permeability (P_e) was determined using the equation **1**:

$$P_e = \frac{-218.3}{t} \text{Log}\left[1 - \frac{2\ C_A(t)}{C_D(t0)}\right] 10^{-6}\ \text{cm/s} \qquad (1)$$

Where *t* is the time express in hours, $C_A(t)$ is the compound concentration at the acceptor compartment after the experiment (time: 4 h) and $C_D(t0)$ is the initial concentration of sample applied to the donor compartment (time: 0 h).

The percentage of transport was calculated following the equation **2**:

$$T\% = \frac{C_A(t)}{C_D(t0)} \cdot 100 \qquad (2)$$

The effective permeability results are summarized in Table **7**. The permeability of the candidates was confirmed by MALDI-TOF analysis of the acceptor compartments.

The ability of a certain compound to permeate this barrier is affected by its pKa and, as the assay is performed at pH 7.4, only the fraction of compound not ionised at this pH should be able to partition through the barrier into the acceptor chamber.

Compound	% Membrane retention	P_e x 10^{-6} (cm/s)	% PAMPA transport after 4h
***cyclo*-4a**	< 5	0.8	1.6
***cyclo*-4b**	< 5	0.8	1.6
THRre *cyclo*-4a	< 5	0.047	0.1
THRre *cyclo*-4b	< 5	0.095	0.2
Propranolol	< 5	19.3	28

Table 7. Membrane retention (%), effective permeability (P_e) and percentage of transport, after 4 h in the PAMPA assay of the candidates (unconjugate and conjugate with the BBB-shuttle) and the control compounds (Propranolol). Low permeability: P_e (cm/s) < 0.1 x 10^{-6}.Medium permeability P_e (cm/s) 0.1 x $10^{-6} \leq P_e <$ 1x 10^{-6}. High permeability: P_e (cm/s) ≥ 1x10^{-6}.

The peptides alone exhibit a medium permeability towards the artificial membrane, probably due to their intrinsic lipophilic character and to the intramolecular hydrogen bonds (suggested by the NMR results) which increase their lipid solubility.

The PAMPA experiment provided a general indication on the ability of these candidates to cross the cell barrier. Nevertheless, due to the artificial nature of the assay membrane (non-bilayer lipid structure) and the only passive transport mechanisms considered, the PAMPA assay will never be a precise model of the brain endothelial cell membrane. To overcome this limitation, the peptides were also evaluated in a more realistic BBB model.

2.6.2. BBB transport evaluation using a BBB in vitro model.

Two BBB shuttle-cyclopeptides and the unconjugated ones have been tested in an *in vitro* BBB model in the group of Prof. Giralt (IRB) by Benjamin Ollèr.

The BBB transport evaluation was done with the most widely used *in vitro* BBB model, which consist on a co-culture of bovine brain endothelial cells (BBECs) and rat astrocytes.[29-32] This type of model shows a remarkable correlation between *in vitro* and *in vivo* BBB permeability data, both for passive diffusion and active transport.

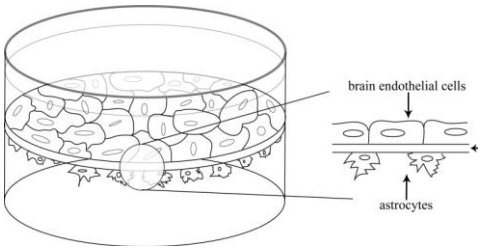

Figure 9. Mono-culture of brain endothelial cells in transwells. Cells are seeded in the filter of the transwell and are cultured until confluence.

The *in vitro* BBB model that will be used in this project is formed by a co-colture of BBECs and newborn rat aristrocytes that are co-coltured until the transendothelial electrical resistance (TEER) measures showed that the system was ready for transport studies.
In parallel, the permeability assay was performed with Lucifer yellow (LY) to check the integrity of the barrier *in vitro*, in order to validate the analysis.
After incubation, the contents of the acceptor and donor compartments were analyzed by RP-HPLC and the permeability and percentage of the transport was determined according to equations 1 and 2 (see page 165). The transport of the peptides was confirmed by MALDI-TOF analysis of the acceptor compartment. P_e and transport results are summarized in Table **8**.

All the compounds tested are able to cross the endothelial membrane. The conjugated cyclopeptides with the BBB shuttle have lower permeability efficiency compared to the unconjugated one and they have to cross the BBB by using the active transport via transferrin receptor, resulting in a more selective transport. On the other hand, the high values observed for the cyclic peptides alone are not surprising due to their permeability by passive diffusion through the membrane.
Nevertheless, this model is highly sensitive and any external influence can easily disturb the cell barrier, causing the premature disruptions between the cell junctions. This fact may

induce false positives during the permeability assays and it must be repeated to confirm and validate the obtained results.

Compound	% Membrane retention	P_e x 10^{-6} (cm/s)	% Transport after 4h
THRre	9.0	3.1	3.7
***cyclo*-4a**	22.5	4.2	5.0
***cyclo*-4b**	16.7	5.1	6.0
THRre *cyclo*-4a	6.2	0.7	0.8
THRre *cyclo*-4b	5.3	0.5	0.6

Table 8. Ranking of the results obtained using the BBB cellular model. Candidates were incubated with the cells at a concentration of 50 µM for 24 h at 37ºC using HBSS as buffer.

2.7. Validation of NMR result for VEGF-ligand binding

Different biophysical assays have been considered to validate the VEGF-ligand binding results obtained by NMR technique. Methods such as surface plasmon resonance (SPR), isothermal titration calorimetry (ITC), surface acoustic wave coupled to mass spectrometry (SAW)[33-35] and competition fluorescence polarization assay (FP) can be used to perform the thermodynamic and kinetic studies of VEGF-ligand binding.[36]
Among these techniques, we have focused on the competition fluorescence polarization assay (FP) because this method has been recently reported to identify molecules that bind to the VEGF dimer in the region that is recognized by the cell surface receptors[37] and because the experimental conditions are already known and may be used to screen our candidates. Moreover, FP does not required ^{15}N-labelled protein which expression represents one of the limiting factors for the NMR analysis allowing the use of commercially available protein. Nevertheless, FP requires a tracer fluorescent ligand that could be displaced by the candidate inhibitors.

Fluorescence polarization is based on the observation that fluorescent molecules in solution that are excited with plane-polarized light will emit light in a fixed plane. However, as the molecules rotate and tumble, the plane into which the light is emitted may vary from the plane used for the initial excitation. The rate at which a molecule rotates and tumbles depends on the size. If a molecule is very large, little rotation will occur whereas if a molecule is small, the rotation will be faster. Therefore, a molecule can be excited with vertically polarized light and the intensity of emitted light can be monitored in the vertical and the horizontal planes to determine the relative mobility of the fluorescently labeled molecule. If the fluorescent probe is bound to the protein, the emission light will remain highly polarized relative to the excitation plane, but if the probe is free in solution it will rotate quicker and the light will be depolarized relative to the excitation plane.

The reported FP assays are performed employing two different fluorescent tracers based on the same peptide sequence but with different fluorophore moieties: BODIPY or fluorescein.
BODIPY is defined as a red-shifted fluorophore that tend to lower common assay interferences, such as those arising from compound aggregation or fluorescent impurities.

We have performed the first PF experiment using a BODIPY-labeled ligand as fluorescent tracer using the experimental conditions reported in literature[37] with unsuccessful results, probably due to the low quality of the tracer or to the perturbation of the outcome fluorescent signal by the cyclic peptides, for example due to the peptide aggregation.

To overcome this problem, a new synthesis was developed to obtain a fluorescein-labeled ligand which has reported to have a Kd greater than the BODIPY-analogue and for this reason may be displaced by the candidate which present a low affinities towards the VEGF, representing a throughput method with a high sensitivity to identify weakly binding inhibitors.

2.7.1. Synthesis of the FP-tracer

The FP tracer is a peptide composed of 15 amino acids (CDIHVMWEWECFERL), bearing a disulfide bridge between the two cysteines in the sequence. In addition it has a [2-(2-amino ethoxy)-ethoxyl] acetic acid spacer located at the *N*-terminal between the peptide and the fluorophore.

The synthesis of the fluorescein-labelled tracer (Figure **9**) was performed using Aminomethyl-ChemMatrix resin as solid support functionalized with Fmoc-Rink-Linker, which, not only reduces the resin functionalization, but also provides a *C*-terminal amide after the peptide cleavage from the resin.
The peptide elongation was carried out by automated microwave assisted technology following the Fmoc/*t*Bu strategy and using TBTU and DIEA as coupling reagent system.
After completing the linear peptide assembly by microwave, the intermediate **9** was characterized through the analysis of a crude sample, obtained from the cleavage of a little portion of resin with a proper cleavage cocktail. The RP-HPLC and MALDI-TOF analysis show the good outcome of the reaction. Subsequently, the coupling with the spacer was performed manually by SPPS using HBTU-DIEA, yielding the product **10**.

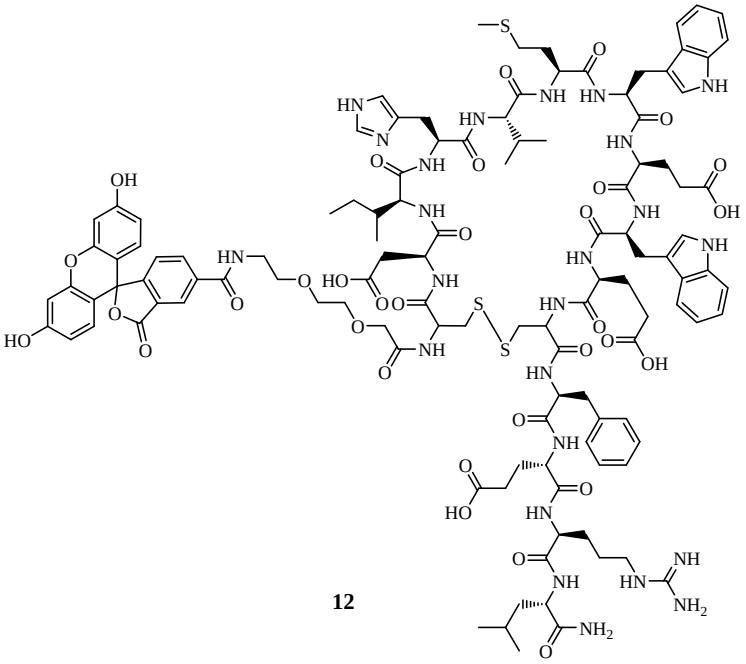

12

Figure 9. Structure of FP fluorescein-labelled tracer.

The next synthetic step, related to the removal of the trityl (S-Trt) protecting groups on the cysteines and their subsequent oxidation to form a disulfide bond, was the subject of an intensive investigation, with the aim to indentify an efficient methodology to perform the reaction on solid phase instead of in solution as previously done.

Typically, the cyclization of linear peptides on the solid support, where pseudodilution is achieved, presents an important benefit for the intramolecular disulfide bond formation.[38,39] Solid phase disulfide bridge formation has the advantage that it favors the intramolecular reactions, avoiding the intermolecular one. Moreover, on-resin oxidations can be carried out in small solvent volumes that can be easily removed together with the excess oxidizing agent by filtration. Several protocols have been developed for on-resin disulfide bond formation and include the use of hazardous oxidizing agents like thallium and mercury complexes, or iodine-mediated methods.[40,41] Furthermore, the common on-resin oxidation methods provide reduced by-product formation, especially when sensitive residues as Trp and Met are present in the peptide sequence.[42]

Since Kamber et al.[43] discovered that in peptides where thiols are protected by acetamidomethyl (Acm) groups, iodine offered the potential to carry out removal and simultaneous oxidative disulphide bond formation in one-single step, several disulphide-bonded peptides have been synthesized using this strategy.[44] Unfortunately, side reactions are often associated with this procedure including, for example, iodination of some sensitive residues such as Tyr, Met, and Trp. To limit these undesired side reactions, the excess of iodine should be quenched or adsorbed after completion of the disulfide reaction by addition of sodium bisulfate or thiosulfate, ascorbic acid, powdered zinc dust, activated charcoal, or by dilution with water followed by extraction with carbon tetrachloride.

Starting from the several reported methodologies, we have focussed on the study of the I_2-mediated disulfide bonds on solid phase. Several trials have been performed changing the equivalents of iodine and the time of the treatment. The best reaction conditions were identified in two treatments of 15 minutes with 5 equivalents of I_2 in DMF followed by a quench (3x1 min) with a saturated solution of sodium bisulfate in DMF to eliminate the iodine and to prevent the iodination of the methionine. Under these conditions the cleavage of the Trt-cysteine protecting groups and the cyclization happen in only a single reaction step leading to the product **11** in almost quantitative yield. It is important to notice the difficulty to monitor the reaction evolution by RP-HLPC due to the similar retention times of the oxidized and the reduced form independently on the elution gradient used. In the same way, MALDI-TOF analysis was not providing clear statement of the reaction due to the detected isotopic cluster which complicates the spectra interpretation. Only by HR-ESMS it was possible to clarify the course of the reaction.

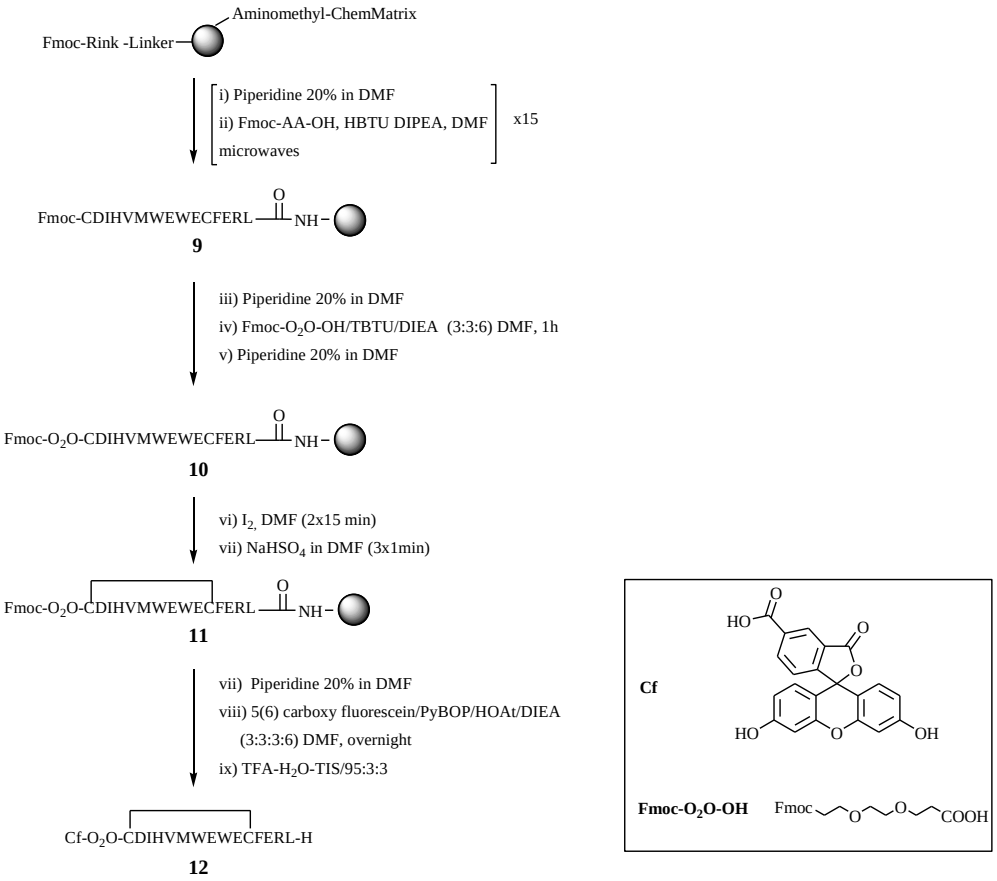

Scheme 1. Synthetic scheme of the FP fluorescein-label tracer.

The fluorescent moiety has been introduced by the coupling with the 5(6) carboxyfluorescein performed using PyBOP-HOAt-DIEA/3:3:6, overnight.

The cleavage of the peptide from the resin and the complete removal of side-chain protecting groups were accomplished by treatment with TFA solution containing water and TIS as scavengers (TFA-TIS-H_2O/95:3:3, 2h). The solvent was removed *in vacuo* and the peptide **12** was precipitated with TBME, dissolved in a mixture of acetonitrile-water (1:1) and lyophilized.

The crude was purified by RP-HPLC at semi-preparative scale providing the final product **12** in 11% overall yield and with a purity higher than 98% (Figure **10**). The pure product was fully characterized by RP-HPLC, HR-ESMS, MALDI-TOF and amino acids analysis.

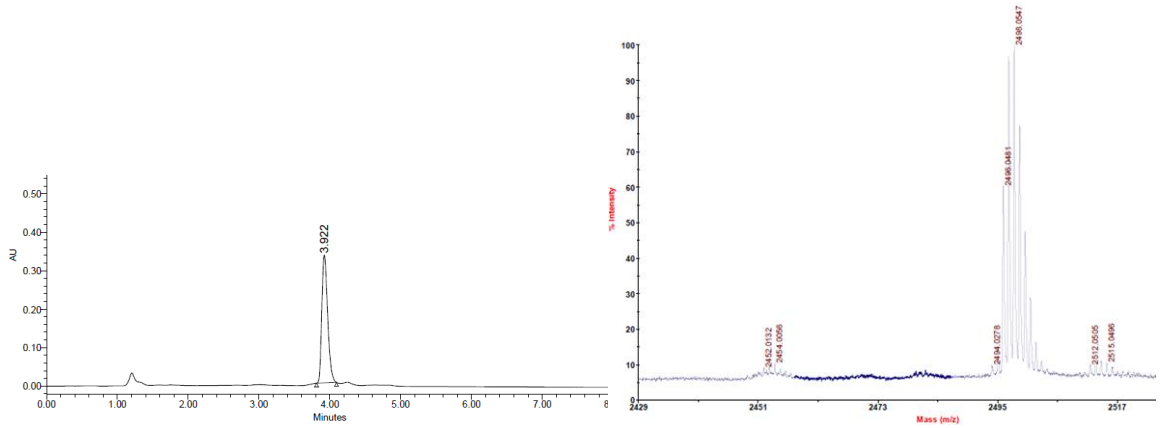

Figure 10: HPLC and MALDI-TOF traces of the FP fluorescein-labelled tracer **12**. HPLC were recorded using a 30-60% B gradient in 8 min (A = 0.045% TFA in H_2O and B = 0.036% TFA in ACN).

2.7.2. FP: validation experimental conditions

The fluorescein-labelled tracer has been used to perform a preliminary FP assay with the aim to set up the experimental conditions and to evaluate the behavior of the tracer during these experiments.
A direct binding assay was initially performed with the fluorescein-labelled tracer **12** and VEGF, obtaining a Kd values of the tracer in accordance with those reported in literature (Table **9**).[37]

Peptide	Sequence	Literature K_d (nM)	Experimental K_d (nM)
12	Cf-X-CDIHVMWEWECFERL-NH_2	140 ± 40	146 ± 32

Table 9. Direct binding FP assay of fluorescein-labelled tracer **12**. X = [2-(2-amino-ethoxy)-ethoxy]-acetic acid.

Based on the Kd value determined in direct binding FP experiments described above, we established a competition FP assay in which a well-known peptidic VEGF inhibitor (v107)[45] can be screened for its ability to displace the tracer **12** from VEGF.
Affinity of competitor for VEGF was quantified as an equilibrium dissociation constant (Ki value), which was calculated from the inhibition curve.[46]
The unlabeled peptide 107 was able to compete with tracer **12** for binding to VEGF; with a Ki value of 0.4 ± 0.03 μM.

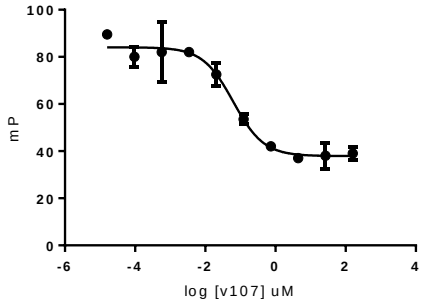

Figure 11. v107 competition assay graph. V107 sequence: H-GGNECDIARMWEWECFERL-NH_2.

The same experimental conditions will be used to screen the cyclic hexapeptides of the library and to evaluate their interaction with the protein. This assay is a complementary approach to the NMR studies to measure the interaction of the cyclic hexapeptides to the VEGF. Moreover, this method can also provide information about the interaction site exploiting the competition with the tracer which is known to interact with VEGF in a region recognized by its receptor.

2.7.3. A Fluorine-labelled tracer

In spite of the NMR spectroscopy has gained increasing importance for the identification of compounds that bind to macromolecules, screening of chemical libraries using traditional spectroscopic methods produces complex ^{1}H-NMR spectra and requires labelled protein samples.
The ^{19}F-NMR spectroscopy represents an alternative simple methodology for the screening of ligands that bind to proteins, which also provides qualitative information about the relative binding strengths and the presence of multiple binding sites.

^{19}F nucleus has lately attracted much attention in the screening field for various reasons. First and most important is its high sensitivity; this is due to ^{19}F's high gyromagnetic constant ($\gamma F \sim 0.94\ \gamma H$) but also to its 100% natural abundance. Moreover, fluorine displays a wide chemical shift range, which makes it unlikely for overlapping to occur. Other useful properties include its high sensitivity towards binding events; this often induces important changes to fluorine chemical shift and line width due to fluorine's large CSA (*Chemical Shift Anisotropy)*. Given the remarkable relaxation properties above, binding detection can often be performed simply by acquiring 1D spectra in with and without the target protein. Nonetheless, a more general approach to discriminate between fluorine containing ligands among non-binders consists on the determination on transversal relaxation rates (T_2), either by direct measurement of linewidth or by using T_2 filters.[47,48]
Obviously such experiments are limited to some extent, as they require the presence of fluorine atoms in the assayed compounds. This element, however, is rather common in commercial drugs and often, medicinal chemists enhance metabolic stability or modulate compound lipophilicity by incorporating such element. On the other hand, fluorine is seldom found in natural sources or solvents; for these reasons it has been proposed as an alternative to avoid background resonances arising from the protein or the annoying solvent signals, which often have deleterious consequences for the performance of ligand based experiments.

In the field of ^{19}F spectroscopy, recently FAXS (*fluorine chemical shift anisotropy and exchange for screening*) has been reported as a ligand-based binding competition screening experiment[49-51] that utilizes a weak affinity spy molecule containing a CF_3 or CF moiety and ^{19}F as the nucleus of detection. The FAXS approach has some distinct advantages. The absence of overlap allows the screening of large chemical mixtures and the automated spectra analysis. The large CSA of fluorine results in a large difference in line width for the spy molecule in the free and bound states, especially at the high magnetic fields currently used. This phenomenon, combined with the large exchange contribution, allows for the selection of a weak-affinity spy molecule, thus resulting in both a lower binding affinity threshold for the identified NMR hits and protein consumption.

We have focused on this technique as an alternative (or parallel) method to FP for screening the cyclic peptides of our library, in order to confirm if the candidate peptides interact with the VEGF in its site of recognition with the VEGFR. A fluorine version of the FP tracer has been synthesized using the same methodology previously described for the FP tracer **12**. The coupling with a fluorine moiety instead of with the carboxyfluorescein was performed in the last step, just before the resin cleavage. This tracer will be used as spy molecule in the ligand-based binding competition screening experiment based on ^{19}F as the nucleus of detection.

After the synthesis of the linear peptide **11**, the fluorine moiety has been introduced by the coupling with the 4,4,4-Trifluoro-3-(trifluoromethyl)butanoic acid performed using PyBOP-HOAt-DIEA/20:60:60, in DMF for 1.5 hours.

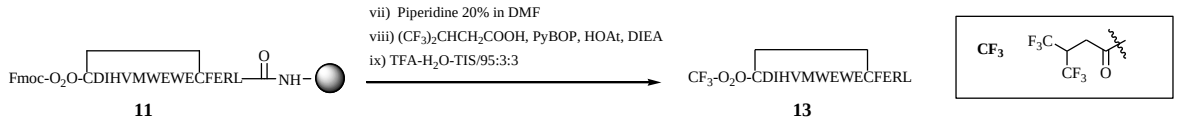

Scheme 2. The last step of the synthesis of fluorine-labelled tracer.

The cleavage of the peptide from the resin and the complete removal of side-chain protecting groups were accomplished by treatment with TFA solution containing water and TIS as scavengers (TFA-TIS-H_2O/95:3:3, 2h). The crude was purify by RP-HPLC at semi-preparative scale providing the product **13** in 8% overall yield and with a purity higher than 98% (Figure **12**). The pure product was fully characterized by RP-HPLC, RP-HPLC-MS, MALDI-TOF and amino acids analysis.

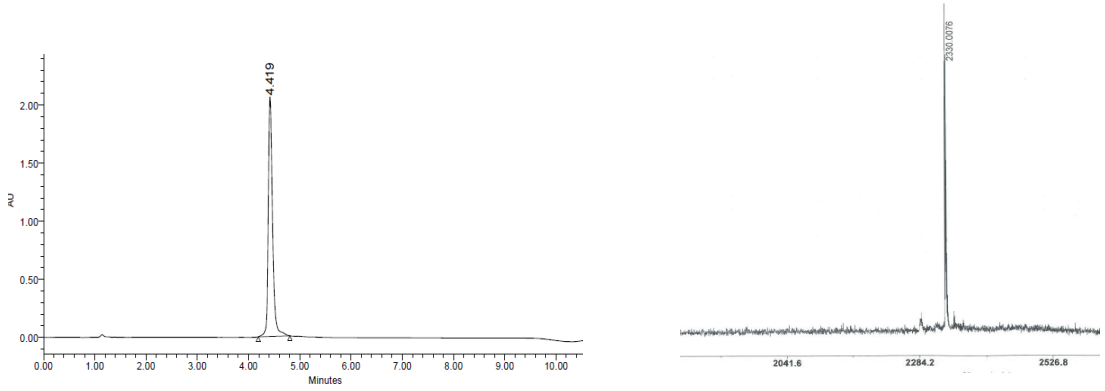

Figure 12. HPLC and MALDI-TOF traces of the fluorine-labelled tracer **13**. HPLC was recorded using a 30-60% B gradient in 8 min (A = 0.045% TFA in H_2O and B = 0.036% TFA in ACN).

2.8. EGF target protein

One of the target protein proposed at the beginning of this project was the Epidermal Grow Factor (EGF) which is widely involved in tumorigenesis and in the glioma progression.
In order to explore the EGF binding ability of the cyclohexapeptides two main approaches were evaluated.

The first one is based on the NMR observation of ^{15}N-labelled EGF and the use of chemical shift perturbation experiments. As previously described for the VEGF, this approach allows screening over a wide range of affinities (mM-nM). In addition to identify positive binders, this method allows a quantitative characterization of the interactions and the direct identification of the binding site within the protein, but requires the expression of ^{15}N-labelled EGF in *E. coli*. Despite the structure of free EGF has been solved by NMR using recombinant protein,[52] the EGF expression represent a non-trivial problem. Indeed, while the EGF expression was successfully obtained, although with low yield, the further work to produce the ^{15}N-labelled version, proved particularly challenging and it is currently in progress.

As the expression of ^{15}N-labelled EGF was a limiting factor, some alternative binding assays have been evaluated. For example it is possible to use the competition fluorescence polarization assay employing the experimental conditions validated for the VEGF. In such a case, it is necessary to find a fluorescent tracer EGF-ligand that could be displaced by the candidate inhibitors. Nowadays, only Suramin has been described as inhibitor of EGF-

EGFR interaction.[52] Suramin is a symmetric polysulfonate compound that uses half of the molecule to interact with the *C*-terminal region of EGF. Suramin alone is poorly fluorescent and it has not any functional group susceptible of being conjugated with a suitable fluorescent moiety but can give a fluorescent signal according to hydrophobic media and to the target molecule which can induce a conformational change resulting in a fluorescence enhancement.[53] Unfortunately this does not happen when Suramin interacts with EGF, so Suramin can not be used as EGF-fluorescent tracer.

The second approach is based on the thermodynamic characterization of the EGF-ligand binding, by isothermal titration calorimetry (ITC) which is perhaps the most rigorous method for the characterization of protein-ligand interactions. In this method, the interactions are detected by the intrinsic heat change. From ITC measurements it is possible to determine the thermodynamic parameters such as binding enthalpy (H), stoichiometry, entropy (S) and association constant (K) of the binding process. ITC experiments cover an optimum range of dissociation constants from 100 μM to 10 nM; however, modification of experimental design using competition methods can be used to extend this range.

Independently on the type of chosen assay, it is necessary to synthesize the EGF considering the low amount of protein that can be produced by EGF expression and the high cost of the commercially available one.

2.8.1. Attempt to EGF synthesis

The human EGF is 6045-Da protein with 53 amino acid residues, three intramolecular disulphide bridges and a large number of trifunctional amino acids bonds, thus represents a considerable challenge to the peptide chemist. Few procedures are reported for this synthesis which was performed both by assembly of shorter peptide building blocks[54] or by a stepwise manner.[55]

During this project the EGF was synthesized by SPPS in association with the microwaves assisted technology. Aminomethyl ChemMatrix resin was chosen as solid support which was functionalized with an AB linker (3-(4-Hydroxymethylphenoxy) propionic acid) in order to reduce the resin functionalization (0.4 mmol) and to obtain a carboxylic function as *C*-terminal. After the incorporation of the first amino acid by manual coupling (5eq AA/ 5eq DIPCDI/ 0.5 eq DMAP; DCM, 0.5 h x 2) the peptide chain elongation was performed by microwaves assisted synthesis using TBTU/DIEA as coupling reagent in association with the Fmoc/*t*Bu chemistry.

The synthesis progression was monitored at different stages, and up to 35 amino acids it was possible to identify the product by MS-HPLC and MALDI-TOF analysis; nevertheless at the end of the synthesis the crude characterization does not provide any evidences of the desired product and giving a very complex HPLC chromatogram. The complexity of the spectrum could be related to possible deletions of amino acids due to a low efficiency of the attempted synthetic methodology, or to the formation of multiple disulfide bonds between the cysteines in the sequence. Although the peptide has not been subjected to oxidative conditions, it is possible that the six cysteines in the sequence have formed intra and/or inter disulfide bonds leading to a complex mixture of products.

In order to confirm this hypothesis and to simplify the crude, the product was reduced using a large excess of DTT (100 eq 5mg/ml, r.t. 30 min), then it was purified by sephadex: NAP-5 (cut off= 5000 Da). The HPLC after the reduction is significantly simplified and its comparison with the HPLC of the expressed and commercial EGF revealed some common peaks. In any case the MALDI-TOF and MS-HPLC analysis do not identify the mass corresponding to the product.

A new synthesis has been attempted slightly changing the synthetic methodology, by setting a double coupling as default after the first 15 amino acids in order to push the reaction. In this case the product was detected by MALDI-TOF and MS-HPLC up to 40 amino acids, but at the end of the synthesis (53 AA) the product was not identified also after the reductive treatment with DTT.

The products obtained from the two attempted synthesis and the commercial EGF, were subjected to a gel electrophoresis analysis using a polyacrilamide gel. The results reveled that the synthetic products have a smaller size compared to the commercial protein. In addition, by comparison of the two synthetic products it was noticed that the second attempt has provided a peptide with a higher molecular weight than the first one showing that the large excess of reagents used in the double coupling has pushed the reaction but, however, was not enough to obtain the final product.

In conclusion, despite the microwaves assisted heating technology is, in general, an efficient method for the synthesis of peptide with different lengths and amino acids compositions, in this case the synthesis were failed. These results suggest that the stepwise synthetic approach is not probably the best method to produce this protein. Thus, further investigations will be performed to identify an alternative approach to obtain the protein, for example will be evaluated to synthesize EGF exploiting the native chemical ligation or by fragment condensation.

2.9. *In vitro* assays for biological activity evaluation: preliminary results

The candidates *cyclo*-4a and *cyclo*-4b (labeled with the BBB shuttle and the unconjugated ones) were also tested in a viability cell assay at the group of Prof. Seoane in the Vall d'Hebron Institut d'Oncologia of Barcelona (VHIO). The preliminary data showed that one of the compounds active in the VEGF binding assay (*cyclo*-4b) showed a remarkable activity when compared to the control compound (Cetuximab) at work dose of 66 nM. The epimer compound (*cyclo*-4a), which only differs in the chirality of one carbon, was significantly less active. Moreover, the results showed the loss of activity when the compounds are linked to the BBB shuttle indicating that they are in the silent mode when circulating and that a hydrolysable specific linker is required to release the compound when reaching the brain tissue.

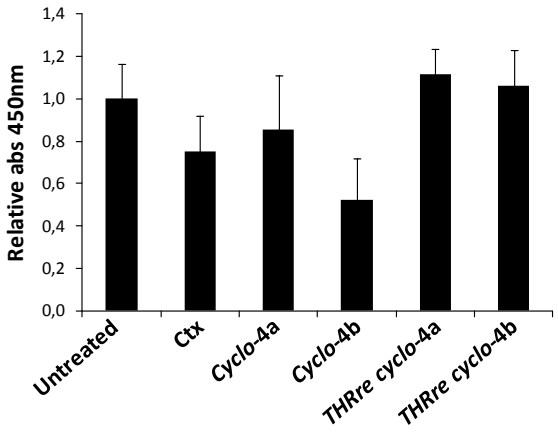

Figure 14. Results of viability assay measured by WST-1 reagent upon 24 h treatment with Cetuximab/Cancertech compounds.

2.10. Conclusion

A library of cyclic haxapeptides to search for anti-EGF and anti-VEGF binders was designed and synthesized. The design of the peptide drugs has been rationalized to obtain symmetric cyclic hexapeptides: *cyclo*-(DPro-XY-DPro-XY) synthetically accessible with drug-like properties as protease resistant and metabolically stable (e.g. by the insertion of unnatural amino acids). Moreover, the design aims the access to rigid structures to increase the binding activities and to obtain a fixed peptidic backbone structure which makes easier the exploration of different amino acid side chains.

In the first stage, the methodology has been explored to identify a synthetic procedure to easily access to the cyclic peptides with high yields and purities. The key points of the optimized synthetic procedure are represented by the use of a 2-Chlorotrityl resin as a polymeric support which allows to obtain the side-chain protected linear precursor and to exploit all the advantages of solid-phase chemistry. The introduction of D-prolines has the double effect to promote the peptide cyclization (being β-turn elements) and to increase the metabolic resistance of the final products (as non natural amino acids). DPPA/$NaHCO_3$ were chosen as the best reagents to perform the cyclization in solution.

A library of cyclic compounds were produced by using a representative base of amino acids for X and Y positions: Trp, Glu, Ile, Ser and Arg and for each combination, one epimer was synthesized.

Different NMR studies have been performed to characterize the structure of the cyclic peptides defining that they contain a rigid structure with a common motive of two β-turns type II'.

The cyclo hexapeptides were tested by NMR for binding interaction against the vascular endothelial growth factor (VEGF) ^{13}CMet-labelled. Despite several tested compounds produce alteration in the chemical shift of the protein, mainly two peptides (*cyclo*-4a, *cyclo*-4b) showed binding interaction in the active binding site, so they could be promising drug candidate.

In order to confirm the NMR results, the same system was evaluated by using fluorescent polarization (FP). Since the problems encountered in the fluorescent signal acquisition during the first trial with a BODIPY-labelled ligand, a new fluorescein-labelled ligand was synthesized.
The synthesis was developed optimizing the previously established procedure to form the disulfide bond, in which the oxidation was carried out in solution using ammonium hydroxide and required five days. With our optimized method, the reaction was performed on solid-phase with only 30 minutes with iodine, allowing the synthesis of the tracer fully on solid phase.
The tracer was used to validate the PF experimental conditions that will be employed to screen the cyclic compounds of the library.

In order to test the peptide library against the epidermal growth factor, the EGF synthesis by microwaves assisted technology was attempted. Despite the failure of the two trials, the results have provided important information about the synthetic approach to use, discarding the stepwise as method of choice. In addition, during this step, it was performed a complete characterization of the commercial EGF, which will be a useful reference during the further attempts that will be performed in order to obtain the EGF both synthetically and by expression.

Two cyclic hexapeptides were evaluated by PAMPA assay which models the passive transport at the BBB and both of them showed passive diffusion ability. Whereas the BBB transport evaluation in a cell based model displayed that these two candidates conjugated with the BBB shuttle were able to cross the BBB by using the active transport via transferrin receptor, resulting in a more selective transport.

Based on the viability cell assay results which show that the two candidates are biological active but when they are linked to the BBB-shuttle become inactive. A hydrolysable link between the cyclopeptide and the BBB-shuttle will be evaluated in order to release the active compound when it reaches the brain tissue keeping its activity.

Based on the structural features of the two compounds identified as the best candidates of this first cyclic hexapeptide library, it will be possible to plan properly the modifications to optimize their interaction with the target protein. Thus a new set of cyclopeptides could be developed, maintaining the same set of amino acids but, for instance, changing the stereochemistry or shifting the residues along the peptide chain, to explore their influence on the structural and conformational properties of the cyclohexapeptides and the consequent effect on the binding with the target.
A different approach could be to introduce and additional level of restriction in the structure through a bicyclic formation or to expand the size of the ring, either by including a third pair of pXY to obtain cyclic nonapeptides, or by including a Z amino acid into the motive pXYZ to obtain cyclic octapeptides.

The hits compounds identified during this first part of the project, could be also validated and characterized in better detail with other throughput methods, either using the same NMR techniques but with different experimental design or using additional techniques, to acquire a wider set of thermodynamic, kinetic and structural data to investigate the compound properties.

An alternative approach could be to develop a new sub-set of cyclopeptides *in silico* and to test them against the target proteins by using computational tools such as docking. The obtained results will provide important information related with the possible activity of these potential therapeutic agents against the tested targets and the most promising candidates will be synthesized so as to be validated.

References

(1) Katz, C.; Levy-Beladev, L.; Rotem-Bamberger, S.; Rito, T.; Rudiger, S. G. D.; Friedler, A. Studying protein-protein interactions using peptide arrays. *Chem. Soc. Rev.* **2011**, *40*, 2131-2145.

(2) Horne, W. S. Peptide and peptoid foldamers in medicinal chemistry. *Expert Opin. Drug Discov.* **2011**, *6*, 1247-1262.

(3) Peczuh, M. W.; Hamilton, A. D. Peptide and Protein Recognition by Designed Molecules. *Chem. Rev.* **2000**, *100*, 2479-2494.

(4) Chiva, C.; Vilaseca, M.; Giralt, E.; Albericio, F. An HPLC-ESMS study on the solid-phase assembly of C-terminal proline peptides. *J. Pept. Sci.* **1999**, *5*, 131-140.

(5) Miller, S. C.; Scanlan, T. S. oNBS−SPPS: A New Method for Solid-Phase Peptide Synthesis. *J. Am. Chem. Soc.* **1998**, *120*, 2690-2691.

(6) Kaiser, E.; Colescott, R. L.; Bossinger, C. D.; Cook, P. I. Color test for detection of free terminal amino groups in the solid-phase synthesis of peptides. *Anal. Biochem.* **1970**, *34*, 595-598.

(7) Christensen, T. Qualitative test for monitoring coupling completeness in solid-phase peptide-synthesis using chloranil. *Acta Chem. Scand. B* **1979**, *33*, 763-766.

(8) Madder, A.; Farcy, N.; Hosten, N. G. C.; De Muynck, H.; De Clercq, P. J.; Barry, J.; Davis, A. P. A Novel Sensitive Colorimetric Assay for Visual Detection of Solid-Phase Bound Amines. *Eur. J. Org. Chem.* **1999**, *1999*, 2787-2791.

(9) Schubert, M.; Labudde, D.; Oschkinat, H.; Schmieder, P. A software tool for the prediction of Xaa-Pro peptide bond conformations in proteins based on 13C chemical shift statistics. *J. Biomol. NMR* **2002**, *24*, 149-154.

(10) Baxter, N.; Williamson, M. Temperature dependence of 1H chemical shifts in proteins. *J. Biomol. NMR* **1997**, *9*, 359-369.

(11) Fairbrother, W. J.; Champe, M. A.; Christinger, H. W.; Keyt, B. A.; Starovasnik, M. A. 1H, 13C, and 15N backbone assignment and secondary structure of the receptor-binding domain of vascular endothelial growth factor. *Protein Sci.* **1997**, *6*, 2250-2260.

(12) Meyer, B.; Peters, T. NMR Spectroscopy Techniques for Screening and Identifying Ligand Binding to Protein Receptors. *Angew. Chem. Int. Ed. Engl.* **2003**, *42*, 864-890.

(13) Homans, S. W. NMR Spectroscopy Tools for Structure-Aided Drug Design. *Angew. Chem. Int. Ed. Engl.* **2004**, *43*, 290-300.

(14) *WO2013/127829* **2013**.

(15) Wohnsland, F.; Faller, B. High-throughput permeability pH profile and high-throughput alkane/water log P with artificial membranes. *J. Med. Chem.* **2001**, *44*, 923-930.

(16) Zhu, C.; Jiang, L.; Chen, T. M.; Hwang, K. K. A comparative study of artificial membrane permeability assay for high throughput profiling of drug absorption potential. *Eur. J. Med. Chem.* **2002**, *37*, 399-407.

(17) Kerns, E. H. High throughput physicochemical profiling for drug discovery. *J. J. Pharm. Sci.* **2001**, *90*, 1838-1858.

(18) Kansy, M.; Senner, F.; Gubernator, K. Physicochemical high throughput screening: parallel artificial membrane permeation assay in the description of passive absorption processes. *J. Med. Chem.* **1998**, *41*, 1007-1010.

(19) Avdeef, A. The rise of PAMPA. *Expert Opin. Drug Metab. Toxicol.* **2005**, *1*, 325-342.

(20) Di, L.; Kerns, E. H.; Fan, K.; McConnell, O. J.; Carter, G. T. High throughput artificial membrane permeability assay for blood-brain barrier. *Eur. J. Med. Chem.* **2003**, *38*, 223-232.

(21) Ottaviani, G.; Martel, S.; Carrupt, P. A. Parallel artificial membrane permeability assay: a new membrane for the fast prediction of passive human skin permeability. *J. Med. Chem.* **2006**, *49*, 3948-3954.
(22) Ottaviani, G.; Martel, S.; Carrupt, P. A. In silico and in vitro filters for the fast estimation of skin permeation and distribution of new chemical entities. *J. Med. Chem.* **2007**, *50*, 742-748.
(23) Kovo, M.; Kogman, N.; Ovadia, O.; Nakash, I.; Golan, A.; Hoffman, A. Carrier-mediated transport of metformin across the human placenta determined by using the ex vivo perfusion of the placental cotyledon model. *Prenat. Diagn.* **2008**, *28*, 544-548.
(24) Kerns, E. H. D., L. . Structure Design and Methods, from ADME to Toxicity Optimization. *Drug-like Properties: Concepts* **2008**, *Chapter 28*, 311−328.
(25) Yoon, C. H.; Kim, S. J.; Shin, B. S.; Lee, K. C.; Yoo, S. D. Rapid screening of blood-brain barrier penetration of drugs using the immobilized artificial membrane phosphatidylcholine column chromatography. *J. Biomol. Screen.* **2006**, *11*, 13-20.
(26) Naik, P.; Cucullo, L. In vitro blood-brain barrier models: current and perspective technologies. *J. Pharm. Sci.* **2012**, *101*, 1337-1354.
(27) Di, L.; Kerns, E. H.; Bezar, I. F.; Petusky, S. L.; Huang, Y. Comparison of blood-brain barrier permeability assays: in situ brain perfusion, MDR1-MDCKII and PAMPA-BBB. *J. Pharm. Sci.* **2009**, *98*, 1980-1991.
(28) Malakoutikhah, M.; Teixido, M.; Giralt, E. Toward an optimal blood-brain barrier shuttle by synthesis and evaluation of peptide libraries. *J. Med. Chem.* **2008**, *51*, 4881-4889.
(29) Hallier-Vanuxeem, D.; Prieto, P.; Culot, M.; Diallo, H.; Landry, C.; Tahti, H.; Cecchelli, R. New strategy for alerting central nervous system toxicity: Integration of blood-brain barrier toxicity and permeability in neurotoxicity assessment. *Toxicol. In Vitro* **2009**, *23*, 447-453.
(30) Culot, M.; Lundquist, S.; Vanuxeem, D.; Nion, S.; Landry, C.; Delplace, Y.; Dehouck, M. P.; Berezowski, V.; Fenart, L.; Cecchelli, R. An in vitro blood-brain barrier model for high throughput (HTS) toxicological screening. *Toxicol. In Vitro* **2008**, *22*, 799-811.
(31) Cecchelli, R.; Berezowski, V.; Lundquist, S.; Culot, M.; Renftel, M.; Dehouck, M. P.; Fenart, L. Modelling of the blood-brain barrier in drug discovery and development. *Nat. Rev. Drug Discov.* **2007**, *6*, 650-661.
(32) Gumbleton, M.; Audus, K. L. Progress and limitations in the use of in vitro cell cultures to serve as a permeability screen for the blood-brain barrier. *J. Pharm. Sci.* **2001**, *90*, 1681-1698.
(33) Lange, K.; Rapp, B. E.; Rapp, M. Surface acoustic wave biosensors: a review. *Anal. Bioanal. Chem.* **2008**, *391*, 1509-1519.
(34) Rocha-Gaso, M. I.; March-Iborra, C.; Montoya-Baides, A.; Arnau-Vives, A. Surface generated acoustic wave biosensors for the detection of pathogens: a review. *Sensors* **2009**, *9*, 5740-5769.
(35) Dragusanu, M.; Petre, B. A.; Slamnoiu, S.; Vlad, C.; Tu, T.; Przybylski, M. On-line bioaffinity-electrospray mass spectrometry for simultaneous detection, identification, and quantification of protein-ligand interactions. *J. Am. Soc. Mass Spectrom.* **2010**, *21*, 1643-1648.
(36) Lea, W. A.; Simeonov, A. Fluorescence polarization assays in small molecule screening. *Expert. Opin. Drug Discov.* **2011**, *6*, 17-32.
(37) Peterson, K. J.; Sadowsky, J. D.; Scheef, E. A.; Pal, S.; Kourentzi, K. D.; Willson, R. C.; Bresnick, E. H.; Sheibani, N.; Gellman, S. H. A fluorescence polarization

assay for identifying ligands that bind to vascular endothelial growth factor. *Anal. Biochem.* **2008**, *378*, 8-14.

(38) Albericio, F.; Hammer, R. P.; Garcia-Echeverria, C.; Molins, M. A.; Chang, J. L.; Munson, M. C.; Pons, M.; Giralt, E.; Barany, G. Cyclization of disulfide-containing peptides in solid-phase synthesis. *Int. J. Pept. Protein Res.* **1991**, *37*, 402-413.

(39) Annis, I.; Chen, L.; Barany, G. Novel Solid-Phase Reagents for Facile Formation of Intramolecular Disulfide Bridges in Peptides under Mild Conditions1,2. *J. Am. Chem. Soc.* **1998**, *120*, 7226-7238.

(40) Barany, G.; Han, Y.; Hargittai, B.; Liu, R.-Q.; Varkey, J. T. Side-chain anchoring strategy for solid-phase synthesis of peptide acids with C-terminal cysteine. *Pept. Sci.* **2003**, *71*, 652-666.

(41) Edwards, W. B.; Fields, C. G.; Anderson, C. J.; Pajeau, T. S.; Welch, M. J.; Fields, G. B. Generally applicable, convenient solid-phase synthesis and receptor affinities of octreotide analogs. *J. Med. Chem.* **1994**, *37*, 3749-3757.

(42) Annis, I.; Hargittai, B.; Barany, G. Disulfide bond formation in peptides. *Methods Enzymol.* **1997**, *289*, 198-221.

(43) Kamber, B.; Hartmann, A.; Eisler, K.; Riniker, B.; Rink, H.; Sieber, P.; Rittel, W. The Synthesis of Cystine Peptides by Iodine Oxidation of S-Trityl-cysteine and S-Acetamidomethyl-cysteine Peptides. *Helv. Chim. Acta* **1980**, *63*, 899-915.

(44) Reddy, K. M. B.; Kumari, Y. B.; Mallikharjunasarma, D.; Bulliraju, K.; Sreelatha, V.; Ananda, K. Large Scale Solid Phase Synthesis of Peptide Drugs: Use of Commercial Anion Exchange Resin as Quenching Agent for Removal of Iodine during Disulphide Bond Formation. *Int. J. Pept.* **2012**, *2012*, 8.

(45) Pan, B.; Li, B.; Russell, S. J.; Tom, J. Y.; Cochran, A. G.; Fairbrother, W. J. Solution structure of a phage-derived peptide antagonist in complex with vascular endothelial growth factor. *J. Mol. Biol.* **2002**, *316*, 769-787.

(46) Roehrl, M. H.; Wang, J. Y.; Wagner, G. A general framework for development and data analysis of competitive high-throughput screens for small-molecule inhibitors of protein-protein interactions by fluorescence polarization. *Biochemistry* **2004**, *43*, 16056-16066.

(47) Dalvit, C.; Mongelli, N.; Papeo, G.; Giordano, P.; Veronesi, M.; Moskau, D.; Kummerle, R. Sensitivity improvement in 19F NMR-based screening experiments: theoretical considerations and experimental applications. *J. Am. Chem. Soc.* **2005**, *127*, 13380-13385.

(48) Dalvit, C.; Fagerness, P. E.; Hadden, D. T. A.; Sarver, R. W.; Stockman, B. J. Fluorine-NMR Experiments for High-Throughput Screening: Theoretical Aspects, Practical Considerations, and Range of Applicability. *J. Am. Chem. Soc.* **2003**, *125*, 7696-7703.

(49) Dalvit, C.; Flocco, M.; Knapp, S.; Mostardini, M.; Perego, R.; Stockman, B. J.; Veronesi, M.; Varasi, M. High-throughput NMR-based screening with competition binding experiments. *J. Am. Chem. Soc.* **2002**, *124*, 7702-7709.

(50) Jahnke, W.; Floersheim, P.; Ostermeier, C.; Zhang, X.; Hemmig, R.; Hurth, K.; Uzunov, D. P. NMR reporter screening for the detection of high-affinity ligands. *Angew. Chem. Int. Ed. Engl.* **2002**, *41*, 3420-3423.

(51) Siriwardena, A. H.; Tian, F.; Noble, S.; Prestegard, J. H. A straightforward NMR-spectroscopy-based method for rapid library screening. *Angew. Chem. Int. Ed. Engl.* **2002**, *41*, 3454-3457.

(52) Huang, H. W.; Mohan, S. K.; Yu, C. The NMR solution structure of human epidermal growth factor (hEGF) at physiological pH and its interactions with suramin. *Biochem. Biophys. Res. Commun.* **2010**, *402*, 705-710.

(53) Zhang, Y. L.; Keng, Y. F.; Zhao, Y.; Wu, L.; Zhang, Z. Y. Suramin is an active site-directed, reversible, and tight-binding inhibitor of protein-tyrosine phosphatases. *J. Biol. Chem.* **1998**, *273*, 12281-12287.

(54) MUNEKATA, S. Y. S. Y. K. M. W. E. Total Solution Synthesis of Human Epidermal Growth Factor (h-EGF) by the Assembly of Nine Building Blocks. *Biosci. Biotechnol. Biochem.* **1992**, *56*, 404-408.

(55) Heath, W. F.; Merrifield, R. B. A synthetic approach to structure-function relationships in the murine epidermal growth factor molecule. *PNAS* **1986**, *83*, 6367-6371.

Chapter 3

Peptides synthesis and characterization

3.1. Linear peptides

3.1.1. Synthesis

All the linear peptides were synthesized by SPPS using the Fmoc/*t*Bu strategy and 2-chlorotrityl (Cl-Trt) resin (f=1.60 mmol/g) in accordance to the experimental procedures reported in the section *6.5* of the Chapter 6. Syntheses were performed at a 200-µmol scale. Solid-phase peptide elongations was done manually in polypropylene syringes, using PyBOP, HOAt and DIEA as coupling reagents. Solvents and soluble reagents were removed by suction. Washings between synthetic steps were done with DMF (5 x 30 s) and DCM (5 x 30 s). During couplings the mixture was left to react with intermittent manual stirring and the good outcome of each coupling was verified by ninhydrin, chloranil or *p*-nitrophenyl ester test, depending on the type of amine which should be detected. After the removal of the last Fmoc group by treatment with 20% of piperidine in DMF, the cleavage of the peptide from the resin was accomplished by treatment with a solution of 2% TFA in DCM (5x 1 min). Crude products were analyzed by RP-HPLC, MS-HPLC and MALDI-TOF. The initial resin loading was determined by UV spectroscopy as reported in the section *6.5.6.*

The overall yield of each linear peptide synthesis was estimated by Fmoc UV detection related to the last cleavage step, whereas the purity of the crudes was determined through analytical HPLC analysis. HPLC chromatograms were recorded on a Waters Alliance 2695 separation module using a Sunfire C18 column flow 1mL/min, solvents H_2O (0.045% TFA) and ACN (0.036% TFA). The gradient (G) is expressed as % of ACN in H_2O (peak detected at λ=220 nm).

3.1.2. Characterization

H-Trp(Boc)-Pro-Arg(Pbf)-Trp(Boc)-Pro-Arg(Pbf)-OH (1a)

Initial loading: 0.53 mmol/g
HPLC: t_R (min, G0100 ACN in 8 min) = 7.27
MS-HPLC calcd for: $C_{80}H_{108}N_{14}O_{17}S_2$, expected: 1600.75, found: 1601.50 $[M+H]^+$
MALDI-TOF, $[M+H]^+$: 1601 Da
Yield: 82 %
Purity: 83 %

H-Trp-Pro-Arg-Trp-Pro-Arg-OH (1a')

Initial loading: 0.53 mmol/g
Cleavage cocktail: TFA/TA/H_2O/TIS/EDT - 81.5:5:5:1:5 (3 h)
HPLC: t_R (min, G0100 ACN in 8 min) = 4.45
MS-HPLC calcd for: $C_{44}H_{60}N_{14}O_7$, expected: 896.48, found: 897.50 $[M+H]^+$
MALDI-TOF, $[M+H]^+$: 897.64 Da
Yield: 86 %
Purity: 80 %

H-D-Trp(Boc)-Pro-Arg(Pbf)-D-Trp(Boc)-Pro-Arg(Pbf)-OH (1b)

Initial loading: 0.56 mmol/g
HPLC: t_R (min, G0100 ACN in 8 min) = 7.86
MS-HPLC calcd for: $C_{80}H_{108}N_{14}O_{17}S_2$, expected: 1600.75, found: 1601.50 $[M+H]^+$
MALDI-TOF, $[M+H]^+$: 1601 Da
Yield: 70 %
Purity: 94 %

H-D-Trp-Pro-Arg-D-Trp-Pro-Arg-OH (1b')

Initial loading: 0.56 mmol/g
Cleavage cocktail: TFA/TA/H_2O/TIS/EDT - 81.5:5:5:1:5 (3 h)
HPLC: t_R (min, G0100 ACN in 8 min) = 4.54
MS-HPLC calcd for: $C_{44}H_{60}N_{14}O_7$, expected: 896.48, found: 897.70 $[M+H]^+$
MALDI-TOF, $[M+H]^+$: 897.53 Da
Yield: 90 %
Purity: 70 %

H-Trp(Boc)-D-Pro-Arg(Pbf)-Trp(Boc)-D-Pro-Arg(Pbf)-OH (1c)

Initial loading: 0.71 mmol/g
HPLC: t_R (min, G0100 ACN in 8 min) = 7.73
MS-HPLC calcd for: $C_{80}H_{108}N_{14}O_{17}S_2$, expected: 1600.75, found: 1602 $[M+H]^+$
MALDI-TOF, $[M+H]^+$: 1601.63 Da
Yield: 75 %
Purity: 83 %

H-Trp(Boc)-Pro-D-Arg(Pbf)-Trp(Boc)-Pro-D-Arg(Pbf)-OH (1d)

Initial loading: 0.50 mmol/g
HPLC: t_R (min, G30100 ACN in 8 min) = 6.70
MS-HPLC calcd for: $C_{80}H_{108}N_{14}O_{17}S_2$, expected: 1600.75, found: 1601.9 $[M+H]^+$
MALDI-TOF, $[M+H]^+$: 1601.71 Da
Yield: 70 %
Purity: 92 %

H-Arg(Pbf)-Pro-Trp(Boc)-Arg(Pbf)-Pro-Trp(Boc)-OH (2a)

Initial loading: 0.60 mmol/g
HPLC: t_R (min, G30100 ACN in 8 min) = 6.55
MS-HPLC calcd for: $C_{80}H_{108}N_{14}O_{17}S_2$, expected: 1600.75, found: 1602 $[M+H]^+$
MALDI-TOF, $[M+H]^+$: 1601.91 Da
Yield: 77 %
Purity: 88 %

H-Arg-Pro-Trp-Arg-Pro-Trp-OH (2a')

Initial loading: 0.60 mmol/g
Cleavage cocktail: TFA/TA/H_2O/TIS/EDT - 81.5:5:5:1:5 (3 h)
HPLC: t_R (min, G0100 ACN in 8 min) = 4.63

MS-HPLC calcd for: $C_{44}H_{60}N_{14}O_7$, expected: 896.48, found: 897.50 $[M+H]^+$
MALDI-TOF, $[M+H]^+$: 897.53 Da
Yield: 90 %
Purity: 83 %

H-D-Arg(Pbf)-Pro-Trp(Boc)-D-Arg(Pbf)-Pro-Trp(Boc)-OH (2b)

Initial loading: 0.55 mmol/g
HPLC: t_R (min, G30100 ACN in 8 min) = 7.50
MS-HPLC calcd for: $C_{80}H_{108}N_{14}O_{17}S_2$, expected: 1600.75, found: 1602.0 $[M+H]^+$
MALDI-TOF, $[M+H]^+$: 1602.08 Da
Yield: 91 %
Purity: 90 %

H-D-Arg-Pro-Trp-Arg-D-Pro-Trp-OH (2b')

Initial loading: 0.55 mmol/g
Cleavage cocktail: TFA/TA/H_2O/TIS/EDT - 81.5:5:5:1:5 (3 h)
HPLC: t_R (min, G0100 ACN in 8 min) = 4.89
MS-HPLC calcd for: $C_{44}H_{60}N_{14}O_7$, expected: 896.48, found: 897.01 $[M+H]^+$
MALDI-TOF, $[M+H]^+$: 897.47 Da
Yield: 85 %
Purity: 70 %

H-Arg(Pbf)-D-Pro-Trp(Boc)-Arg(Pbf)-D-Pro-Trp(Boc)-OH (2c)

Initial loading: 0.43 mmol/g
HPLC: t_R (min, G0100 ACN in 8 min) = 8.25
MS-HPLC calcd for: $C_{80}H_{108}N_{14}O_{17}S_2$, expected: 1600.75, found: 1601.81 $[M+H]^+$
MALDI-TOF, $[M+H]^+$: 1602.11 Da
Yield: 75 %
Purity: 90 %

H-Arg(Pbf)-Pro-D-Trp(Boc)-Arg(Pbf)-Pro-D-Trp(Boc)-OH (2d)

Initial loading: 0.50 mmol/g
HPLC: t_R (min, G0100 ACN in 8 min) = 8.18
MS-HPLC calcd for: $C_{80}H_{108}N_{14}O_{17}S_2$, expected: 1600.75, found: 1602 $[M+H]^+$
MALDI-TOF, $[M+H]^+$: 1601.71 Da
Yield: 89 %
Purity: 73%

H-Ser(*t*Bu)-D-Pro-Trp(Boc)-Ser(*t*Bu)-D-Pro-Trp(Boc)-OH (3a)

Initial loading: 0.73 mmol/g
HPLC: t_R (min, G0100 ACN in 8 min) = 7.13
MS-HPLC calcd for: $C_{56}H_{78}N_8O_{13}$, expected: 1070.57, found: 1071.63 $[M+H]^+$
MALDI-TOF, $[M+H]^+$: 1071.71 Da
Yield: 86 %
Purity: 91 %

H-Ser(*t*Bu)-D-Pro-Trp(Boc)-Ser(*t*Bu)-D-Pro-D-Trp(Boc)-OH (3a')

Initial loading: 0.83 mmol/g
HPLC: t_R (min, G0100 ACN in 8 min) = 7.46
MS-HPLC calcd for: $C_{56}H_{78}N_8O_{13}$, expected: 1070.57, found: 1071.57 $[M+H]^+$.
MALDI-TOF, $[M+H]^+$: 1071.90 Da
Yield: 80 %
Purity: 90 %

H-Glu(O*t*Bu)-D-Pro-Trp(Boc)-Glu(O*t*Bu)-D-Pro-Trp(Boc)-OH (4a)

Initial loading: 0.71 mmol/g
HPLC: t_R (min, G0100 ACN in 8 min) = 7.81
MS-HPLC calcd for: $C_{60}H_{82}N_8O_{15}$, expected: 1154.59, found: 1155.59 $[M+H]^+$
MALDI-TOF, $[M+H]^+$: 1155.71 Da
Yield: 89 %
Purity: 85 %

H-Glu(O*t*Bu)-D-Pro-Trp(Boc)-Glu(O*t*Bu)-D-Pro-D-Trp(Boc)-OH (4b)

Initial loading: 0.81 mmol/g
HPLC: t_R (min, G0100 ACN in 8 min) = 7.77
MS-HPLC calcd for: $C_{60}H_{82}N_8O_{15}$, expected: 1154.59, found: 1155.52 $[M+H]^+$
MALDI-TOF, $[M+H]^+$: 1155.90 Da
Yield: 85 %
Purity: 83 %

H-Ile-D-Pro-Trp(Boc)-Ile-D-Pro-Trp(Boc)-OH (5a)

Initial loading: 0.70 mmol/g
HPLC: t_R (min, G0100 ACN in 8 min) = 7.17
MS-HPLC calcd for: $C_{54}H_{74}N_8O_{11}$, expected: 1010.55, found: 1011.5 $[M+H]^+$
MALDI-TOF, $[M+H]^+$: 1011.56 Da
Yield: 84 %
Purity: 95 %

H-Ile-D-Pro-Trp(Boc)-Ile-D-Pro-D-Trp(Boc)-OH (5b)

Initial loading: 0.72 mmol/g
HPLC: t_R (min, G0100 ACN in 8 min) = 7.55
MS-HPLC calcd for: $C_{54}H_{74}N_8O_{11}$, expected: 1010.55, found: 1011.5 $[M+H]^+$
MALDI-TOF, $[M+H]^+$: 1011.56 Da
Yield: 78 %
Purity: 97 %

H-Ser(*t*Bu)-D-Pro-Glu(O*t*Bu)-Ser(*t*Bu)-D-Pro-Glu(O*t*Bu)-OH (6a)

Initial loading: 0.90 mmol/g
HPLC: t_R (min, G0100 ACN in 8 min) = 5.82
MS-HPLC calcd for: $C_{42}H_{72}N_6O_{13}$, expected: 868.52, found: 869.44 $[M+H]^+$
MALDI-TOF, $[M+H]^+$: 869.56 Da

Yield: 88 %
Purity: 80 %

H-Ser(*t*Bu)-D-Pro-Glu(O*t*Bu)-Ser(*t*Bu)-D-Pro-D-Glu(O*t*Bu)-OH (6b)

Initial loading: 0.85 mmol/g
HPLC: t_R (min, G0100 ACN in 8 min) = 5.58
MS-HPLC calcd for: $C_{42}H_{72}N_6O_{13}$, expected: 868.52, found: 869.50 $[M+H]^+$
MALDI-TOF, $[M+H]^+$: 869.55 Da
Yield: 80 %
Purity: 80 %

H-Ser(*t*Bu)-D-Pro-Ile-Ser(*t*Bu)-D-Pro-Ile-OH (7a)

Initial loading: 0.73 mmol/g
HPLC: t_R (min, G0100 ACN in 8 min) = 5.88
MS-HPLC calcd for: $C_{36}H_{64}N_6O_9$, expected: 724.47, found: 725.30 $[M+H]^+$
MALDI-TOF, $[M+H]^+$: 725.51 Da
Yield: 80 %
Purity: 94 %

H-Glu(O*t*Bu)-D-Pro-Ile-Glu(O*t*Bu)-D-Pro-Ile-OH (8a)

Initial loading: 0.90 mmol/g
HPLC: t_R (min, G0100 ACN in 8 min) = 5.82
MS-HPLC calcd for: $C_{40}H_{68}N_6O_{11}$, expected: 808.49, found: 809.34 $[M+H]^+$
MALDI-TOF, $[M+H]^+$: 809.54 Da
Yield: 77 %
Purity: 95 %

3.2. Cyclic peptides

3.2.1. Synthesis

The *head-to-tail* peptide cyclizations were performed according to the protocol G described in the section *6.7* of the chapter 6 *General methods and procedures*. The linear peptides were dissolved in DMF (5 mM solution) and to the solution were added $NaHCO_3$ (8 eq) and DPPA (2 eq). The reaction was left to proceed at r.t. under stirring and monitored by analytical HPLC. $NaHCO_3$ was removed by filtration and the solvent was evaporated under reduced pressure**.**

Complete deprotection of the peptide was performed by acidolytic treatment with a TFA/TIS/H_2O solution or TFA/phenol/H_2O/TA/EDT for Arg containing peptides. The reaction was carried out at r.t. for 1 hour on orbital shaker. For the cleavage of Arg containing peptides the reaction time was increased to 3 h. The crude was precipitated through addition of cold *tert*-butyl methyl ether. The suspension was centrifuged at 4000 rpm and 4ºC for 10 min. The ether fraction was discarded and the process repeated up to 3

times. The peptide residue was dried under a N_2 flow stream, dissolved in a mixture of H_2O/ACN (1:1) and lyophilized.

The cyclopeptides were purified by automated flash chromatography using IscoCombi flash equipment or by HPLC at semi-preparative scale. Purifications were run using ReadySep C18 column (or C18 Sunfire column for the semi-Prep-HPLC) and a 30 min linear gradients of ACN in H_2O which were optimized for each sample. Peaks of interest were analyzed by analytical HPLC, combined and lyophilized.
The final products were analyzed and fully characterized by MALDI-TOF, HR-ESMS and amino acids analysis. Purity was checked by analytical HPLC. The yield of each cyclopeptide was determined by amino acid analysis.

3.2.2. Characterization

&D-Trp-Pro-Arg-D-Trp-Pro-Arg& (*cyclo*-1b)

Cleavage cocktail: TFA/TA/H_2O/TIS/EDT - 81.5:5:5:1:5 (3 h)
Purification by automated flash chromatography with RediSep C18 (0:20 to 20:25 H_2O/ACN + 0.1% TFA, gradient over 30 min). (20 mg, 75%). Purity: 95%
HPLC: t_R (min, G1060 ACN in 8 min) = 2.978
HR-ESMS calcd for: $C_{44}H_{58}N_{14}O_6$, expected: 879.47365, found: 879.4759 (m/z)

&Trp-D-Pro-Arg-Trp-D-Pro-Arg& (*cyclo*-1c)

Cleavage cocktail: TFA/TA/H_2O/TIS/EDT - 81.5:5:5:1:5 (3 h)
Purification by automated flash chromatography with RediSep C18 (0:20 to 20:25 H_2O/ACN + 0.1% TFA, gradient over 30 min) (60 mg, 80%). Purity: 95%
HPLC: t_R (min, G2070 ACN in 8 min) = 2.99
HR-ESMS calcd for: $C_{44}H_{58}N_{14}O_6$, expected: 879.47365, found: 879.47546 (m/z)

&Trp-Pro-D-Arg-Trp-Pro-D-Arg& (*cyclo*-1d)

Cleavage cocktail: TFA/TA/H_2O/TIS/EDT - 81.5:5:5:1:5 (3 h)
Purification by automated flash chromatography with RediSep C18 (0:20 to 20:25 H_2O/ACN + 0.1% TFA, gradient over 30 min) (10 mg, 20%). Purity: 95 %
HPLC: t_R (min, G0100 ACN in 8 min) = 4.12
HR-ESMS calcd for: $C_{44}H_{58}N_{14}O_6$, expected: 879.47365, found: 879.47449 (m/z)

&D-Arg-Pro-Trp-D-Arg-Pro-Trp& (*cyclo*-2b)

Cleavage cocktail: TFA/TA/H_2O/TIS/EDT - 81.5:5:5:1:5 (3 h)
Purification by automated flash chromatography with RediSep C18 (0:20 to 20:25 H_2O/ACN + 0.1% TFA, gradient over 30 min). (30 mg, 84%). Purity: 97 %
HPLC: t_R (min, G1060 ACN in 8 min) = 4.75
HR-ESMS calcd for: $C_{44}H_{58}N_{14}O_6$, expected: 879.47365, found: 879.47377 (m/z)

&Arg-D-Pro-Trp-Arg-D-Pro-Trp& (*cyclo*-2c)

Cleavage cocktail: TFA/TA/H_2O/TIS/EDT - 81.5:5:5:1:5 (3 h)

Purification by automated flash chromatography with RediSep C18 (0:20 to 20:25 H_2O/ACN + 0.1% TFA, gradient over 30 min). (60 mg, 80%). Purity: 95 %
HPLC: t_R (min, G0100 ACN in 8 min) = 4.34
HR-ESMS calcd for: $C_{44}H_{58}N_{14}O_6$, expected: 879.47365, found: 879.47429 (m/z)

&Arg-Pro-D-Trp-Arg-Pro-D-Trp& (*cyclo*-2d)

Cleavage cocktail: TFA/TA/H_2O/TIS/EDT - 81.5:5:5:1:5 (3 h)
Purification by automated flash chromatography with RediSep C18 (0:20 to 20:25 H_2O/ACN + 0.1% TFA, gradient over 30 min). (30 mg, 30%). Purity: 95 %
HPLC: t_R (min, G0100 ACN in 8 min) = 4.60
HR-ESMS calcd for: $C_{44}H_{58}N_{14}O_6$, expected: 879.47365, found: 879.47481 (m/z)

&Ser-D-Pro-Trp-Ser-D-Pro-Trp& (*cyclo*-3a)

Cleavage cocktail: TFA/H_2O/TIS - 95:2.5:2.5 (1 h)
Purification by automated flash chromatography with RediSep C18 (0:20 to 20:50 H_2O/ACN + 0.1% TFA, gradient over 30 min). (33 mg, 70%). Purity: 98 %
HPLC: t_R (min, G0100 ACN in 8 min) = 5,47
HR-ESMS calcd for: $C_{38}H_{44}N_8O_8$, expected: 741.33549, found: 741.33646 (m/z)

&Ser-D-Pro-Trp-Ser-D-Pro-D-Trp& (*cyclo*-3b)

Cleavage cocktail: TFA/H_2O/TIS - 95:2.5:2.5 (1 h)
Purification by automated flash chromatography with RediSep C18 (0:20 to 20:50 H_2O/ACN + 0.1% TFA, gradient over 30 min) (27 mg, 60%). Purity: 98 %
HPLC: t_R (min, G0100 ACN in 8 min) = 5,59
HR-ESMS calcd for: $C_{38}H_{44}N_8O_8$, expected: 741.33549, found: 741.33646 (m/z)

&Trp-D-Pro-Glu-Trp-D-Pro-Glu& (*cyclo*-4a)

Cleavage cocktail: TFA/H_2O/TIS - 95:2.5:2.5 (1 h)
Purification by automated flash chromatography with RediSep C18 (0:30 to 30:80 H_2O/ACN + 0.1% TFA, gradient over 30 min). (67 mg, 50%). Purity: 97 %
HPLC: t_R (min, G30100 ACN in 8 min) = 3.44
HR-ESMS calcd for: $C_{42}H_{48}N_8O_{10}$, expected: 825.35662, found: 825.35695 (m/z)

&Trp-D-Pro-Glu-Trp-D-Pro-D-Glu& (*cyclo*-4b)

Cleavage cocktail: TFA/H_2O/TIS - 95:2.5:2.5 (1 h)
Purification by automated flash chromatography with RediSep C18 (0:30 to 30:50 H_2O/ACN + 0.1% TFA, gradient over 30 min). (95 mg, 60%). Purity: 95 %
HPLC: t_R (min, G30100 ACN in 8 min) = 3.67
HR-ESMS calcd for: $C_{42}H_{48}N_8O_{10}$, expected: 825.35662, found: 825.35545 (m/z)

&Ile-D-Pro-Trp-Ile-D-Pro-Trp& (*cyclo*-5a)

Cleavage cocktail: TFA/H_2O/TIS- 95:2.5:2.5 (1 h)
Purification by automated flash chromatography with RediSep C18 (0:30 to 30:80 H_2O/ACN + 0.1% TFA, gradient over 30 min). (59 mg, 75%). Purity: 95 %

HPLC: t_R (min, G30100 ACN in 8 min) = 6.04
HR-ESMS calcd for: $C_{44}H_{56}N_8O_6$, expected: 793.43956, found: 793.44013 (m/z)

&Ile-D-Pro-Trp-Ile-D-Pro-D-Trp& (*cyclo*-5b)

Cleavage cocktail: TFA/H_2O/TIS - 95:2.5:2.5 (1 h)
Purification by automated flash chromatography with RediSep C18 (0:40 to 40:70 H_2O/ACN + 0.1% TFA, gradient over 30 min). (53 mg, 68%). Purity: 96 %
HPLC: t_R (min, G30100 ACN in 8 min) = 6.04
HR-ESMS calcd for: $C_{44}H_{56}N_8O_6$, expected: 793.43956, found: 793.43955 (m/z)

&Ser-D-Pro-Glu-Ser-D-Pro-Glu& (*cyclo*-6a)

Cleavage cocktail: TFA/H_2O/TIS - 95:2.5:2.5 (1 h)
Purification by HPLC-semi-preparative (SunFirePrep C18, 0:50 H_2O/ACN + 0.1% TFA, linear gradient over 30 min). (35 mg, 15%). Purity: 95 %
HPLC: t_R (min, G050 ACN in 8 min) = 4.61
HR-ESMS calcd for: $C_{26}H_{38}N_6O_{12}$, expected: 627.26205, found: 627.26162 (m/z)

&Ser-D-Pro-Glu-Ser-D-Pro-D-Glu& (*cyclo*-6b)

Cleavage cocktail: TFA/H_2O/TIS - 95:2.5:2.5 (1 h)
Purification by HPLC-semi-preparative (SunFirePrep C18, 0:50 H_2O/ACN + 0.1% TFA, linear gradient over 30 min). (80 mg, 41%). Purity: 95 %
HPLC: t_R (min, G050 ACN in 8 min) = 4.50
HR-ESMS calcd for: $C_{26}H_{38}N_6O_{12}$, expected: 627.26205, found: 627.26186 (m/z)

&Ser-D-Pro-Ile-Ser-D-Pro-Ile& (*cyclo*-7a)

Cleavage cocktail: TFA/H_2O/TIS - 95:2.5:2.5 (1 h)
Purification by automated flash chromatography with RediSep C18 (0:10 to 10:30 H_2O/ACN + 0.1% TFA, gradient over 30 min). (57 mg, 50%). Purity: 98 %
HPLC: t_R (min, G2070 ACN in 8 min) = 3.62
HR-ESMS calcd for: $C_{28}H_{46}N_6O_8$, expected: 595.34499, found: 595.34503 (m/z)

&Glu-D-Pro-Ile-Glu-D-Pro-Ile (*cyclo*-8a)

Cleavage cocktail: TFA/H_2O/TIS - 95:2.5:2.5 (1 h)
Purification by automated flash chromatography with RediSep C18 (0:10 to 10:40 H_2O/ACN + 0.1% TFA, gradient over 30 min). (104 mg, 70%). Purity: 95%
HPLC: t_R (min, G0100 ACN in 8 min) = 5.11
HR-ESMS calcd for: $C_{32}H_{50}N_6O_{10}$, expected: 595.34499, found: 595.34503 (m/z)

3.3. Synthesis of fluorine and carboxyfluorescein labelled peptides (12-13)

L*inear peptide sequence: H-CDIHVMWEWECFERL-NH₂ (9)*

The synthesis was performed at 100 μmol scale. Aminomethyl ChemMatrix resin (300 mg, f=0.58 mmol/g) was functionalized with the AB linker by treatment with Fmoc-Rink Linker (64.75 mg, 3 eq), TBTU (38.53 mg, 3 eq) and DIEA (42 μl, 6 eq) in DMF. The

coupling was performed manually and the reaction was left to proceed 1 h, then the solvent was removed by filtration and the peptide washed with DMF (5x1 min) and DCM (5x1 min). The capping was performed adding Ac_2O (113 µl, 10 eq) and DIEA (209 µl. 10 eq) in DMF and stirring manually for 15 min. The resin was transferred into the microwaves reactor and the peptide chain elongation was performed by microwaves assisted heating technology, according to the conditions described in the section *6.5.13.* TBTU/DIEA were used for the amino acid coupling reactions and piperidine 20% in DMF for the Fmoc deprotection. A double coupling was set as default for each coupling.
At the end of the linear peptide synthesis a small amount of resin was subjected to deprotection by treatment with TFA/TIS/H_2O-94:3:3 cleavage cocktail solution (3 h). The identity of the product was confirmed by MALDI-TOF and the quality of the reaction was checked by analytical HPLC.

Initial loading: 0.33 mmol/g
HPLC: t_R (min, G0100 ACN in 8 min) = 4.73
MALDI-TOF calcd for: $C_{90}H_{127}N_{23}O_{23}S_3$, expected: 1993.86, found: 1995.2570 $[M+H]^+$

O_2O-CDIHVMWEWECFERL-NH_2 (10)

Fmoc-8-amino-3,6-dioxaoctanoic acid (115.5 mg, 3 eq) and HBTU (96,33 mg, 3 eq) were sequentially added to the peptide-resin **9** in DMF, followed by DIEA (140 µl, 6 eq). The mixture was allowed to react with intermittent manual stirring for 1 h. The solvent was removed by filtration, and the resin was washed with DMF (5 x 1 min) and DCM (5 x 1 min). Finally the Fmoc group was removed by treatment with piperidine 20% in DMF. A small amount of resin was subjected to deprotection by treatment with a cleavage cocktail solution (TFA/TIS/H_2O-94:3:3, 3 h). The identity of the product was confirmed by MALDI-TOF and the quality of the reaction was checked by analytical HPLC.

HPLC: t_R (min, G0100 ACN in 8 min) = 4.76
HR-MS calcd for: $C_{96}H_{138}N_{24}O_{26}S_3$, expected: 2138.94, found: 2141.60 $[M+H]^+$
MALDI-TOF: $[M+H]^+$: 2141.29

O_2O-C(&)-DIHVMWEWEC(&)-FERL-NH_2 (11)

To the peptide-resin **10** in DCM, I_2 (19 mg, 5 eq) was added. The reaction was left with intermittent manual stirring for 15 min. The solvent was removed and the treatment was repeated again. The peptide resin was washed with DMF (5x1 min), a saturated solution of $NaHSO_4$ (5x1 min) and $CHCl_3$ (5x1 min). A small amount of resin was subjected to deprotection by treatment with a cleavage cocktail solution (TFA/TIS/H_2O-94:3:3, 3 h) and the accomplishment of the reaction was monitored by HS-ESMS and MALDI-TOF analysis.

HPLC: t_R (min, G0100 ACN in 8 min) = 4.77
HR-ESMS calcd for: $C_{96}H_{136}N_{24}O_{26}S_3$, expected: 2136.92, found: 2136.9223 (m/z)
MALDI-TOF, $[M+H]^+$: 2139.03 Da

Cf-O_2O-C(&)-DIHVMWEWEC(&)-FERL-NH_2 (12)

A mixture of 5(6)-carboxyfluorescein (15.67 mg, 3 eq), PyBOP (23.4 mg, 3 eq) and HOAt (6.12 mg, 3 eq) was dissolved in the minimum volume of DMF and pre-activated by adding DIEA (15.67 μl, 6 eq). After 1 min the mixture was added to the peptide-resin **11**. The mixture was allowed to react overnight. The solvent was removed by filtration and the resin was washed with DMF (5x1 min) and DCM (5x1 min). The treatment with the cocktail cleavage solution TFA/TIS/H_2O-94:3:3 (3 h) provided the peptide complete deprotection and cleavage from the resin. The purification by HPLC-semi-preparative (SunFirePrep C18, 30:60 H_2O/ACN + 0.1% TFA, linear gradient over 25 min) yielded the product **12** as white solid. (10 mg, 11 %). Purity: 95%.

HPLC: t_R (min, G3060 ACN in 8 min) = 3.92
MS-HPLC calcd for: $C_{117}H_{146}N_{24}O_{32}S_3$, expected: 2494.97, found: 1249 $[(M+2H)/2]^+$, 833.22 $[(M+H)/3]^+$
MALDI-TOF, $[M+H]^+$: 2496.36 Da

CF_3-O_2O-C(&)-DIHVMWEWEC(&)-FERL-NH_2 (13)

A mixture of 4,4,4-Trifluoro-3-(trifluoromethyl)butanoic acid (83 μl, 20 eq), PyBOP (312 mg, 20 eq) and HOAt (245 mg, 60 eq), was dissolved in the minimum volume of DMF and pre-activated by adding DIEA (313 μl, 60 eq). After 1 min the mixture was added to the peptide-resin **11**. The mixture was allowed to react with intermittent manual stirring 1.5 h. The solvent was removed by filtration and the resin was washed with DMF (5x1 min) and DCM (5x1 min). The peptide complete deprotection and cleavage from the resin was accomplished by acidolytic treatment with the cocktail cleavage solution TFA/TIS/H_2O-94:3:3 (3 h). The purification by HPLC-semi-preparative (SunFirePrep C18, 30:60 H_2O/ACN + 0.1% TFA, linear gradient over 25 min) yielded the product **13** as white solid. (9 mg, 8 %). Purity: 98%

HPLC: t_R (min, G3060 ACN in 8 min) = 3.92
MS-calcd for: $C_{101}H_{138}F_6N_{24}O_{27}S_3$, expected: 2328.92, found: MALDI-TOF, $[M+H]^+$: 2330.0076 Da

ACKNOWLEDGEMENTS

At the end of my thesis, it is a pleasant task to express my thanks to all those who contributed in many ways to the success of this study and made it an unforgettable experience for me.

Foremost, I would like to express my sincere gratitude to my advisor Prof. Luigi Panza for his unflagging support to my Ph.D study and research.

My sincere thanks to Prof. Ernest Giralt for giving me the opportunity to work in his research group at IRB in Barcelona. Thanks for letting me to be involved in an exciting project and leading me to grow professionally in the world of synthesis on solid phase. A special thank to Dr. Meritxell Teixido for giving me the great scientific support throughout the course of my research at IRB.

Thanks to the Panza's group for your wonderful patience, continual support and warm humour. I am lucky to have made such great friends.

To all the staff and labmates at IRB (Barcelona), I am grateful for the chance to be a part of the lab and for making the time spent in Barcelona so enjoyable and unforgettable.

I would like to thank my family for all the moral support, the continuous confidence and motivation they've given me over the years. Grazie!